(12)

THE HIGH CURRENT RF (HCRF) LINAC PROGRAM

Final Report

PIFR-3863

November 1992

Prepared for

Office of Naval Research
Department of the Navy
800 N. Quincy Street
Arlington, VA 22217-5000

Under Contract N00014-88-C-0267

Prepared by

Physics International Company
2700 Merced Street
San Leandro, CA 94577

TABLE OF CONTENTS

Dist A. per telecon Dr. V. Smiley
NOSC Code 804
27 Catalina Blvd
San Diego, CA 92152
12/10/92 CG

SECTION 1

INTRODUCTION AND OVERVIEW

The High Current Radio Frequency (HCRF) Accelerator program began as an effort funded by the Strategic Defense Initiative Office (SDIO) through the Office of Naval Research (ONR) under contract number N00014-88-C-0267 awarded to Physics International Company (PI) on August 15, 1988. The ONR Scientific Officer in charge of monitoring technical progress throughout the program's duration was Dr. Vern Smiley. The original contract was negotiated in the amount of $219,225 for an initial study with three options that could be exercised at the Government's discretion. The three options carried a negotiated total of $3,731,115 so that the total negotiated amount was $3,950,340. SDIO only provided $600,000 for the effort, and only one of the three options was exercised. An additional $310,000 was provided by DARPA, the Office of Naval Technology (ONT) and the Naval Ocean System Center (NOSC) for a collaborative effort to explore an RF technology application in naval surveillance (ultra-wideband radar), an activity covered by the HCRF statement of work. Technical work on the HCRF program consisted of in-depth technology studies and experimental support on the naval radar task. This final report describes that work; a brief overview follows.

1.1 HCRF STUDIES.

The overall goal of the HCRF program was to develop a fundamentally new technology for compact (high gradient) electron accelerators that can efficiently drive high gain, single pass FEL amplifiers producing output radiation at a wavelength of approximately one micron or less in a pulsed format for boost phase and mid-course SDIO missions. SDIO mission requirements dictated that the accelerator technology goals be consistent with a laser system that can produce greater than ten megawatts of average optical power during a 200 second battle from a space platform placed in orbit with a single heavy lift booster (see Section 2.1 for more background on the SDIO requirements). The overall system mass and length could not exceed 70 tonnes and 60 meters. These constraints not only meant that the accelerator had to be as small and light as possible, it also had to be efficient to keep its demands for prime power and thermal management from driving total system mass and size over the limits.

SDIO/ONR had been developing an accelerator for the SBFEL program for two years when PI began work on the HCRF program in August 1988. The other program, then being executed by TRW, is based on using a CW RF accelerator with superconducting cavities to drive an FEL oscillator. The HCRF accelerator approach is fundamentally different in that it uses a pulsed format to drive a single-pass, master oscillator power amplifier (MOPA) FEL wiggler, operates at ambient temperature and can be constructed with low Q aluminum cavities. These differences promise several advantages over the superconducting accelerator (SCA) approach including the elimination of a large and complex ring resonator, less sensitivity to acoustic and thermal variations in cavities (because of the low Q), a shorter structure (because of higher real-estate gradients), rapid turn on/off capability, and the option of locating the beam director away from the high power laser platform.

To achieve these advantages, several technology hurdles had to be surmounted. The key technical issues for the accelerator lay in three areas, efficiency, electron beam quality, and high power RF radiation sources. The original $4 million program was intended to address these issues in phase one of a seven year program to develop a fully space qualifiable HCRF-based FEL system. The program began with a study to provide baseline system requirements and to plan future experimental work. The remainder of the phase one effort was to have been a series of experiments culminating in a 20 MeV, 1 kA proof of principle demonstration. A full description of this program plan is in Section 2.2. Unfortunately, because only 15 percent of the negotiated funds became available from SDIO, no experimental work was possible. Instead, ONR directed PI to expand the scope of its studies to make sure that overall system issues could be addressed more cost effectively should full funding become available. Such funding never materialized so the HCRF accelerator effort never progressed beyond the study phase.

Despite the lack of funding, several noteworthy accomplishments were completed in the HCRF program. Among those are the following:

- A baseline point design for a 200 MeV HCRF accelerator based on delivering a 100-MW average power electron beam to a MOPA FEL.
- Identification of key technology issues in all subsystems and comparison of existing state of the art to requirements.
- A preliminary computer analyses (using the code SUPERFISH) on the baseline cavity design to verify suitable mode separation.

- Numerous trade off studies to vary parameters about the baseline point design in order to optimize the system design and to refine the experimental technology road map. All aspects of accelerator design were considered including fundamental frequency, beam loading fraction, gradient, efficiency, pulse length, repetition rate, cavity material, intrinsic Q values, wall losses, etc.

- Preliminary mass estimates for required prime power and burst power conditioning subsystems and a comparison of the results to published estimates for cryogenic accelerators.

- A complete analysis of accelerator efficiency and the impact of using very high beam loading fractions (95%) on longitudinal energy spread.

- A thorough study of electron beam quality and stability within the accelerator structure. Calculations using the codes SUPERFISH and PARMELA were carried out to predict longitudinal beam energy spread and the results documented.

- Preliminary analyses of the effects of multi-bunch and single-bunch wakefield effects on beam breakup and emittance degradation during beam transport through the accelerator.

- Partial completion of a PC-based system analysis code to use in further trade-off studies.

- Identification of key conceptual approaches to provide the very high power RF radiation sources required to power the accelerator. Chief among these concepts was a novel series source configuration using relativistic klystrons that promises 90 percent electronic conversion efficiency.

The issue of the RF source feasibility is particularly important. The HCRF accelerator conceptual design uses a pulse format in which RF energy must couple to the electron beam from the RF cavities at a rate of 10 GW during the macropulse duration (see Section 2.3). During the early part of the macropulse, before RF energy begins to flow from the decelerator, this entire RF power pulse must be provided by an ensemble of sources external to the accelerator. In January 1989, a panel of experts assembled by ONR to review both the TRW and PI accelerator approaches (see Section 2.1 and Appendix A) recommended that the PI effort concentrate most heavily on this aspect of the concept. The remainder of the SDIO funds in the program were expended in various aspects of the RF radiation source problem.

Section 2.4 gives a summary of the PI effort on novel RF radiation source concepts. Of special interest is the series source concept that provides a means to increase the overall efficiency of an ensemble of sources by re-accelerating the relativistic electron beam used to power each

source after RF energy is extracted. This concept was selected as the basis for the final task in the HCRF program. In that task, PI executed a conceptual design for an experiment to study the critical issues of using a re-accelerated electron beam for efficiently producing RF energy from series relativistic klystrons. Details of this design study are in Appendix D.

1.2 IMPULSE RADAR EXPERIMENTS.

PI executed this portion of the HCRF program under a provision in the statement of work (SOW) instructing the contractor (PI) to "...study the utility of applying high power RF technology for collateral missions of interest to the Navy and SDIO such as surveillance". The purpose of this provision in the SOW was to apply the expertise and technology of the HCRF program outside the space based laser arena in order to maximize the effectiveness of government funds. The impulse radar experiments provided an excellent opportunity to take advantage of such cost saving features for the government.

The study of impulse radar for surveillance is an important effort for the Navy. The HCRF program had the necessary expertise in high power RF technology to support it, and, because of the SDIO funding shortfall, there were unfunded experimental tasks in the HCRF contract that were a perfect match to the impulse radar requirements. For these reasons, The ONR scientific officer, Dr. Vern Smiley, directed PI to support experiments being planned by Dr. Vince Pusateri of the Naval Ocean System Center (NOSC, Code 705). Dr. Pusateri's program was being funded by the Office of Naval Technology (ONT-21) and DARPA (under a BTI effort managed by Dr. Dominic Giglio). Funds were provided by Dr. Pusateri to cover all impulse radar work carried out under the HCRF contract.

Impulse radar is a special type of ultra-wideband radar (UWB). UWB radars are, as the name implies, characterized by bandwidths large compared to conventional radars. Bandwidth can be achieved with spread spectrum techniques or by using short pulses where the time-bandwidth product is of order unity. This latter technique is generally referred to as an impulse radar. Impulse radars have relative bandwiths of order 100 percent, meaning that the spectral width of the pulse is roughly equal to its carrier frequency. The interest in impulse radars partly derives from their very high range resolution capability. They are also regarded as potentially effective in foliage penetration, target identification, ground probing, terrain mapping, and other applications where a combination of low frequency and high range resolution are helpful. There has also been talk

about impulse radar's effectiveness as a counter-stealth tool but that is a controversial subject and has generally been discounted by a DARPA panel convened to study the problem.

The Navy's interest in impulse radar is specific to its potential role in detecting low flying, supersonic cruise missiles (sea-skimmers). These threats are a serious ship defense problem for the Navy and remain difficult to counter. Impulse radar, however, is not a proven technology and there is still a great deal of controversy surrounding it. To address feasibility questions, Dr. Pusateri initiated a program at NOSC to begin collecting basic design data in late 1988. One important type of data lies in the sea echo environment. To collect such data, a powerful impulse source that can broadcast UWB RF signals at long range (several kilometers) is needed. The PI portion of this effort was to provide such a source for sea clutter and multipath measurements.

Section 3 of this report presents details of the PI effort. PI provided a high power impulse source to mate with a 30 foot diameter parabolic dish provided by NOSC at a site on Point Loma in San Diego, California. The short pulse radiation signals were directed to sea and returns measured with a separate dish and signal detection system provided by SRI under a subcontract to PI. The experiments were successful and represented the first time a high power RF source was used in an impulse radar experiment at long range.

The remaining sections of this report give further details of the work accomplished under the HCRF program. Section 2 concentrates on the HCRF portion and Section 3 on the impulse radar work. Several appendices augment the report by presenting selected details in more depth.

SECTION 2

HCRF PROGRAM REVIEW

2.1 SDIO SBFEL PROGRAM BACKGROUND.

On March 23, 1983, President Reagan announced his intention to establish the Strategic Defense Initiative Organization (SDIO) with the mission to create an impenetrable defense system to negate nuclear armed Intercontinental Ballistic Missiles (BMD). At the time, this announcement was viewed as a bolt out of the blue; however, it was based on over two decades of intense R&D and systems analysis pursued under various Navy, Army, Air Force and DARPA programs. A major component of the conceptual BMD system was based on the use of High Energy Lasers (HEL), since the speed of light of the weapon pulse greatly reduced system response time and appeared to be a critical enabling technology. Use of the HEL appeared to be within reach as a result of remarkable progress made under the DARPA HEL program initiated shortly after the first laser demonstration by T. Maiman at Hughes Research Laboratory in 1960. By 1983 the output of pulsed lasers had been increased from the original microjoules per pulse to tens of kilojoules per pulse, and for CW lasers output had been increased from milliwatts to megawatts of average power. In addition, major progress had been made in the propagation of intense laser beams through the atmosphere.

By the fall of 1984 SDIO was in operation, with funding provided by transfer of funds from other DoD organizations and a core of staff from DARPA. SDIO immediately addressed the architecture required for the envisioned BMD system. It quickly became apparent that to achieve an acceptable leak rate, the system would have to have multiple components in a tightly interlinked system. Both ground based (GBL) and space based (SBL) laser systems were projected to have a crucial role in the overall system. The leading candidates for the SBL were assumed to be the CW chemical laser and the pulsed x-ray laser, and for the GBL it was assumed that the excimer laser was the primary candidate with the possibility that the free electron laser (FEL) might become a strong contender with further development. Although the first FEL had been demonstrated in 1975, the state of development was still rather immature in 1984. SDIO initiated studies to establish system and component performance requirements and then launched extensive technology development efforts for both the GBL and SBL. In 1986, Office of Naval Research (ONR) established a SBFEL program with SDIO funding. The goal was to achieve a laser system capable

of producing >10 MW of optical power with a total battle time of > 200 seconds, which could be launched on a single heavy lift booster. This placed size and mass constraints on the system. The key limitations were system mass less than 70 metric tonnes and a system length less than 60 meters. Early results from the SBL architecture studies suggested that an FEL based on a superconducting accelerator (SCA) would be the best approach to meet these goals. ONR had begun R&D on the SCA FEL in 1983 and chose to continue this effort at an accelerated rate. The primary contractors for that effort were TRW and Stanford University.

In March 1987 Physics International began discussions with ONR regarding an alternative approach for the SBFEL. The PI approach was based on use of a high gradient standing wave accelerator (HGA) that could drive a high-gain single-pass FEL amplifier with a total system efficiency of better than 40% with an optical wavelength of about one micron. To achieve the high accelerator gradient, PI proposed to use very high peak RF power to drive the cavities, and to achieve the high efficiency PI chose to use high beam loading with efficient beam energy recovery. The high current RF (HCRF) approach has several potential advantages when compared to the SCA FEL approach. Among these are higher real-estate voltage gradient, room temperature operation, high gain amplifier operation, relatively low power optical resonator for the drive oscillator, shorter overall structure, low Q (noise insensitive) cavities, rapid turn on/off capability and use of a remotely located high power beam director. After lengthy discussions with ONR and SDIO, the HCRF program was initiated in August 1988 to address the crucial technical issues for the HCRF approach.

The long range goal of ONR/SDIO was to develop the HCRF technology and incorporate it into a space qualifiable weapon device over a period of about seven fiscal years. To achieve this goal, a plan was conceived with three segments consisting of a baseline program, supporting technology development and a multi-MW optical power device. Continuation of the program from one segment to the next was contingent on the success of the prior segment and on the relative merits of the HCRF approach compared to other SBFEL approaches. The initial segment of the program, the baseline program, contained four elements. These were a system study, a proof of principle (PoP) experiment, an extended pulse accelerator (EPA) experiment and development of a high power microwave (HPM) source. Due to the expense and high risk of the EPA development, the baseline program was divided into two phases. The first phase was to include developing an EPA with a 50-MeV, 1-kA, 0.15-μs pulse, with the second phase extending this to 200-MeV, 2 kA, 0.5-μs pulse. The Phase I baseline program was incrementally funded with 200k$ of FY88

funds with the intention of providing sufficient funds in FY89 to vigorously pursue the program. In view of the limited amount of FY88 funding available, a decision was made to initially concentrate on the system study.

Unfortunately, the FY89 budget of SDIO only permitted release of an additional 200k$, which was insufficient to allow initiation of experimental work. Furthermore, the outyear budget prospects for SDIO were not optimistic. In view of this situation, the ONR/SDIO technical program managers reviewed the baseline program plan. A technical review group was selected by ONR to review the two SBFEL approaches. Reviews of both the SCA and HCRF approaches were performed in January 1989. The general finding of the TRG was that the SCA approach was at a more advanced stage of development than the HCRF approach and appeared to be a lower risk approach, in that there did not appear to be any "show stoppers." The TRG identified the crucial technology issue for the HCRF approach as development of the high power RF power source required to drive the HGA. The TRG report was delivered to ONR/SDIO in March 1989, with the results subsequently relayed to PI. The ONR/SDIO technical program managers advised the PI technical program manager to modify the program plan in concert with this recommendation. The program was then redirected to concentrate on development of the HPM source, including technical approaches beyond the relativistic magnetron originally selected for this application. In FY90, a final increment of 200k$ of funding was provided by SDIO.

2.2 FUNDAMENTAL PREMISE AND PROGRAM TIME LINE.

The primary goal of PI's High Current Radio Frequency (HCRF) accelerator program was to prove the feasibility of a novel electron beam accelerator meant to drive a free electron laser (FEL) wiggler to compete against the other technologies in SDIO's Space Based Free Electron Laser (SBFEL) program. Only two types of accelerators hold promise for high power free electron lasers: the induction linac and the RF accelerator. Both types can produce the high quality (high brightness and monoenergetic), and high voltage (of order of 100-200 MeV), electron beams needed to drive the FEL wigglers. Of these two, the induction linac concepts suffer size disadvantages because they are designed with relatively low accelerating field "real estate" gradients and use heavy magnetic materials in the acceleration cavities. Their advantage over most RF accelerator concepts is that they produce high currents. These high currents (of order of a few kA) simplify the FEL wiggler subsystem by allowing it to operate as a single pass amplifier. At lower currents, the wiggler must be configured as a master oscillator and requires a large and

complex ring resonator with either grazing incidence optics or gas lenses to re-circulate the optical beam power.

The motivation for PI's approach derives from these facts and a desire to overcome any shortcomings of SDIO's leading SBFEL technology choice, based on a CW superconducting RF electron beam accelerator. The superconducting accelerator (SCA) requires a cryogenic system that PI considered more complex and, potentially, larger and heavier than the thermal management system for an HCRF accelerator. Also, the high intrinsic Q value characteristic of SCA structures limits the electron beam microbunch currents to values less than 200 A (due to the excitation of transverse beam instabilities at high current) and causes the operation of the accelerator to be sensitive to minute perturbations induced by either mechanical vibrations or small fluctuations in the RF phase. Furthermore, CW operation drives up the average rf power handling requirements and limits the real estate gradient to values < 10 MV/m. The challenge, then, is to achieve high peak micropulse currents with a compact (high accelerating field gradient), room temperature, RF accelerator design that avoids transverse beam instabilities and efficiently converts RF energy to electron beam energy.

The HCRF program proposed to meet this challenge by using high peak power RF sources (3-10 GW per source) to drive the HCRF accelerator. The HCRF accelerator would operate at ambient temperature and use low Q cavities. Transverse instabilities are suppressed with damping probes and segmented cavity designs to reduce the Q's of the dangerous modes to values less than 100. Because of the low Q design, very large cavity apertures are possible. Hence, wakefield effects are reduced sufficiently at the fundamental driving frequency of 500 MHz to allow acceleration of 2 kA or more current in the micropulse without significant emittance growth or energy spread. The large aperture cavities have relatively low longitudinal shunt impedance but the RF to electron beam energy conversion efficiency is maintained by filling every RF bucket and operating at a macropulse current near 50 A. These features are all revisited in more detail in subsection 2.3. The advantages of the HCRF approach are summarized in Table 2.1.

The road map for the HCRF technology program is shown schematically in Figures 2.1 through 2.4. The overall program was composed of the Baseline and the Supporting Technology Development Elements. In the Baseline Element, a high gradient accelerator fed by single shot, phase-locked, high power microwave sources was to be constructed to prove the critical transverse beam instability suppression principles. In the parallel Technology Development Element a high quality electron beam injector and a moderate duty factor pulsed power driver was to be developed.

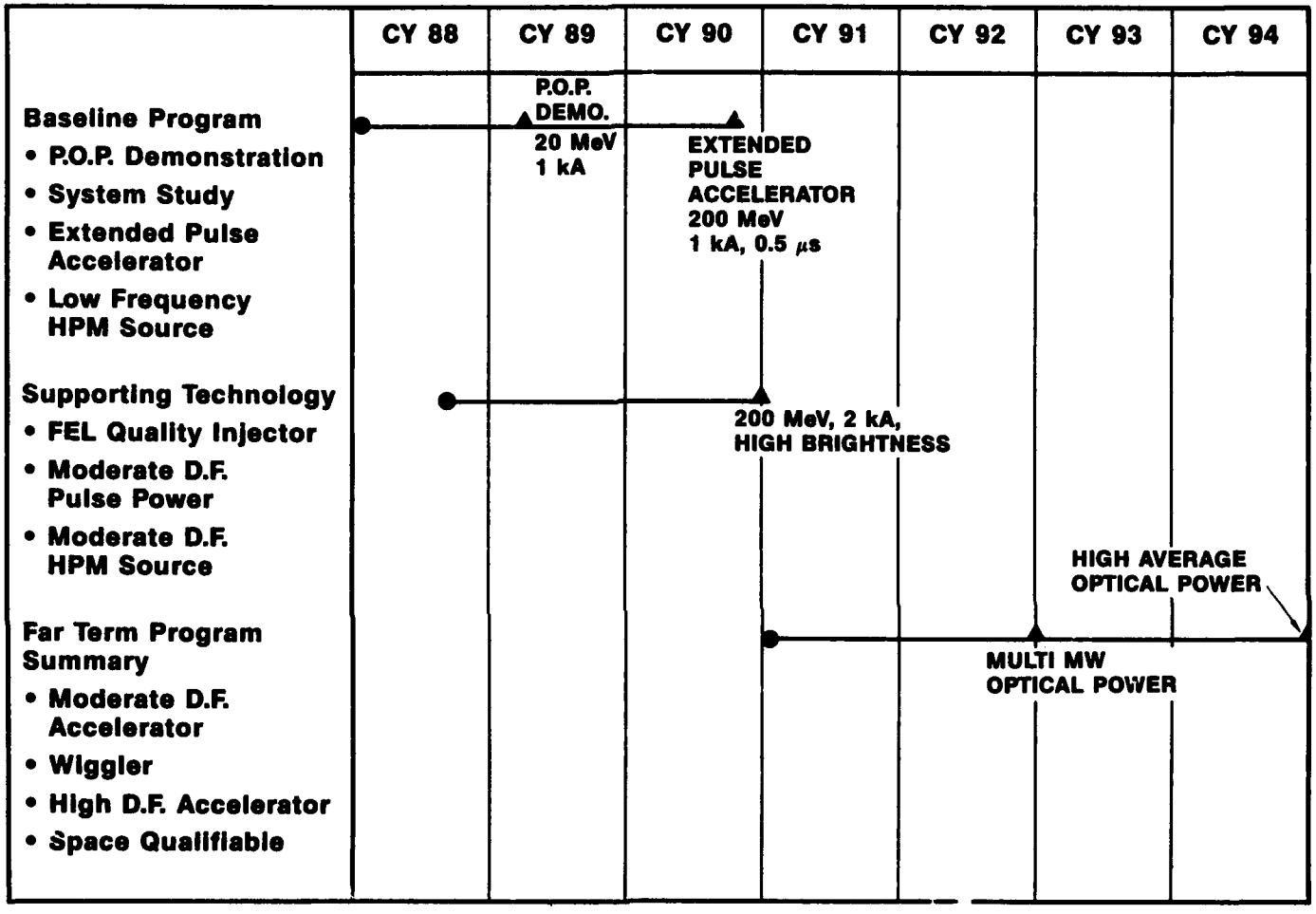

Figure 2.1. HCRF technology roadmap—overview.

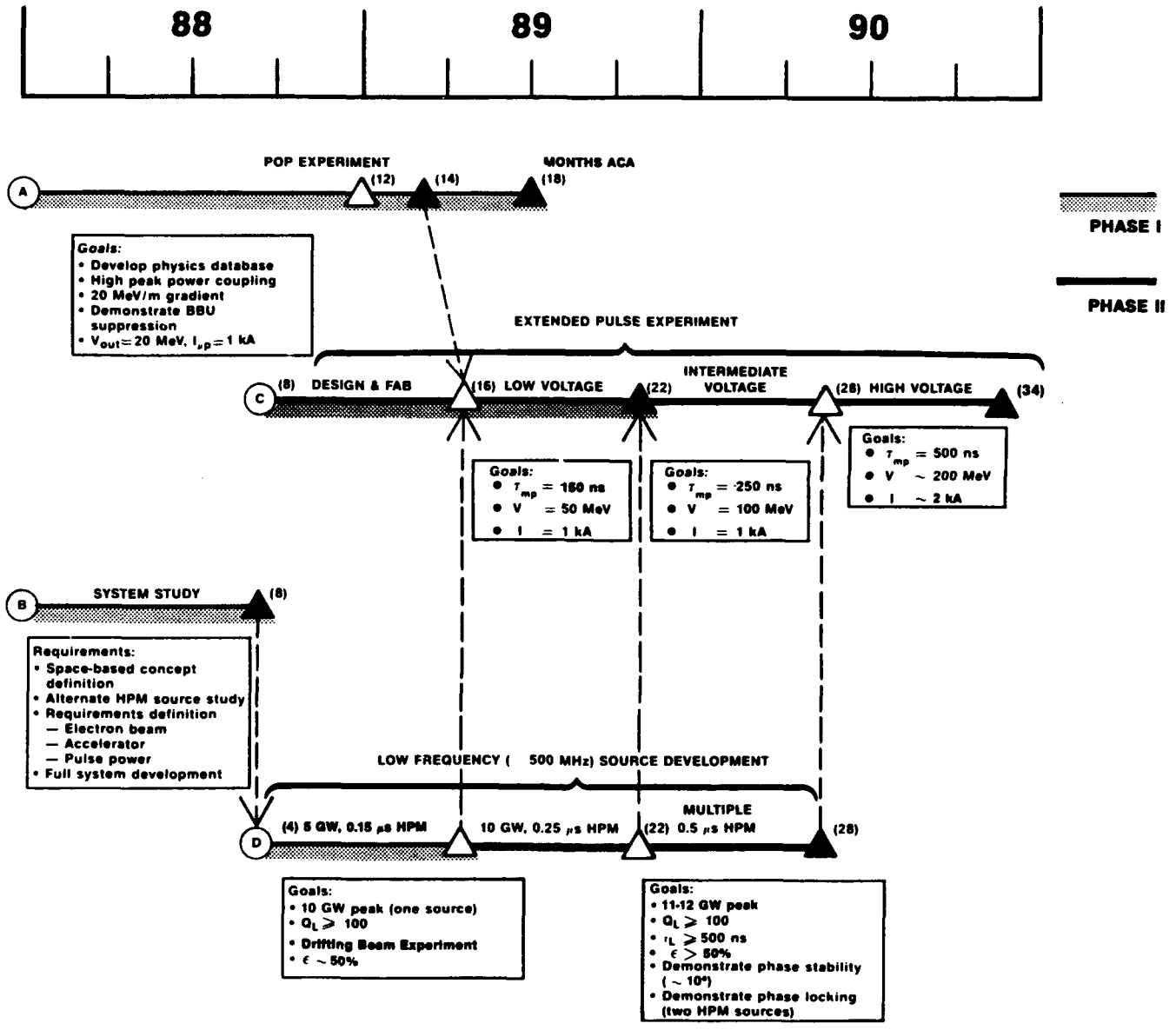

Figure 2.2. Original baseline technology program (Phase I and II)—single shot HCRF demonstration.

87-07-116

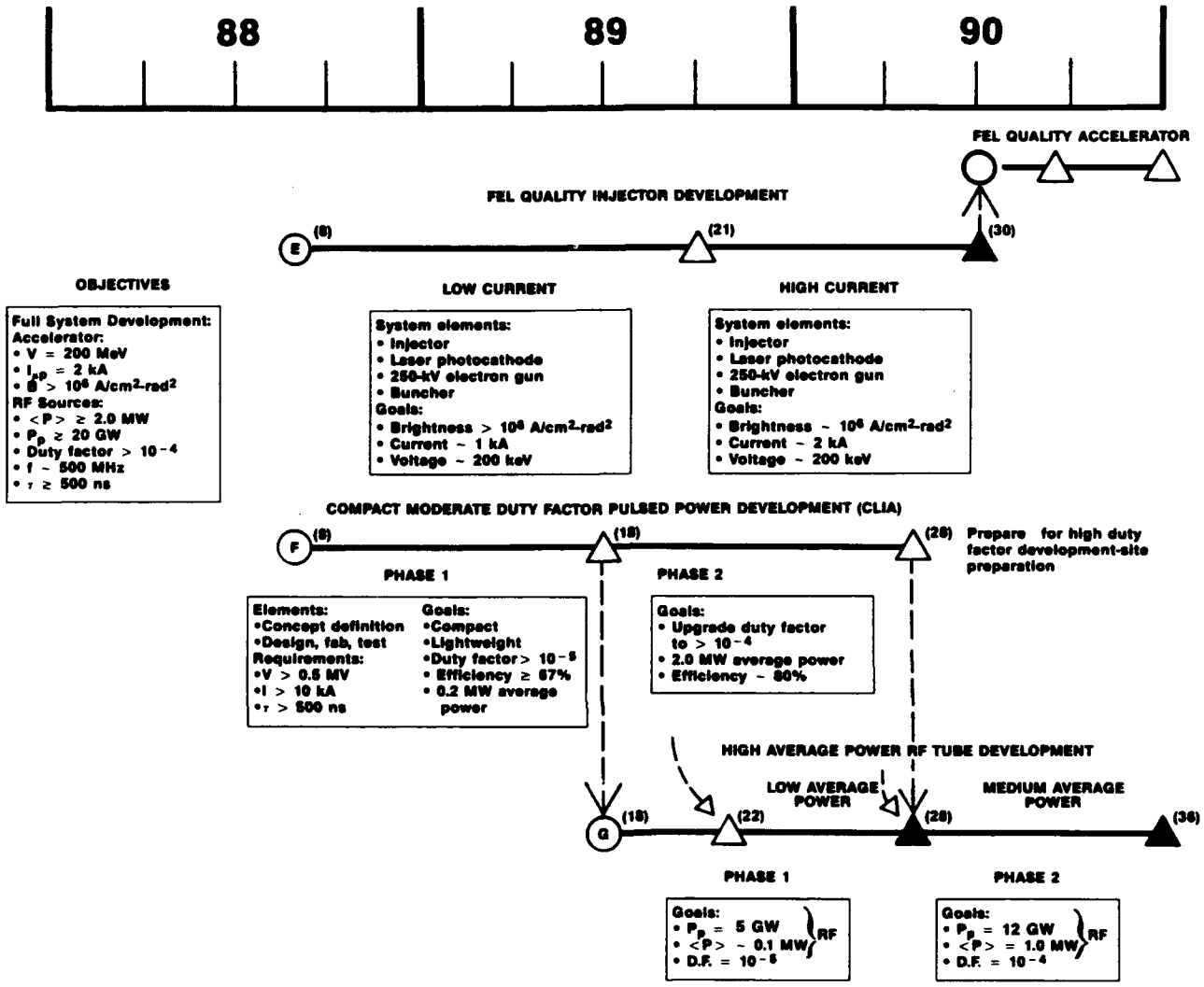

87-07-118

Figure 2.3. Original supporting technology program.

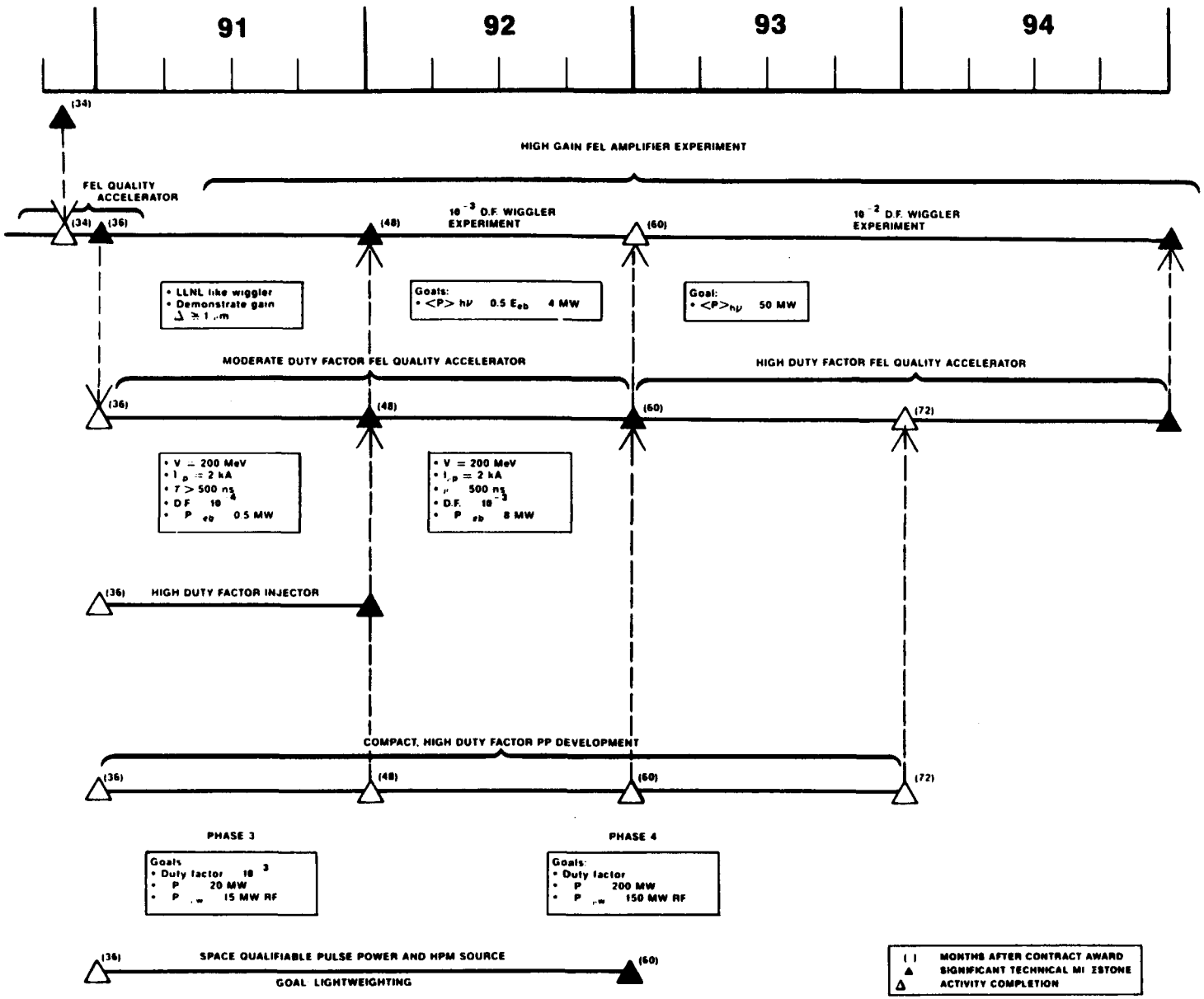

Figure 2.4. Original far term program.

The proposed follow-on to this program was to have used the injector and the HPM sources as well as results from the proof-of-principle demonstration to construct and test a high gain FEL amplifier experiment. The detailed program goals associated with each of these program elements are summarized in Table 2.2 and the technology issues to be resolved by each element are described in Table 2.3.

Table 2.1. Advantages of HCRF approach.

- More compact and lighter accelerator
  - Higher real estate gradient (≥ 20 MeV/m versus < 10 MeV/m for CW)
  - No cryogenics
  - Low Q cavities are a much more robust technology than high Q systems
- More compact and efficient wiggler configuration
  - High current allows high gain, single pass amplifier configuration for wiggler
  - No grazing incidence optics
- Much smaller and simpler space platform
  - No complex support systems required by high Q structures - relatively insensitive to shock, vibration, temperature variation, and start-up conditions
  - Fighting optics on separate platform
  - Does not require beam energy recovery system
- Greater overall electrical efficiency
  - High gain, single pass amplifier configuration is more efficient than master oscillator configuration.

2.3 HCRF ACCELERATOR DESIGN.

2.3.1 Operational Parameters.

The design parameters for the HCRF accelerator were selected to respond to the totality of technology issues summarized in Figure 2.5. As the figure shows, the key issues fall into three main categories having to do with the overall efficiency of the accelerator, the electron beam quality, and the high power RF sources that drive the accelerator. Elements of each of these main issues will be discussed below.

Table 2.2. HCRF Program goals.

Baseline Program - Low Frequency HPM Source and Extended Pulse Accelerator

- Using existing high power microwave source (1 or 3 GHz relativistic magnetron), demonstrate efficient acceleration of a high peak current electron beam (1 kA) to high energy (20 MeV) in a high gradient structure (20 MeV/m)
- Demonstrate matched coupling from a high power intense microwave source to a resonant accelerating structure
- Demonstrate the effectiveness of methods for suppression of transverse (beam breakup) instabilities
- Generate a database to understand the physics of high current rf accelerators
- Extend the operating range of HPM source to:
  - Higher peak power (10 GW) and total power (20 GW)
  - Low frequency (500 MHz)
  - Long pulse operation (0.5 μs)
- Using low frequency, long pulse HPM source, demonstrate acceleration of high peak current in microbunch (1 kA) to 200 MeV at a gradient of 20 MeV/m
- Scale the physics database developed in P.O.P. program to lower frequency (~ 500 MHz) and long macropulse (~ 0.5 μs)

Supporting Technology Program - Overall Goals

- Accelerate the high current (2 kA) FEL quality beam ($\Delta\gamma/\gamma < 0.5\%$, B ~ 1 to 2 x 10^6 A/cm^2·R^2 to 200 MeV using the extended pulse accelerator developed under baseline technology program
- Develop the necessary supporting technologies to provide a repetition rate capability for the extended pulse accelerator
  - Develop a high current, high brightness injector - 2 kHz and 1-2 x 10^6 A/cm^6·R^2
  - Develop moderate duty factor (10^{-4}-10^{-3}), moderate average power (2 MW), compact pulse power driver
  - Demonstrate high average power (> 1 MW) capability for HPM source

Table 2.3. Technology issues resolved in each program element.

	Q1 '89	Q2 '89	Q4 '89	Q2 '90	Q4 '90	Q4 '91	Q4 '92	Q4 '94
• Baseline Program	20 MeV	50 MeV	100 MeV	200 MeV				
Current Limits	1 kA	1 kA	1 kA	1 kA	2 kA			
BBU	X	X	X	X	X			
Wake field Effects	X	X	X	X	X			
High Power Coupling	X	X	X	X	X			
High Gradient	X	X	X	X	X			
Voltage	2 MeV	50 MeV	100 MeV	200 MeV				
RF Source at 500 MHz	5 GW	10 GW	20 GW					
Pulse Duration		100 ns	250 ns	500 ns				
• Supporting Technology								
High Brightness				Injector	X			
Low $\Delta\gamma/\gamma$ ($\leq$ 0.5%)				Injector	X			
Pulse Power (size, wt., power)					DF = 10^{-4}	10^{-3}		10^{-2}
RF Source Duty Factor					DF = 10^{-4}	10^{-3}		10^{-2}
End-to-End Efficiency							X	
FEL Demonstration						Single	DF = 10^{-3}	10^{-2}
Space Qualifiable						Pulse		
							X	

X = Demonstrated at full system level.

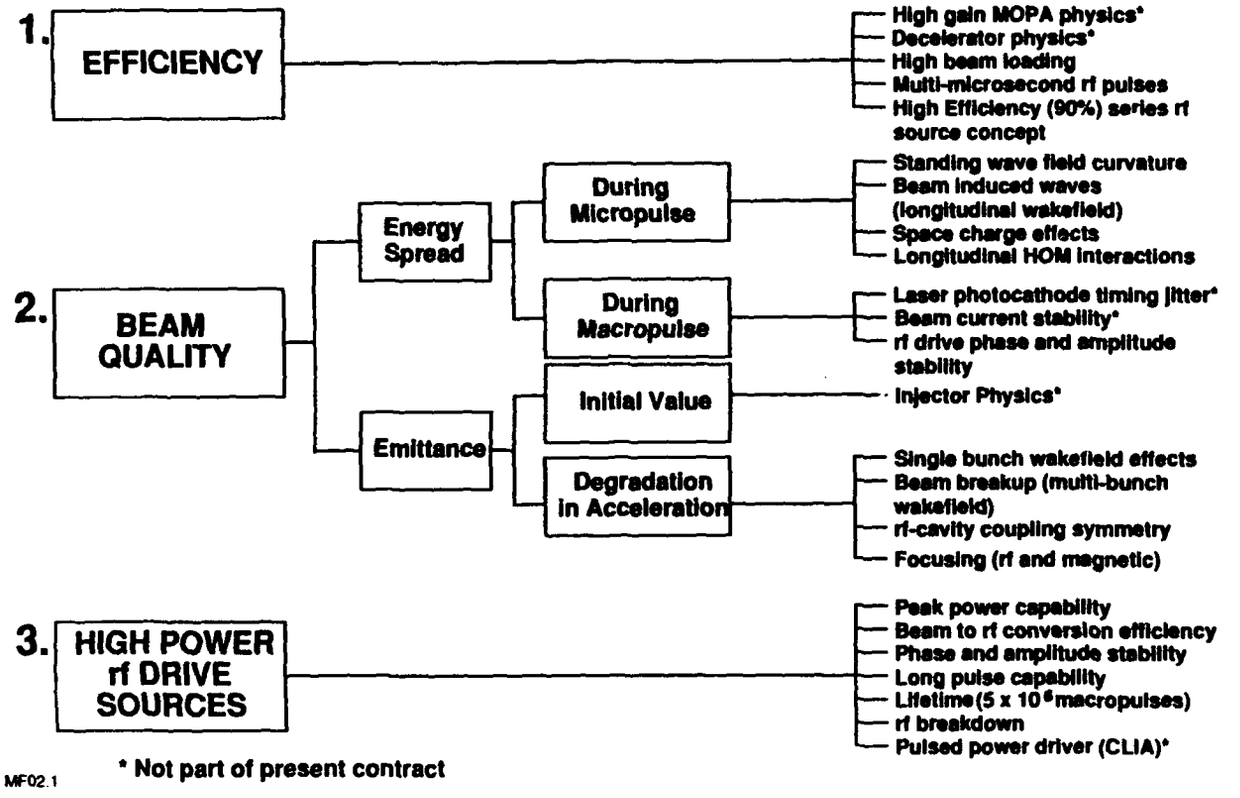

Figure 2.5. Key accelerator technology issues tree.

The HCRF accelerator concept is shown schematically in Figure 2.6 and the temporal pulse format of the electron beam is shown in Figure 2.7. Figure 2.6 also shows the evolution of the beam pulse width and energy as it moves through the injector, the buncher and the accelerator. The injector shown in Figure 2.6 produces a 0.5 MeV, 200 A (1 cm^2 area) photocathode electron beam train. This beam consists of micropulses of 500 ps duration. Each micropulse coincides with each cycle of the 500 MHz RF wave, thereby filling every RF bucket, and gives the train of micropulses shown in Figure 2.7, which repeat every 2 ns for the entire duration of the macropulse.

The injector design for the concept shown in Figure 2.6 is based upon the recent work on high brightness, high current electron guns developed at both LANL and Thermal Electron Corporation. A low power laser is used to irradiate a suitable photocathode (Cs_3Sb) that provides from 200 to 500 A/cm^2 of emitted current density. The injector is powered by a low voltage (200 to 500 keV) electron gun. The low power laser is Q-switched and mode locked to the RF accelerating power train and can also serve as the seed laser for the FEL wiggler.

The next device along the accelerator structure is the buncher. The buncher is a RF cavity that impresses a ramp on the accelerating pulse so that the tail of the micropulse can catch up to the head. For example, a 60-kV ramp in a 0.5-meter-long buncher is sufficient to bunch the initial 500 ps pulse to 50 ps and still restrict the energy spread in the fully accelerated pulse to < 0.50%. The pulse leaves the buncher with approximately the same 500 keV peak electron energy but the peak current is increased from 200 A to 2 kA. The beam enters the high gradient accelerating cavities after passing through a beam conditioning section, (which is not shown) to clean up the rise and fall of the micropulses.

The accelerating cavities (Figure 2.8) provide the final energy amplification. In this case, the end point energy is 200 MeV and the peak current in each 50 ps micropulse is 2 kA. To obtain the desired average electron beam power, the macropulse is repeated at the required repetition rate. For 100-MW average power in the electron beam, at a 200-MeV input energy, one needs an average current of 0.5 A. This is achieved by repeating the micropulse train with the characteristics of Figure 2.7 at a repetition rate of 20 kHz for a .5 microsecond long macropulse or 5 kHz for a 2 microsecond long macropulse. A summary of the parameters chosen for the HCRF accelerator is given in Table 2.4. Table 2.5 provides mass estimates of the primary system components.

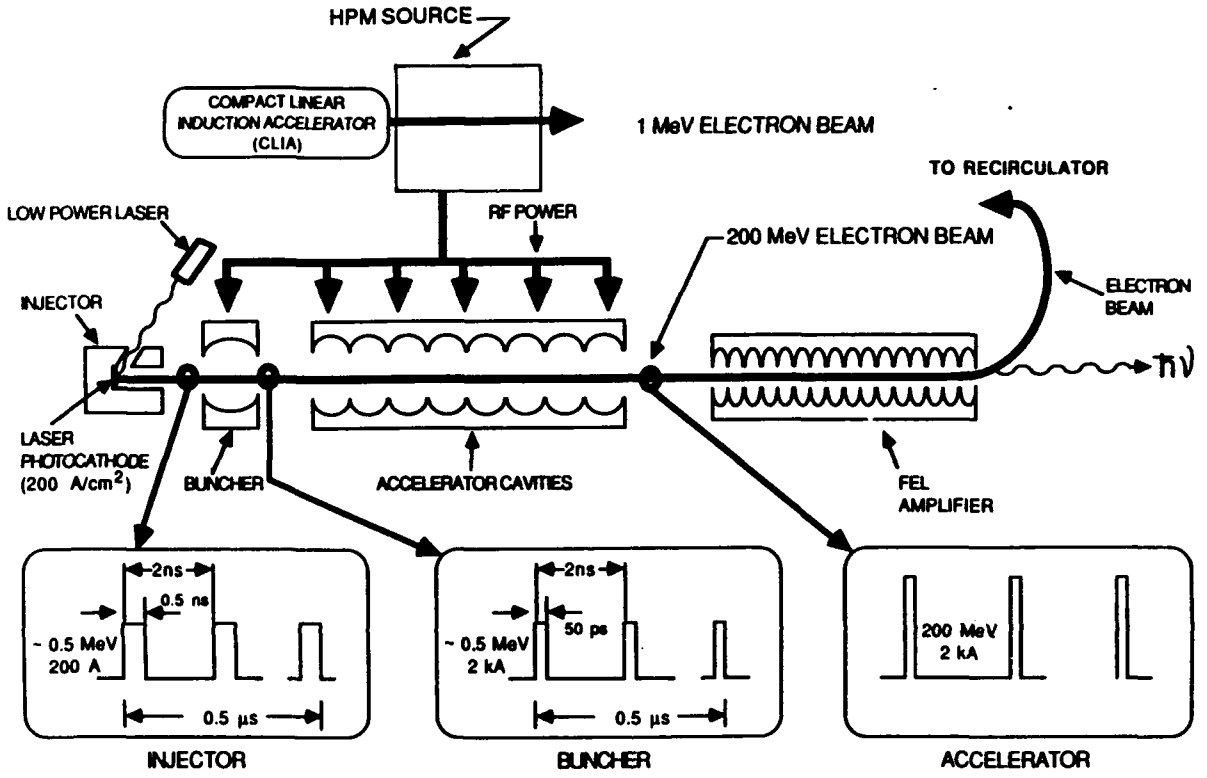

Figure 2.6. HCRF accelerator schematic and electron beam pulsewidth and energy evolution

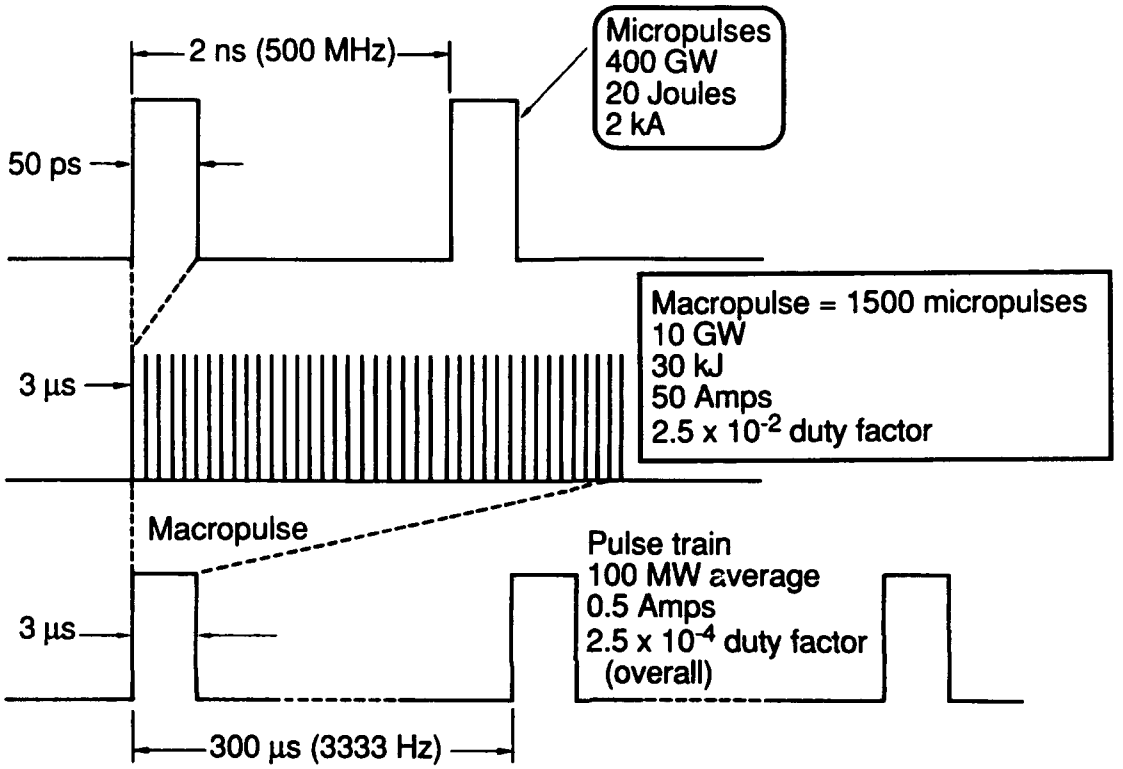

Figure 2.7. Two-hundred-MeV electron beam pulse format for HCRF.

- **Follows CERN SC design** (P. Bernard, et.al IEEE Trans. Nucl. Sci. Vol. NS-30, No. 4, August 1983) **but, with center cell input coupling.**

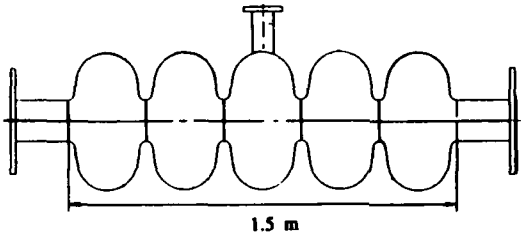

- **Initial SUPERFISH analysis shows suitable separation of normal modes**

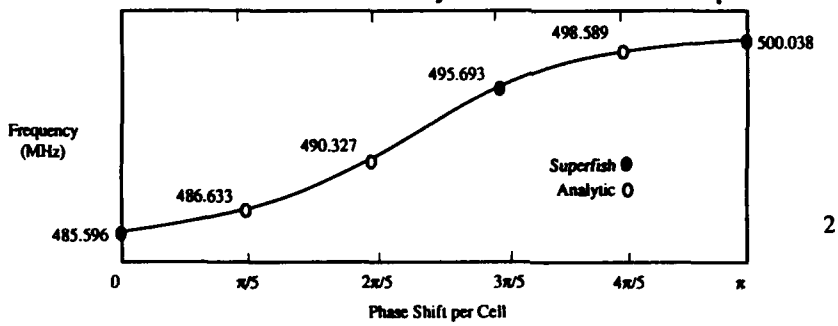

Bandwidth:

$$2\frac{(f_\pi - f_0)}{f_\pi + f_0} = 2.93\ \%$$

Figure 2.8a. Five cell cavity concept.

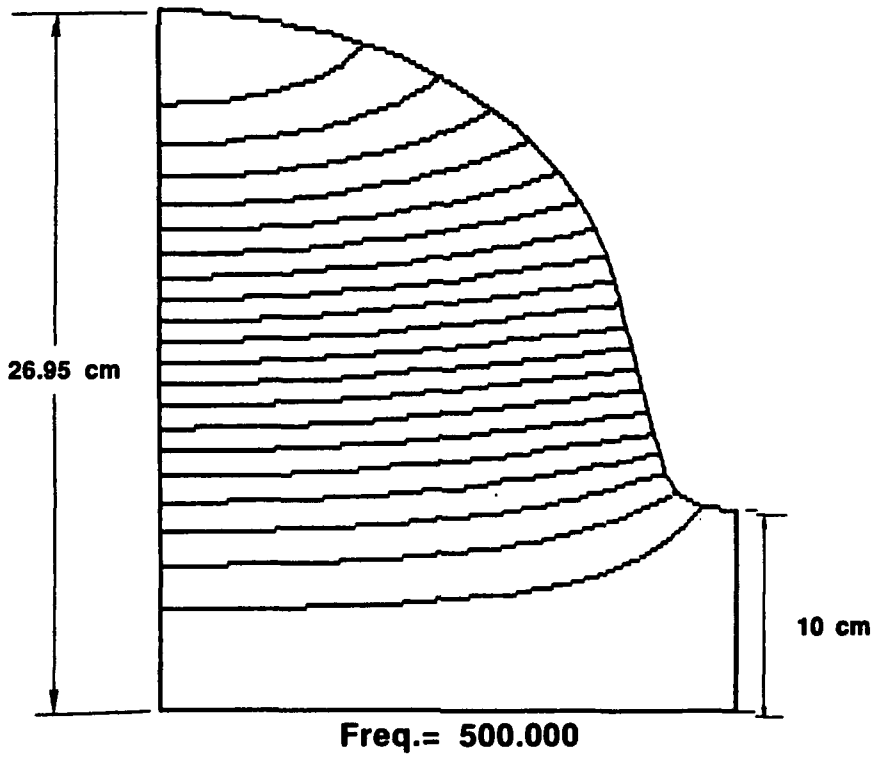

Figure 2.8b. Baseline cell design for 500 MHz accelerator.

Table 2.4. HCRF system parameters.

Accelerator Parameter Requirements

		circa 8/89	circa 8/90
Fundamental Frequency	f (GHz)	0.5	0.5
Beam Loading Fraction	α	0.98	0.95
Shunt Impedance	R/Q (Ω/m)	320	320
Stored rf Energy	U (kJ)	2.98	848
Intrinsic Q Value	Q_o	4.6 (10^4)	8.4 (10^3)
Accelerating Gradient	Eg (MV/m)	15	7.1
Accelerator Length	L (m)	13.3	16.9
Accelerator Efficiency	η (%)	90	90
Cavity Fill Time	τ_{fill} (μs)	0.5	0.19
RF Pulse Duration	τ_o (μs)	5	3.19
CW Wall Losses	$\langle P_{wall} \rangle \left(\frac{kW}{m}\right)$	150	166

The lower beam loading fraction and accelerating gradient no longer represent technology extrapolations. The reduced intrinsic Q value can be realized by using copper-nickel alloys.

Accelerator

- Utilize lower required endpoint energy, and reduced emphasis on accelerator mass minimization* to reduce accelerator real-estate gradient.
- Despite the increased accelerator length, the reduced gradient results in significantly lower stored rf energy, which in turn, significantly relaxes the operational requirements on the rf source.

* An estimate which breaks down the system mass component-by-component reveals that the accelerator mass is small relative to the thermal management components. This is quantified in Table 2.5.

Table 2.5. Mass estimates for prime power and burst power conditioning HCRF concept vs. cryocooled accelerator concept.

Assumptions: FEL output power = 10 MW @ $\lambda = 1\ \mu m$
Overall wall plug efficiency = 40% (25 MW input, 45 MW recirculating)

Component	HCRF (metric tons)		Cryogenic Accelerator* (metric tons)
Baseload, prime power, burst power	12		12.5
LH_2, tankage, structure	6.5	1.5 fuel 2.5 cool HCRF 2.5 cool dep. coll.	18
Pulsed power or RF conditioning (drivers & tubes)	6.4		6.6
Accelerator	3.4		1.3
	28.3		38.4

* ACDTI Studies and D. Reed at LANL

The high power microwave source that powers both the accelerator cavities and the buncher furnishes RF energy at a rate sufficient to maintain a 10-GW average beam power for the full 0.5 to 2 microsecond macropulse duration. For 90-95% beam loading, a single source or a group of phase locked sources supplying approximately 11-12 GW for 0.5 to 2 microseconds, coupled into a low loss waveguide network, can power such a beam. The technology choice for these sources are discussed in subsection 2.4.

2.3.1.1 Accelerator Efficiency. To a large extent the overall accelerator efficiency, the ratio of the electron beam energy to the RF energy in each macropulse, determines the overall free electron laser system size, in as much as it determines the required RF power as well as the amount of cooling required for the accelerator. Figure 2.9 shows that the accelerator efficiency is made up of the product of three separate parameters: 1) The transmitted to incident RF power ratio, 2) the beam loading fraction, and 3) the ratio of the duration of the accelerating phase (the total RF pulse width minus the fill time) to the total RF pulse duration. Each of these parameters is briefly discussed in the following.

The plan that has been adopted to fill the cold accelerator with RF energy is shown schematically in Figure 2.10. If the electron beam is turned on at the precise instant that the RF fields have built to their final steady state value with the beam on, then the exponential transients corresponding to the filling of the RF structure and the electron beam loading will precisely cancel and the steady state will be achieved instantaneously. For the overall accelerator efficiency to be high, the microwave source must be matched to the accelerator cavities with the beam on. This efficiency figure can be improved somewhat by overmatching the source and accelerator and thereby increasing the percentage of RF pulse duration available for acceleration at the expense of increased reflected power prior to the electron beam turn on. Figure 2.11 shows that under this scheme a broad maximum in the accelerator efficiency exists around a VSWR equal to ~ 1.2.

The high beam loading fraction (> 95%) is one of the key differentiations between this novel HCRF accelerator and existing accelerator designs. The analysis in Figure 2.12 shows that if a longitudinal shunt impedance of 320 Ω/m can be realized with a beam power of 10 GW, then beam loading fractions exceeding 95% (while filling every RF bucket) are achievable with either aluminum or copper cavities. Additional thermal analyses show that with a gradient as high as 20 MV/m and RF pulse lengths up to 6 μs, the maximum local heat flux never exceeds ~ 2 kW/cm^2, implying that there is no serious heat removal problem. The only open issue

- The conversion efficiency from RF to e-beam power is the product of three factors

$$\eta = \left[\frac{4V}{(1+V)^2}\right] x [\alpha] x \left[1 - \frac{\tau_{fill}}{\tau_o}\right]^* \left(\frac{\text{Coupled Power}}{\text{Source Power}}\right) x \left(\frac{\text{Beam Power}}{\text{Coupled Power}}\right) x \left(\frac{\text{Macropulse Duration}}{\text{rf Pulse Duration}}\right)$$

*(R. H. Miller, "Comparison of Standing-Wave and Traveling-Wave Structures," 1986 Linear Accelerator Conference Proceedings, SLAC-Report-303, p. 200).

$$\tau_{fill} = \tau \, Ln \left\{\frac{2\beta^{1/2} (RLP_{in})^{1/2}}{IRL}\right\}$$

$\tau = Q_o/\pi f (1 + \beta)$
f = frequency
Q_o = implicit Q
V = VSWR with e-beam on
β = VSWR with e-beam off
R = shunt impedance
L = accelerator length
I = macropulse current
P_{in} = coupled power

Figure 2.9. Parametric dependence of RF to E-beam conversion efficiency.

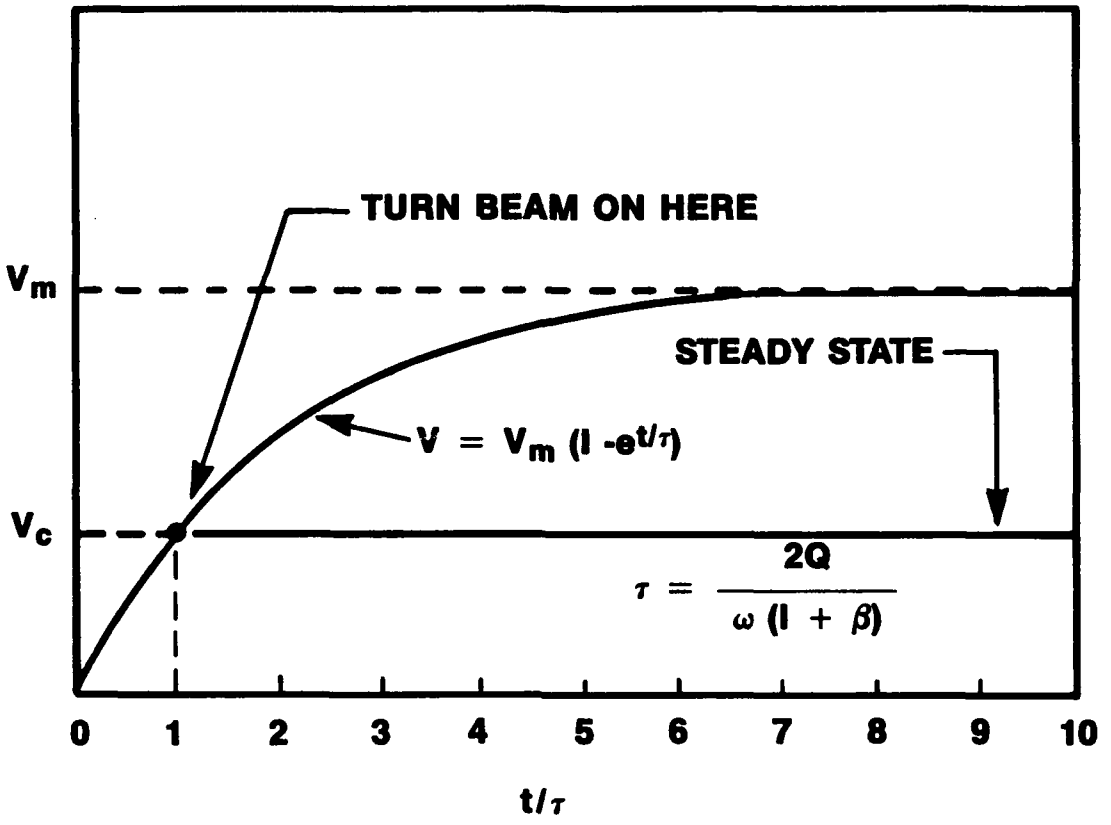

87 06-168

Figure 2.10. Energy transients in standing-wave accelerators.

1.3.1 Variation of (RF → e-beam) efficiency, η, with VSWR (beam on), V, and beam loading fraction, α

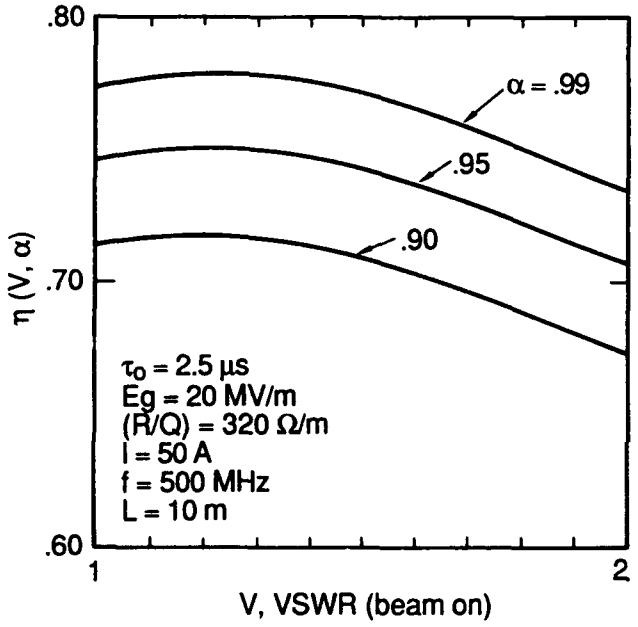

- Broad maximum near V = 1.2
- Two issues:
  - (i) High reflected power during filling time requires:
    - (a) high power isolator, with a
    - (b) high power load
  - (ii) Maximum achievable beam loading fraction limited by cavity material

Figure 2.11. Parameter optimization and trade-offs.

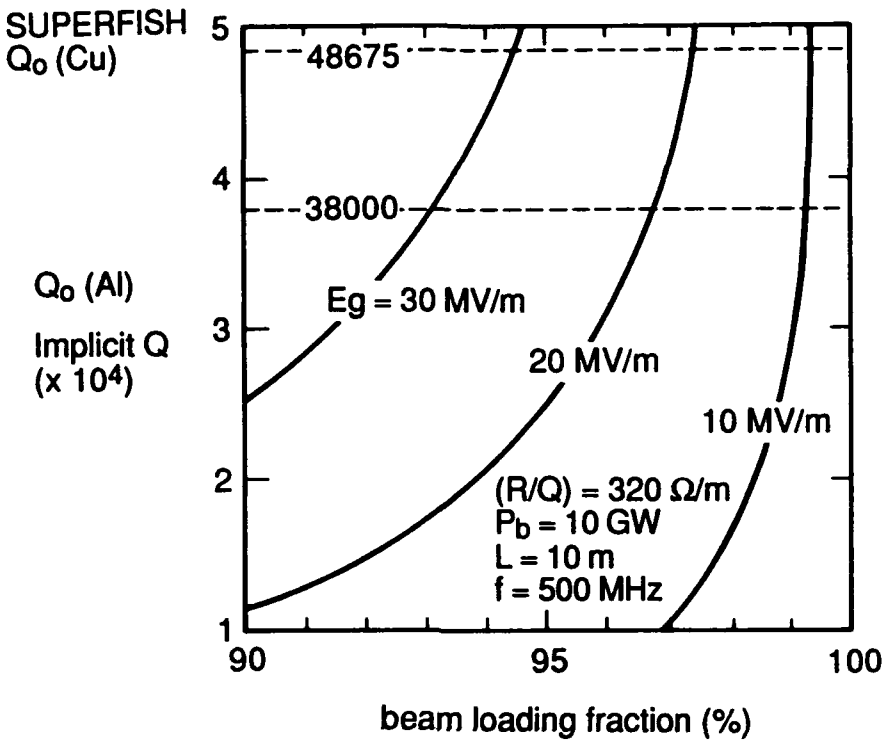

- Must evaluate longitudinal energy spread due to single bunch loading to further assess feasibility of very high beam loading fraction.

Figure 2.12. Beam loading fraction = 95% with (real estate) gradient = 20 MV.m in aluminum cavities is achievable.

89-01-038

associated with a high beam loading is the possibility of introducing longitudinal energy spread in a single microbunch. This is assessed in the next subsection.

The various channels under which RF drive power is partitioned are shown schematically in Figure 2.13. During the 3-μs-long electron beam macropulse, the 200-MeV, 50-A beam extracts 30 kJ of RF energy. Since the beam loading fraction (the ratio of the RF energy coupled into the beam to the RF energy fed into the accelerator) exceeds 95%, the energy lost to heating the cavity walls is < 1.5 kJ. 4 kJ are invested to fill the accelerator to its steady state field level, and this energy is lost when the electron beam macropulse terminates and the accelerator fields decay. Finally, during the transient field time (before the beam is turned on) the accelerator and RF source are mismatched and 1.0 kJ is reflected from the accelerator structure. The overall efficiency is 82%. In order to achieve higher accelerator efficiencies, longer RF drive pulses and longer electron beam macropulses must be used. Schemes to decelerate the beam, exiting the FEL wiggler to recover its energy, have also been investigated.

2.3.1.2 Beam Quality and Stability. The various mechanisms of beam quality degradation have been thoroughly surveyed. They are listed in Figure 2.5. In the following, the two mechanisms that have been identified in a preliminary estimate to cause the greatest energy spreads in the micropulse and the macropulse are briefly discussed.

The FEL can only operate efficiently if the longitudinal energy within a single micropulse is kept < 0.50%. Figure 2.14 shows that there exists an intrisinic spread due to the finite micropulse duration. The electrons in the head of the bunch experience accelerating fields that differ from those in the center of the bunch. This spread is analytically estimated to be 0.31%; this value has been confirmed with more detailed calculations carried out with the SUPERFISH and PARMELA accelerator design codes. This energy spread will probably add in quadrature with other energy spreads due to beam induced wakefields and injector and RF source jitter. However, this total energy spread during the micropulse can be suppressed by factors of 4-6 simply by adjusting the relative timing of the RF phase and the micropulse injection (Figure 2.14). Energy spreading within the micropulse is not considered a limiting factor of HCRF operation.

During the macropulse, the FEL operation can only tolerate energy variations ~ 2%. The beam instability that endangers this constraint is cumulative beam breakup. In a multi-section accelerator, each section acts like an amplifier which provides a small increase in the amplitude of the transverse beam displacement. For a constant gradient, pulsed accelerator without magnetic

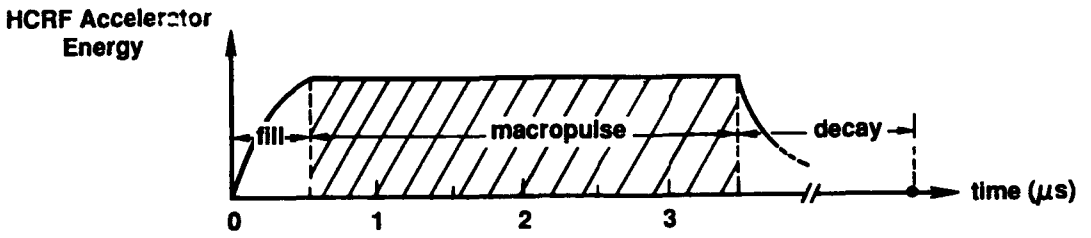

Channels	RF Energy (kJ)
Output e-beam	30
Stored	4
Wall Load	1.5
Fill time mismatch	1.0

$$\text{eff} = \frac{30}{30 + 4 + 1.5 + 1.0} = 82\%$$

Figure 2.13. Schematic of the various channels into which RF energy is partitioned. Higher efficiencies can be obtained by extending the macropulse duration and recovering energy from the FEL wiggler output electron beam.

89-01-057

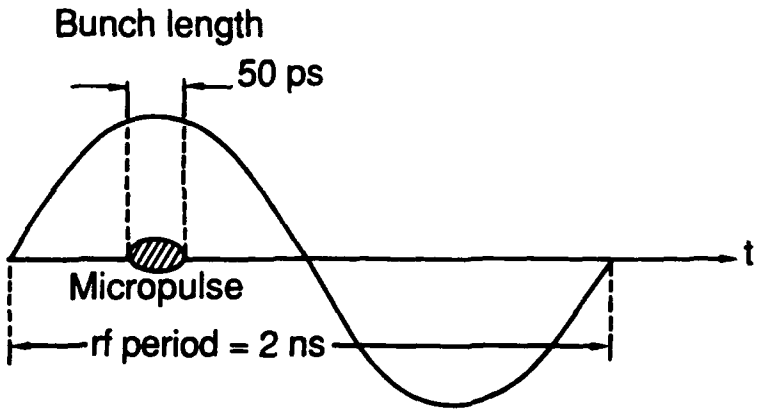

- $\frac{\Delta\gamma}{\gamma} \approx 0.31\%$

- This value consistent with more precise calculation which employs SUPERFISH calculated field structure

- This value also obtained with PARMELA

METHODS TO SUPPRESS BEAM INDUCED SPREADING

- **Balance the variation by moving the bunch ahead of the rf by θ degrees where:**

$$\left(\frac{\Delta\gamma}{\gamma}\right)_{micro} \approx \Delta\theta\tan\theta$$

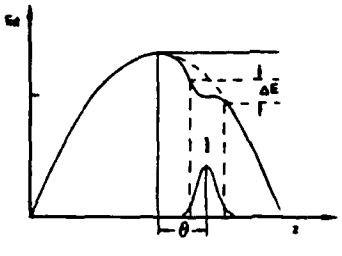

For the point design, $\theta \lesssim 6°$

- **Investigate: "Minimizing the Energy Spread Within a Single Bunch by Shaping its Charge Distribution," (G. Loew and J. Wang, SLAC/AP-25 1984).**

Figure 2.14. The intrinsic longitudinal energy spread in the micropulse is 0.31%. This spread can be suppressed below the FEL constraint by adjusting the relative timing of the RF phase and the micropulse injection.

focussing, the macropulse current which generates 20 e-fold growths over the accelerator length is $I = 30E_g\lambda^2/Lc\tau_p(R/Q)\perp$. Here E_g is the gradient, λ the RF wavelength, L the accelerator length, c the speed of light, and τ_p the macropulse duration. The transverse shunt impedance $(R/Q)\perp$ is estimated (by comparison to similar existing accelerators) to be 200 Ω/m. With the point design parameters, the critical current is I = 120 A. Since the point design macropulse current is only 50 A, this estimation suggests that beam transport through the accelerator is not threatened; however, strong magnetic focussing will probably be required to minimize the beam displacement for efficient FEL operation.

2.3.2 System Analysis Issues and Design Code.

The original HCRF baseline program included a system study to address the overall space based accelerator concept. To aid in that study, PI began to develop a PC based computer code. After the Technical Review Group (see Sections 1.0, 2.1, and Appendix A) recommended shifting HCRF program focus to RF source studies, work on the accelerator system code was discontinued. A significant "shell," however, was completed. All graphics and user interfaces are functional. Should anyone choose to add physics models and calculational subroutines, a very useful code would result. For that reason, this report includes a complete source listing (Appendix B). The following paragraphs briefly describe the code.

In order to make decisions regarding the important dependencies in a system like an HCRF-based FEL, the effect that changes in component performance has on output parameters and observables must be assessed. One way of performing such an assessment is to break the system down into subsystems, each of which can be assigned simple scaling relationships for performance and observables. This type of approach can quickly help to identify technology "bottlenecks," estimate system weight and size, and to assess thermal management requirements. To the extent that simple relationships for the subsystems can be formulated, this approach can work very well.

The HCRF computer program was developed on a IBM compatible PC in Microsoft QuickBASIC, a compiled BASIC language system. This language allows creation of a stand-alone executable file that can be invoked without the QuickBASIC software. A listing of the code as it now stands is in Appendix B.

The code works by defining a 2x11 array for each parameter of the system that can vary in a parametric study. The first 1x11 row contains miscellaneous information about the parameter

(whether it is an input or output, minimum and maximum values, default step size, units, etc.). The second 1x11 row contains the 11 values of this parameter for a scan. There are also parameters, defined as single, which cannot be scanned. These are mostly weight scaling factors for various components and subsystems.

The code can be broken up into three sections—input, calculation, and output. The input section presents the user with two screens. The first screen, present at program startup, allows the user to set up the values of parameters for the study. Twelve parameters are displayed along with their default values. The user can use the up/down cursor keys to select a parameter value to modify. He or she then has the choice of using the left/right cursor keys to increase/decrease the value, using the INS key to enter a new value from the keyboard, or pressing the TAB key to make this the parameter over which a scan of values will take place. When satisfied with the values, the user can press ENTER to proceed with the calculations. Alternatively, the PgDn key brings up a second input screen. On this screen, single-valued parameters are available to be altered if desired. Also, the user can decide on the type of energy recirculation used (rectenna or depressed collector) and the type of display (CGA or EGA). This screen also allows the setup to be saved on or recalled from disk so that different sets of parameters can be analyzed easily.

The calculation section of the code was not completed. Some relationships are in the code to give an idea of how it might work if a set of equations can be developed which describe such a system. These calculations are performed in a FOR/NEXT loop, which is performed either once or eleven times depending on whether a scan or a single point calculation is being done.

After the calculations are done, the output section is entered. If a single point calculation was done, the values of the output parameters are displayed. If a scan was done, the user is asked to select an output parameter to plot against the input parameter over which the scan was done. When this parameter is selected, a plot is produced. While the plot is on the screen, the user can select new scales, select a different output parameter to plot, or go back to the input screen. There is no printing utility in the program; therefore, hardcopy can be generated only by using screen dumps.

In summary, a QuickBASIC code has been developed that has the proper structure to analyze any system that can be defined by a set of input parameters, a set of output parameters, and a set of equations that transform the former into the latter. The code is reasonably flexible and friendly and can be expanded to fit the parameter space of the problem under study. The physics

models and scaling calculation code is not complete but could be added to the code's basic shell later.

2.4 NOVEL HIGH EFFICIENCY RF SOURCE CONCEPTS.

After the Technical Review Panel recommended that the HCRF program focus on RF sources instead of accelerator issues (see Sections 1.0, 2.1, and Appendix A), several steps were taken. First, a survey of existing high power sources was made to determine which ones held the most promise for HCRF. Table 2.6 compares state of the art performance for two of the most promising sources identified to brassboard demonstrator requirements. The brassboard requirements were derived from the basic HCRF accelerator conceptual design described in the preceding section.

The required peak and average power, repetition rate, pulse length and electron conversion efficiency shown in Table 2.6 all exceed the existing state of the art. Since HCRF program funding did not allow developing a source that could satisfy all requirements simultaneously, a decision was made to focus on the most critical requirement, electronic conversion efficiency. A 90 percent conversion efficiency is necessary to meet the overall efficiency goals of HCRF. The other RF source development needs (increasing pulse length, average power, etc) were considered to be somewhat lower risk. Efficiency was judged most important because it could be a show stopper.

The next step taken was to analyze a high efficiency PI concept introduced during the Technical Program Review of January 12, 1989. The concept (Figure 2.15) uses multiple series RF sources to increase overall efficiency. Efficiency is increased by extracting RF energy from the electron beam more than once. Efficiency improves as more series sources are added. Figure 2.15 illustrates the concept.

Figure 2.15 shows the PI source concept using series relativistic klystron amplifiers (RKA). An electron beam generated by a linear induction accelerator is injected into the first relativistic klystron (RK1). RF energy produced in RK1 is then extracted. The depleted electron beam energy from RK1 is replaced by a beam energy replacement (BER) stage immediately downstream of RK1 with the emerging beam then used to drive the second relativistic klystron (RK2). This energy refurbishing/extraction cycle is repeated to achieve high system efficiency.

Table 2.6. Demonstrated HPM Source Operation.

	Brassboard Demonstrator Requirement	Relativistic Klystron		Relativistic Magnetron		
		Circa 1988	Circa 1992(2)	Circa 1988(3)	Circa 1992(4)	
Frequency (GHz)	0.5	1.3	1.3	2.8	1.1	1.1
Peak Power Capacity (GW)	10	0.5	.5	3.6	1.0	0.6
Electronic Efficiency (%)	90	40	--	30	30	--
Phase Stability (%)	2	2	--	2	--	--
Amplitude Stability (%)	1	2	(Triangular pulse)	(Triangular pulse)	(Triangular pulse)	(Triangular pulse)
Pulse Duration (ns)	3500	140	160	30	50	50
Repetition Rate (kHz)	3.3	--	--	--	0.1	1.0
Lifetime (no. shots)	5×10^6	--	--	--	$> 10^3$	--

(1) M. Friedman, J. Krall, Y.Y. Lau, and V. Serlin, "Externally Modulated Intense Relativistic Electron Beams," J. Appl. Phys. 64, 3353 (1988).

(2) M. Friedman, V. Serlin, Y.Y. Lau and J. Krall, "Relativistic Klystron Amplifier I - High Power Operation," in Intense Microwave Particle Beams, Vol. 1407, p. 2, 1991.

Experiments are also on-going at PI for repetitive RKA. The design goal is 1 GW peak power at 250 Hz. For progress status, please refer to the following paper:

N. Aiello, J. Benford, N. Cooksey, B. Harteneck, J. Levine, D. Price, R. Smith, D. Sprehn and M. Willey, "High Power Microwave Generation at High Repetition Rates," Pro. 9th Int. Conf. on High-Power Particle Beams (Washington, DC), 1992.

(3) H. Sze, B. Harteneck, J. Benford, T.S.T. Young, "Operating Characteristics of a Relativistic Magnetron with a Washer Cathode," IEEE Trans. Plasma Sci. Vol. PS-15, 327 (1987).

(4) S. Ashby, R.R. Smith, N. Aiello, J.N. Benford, N. Cooksey, D.V. Drury, B.D. Harteneck. J.S. Levine, P. Sincerny, L. Thompson and L. Schlitt, "High Peak and Average Power with an L-Band Relativistic Magnetron on CLIA," IEEE Trans. Plasma Sci., Vol. 20 p. 344, 1992.

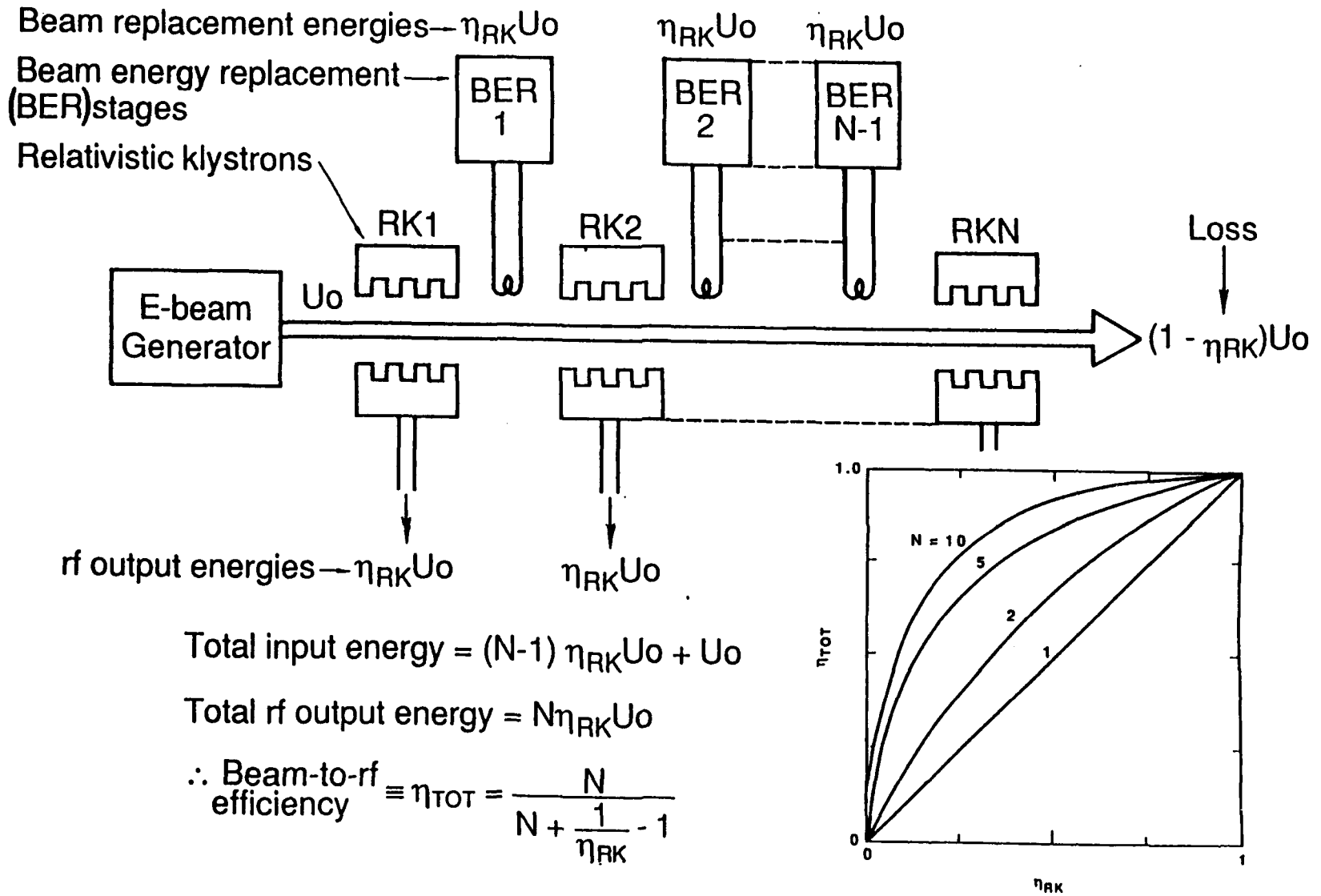

Figure 2.15. A series RF source concept.

A major conclusion drawn from studying the PI series RF source concept was that key critical issues could be addressed economically with existing facilities if funding were to be made available in the future. Since SDIO budget realities meant that at least a hiatus would occur after work on the the current funding increment ended, ONR directed PI to execute a design study for an experiment that could be conducted later. That approach would place the HCRF program in a holding mode with a promising experiment "on the shelf". This design study was completed as the final technical task for the program. Appendix D is a full description of the selected experiment. which addresses the critical issue of electron beam energy replacement. The remaining paragraphs in this section briefly review the reasoning that led to this choice.

An experiment on beam energy replacement was selected as the first step in proving the series source concept for achieving high efficiency electronic conversion to RF because of the importance of assessing beam quality in downstream sources. The series RF source concept requires that the electron beam be re-accelerated each time one of the sources extracts energy from it. Recent experiments in re-acceleration (References 4, 5, and 6) indicate that such a scheme holds promise. Since re-acceleration can excite transverse instabilities and induce transverse emittance growth, more experiments are needed to quantify how the electron beam quality changes as it propagates down the structure. Such experiments can also provide a means to study source-to-source phase coherency between the klystrons, a critical issue for driving RF accelerator cavities.

Another reason for choosing a re-acceleration experiment was the possibility that existing facilities might be used to reduce costs. The Compact Linear Induction Accelerator (CLIA) designed and built by PI and operated as a facility at the company's San Leandro, California headquarters (Reference 1) could provide the required electron beam if certain modifications or additions were made.

Figure 2.16 shows the CLIA accelerator, which delivers a 750-kV, 10-kA, 60-ns, 200-Hz electron beam. CLIA has successfully served as a driver to generate high current RF power. An L-band magnetron on CLIA has produced 1 GW peak RF power, and 4 kW average power at 100 Hz (Reference 2). In addition, CLIA has driven a repetitive L-band relativistic klystron amplifier experiment under another SDIO contract. The RKA on CLIA has produced an electron beam of 500 kV, 5 kA with a 50% modulation at 1.32 GHz (Reference 3).

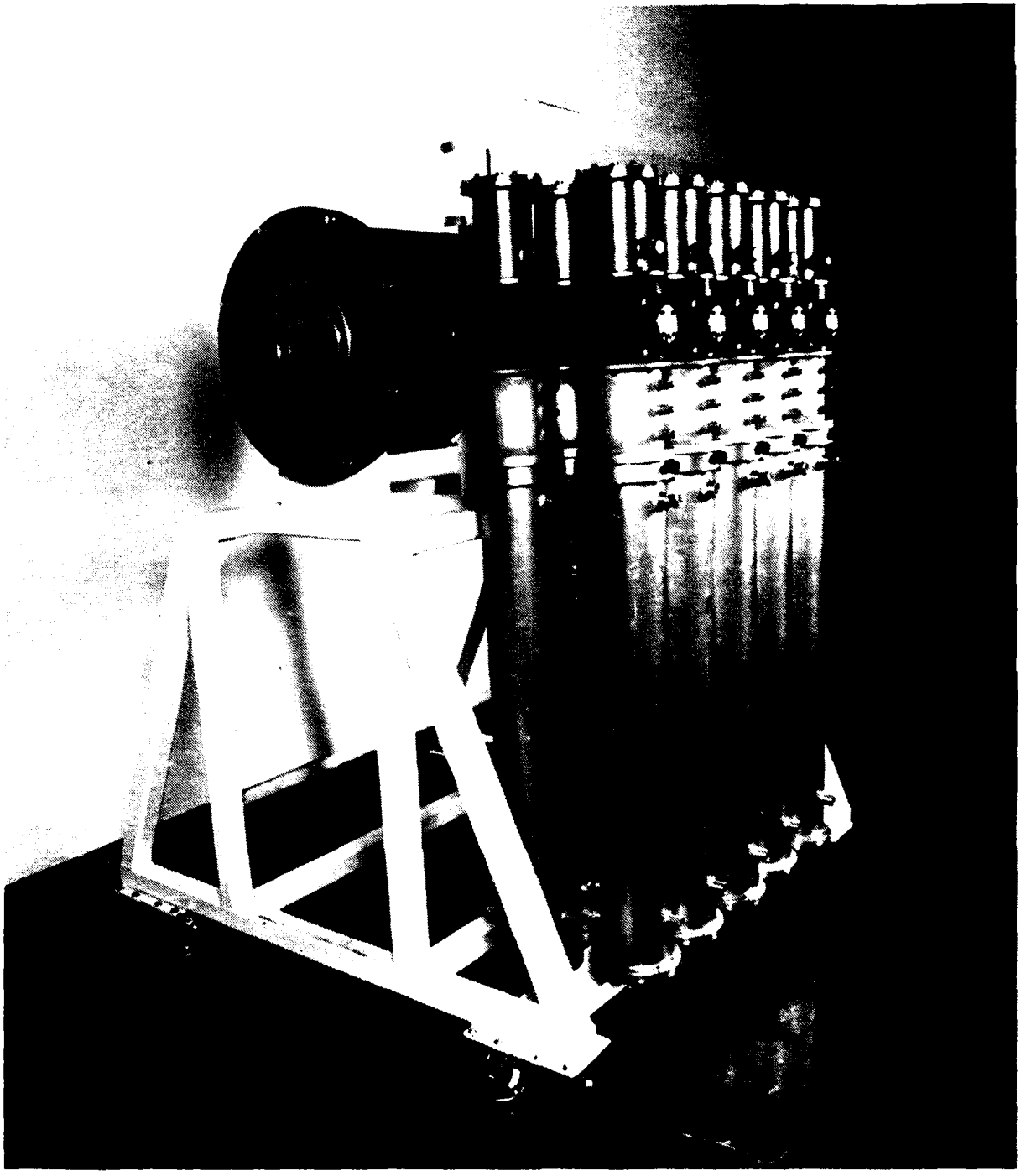

Figure 2.16. The CLIA accelerator and its PFL's.

In summary, the final technical task of the HCRF program was to execute a conceptual design for an experiment to study the critical issues of using a re-accelerated electron beam for efficiently producing RF energy from series relativistic klystrons. The details of the design study are in Appendix D. For economy, the design effort was constrained to use existing hardware wherever possible. The final conclusion of the effort was that some new accelerator hardware would be required to make the experiment viable. The details that led to this conclusion are in the appendix.

1. S. Ashby, D. V. Drury, P. Sincerny, L. Thompson, and L. Schlitt, "CLIA - A Compact Linear Induction Accelerator System", in Pro. 9th Int. Conf. on High-Power Particle Beams (Washington, DC), 1992.

2. S. Ashby, R. R. Smith, N. Aiello, J. N. Benford, N. Cooksey, D. V. Drury, B. D. Harteneck, J. S. Levine, P. Sincerny, L. Thompson, and L. Schlitt, "High Peak and Average Power with an L-Band Relativistic Magnetron on CLIA", IEEE Trans. Plasma Sci., Vol. 20, p. 344, 1992.

3. J. S. Levine, N. J. Cooksey, B. D. Harteneck, S. R. Pomeroy, and M. J. Willey, "Design and Initial Operation of a Repetitively-Pulsed High-Current Relativistic Klystron", in Intense Microwave Particle Beams, Vol. 1629, p. 22, 1992.

4. R. B. Miller, W. F. McCullough, K. T. Lancaster, and C. A. Muechlenweg, "Super-reltron Theory and Experiments", IEEE Trans. Plasma Sci., Vol. 20, p. 332, 1992.

5. T. L. Houck, D. Rogers, R. D. Ryne, G. A. Westenskow, "Relativistic Klystron Research for Future Linear Colliders", in Intense Microwave Particle Beams, Vol. 1629, p. 481, 1992.

6. T. L. Houck and G. A. Westenskow, "Status of the Choppertron Experiments", in Pro. 16th Int. LINAC Conference, Ottawa, Ontario, Canada, 1992.

SECTION 3

IMPULSE RADAR EXPERIMENTS

3.1 INTRODUCTION.

The HCRF contract statement of work instructed PI to apply HCRF related technologies to problems of interest to SDIO or the Navy, at the direction of the contract technical monitor, to the extent that such work could be accommodated within available funding. The work described in this section fits into this "spin-off" category. The HCRF technology used was the expertise PI possesses in generating high power RF radiation. The problem of interest to the Navy was that of detecting supersonic sea-skimming missiles. To solve that problem, the Navy is investigating the use of ultra-wideband (UWB) radar. In a joint effort in which the Office of Naval Technology and the Naval Ocean System Center provided funds to the Office of Naval Research through the HCRF program, PI participated in an experiment to measure sea echoes from high power electromagnetic impulses, data that is important to UWB radar. The effort was jointly managed by Dr. Vern Smiley, the HCRF technical monitor and Dr. Vince Pusateri of the Naval Ocean System Center. This section describes the results of that effort.

Recent interest in ultra-wideband (UWB) radar systems and their possible application to ship defense against low-altitude missiles (sea skimmers) has led to the realization that very little data are available in the literature on ocean backscatter from UWB systems (References 1 and 2). Of particular interest is the region from 400 MHz down to the resonant frequencies of possible sea-skimming targets (around 60 MHz). The effort described in this section supports a Naval Ocean Systems Center (NOSC) program to provide measurements from 200 to 1000 MHz on ocean backscatter and on the visibility of certain specific targets in the presence of the radar clutter from the ocean.

3.2 OBJECTIVES.

The overall goal of this effort is to characterize the sea echo environment in which a working impulse radar* must operate to satisfy the Navy anti-ship missile defense requirement. Specific objectives are:

1. Develop an antenna feed geometry that allows a 30-ft parabolic reflector to transmit an ultrawideband radar pulse at an effective radiated power of greater than 5 GW.

2. Demonstrate the ability to receive and characterize sea echoes produced by ultrawideband signals radiated by the antenna configuration described in objective 1.

3. Collect sufficient data in a real environment to characterize sea clutter for a variety of sea states.

3.3 APPROACH.

PI followed the programmatic approach outlined below:

1. Use existing contractor-supplied equipment for the transmitter and receiver subsystems to minimize cost and to maximize data recovery.

2. Use existing government equipment for the same reasons.

3. Develop remaining components early in the program and conduct low power validation tests to minimize time in the field.

4. Conduct full-scale experiments at a NOSC site at Point Loma in San Diego, California.

The program was executed in two phases:

Phase 1 covered the construction and testing of the transmitter assembly, and completion of the overall UWB radar design.

Phase 2 covers the construction of the radar system, deployment at Point Loma, and acquisition and analysis of the set of sea-clutter data necessary to evaluate the UWB radar.

---

* Impulse radar is a particular type of ultra-wideband (UWB) radar in which UWB signals are generated from short duration (of order 1 ns) impulses.

3.4 RESULTS.

3.4.1 Overview.

PI successfully completed the phase 1 and 2 tasks. Phase 1 of the program started in July 1990. PI issued a subcontract to SRI International to provide expertise in impulse antenna systems, field test ranges, and data acquisition systems. PI first performed a system study on the sea clutter UWB radar, selected a broadband antenna feed design, and carried out laboratory tests at PI and field tests at SRI to finalize the feed geometry. In addition, PI fabricated and tested the high-power hardware in preparation for the NOSC field measurements in phase 2. Work on phase 2 began in April 1991. Under NOSC's direction, PI collaborated with SRI to measure UWB radar sea clutter at the NOSC site on Point Loma, San Diego, California. PI first prepared the transmitter for the field test. In July 1991, PI installed the transmitter and its antenna feed-horn for the 30 ft. dish installed by NOSC personnel on Point Loma. After checking out the transmitter equipment, PI operated the transmitter for NOSC during all UWB radar sea clutter measurements.

The impulse radar system was located adjacent to Building 593 at the Point Loma NOSC site. The facility is about 400 feet above the sea level, and has an unobstructed view of the ocean to the west. Figure 3.1 illustrates the setup for the ultrawideband radar measurements. PI's ultrawideband high-power source excites a wideband feedhorn for a 30-ft dish antenna. The target is illuminated by a direct path and by the forward scattered signal. Signals return to the radar by the direct path and by the scattering path. Clutter signals also return from the clutter path to the receiving antenna. A separate receiving antenna, consisting of a 30-ft parabolic dish and a wideband horn, was used to provide isolation from the high-power transmitter. The transmitting and receiving antennas are very similar in design, differing only in the higher power-handling capability needed for the transmitter. Figure 3.2 is a detailed system block diagram for the UWB radar facility. The receiver and data acquisition system were designed and supplied by SRI International. A brief account of those radar components is given in Appendix C.

UWB radar signatures of a calibration sphere, sea clutter, corner reflectors, a helicopter, boats and ships (Reference 3) were recorded. Figure 3.3 is the unprocessed radar return from a 44-inch sphere hung from a helicopter. The radio frequency interference (RFI) at the test site was found to be rather strong; NOSC later successfully developed practical RFI canceling techniques to process target signatures and some sea clutter data even for the relatively calm sea states in July and August 1991. The advantage of the RFI canceling techniques is clearly shown in the comparison

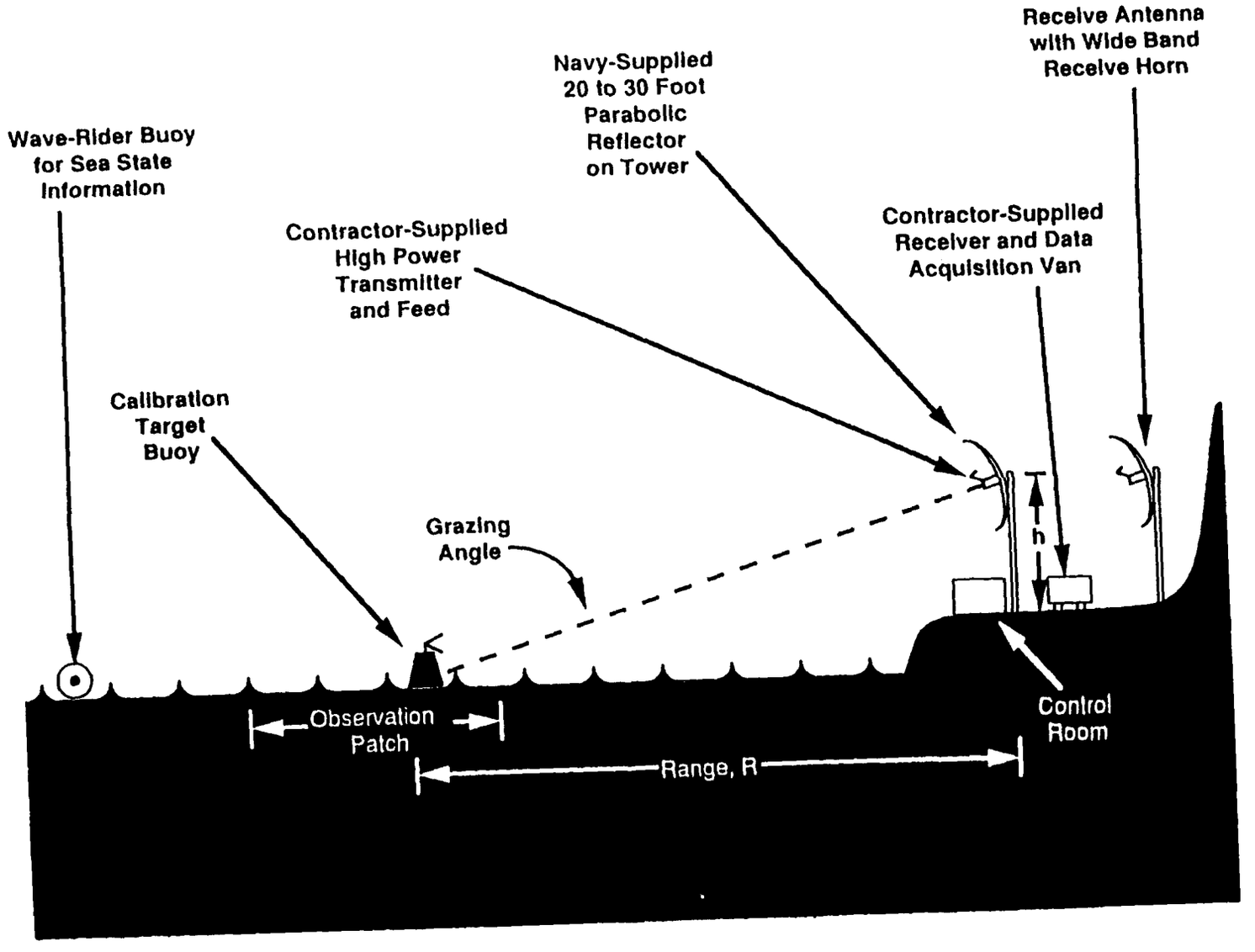

Figure 3.1. The basic setup for impulse radar sea-clutter measurement.

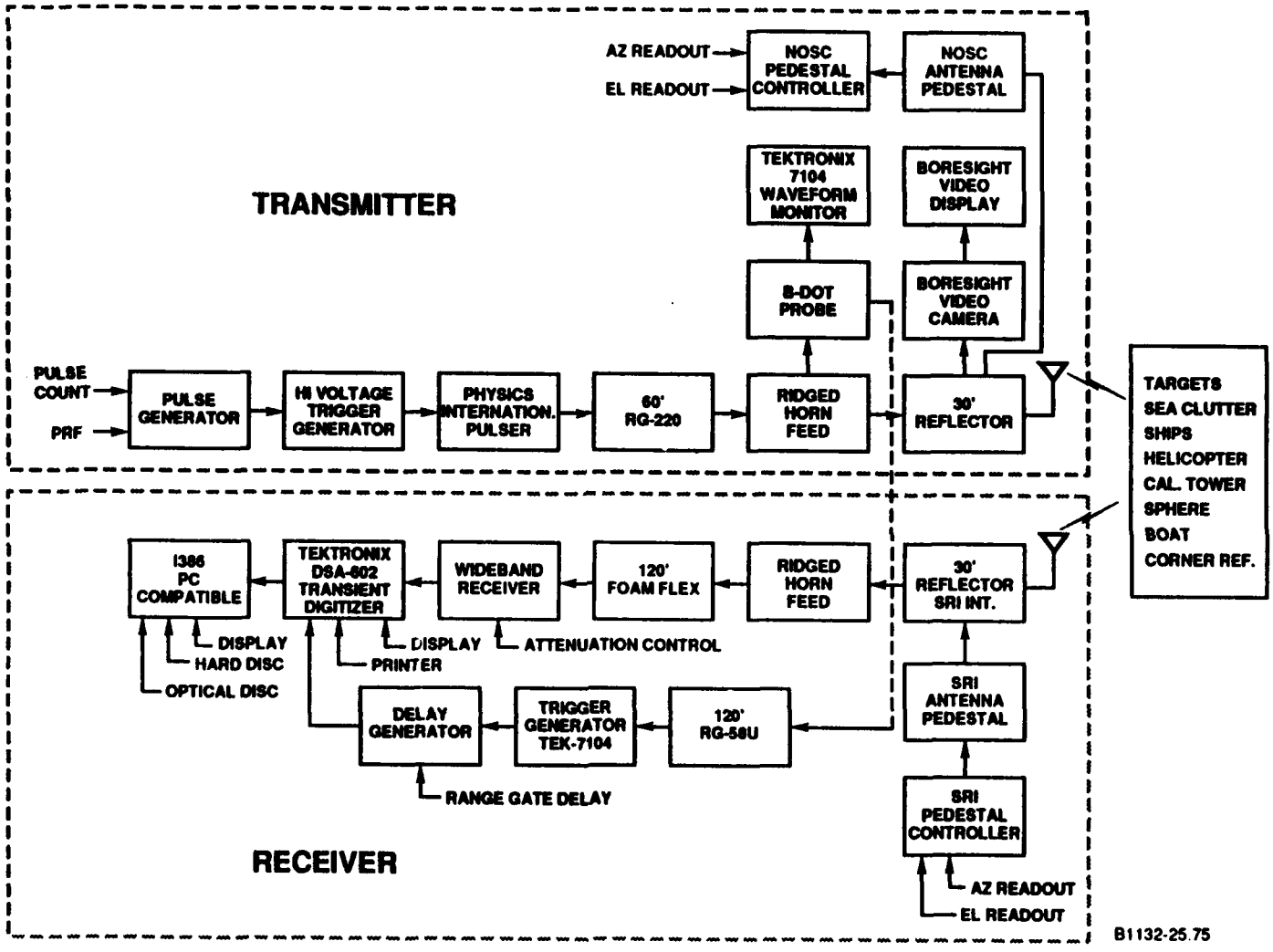

Figure 3.2. The system block diagram for the NOSC ultra-wideband radar facility.

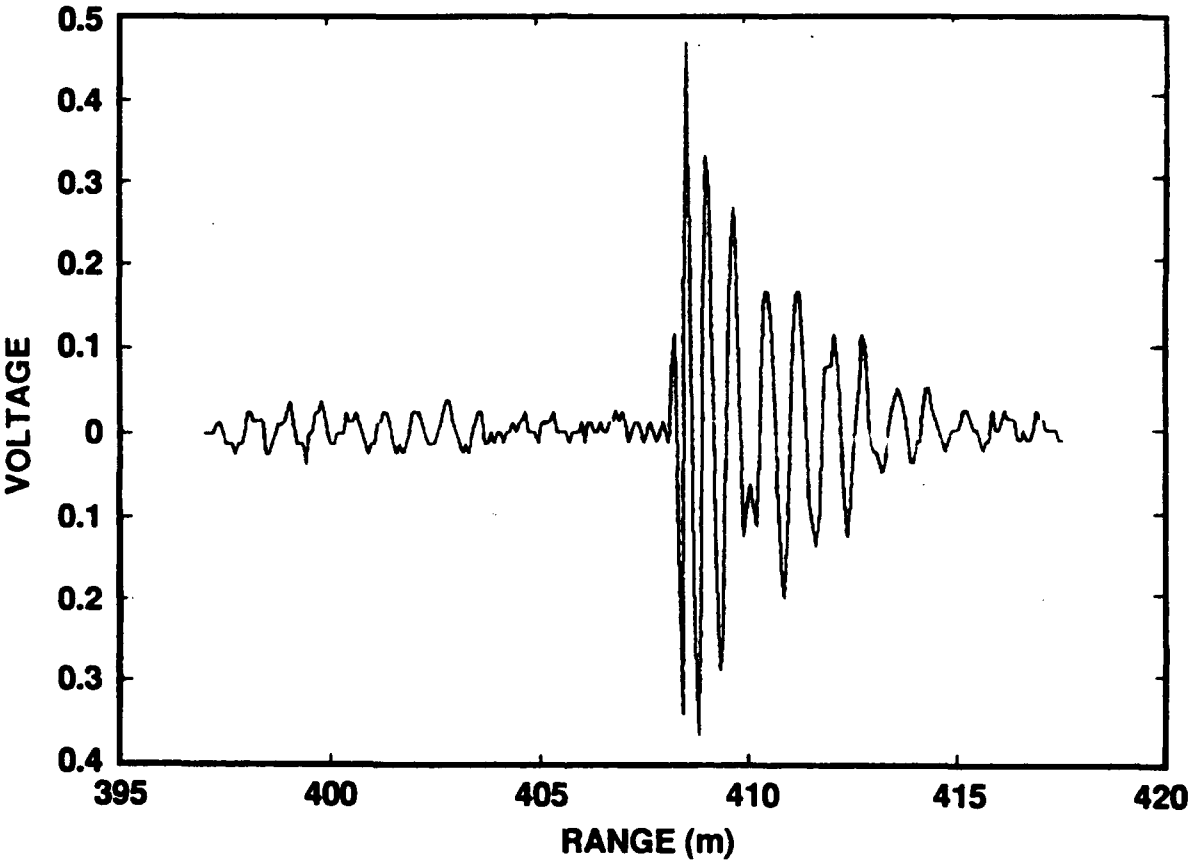

Figure 3.3. An unprocessed impulse radar return from a 44-inch sphere hung from a helicopter.

of the unprocessed and processed signatures of the boat and corner reflector, given in Figures 3.4 and 3.5, respectively.

The rest of this section describes the UWB source, the antennas, and the beam profile obtained with a low-power source which yielded a waveform very similar to the output waveform of the high-power source.

3.4.2 Ultrawideband Radar Source.

PI provided the RF source for the ultra-wideband transmitter used in this effort. The source was developed with PI internal funds for other purposes but fortuitously was an ideal impulse generator for the sea clutter experiments. PI loaned the equipment to the government free of charge except for the work required to adapt it for the experiment. The output characteristics of the PI wideband impulse source are summarized in Table 3.1.

Table 3.1. PI Source Output Characteristics Into A 50-Ω Cable.

Peak Transmitted Power	200 MW
Pulse Shape	1 ns impulse
Energy Per Pulse	200 millijoules
Pulse Repetition Frequency	single-shot or burst mode operation up to 80 pps.

The source output is routed to a double-ridged horn of 50-Ω input impedance, via a 50-Ω coaxial cable. This feed horn is used to illuminate a parabolic reflector. The source can be operated in burst mode up to a couple of minutes from single-shot to 80 pulses per second to facilitate data acquisition.

Figure 3.6 is a picture of the wideband source-feed system that was used in the NOSC sea clutter measurements. The high voltage power supply, the trigger generator, and the pressurized air and oil subsystems are available commercially. Figure 3.7 is a close-up picture of the pulsed-power driver (a Marx generator) with the impulse source. Figures 3.8 and 3.9 show, respectively, the typical output waveform and Fourier spectrum of the voltage pulse injected into a 50-Ω cable. The antenna feed is shown in Figure 3.10, and will be separately discussed later.

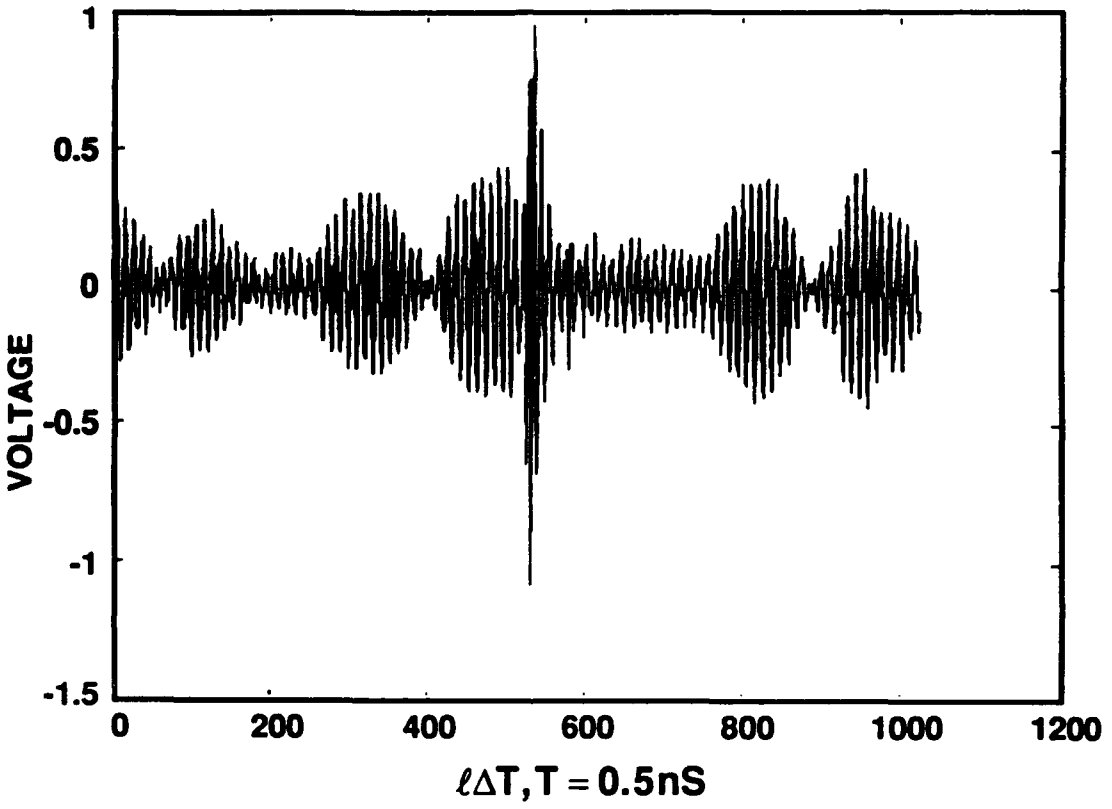

Figure 3.4. An unprocessed impulse radar return from a corner reflector on a boat.

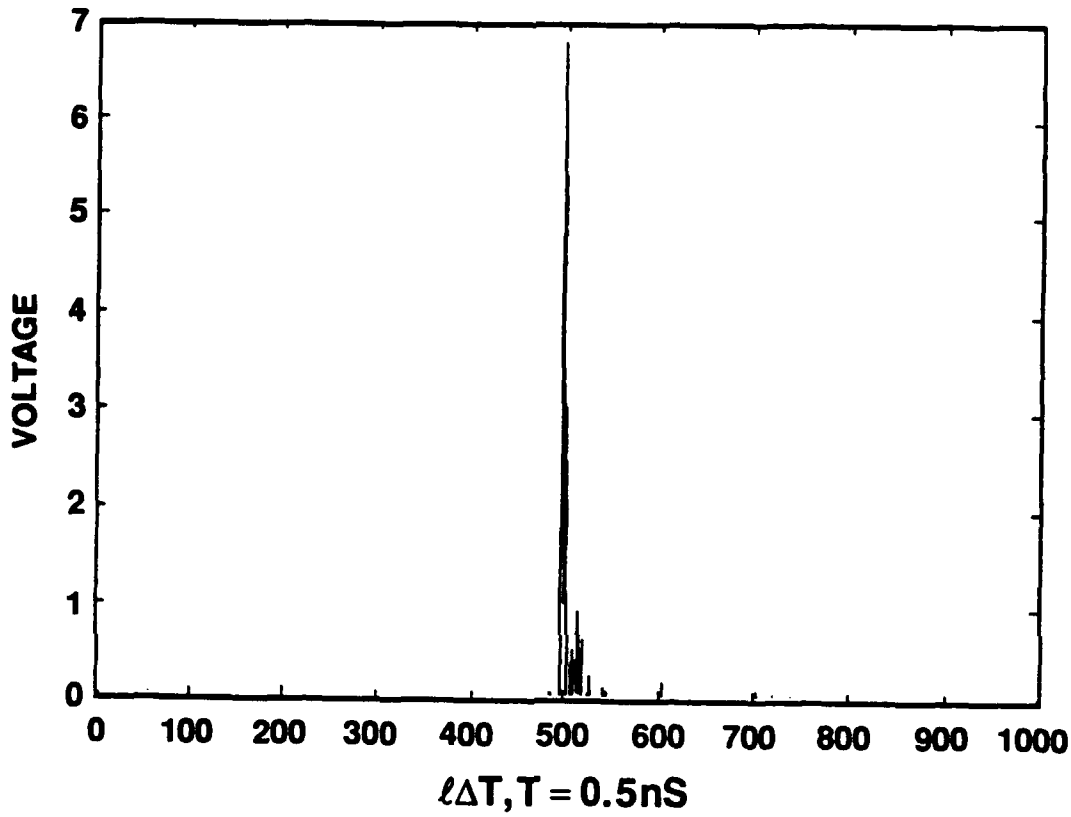

Figure 3.5. **The radar return of Figure 3.2, obtained by differential processing.**

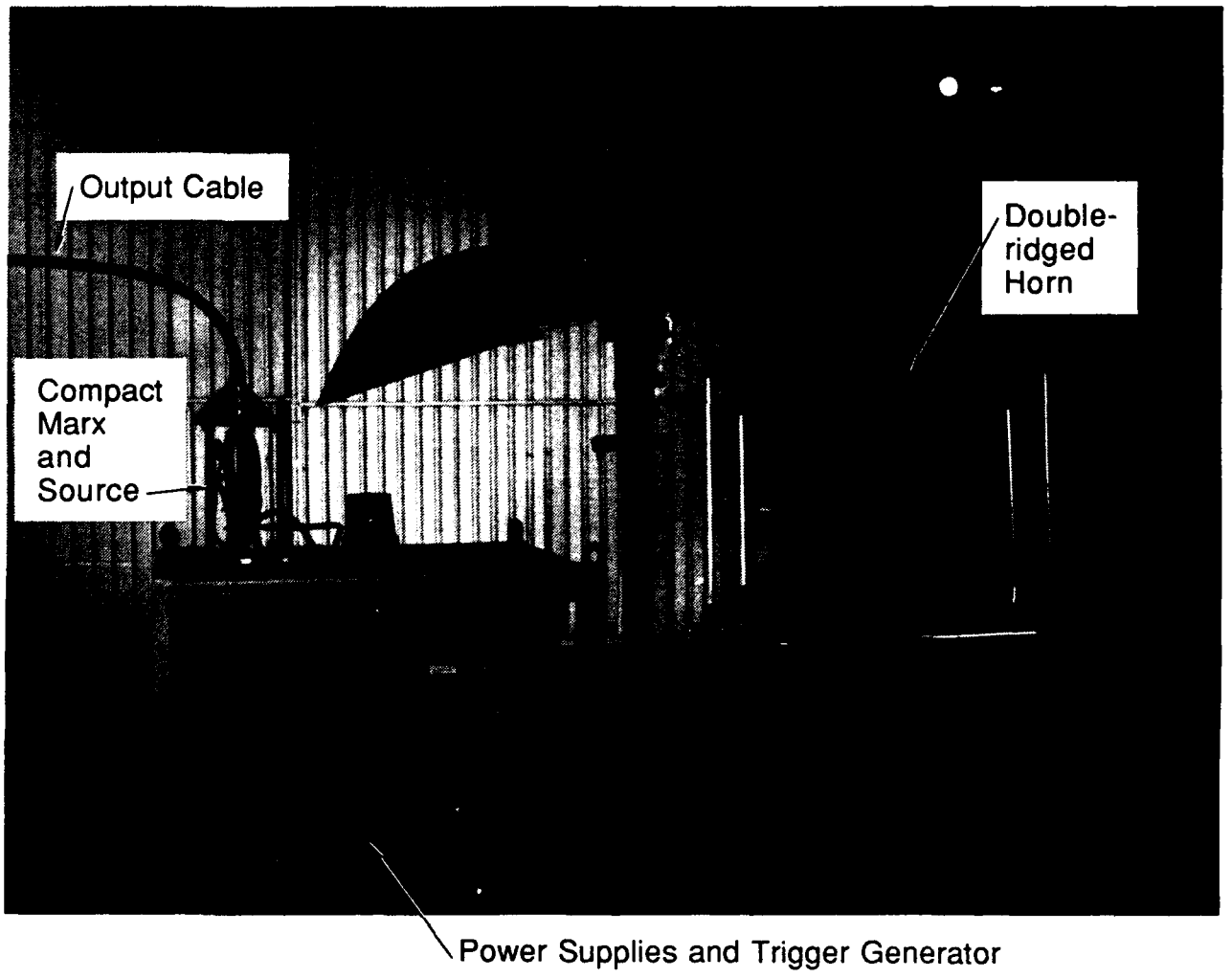

Figure 3.6. The compact UWB source-feed system used in the NOSC sea clutter measurement. Note that only the front feed horn was used for this experiment.

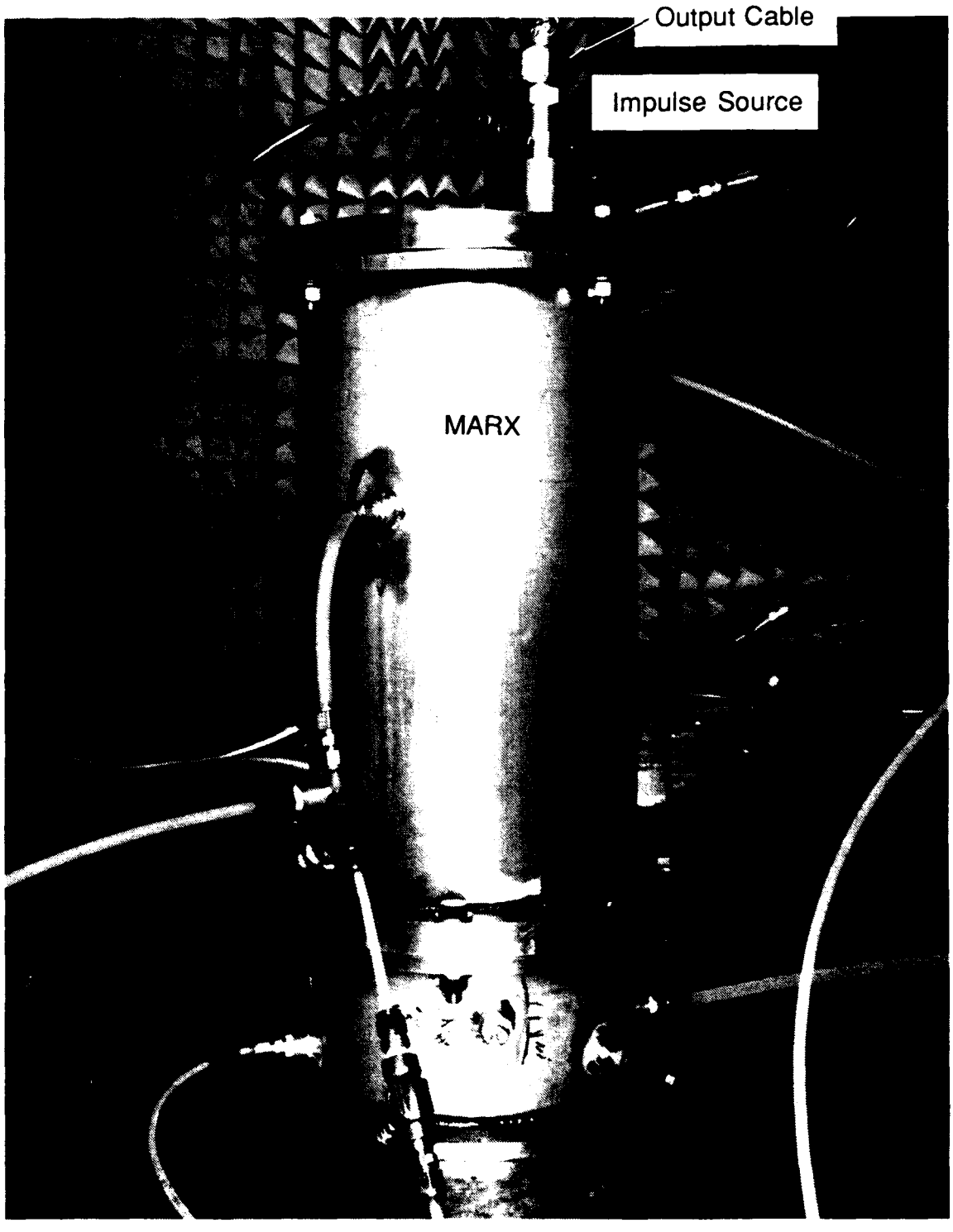

Figure 3.7. The impulse source with its pulsed power driver.

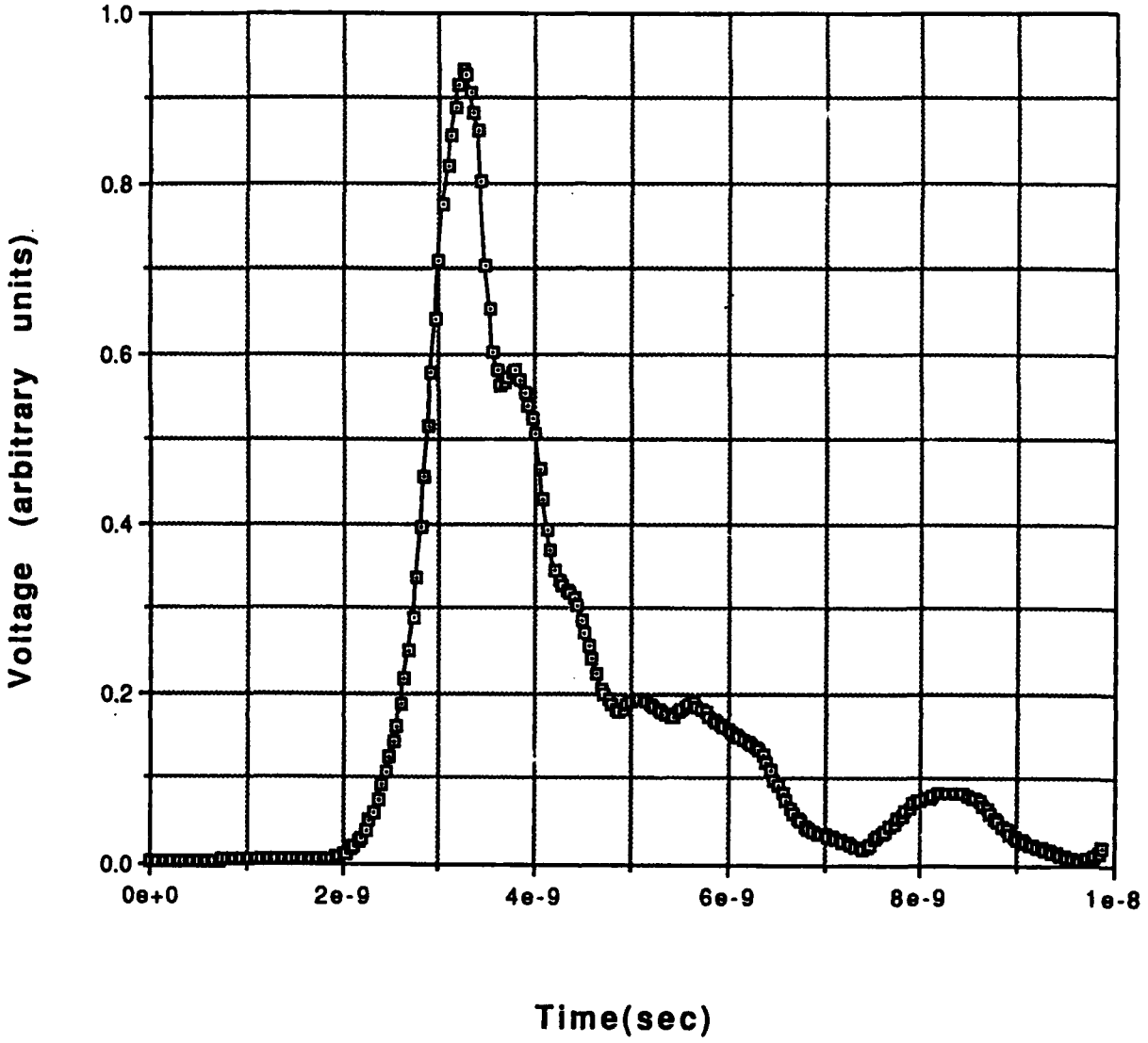

Figure 3.8. Voltage impulse waveform from the source into a 50-Ω coaxial cable.

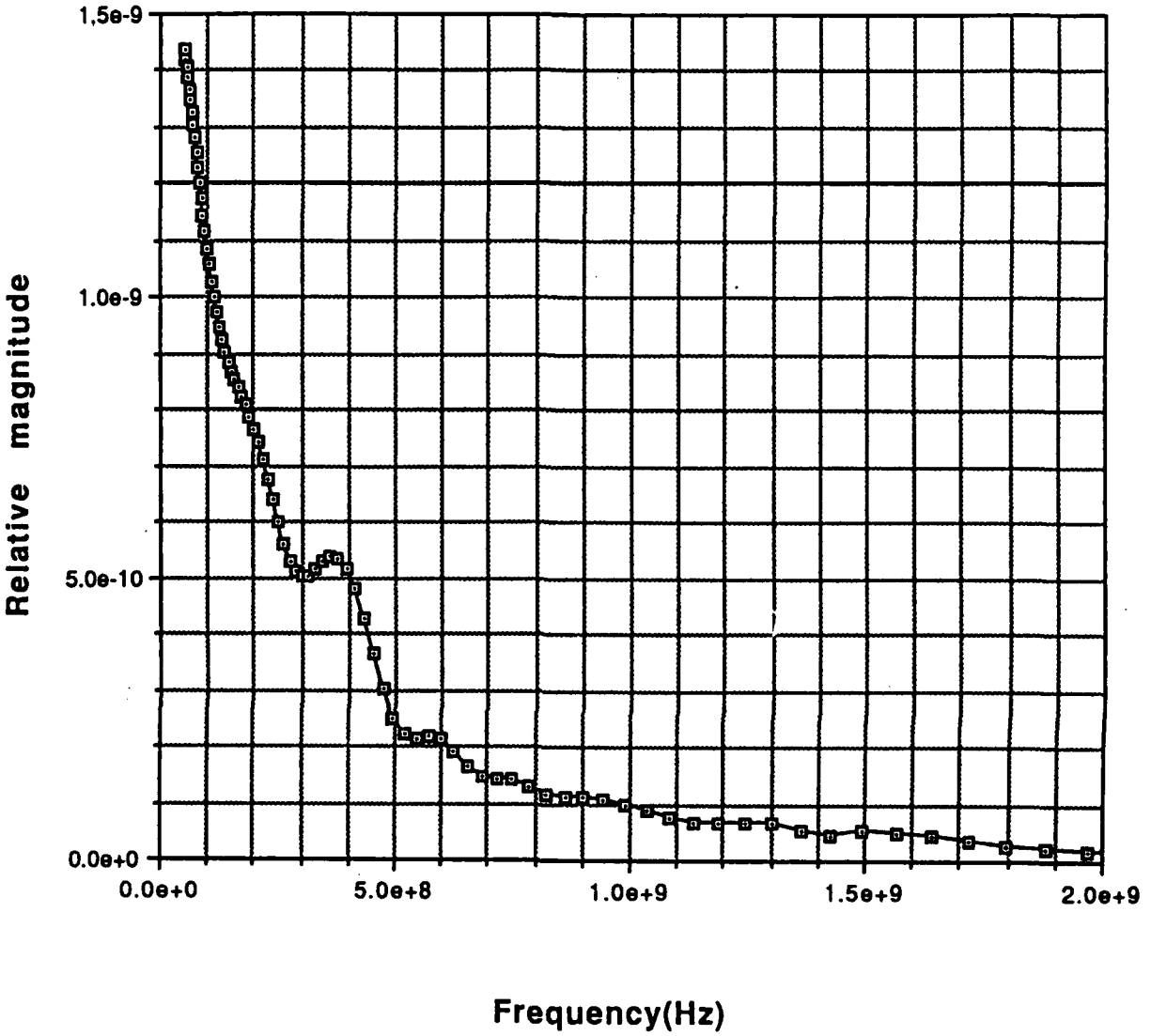

Figure 3.9. Fourier spectrum of the voltage impulse of Figure 3.8.

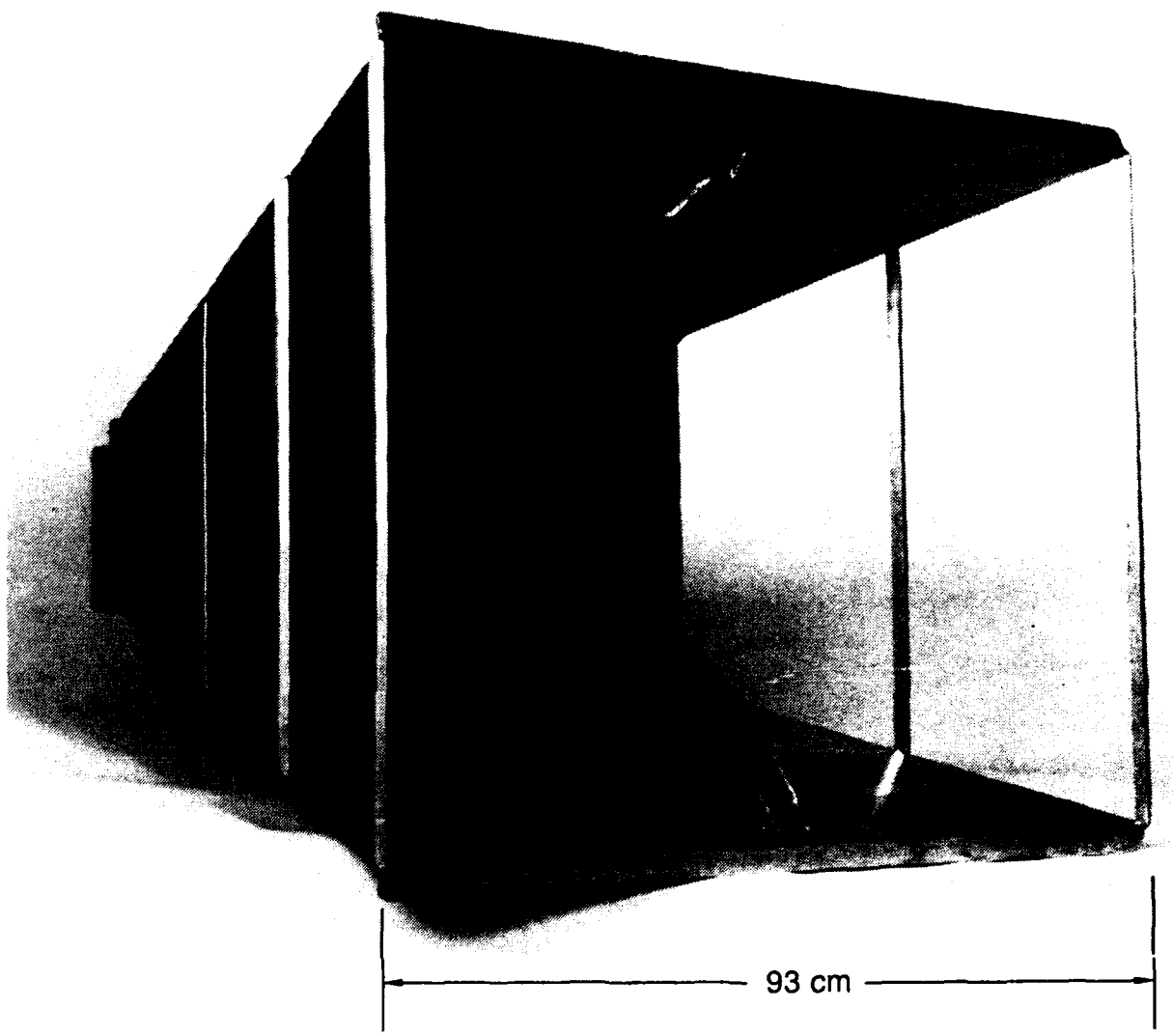

Figure 3.10. The antenna feed is a wideband double-ridged horn.

The PI source generates a fast-rise impulse of about 1 ns FWHM. The impulse source extracts energy from a short pulse forming transmission line into an output cable that leads to the antenna feed. An electrical schematic diagram of the circuit is shown in Figure 3.11. The pulse forming line (PFL) is initially charged by a separate high-voltage driver circuit. When the switch closes, the PFL discharges via the fast closing switch into the output cable. Oil insulation is used for the PFL and the switch. Transformer oil is filtered and circulated during operation of the source by the pressurized oil system.

The pulsed-power driver supplies high voltage to the impulse source. We use pulse-charging to transfer high voltage from the driver to the source. The driver for the source is a compact 10-stage Marx generator system that operates reliably up to 80 Hz. The Marx capacitors are initially charged in parallel up to a dc voltage of 25 kV. When triggered, the spark gaps fire, causing the 10 capacitors to discharge in series into the impulse source. The Marx generator is housed in a sealed metal enclosure about 1 foot in diameter and 2.5 feet tall (Figure 3.7). The dc high-voltage power supply is a 30-kV, 3-kW rack-mount unit made by ALE Systems. The Marx generator is triggered by a Pulspak 10A, a rack-mount unit made by PI. Spark gaps in the Marx generator are insulated by filtered compressed air. Other high voltage Marx generator components are insulated by sulfur hexafluoride gas (SF_6). In general, no replacement of the SF_6 gas is needed during driver operation. After the interior of the Marx housing is exposed to atmosphere, the housing is flushed and filled with SF_6 gas.

3.4.3 Antennas and Beam Profile.

The transmitting antenna was designed to produce a small beam width (and consequently high gain) with little overall distortion in the frequency range of 200 MHz to 1000 MHz. One reason the double-ridged horn (Reference 4) was chosen is because it has suitable E and H field patterns for illuminating a parabolic reflector. The field patterns for the horn at 0.2 and 1.0 GHz are reproduced in Figure 3.12. In order to produce a UWB beam of constant width over all the passband, the reflector must be under-illuminated at the high frequency end and fully illuminated at the low frequency end, so that wavelength-to-diameter ratio stays constant. The focus-to-diameter ratio of the 30-ft transmitting dish was 0.35, which gives a subtended angle at the feed of approximately 110 degrees. At this angle, the pattern of the feed tapers down to -5 dB at 200 MHz, which provides a nicely tailored pattern with minimal sidelobes.

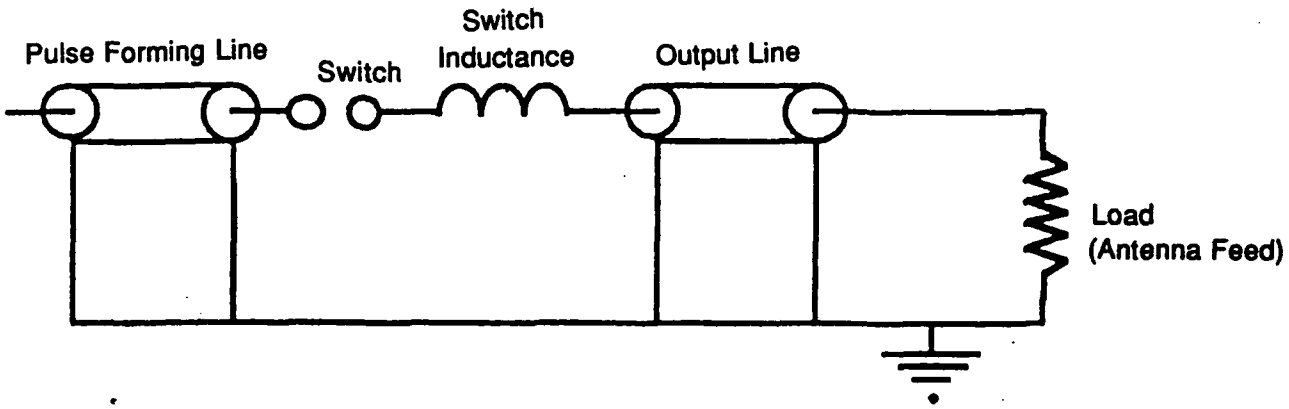

Figure 3.11. Electrical schematic of the impulse source.

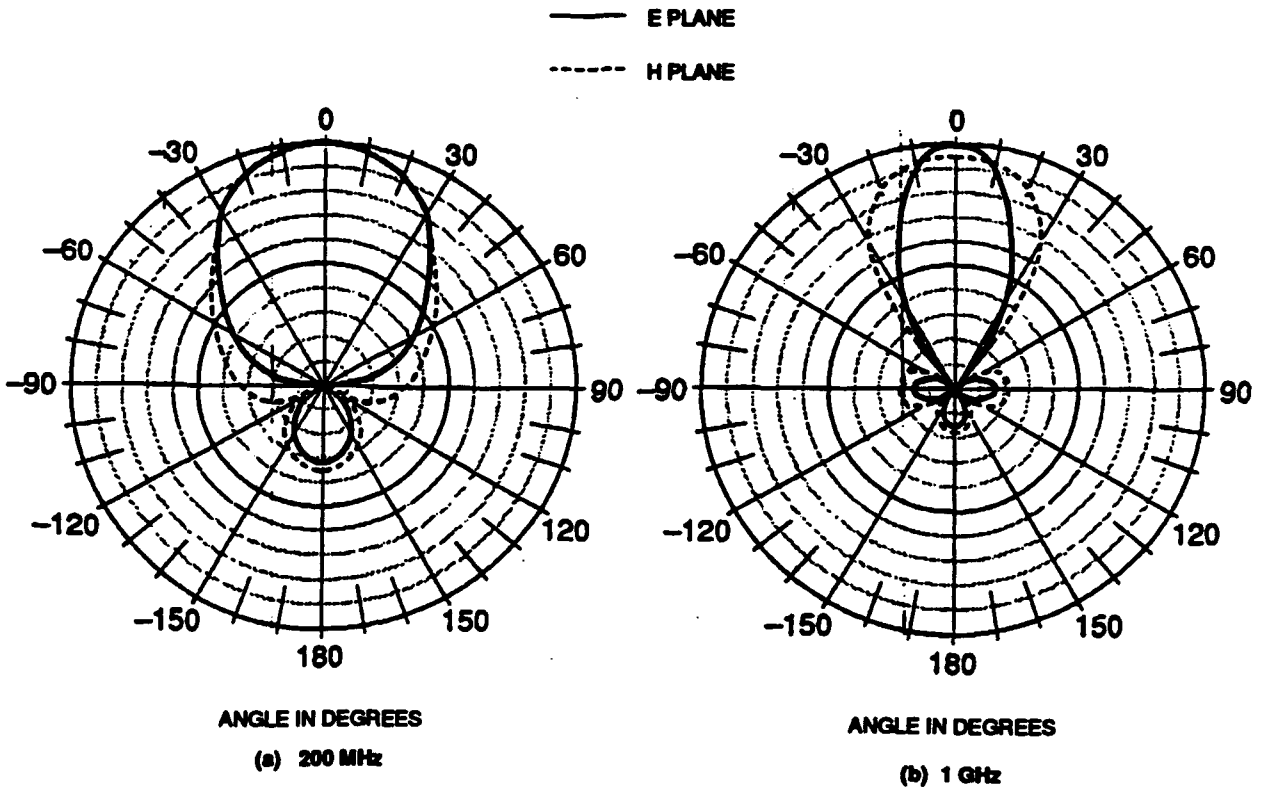

Figure 3.12. Beam patterns of the antenna feed horn at 200 MHz and 1 GHz.

A conventional horn is only adequate for pulse operation up to a few kV. To accommodate the high-power injected impulse, PI sealed the closely spaced waveguide section of the transmitter horn and used sulfur-hexafluoride gas (SF_6) at ambient pressure to provide high-voltage insulation. Laboratory tests showed that the modification did not change the horn characteristics.

Field tests of the transmitting antenna were conducted in September and October of 1990, at SRI's Stanford field site in Menlo Park, California. Swept frequency and pulsed measurements were made for a 200-meter transmission path. The swept frequency measurements yielded beamwidth and gain of the transmitting antenna in the frequency domain. The measurement results were as expected from frequency consideration of the antenna, and are discussed in detail in Appendix C. In the pulsed measurements, we used a low-power UWB source that yielded a waveform very similar to the output waveform of the high-power source. The pulsed tests determined the radiated waveforms, the beam pattern in the time-domain, and the relationship between impulse peak voltage and radiated power. Direct extrapolation of the pulsed test data from low-power test source to the PI high power source allowed us to predict the performance of the UWB system in the sea clutter measurement.

Transmitted waveforms propagated over a 200-meter distance were measured by feeding the wideband horn with a 3-kV impulse generator. The geometry of the path was chosen to minimize multipath effects. The electromagnetic signals were detected by a double-ridged wideband horn, and an EG&G ACD-4 D-dot sensor which records the time-derivative of the electric field. This sensor is especially useful in determining the absolute free-field time domain waveform radiated over the ocean. Measurements of the transmitted waveform by both detectors were recorded with 1-GHz bandwidth instruments (Tektronix 7104 scope and DSA-602 analyzer), as a function of angle off boresight in azimuth and elevation. Some examples of these data are presented in Figures 3.13 and 3.14, respectively, for the electric fields and the receiver horn signals.

From an ideal antenna with constant beamwidth over the bandwidth of the system, the transmitted signal as a function of the angles should vary only in amplitude. This implies preservation of the characteristic shape of the transmitted signal as a function of angle. We observed that this is generally the case within the main beam, but that there are perturbations and distortions visible both within the main beam and at the beam edge. These variations may have resulted from the presence of spurious reflections in the test setup at the field site and the non-ideal behavior of the transmitting antenna assembly. Figure 3.15 and 3.16 plot the peak power density

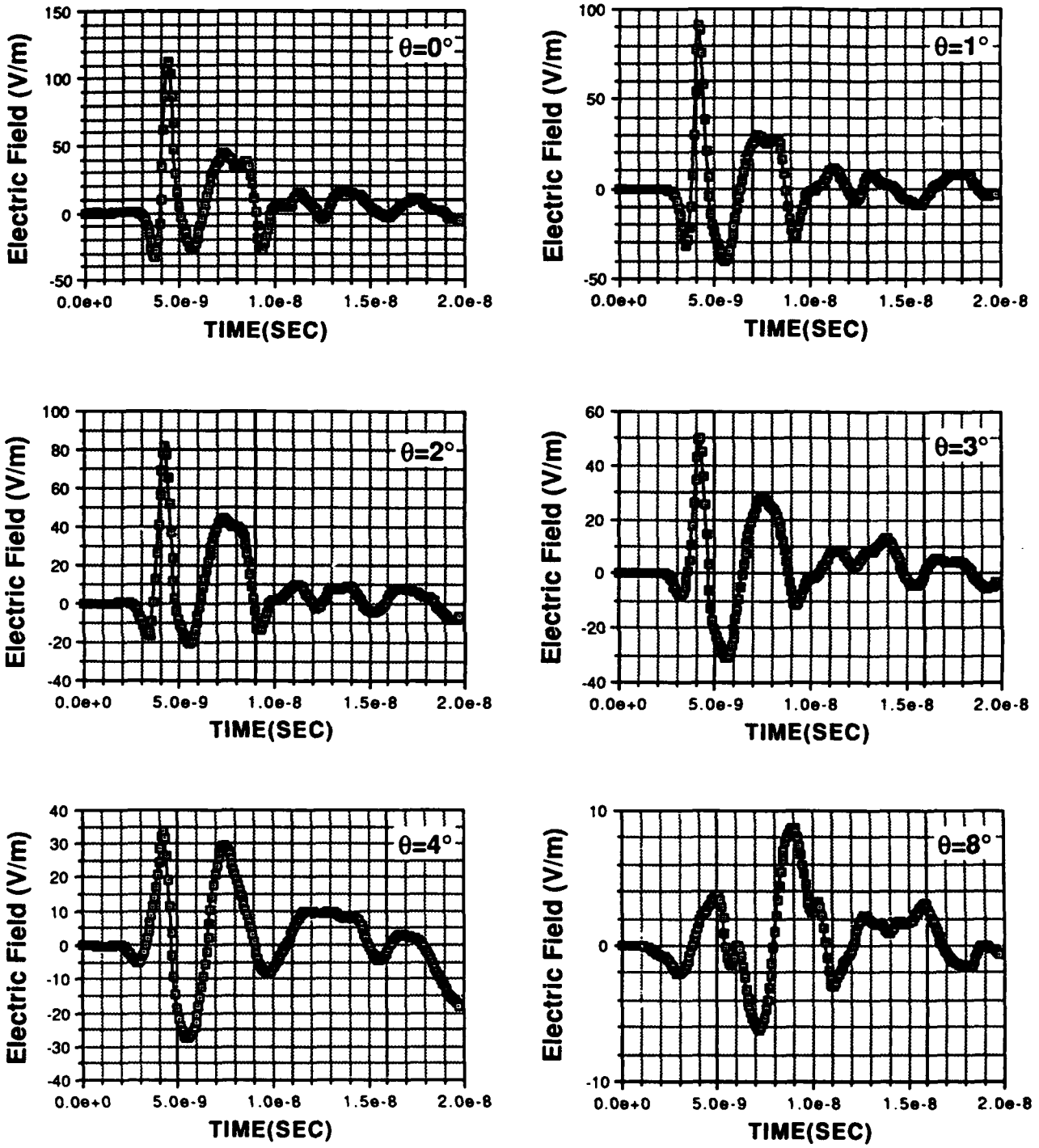

Figure 3.13. Typical transmitted electrical fields, as a function of azimuth offset angle θ, at 200-m away from the UWB horn-dish antenna. The elevation angle was fixed at 0 degree.

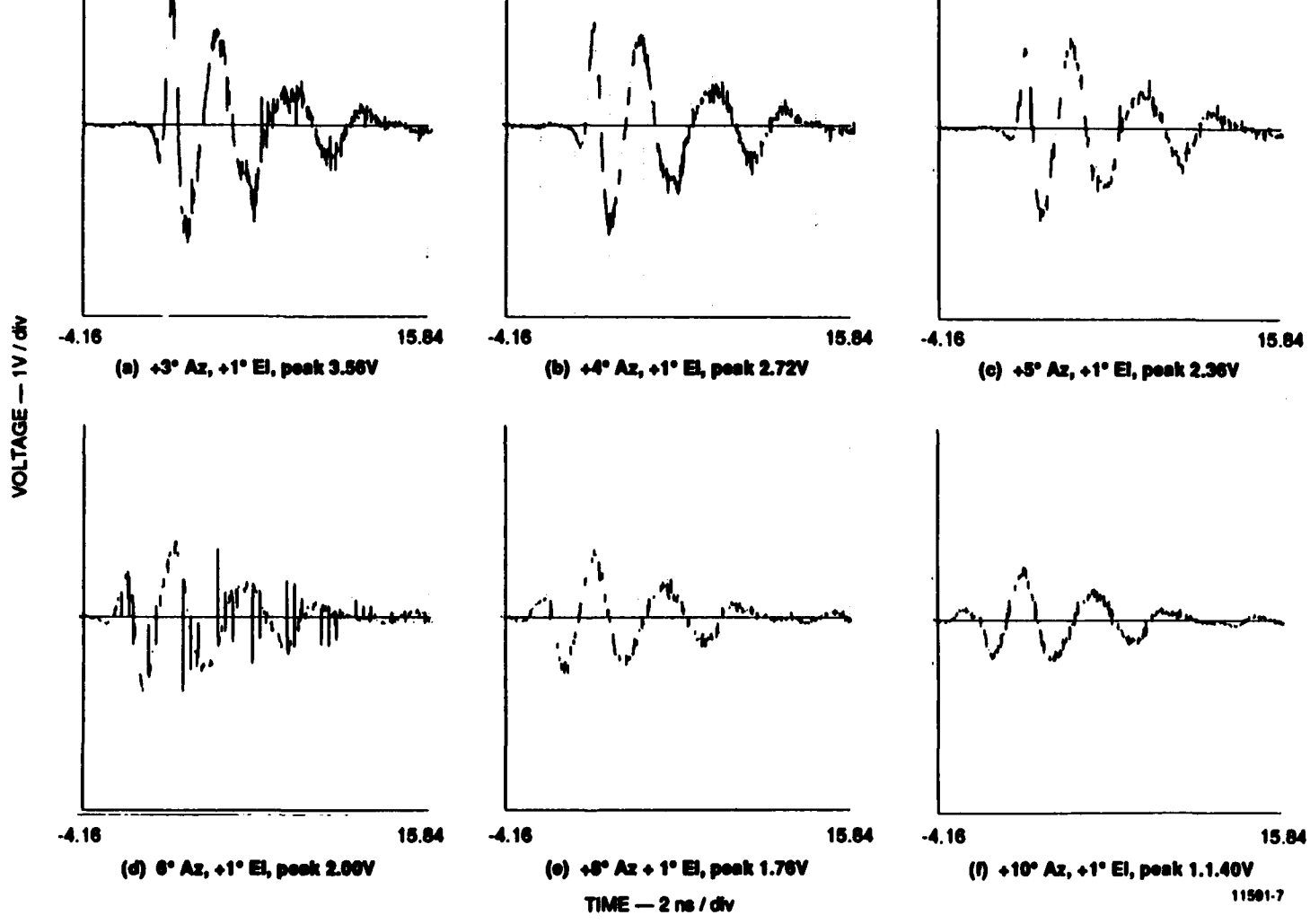

Figure 3.14. Typical received waveforms by a double-ridged horn, as a function of azimuth offset angle, at 200-m away from the UWB horn-dish antenna. The elevation angle was fixed at 0 degree.

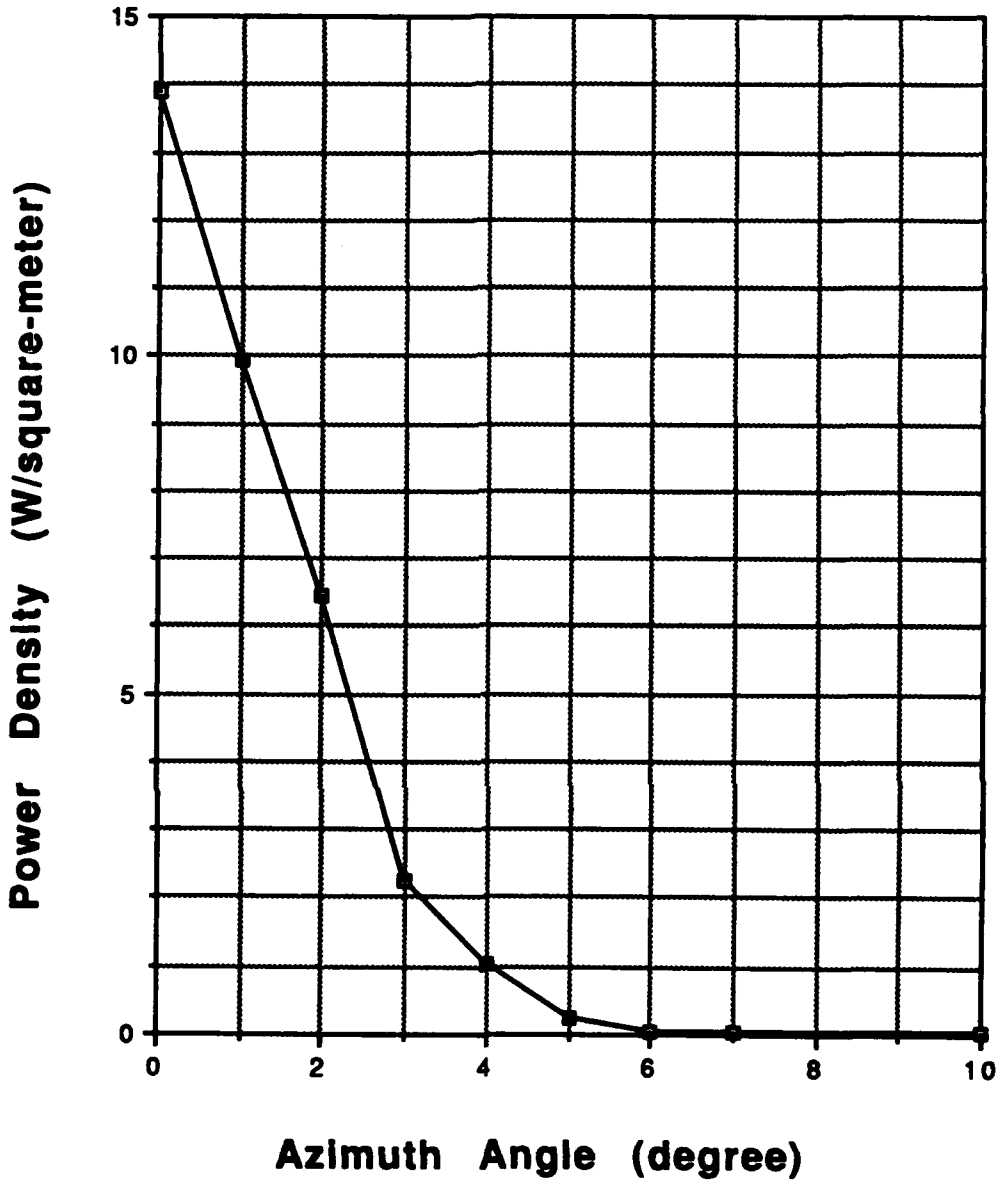

Figure 3.15. Peak power density of the beam as a function of azimuth and elevation angles.

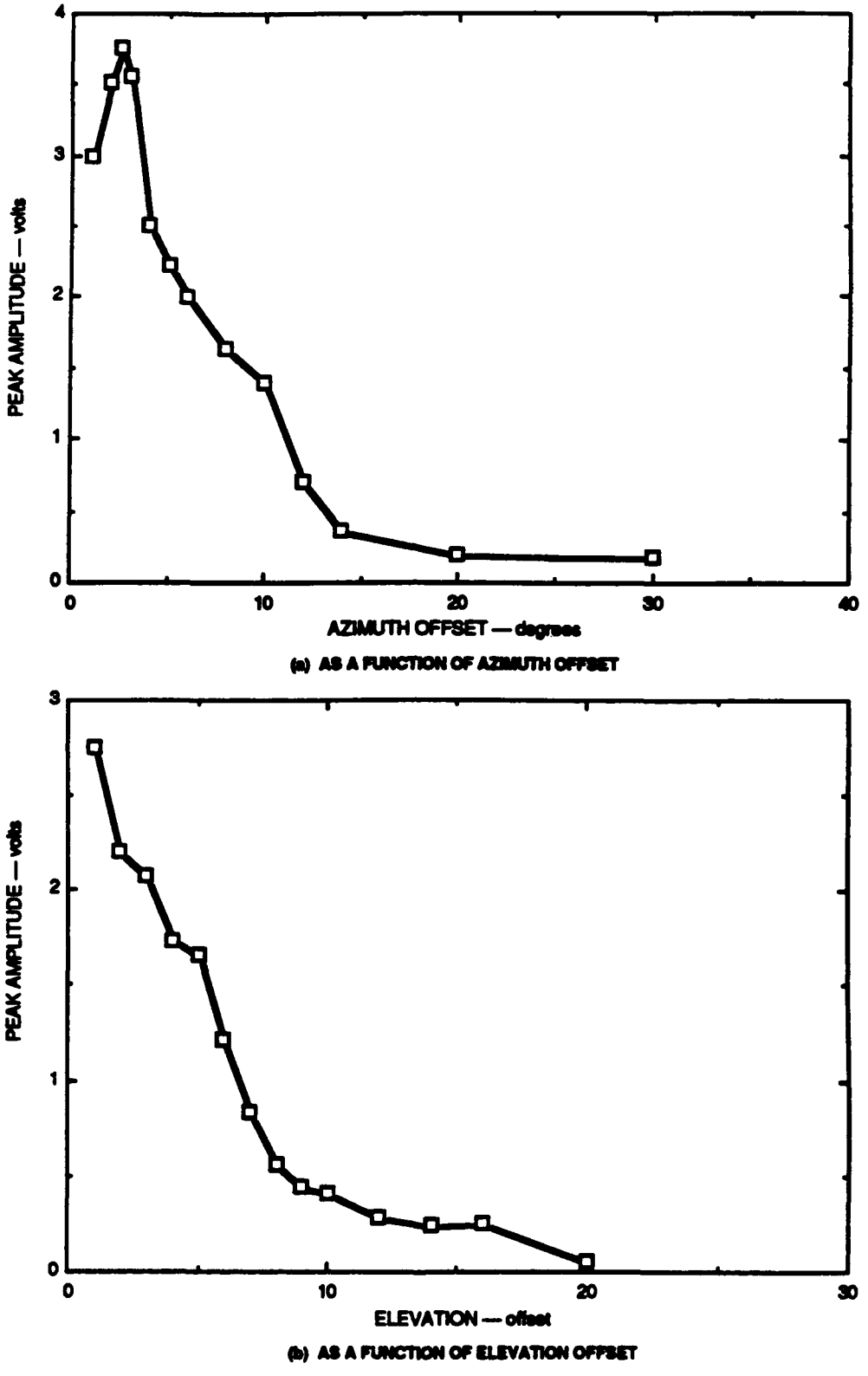

Figure 3.16. Peak amplitude of the beam as received by a double-ridged horn as a function of azimuth and elevation angles.

and voltage amplitude as a function of azimuth angle for the electric fields and the receiver horn signals.

Figure 3.17 is a power spectrum of the transmitted electric field on axis. This spectrum was constructed from the first 5 nanoseconds of the electric field temporal history, a valid process since the clear time in the field measurement was relatively short (of the order of a couple nanoseconds). The transmitted power is concentrated around 450 MHz, with a 90% (about 400 MHz) bandwidth. On the other hand, comparison of the power spectrum and the spectrum of the injected voltage impulse (Figure 3.9) clearly shows the expected high-pass filtering effects of the antenna assembly.

The measured E-field of Figure 3.13 may be used to estimate the effective peak radiated power from the antenna assembly for the injected impulse peak voltage. The peak field on-axis is 110 V/m at a distance of 200 meters away from the transmit antenna for an impulse of 3-kV peak voltage. This field intensity corresponds to a power density of 33 W/m^2. Multiplying the power density by the area of $2\pi R^2$ gives the effective peak transmitted power of about 8 MW. Since the transmitted power is directly proportional to the square of the source voltage, we estimate the effective radiated power for an impulse of 100-kV peak voltage to be 9 GW, exceeding the 5 GW design goal of the experiment.

3.4.4 Conclusion.

The ONR/NOSC sea clutter measurement effort represented the first time a high peak-power impulse radar was operated at extended range (up to 10 km). For the first time, measurements enabled radar designers to determine the operational parameters of an UWB radar designed to detect low-altitude, low-observable targets in the presence of clutter returns from the sea. The experiment was judged a success.

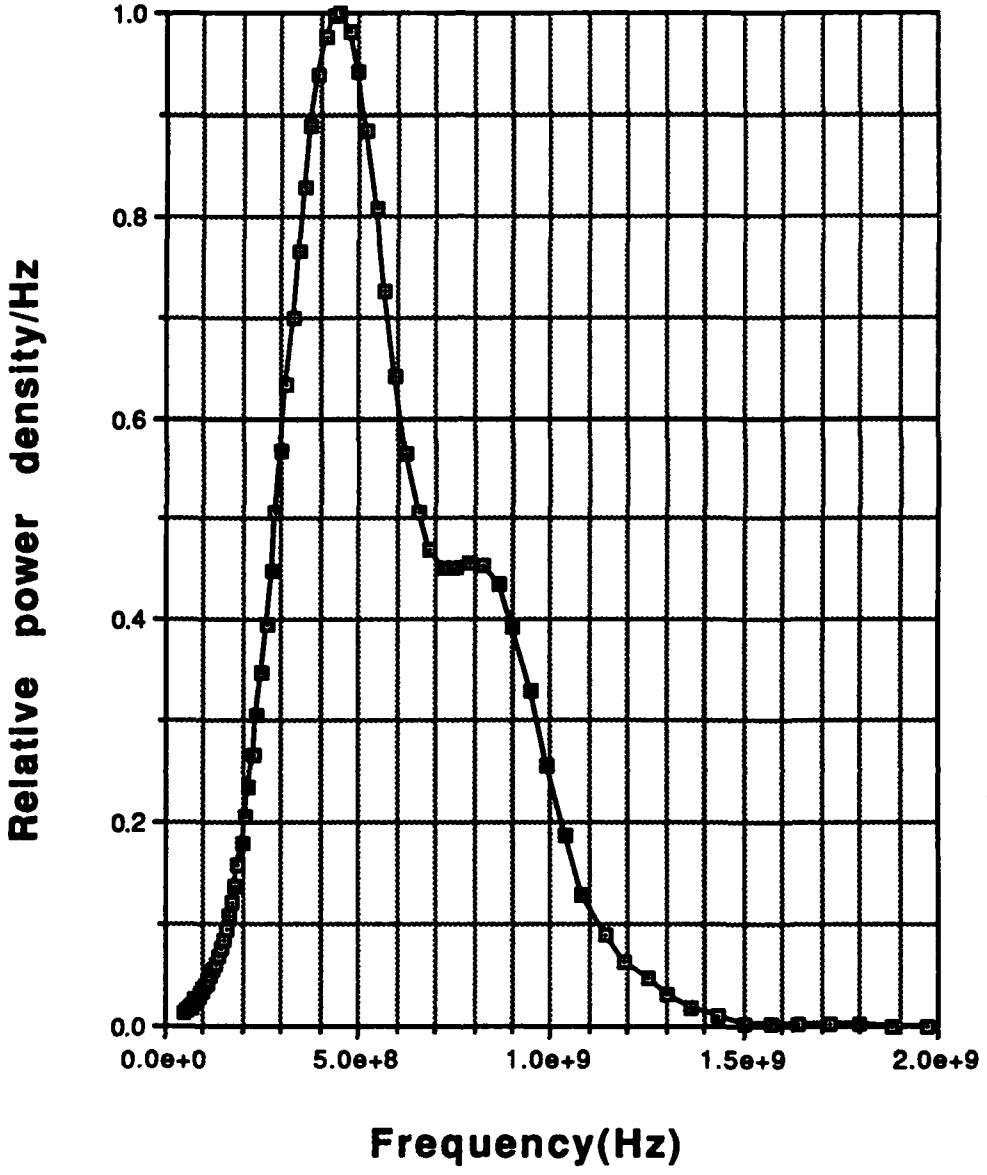

Figure 3.17. Power spectrum of the transmitted electric field on axis.

1. Nobel B., 1991, *1990 Ultra-Wideband Radar Symposium*, Littleton, MA: CRC Press.

2. OSD/DARPA Ultra-wideband Radar Review Panel, 1990, *Assessment of Ultra-wideband (UWB) Technology*, Battelle Tactical Technology Center, Report R-6280.

3. Pollock M. A., Pusateri V. P., Tice T. E., Wehner D. R., and Ott R. H., *Ultrawideband Radar Facility and Measured Results at the Naval Ocean Systems Center*, presented in the 1992 SPIE Ultrawideband Radar meeting (Los Angeles, CA, January 19-25, 1992).

4. Kerr, J. L., 1973: "Short Axial Length Broadband Horns," IEEE Trans. Ant. & Prop., pp 711-714 (September).

APPENDIX A

ONR/SDIO TECHNICAL REVIEW OF JANUARY 12, 1989

A.1 INTRODUCTION.

The HCRF program at Physics International (PI) began in August 1988. At that time, another space based free electron laser (FEL) accelerator effort had already been underway for two years. The other effort, being conducted by TRW (the prime contractor) and Stanford, was based on using a superconducting accelerator (SCA) operating CW to power an FEL oscillator. The HCRF approach is fundamentally different in that it uses a pulsed format to drive a single-pass, master oscillator power amplifier (MOPA) FEL wiggler, operates at ambient temperature and can be constructed with low Q aluminum cavities. These differences promise several advantages over the superconducting accelerator (SCA) approach including the elimination of a large and complex ring resonator, less sensitivity to acoustic and thermal variations in cavities (because of the low Q), a shorter structure (because of higher real-estate gradients), rapid turn on/off capability, and the option of locating the beam director away from the high power laser platform. For these and other reasons, the HCRF program was initiated as an alternative to the SCA approach.

Unfortunately, the FY89 budget of SDIO was insufficient to allow initiation of experimental work on the HCRF program. Furthermore, the outyear budget prospects for SDIO were not optimistic. In view of this situation, the ONR/SDIO technical program managers reviewed the baseline program plan. A technical review group was selected by ONR to review the two SBFEL approaches. Reviews of both the SCA and HCRF approaches were performed in January 1989. The general finding of the TRG was that the SCA approach was at a more advanced stage of development than the HCRF approach and appeared to be a lower risk approach, in that there did not appear to be any "show stoppers." The TRG identified the crucial technology issue for the HCRF approach as development of the high power RF power source required to drive the HGA. The TRG report was delivered to ONR/SDIO in March 1989, with the results subsequently relayed to PI. The ONR/SDIO technical program managers advised the PI technical program manager to modify the program plan in concert with this recommendation. The program was then redirected to concentrate on development of the HPM source, including technical approaches beyond the relativistic magnetron originally selected for this application.

The TRG reviewed the HCRF program at PI on January 12, 1989. The TRG was chaired by the ONR scientific officer, Dr. Vern Smiley with Dr. Robert E. Behringer acting as executive secretary. The TRG members were Dr. William Herrmannsfeldt (Stanford), Dr. Joseph L. Kirchgessner (Cornell), Dr. Phil Morton (Stanford), and Dr. Samuel Penner

(IDA). The next section of this appendix presents the findings of the TRG exactly as they were transmitted to ONR/SDIO in March 1989. The TRG findings on the SCA approach were not made available to PI. The rest of the appendix presents the vue graph package assemble by PI for the review.

A.2 REPORT FROM THE TECHNICAL REVIEW GROUP.

A.2.1 PI Review.

In contrast to the TRW contract which has been underway since June 1986 with a cumulative funding level of over twelve million dollars preceded by several years of funded efforts leading up to that contract, the PI contract was initiated in September 1988 and has received a total of only $400,000 to date. Thus, the PI effort has been limited to only a small paper study effort.

The Program Manager for the PI program is G. Frazier. He gave an overview of the PI SBFEL program which was followed by detailed technology reviews by key members of the scientific and engineering staff and a tour of the laboratory facilities devoted to this program. Dr. D. Price discussed accelerator efficiency and beam quality issues, RF source considerations and the proof-of-principle experimental plan. Preliminary beam transport calculations were presented by Dr. R. Kares, Berkeley Research Associates, a subcontractor to PI. Dr. P. Sincerny described the compact linear induction accelerator (CLIA) concept for generating high current RF (HCRF) power. The tour of the PI facilities was conducted by Frazier and Dr. M. Krishnan.

Frazier said that they have used the results of the CDTI studies done for SDIO/AFSD by LMSC and NAR to determine the requirements for a SBFEL system. PI looked at the differences in a SCA FEL oscillator and an HCRF FEL MOPA approach to meeting those requirements. The key differences are that the SCA operates at cryogenic temperatures with very high cavity Q's and requires superconducting materials whereas the HCRF operates at room temperature with low cavity Q's and can be fabricated with aluminum. Choice of a MOPA configuration for the HCRF approach leads to a requirement for very high peak current, ~2 kA for the MOPA vs ~300 A for the SCA oscillator approach. PI believes the HCRF approach is capable of achieving voltage gradients several times that achievable in the SCA approach which would result in a significant decrease in device size. However, projected efficiency would be about the same so that it is not clear whether there would be any clear advantage in system size and weight. Furthermore, PI was overly optimistic in using the on-axis gradient in their projections, whereas it is really the wall gradient

that determines operational limits due to electrical breakdown. The wall gradient is typically only half that of the on-axis gradient.

To maximize efficiency, PI has chosen a standing wave accelerator approach with very high beam loading. Even though beam loading is very high, power loss to the walls is still very large at the operational power levels contemplated and the required cooling per unit length would exceed the current SoA. Furthermore, cavity fill time significantly lowers total system efficiency. Choice of a standing wave accelerator helps since it has a faster fill time than a traveling wave accelerator, however, the losses during the fill time can still be substantial. An estimate of RF to e-beam efficiency was made assuming rise and fall times of 0.5 microsecond and a flat-top pulse length of 3 microsecond. This yielded a value of 82% whereas their point design requires a value of 90%. To achieve 90% a pulse length of at least 4 to 5 microsecond and possibly 6 to 7 microsecond would be required. This would require an order of magnitude increase in the current SoA which is less than one microsecond.

The preliminary calculations on beam transport were based on a very simplistic model and to some degree independent of the existing theoretical and experimental data base. This led to an inconsistency in the focusing system required to suppress beam breakup instability (BBU). The theoretical calculation assume a 30 cm drift space was sufficient to incorporate a pair of quadruple magnets, however, that is inadequate for a beam pipe with an ID of 18 cm as would be the case for the PI system.

Development of the high power RF (HPM) source required to drive the HCRF is probably the most critical element of the proposed PI approach. In the original proposal PI planned to use REB magnetrons for the HPM but have since switched to the concept of series REB klystrons. While BBU instability is a concern for the HCRF LINAC and is being investigated by PI, it is also an issue for the REB klystrons and has not adequately been addressed. Source-to-source coherence for the series klystrons is also an important issue which needs to be explored. It appears that PI has relied heavily on data for the REB klystrons generated by NRL although the regime of operation planned by PI is not covered by the NRL data. In view of the critical nature of the HPM source to the PI SBFEL approach and the technical issues related to the HPM approach being pursued by PI, it is advisable that alternate HPM source technologies be explored.

PI has chosen a compact linear induction accelerator (CLIA) concept to drive the REB klystrons. Development of the CLIA is partly funded under the DoD Balanced Technology

Initiative and partly under the Olin Research Council funds. For the SBFEL, two CLIA's would be used, each feeding five beam energy replacement stages (BERS). This is a modification of the approach previously proposed. To obtain the required pulse length for the HCRF the pulses from the REB klystrons would be interleaved in time. Although in principle this sounds simple, in practice difficult technical problems arise. Although the CLIA approach has much to commend it, the weight of a CLIA is substantial. Whether or not this would constitute a significant or driving factor for the system as a whole has not yet been determined.

To prove the basic HCRF accelerator FEL concept PI had proposed a proof-of-principle experiment at S-band. Recent progress by NRL on REB klystrons in the L-band has motivated PI to alter the PoP experiment to operate at L-band. This is actually a step in the right direction since the SBFEL would, in fact, be at an even lower frequency.

A.2.2 Conclusions.

Based on the information presented during the review process the TRG concludes that the recirculating superconducting accelerator approach being pursued by TRW is the leading candidate for the SBFEL application at this time. To meet mission requirements reasonable extensions of the SoA are required and no obvious show-stoppers have been identified. TRW has identified the important technical issues which need to be addressed and has outlined a reasonable program to resolve these issues. Progress on this program has been impeded by the erratic support provided by SDIO. The on-again off-again nature of the funding has made it difficult to manage the program and has led unavoidably to inefficient use of funds and growth in anticipated costs to complete the program.

The high-gradient high-current pulsed accelerator approach being pursued by PI was found to be an interesting, very challenging and potentially valuable technology. Application to the SBFEL mission requires a very large extension in the SoA and several potential show-stoppers exist. PI has identified the important technical issues which need to be addressed and has outlined a reasonable program to resolve these issues. The TRG believes that higher priority should be placed on developing the required high power microwave source and lower priority assigned to the proof-of-principle experiment included in the PI program plan. The compact linear induction accelerator being developed to drive the REB klystron HPM source is interesting and useful technology and is well worth pursuing in its own right.

There are other possible approaches applicable to the SBFEL mission which were not reviewed by the TRG. Two examples which are being considered by other groups are cryogenic CW RF and electrostatic accelerator approaches. Since this field is at a very early stage of development, it is inappropriate to rule out any particular approach at this time. Further investigation and evaluation of all reasonable approaches should be done to clearly identify the best possible technology for the SBFEL application.

A.2.3 Recommendations.

The following recommendations have not been prioritized. Rather the list is intended to state what must be done to determine the viability of the two approaches being pursued for the SBFEL application. To establish priorities and outline a program plan would require a significantly greater effort on the part of the TRG.

A.2.4 PI Pulsed High Current RF Accelerator Technology.

a. Demonstrate the high power RF source required for this approach as soon as possible.

b. Explore alternate HPM sources to meet the requirements of the high gradient pulsed RF accelerator.

c. Perform a detailed system analysis of the weight of the Compact Linear Induction Accelerator (CLIA) driven REB klystron required to generate the very high power RF energy for the SBFEL application to determine practicality of this approach.

d. Demonstrate RF LINAC operation with the very high voltage gradient (50 MV/m) and beam loading (greater than 90%) required by the point design.

e. Demonstrate the feasibility of dissipating the energy per unit length that would be deposited in the walls of the accelerator for the point design.

f. Demonstrate the ability to operate and control two high energy electron beams, generate and transmit very high power RF and dissipate very high power per unit length in a space environment.

g. Demonstrate the ability to tune the accelerator to meet the requirements of the FEL.

TECHNICAL PROGRAM REVIEW OF THE HIGH CURRENT RF ACCELERATOR CONCEPT FOR SPACE-BASED FELs

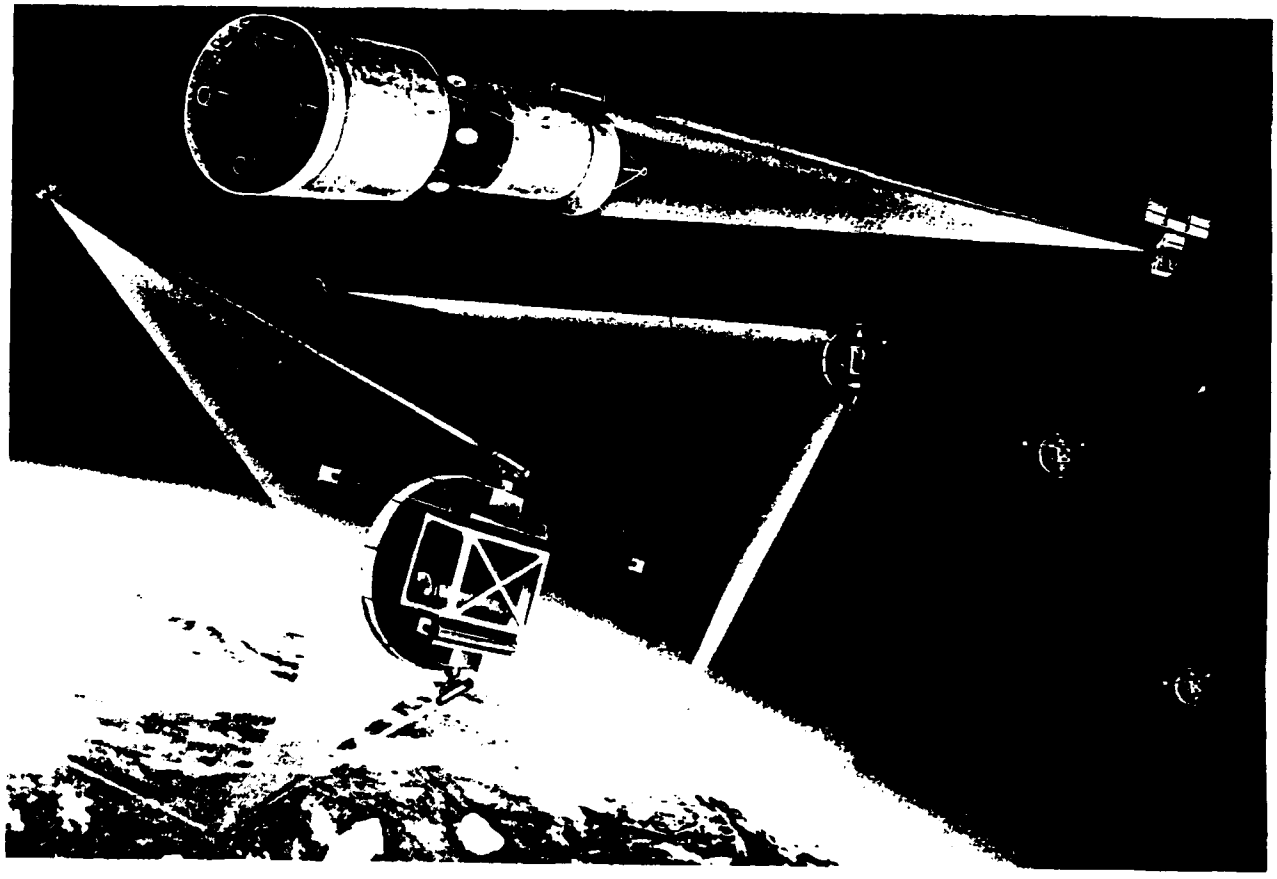

Presented to the
SBFEL Accelerator Technology Review Group

12 JANUARY 1989

Physics International Company
Olin *Defense Systems Group*

SBFEL Accelerator Technology Review Group

CHAIRMAN:

Dr. Vern Smiley
Office of Naval Research
c/o Naval Ocean Systems Center
Code 843
271 Catalina Boulevard
San Diego, CA 92152

EXECUTIVE SECRETARY:

Dr. Robert E. Behringer
Ballena Systems Corporation
1150 Ballena Boulevard
Alameda, CA 94501

TECHNICAL REVIEW PANEL:

Dr. William Herrmannsfeldt
Stanford University
Technical Division
P.O. Box 4349
Stanford, CA 94305

Dr. Phil Morton
Stanford University
Technical Division
P.O. Box 4349
Stanford, CA 94305

Dr. Joseph L. Kirchgessner
Cornell University
124 Newman Laboratory
Ithaca, New York 14853

Dr. Samuel Penner
IDA
10500 Pine Haven Terrace
Rockville, MD 20852

Olin
89-01-007

SBFEL Accelerator Technology Review of tbe Physics International Company High Current RF (HCRF) Linac Program 12 January 1989 Agenda

0830 - 0900	Introductions and Planning	
0900 - 0930	Overview of PI	M. Kolpin
0930 - 1030	HCRF Concept and Program Description	G. Frazier
1030 - 1145	Accelerator Efficiency and Beam Quality Issues	D. Price
1145 - 1245	Lunch (catered)	
1245 - 1330	Tour of PI	G. Frazier/M. Krishnan
1330 - 1400	Beam Transport Calculations	R. Kares
1400 - 1430	RF Source Considerations	D. Price
1430 - 1500	CLIA Considerations for HCRF	P. Sincerny
1500 - 1530	PoP Experimental Plan	D. Price
1530 - 1600	Summary & Conclusion	G. Frazier
1600 - 1700	Government only Caucus	Review Panel
1700 - 1730	Wrap-up	Group

HCRF Concept and Program Description

GEORGE FRAZIER

I. Basic concept description, relevance to SBL program, potential advantages, and key technology issues.

II. Program description, technology roadmaps, budgets and funding needs, evolution of program since inception, current status, and future plans.

List of Contributors

Physics International Company

Susan Ball
Bernie Bernstein
George Frazier
Richard Foster
Ralph D. Genuario
David Price
Robert Raos
Richard Smith
Peter Sincerny
Henry Sze
Lance Thompson

Berkeley Research Associates

William Colson
Robert Kares

University of New Mexico

Stanley Humphries

Stanford Linear Accelerator

Roger Miller

Typical Space Based Laser (SBL) System Hierarchy Description

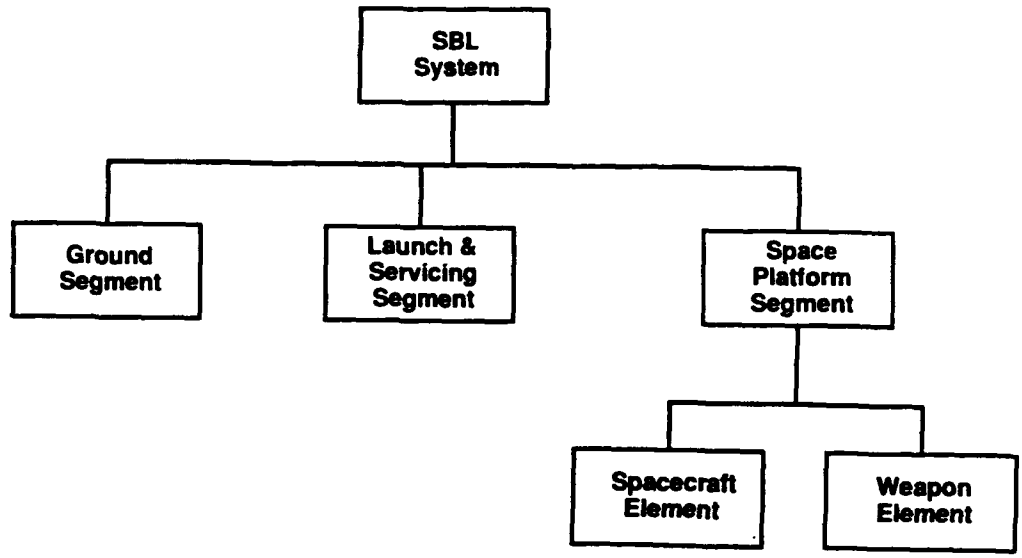

Olin
MF02.1

The scope of the PI HCRF program is limited to a small portion of the weapon element.

Typical SBL Weapon Element Hierarchy*

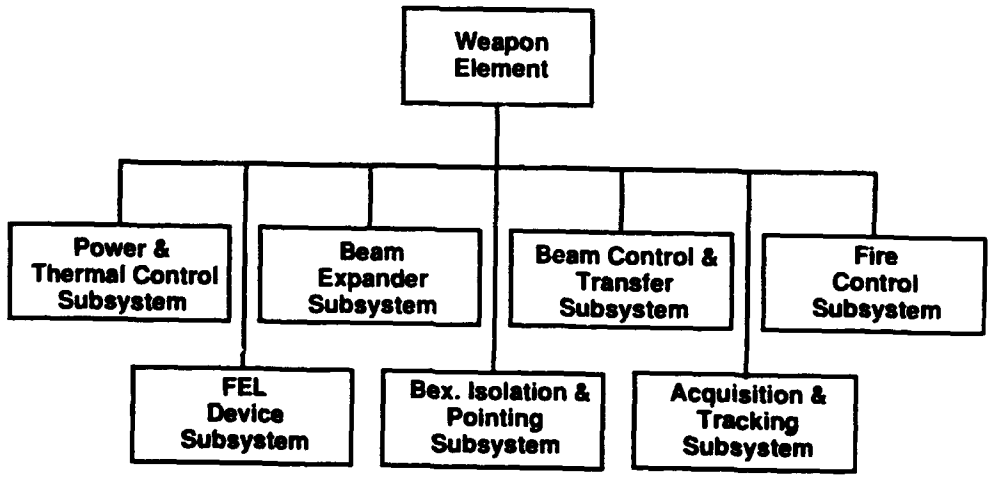

Olin
MF02.1

The FEL device subsystem contains HCRF

* After Lockheed / TRW CDTI Study

Selected Space-Based Laser Technology Choices Showing Where the HCRF LINAC Concept Fits

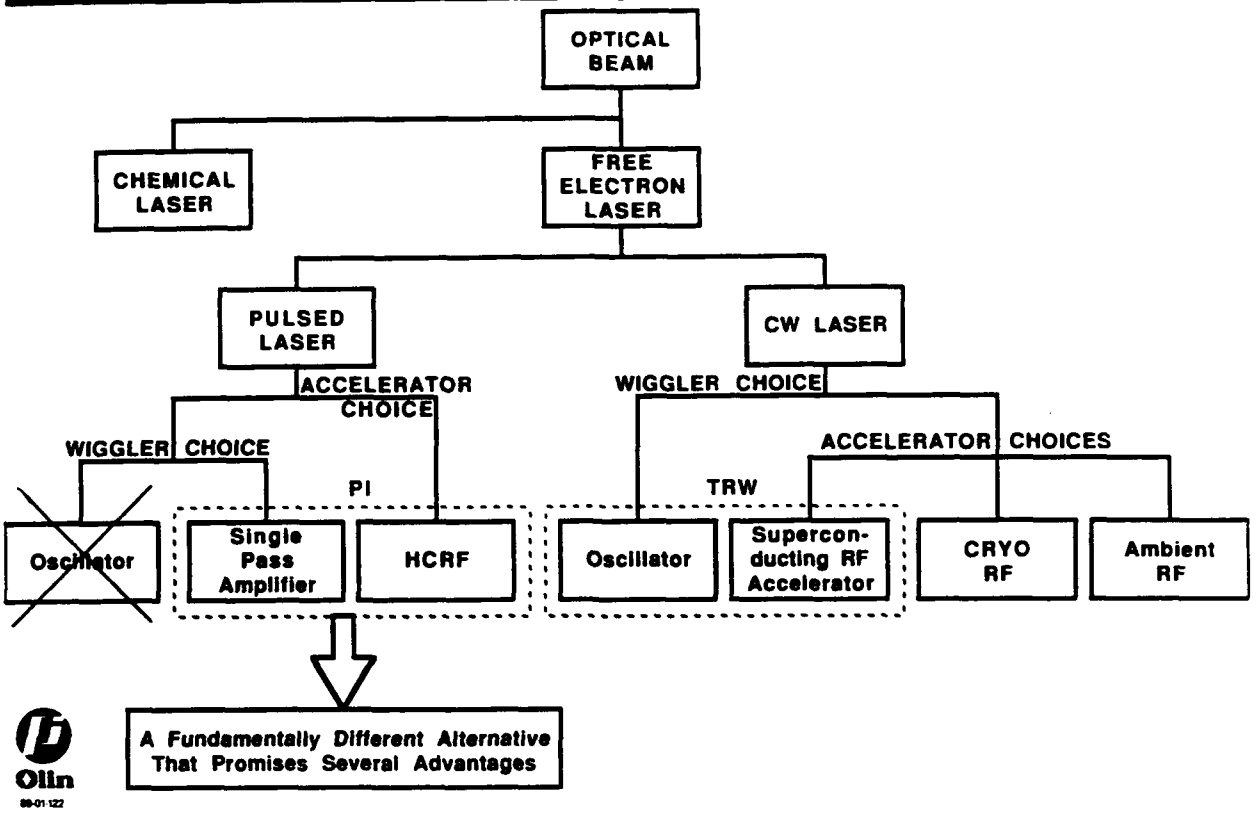

Olin

88-01-122

How HCRF Differs From the CW SCRF Approach

	HCRF	CW SCRF
Loaded Q for fundamental mode	Low (~ 10^3)	High (~ 10^7)
Aperture size	Large (~ 15 cm)	Same?
Cavity material	Aluminum	Niobium?
Cooling required	300-1000K	4-80K
Beam loading goal	95%	99%?
Real estate gradient goal	Up to 30 MeV/m	5-10 MeV/m?
Peak current	2 kA	Few hundred amps
FEL wiggler	Single pass amplifier	Oscillator
Wall-plug-to-light efficiency goal	> 40%	> 40%

Olin

88-01-124

High Current RF Linac Basic Concept

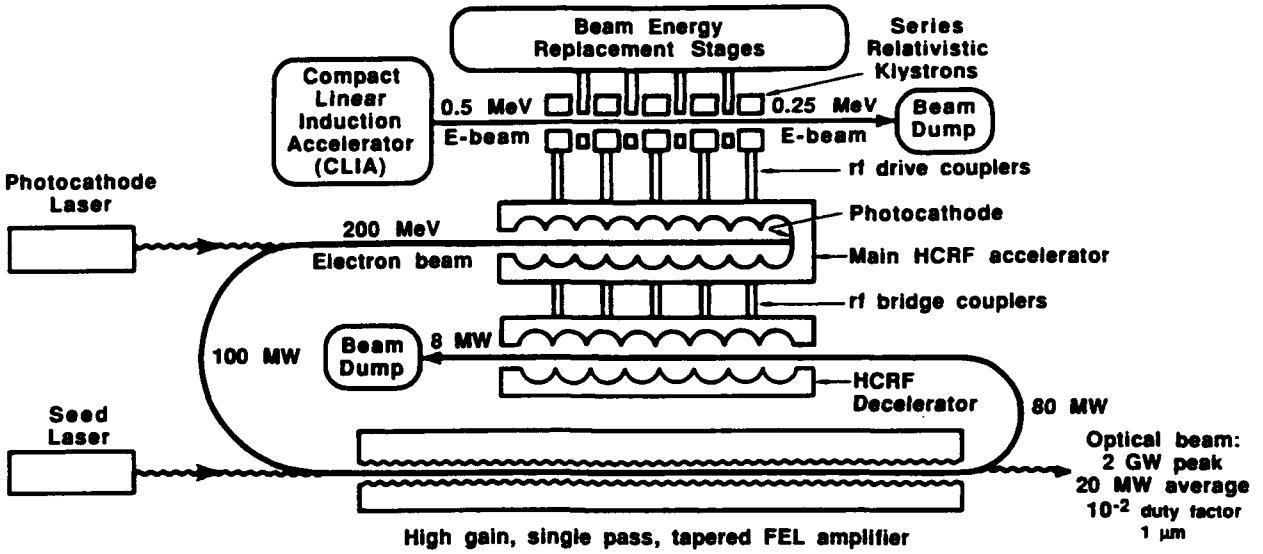

Olin

200 MeV Electron Beam Pulse Format for HCRF

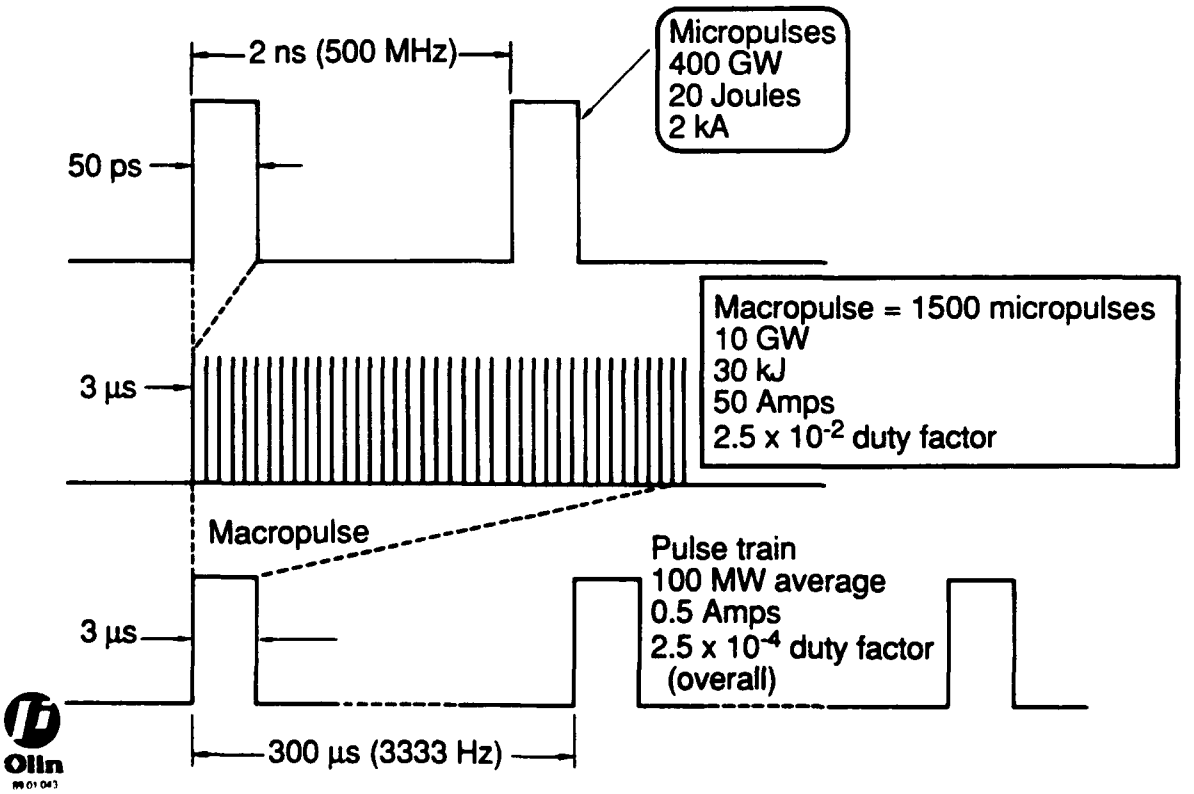

Olin

Potential Advantages of HCRF

- Reduced accelerator weight and volume
  - High real-estate gradient (20 to 30 MeV/m)
  - No refrigeration required
- Simpler, smaller wiggler
  - High gain, single pass amplifier
  - No grazing incidence optics or ring resonator
- Smaller, more robust space platform
  - Low Q structures far less sensitive to shock, vibration, thermal changes and startup
  - Fighting optics can be separated (no beam expander)
  - Single shuttle payload possibility

Darmstadt Data for SC 20 Cell Structure

- STABILITY REQUIREMENTS
  - Amplitude $\Delta V/V \leq 10^{-4}$
  - Phase $\Delta\phi \leq 1^0$
- <u>But</u>: Soft structure, c ≈ 50 kp/mm SENSITIVITY TO VIBRATIONS

$\Delta f_o/\Delta L = 500$ kHz/mm with $f_o = 3 \cdot 10^9$ Hz and $Q_o = 3 \cdot 10^9$

$\Rightarrow \Delta f_o = 1$ Hz $\hat{=}$ $\Delta\phi = 90°$

$\Rightarrow$ $\boxed{\Delta\phi/\Delta L = 45°/\text{nm}}$

for unloaded structure!

<u>But even with $Q_L \approx 3 \cdot 10^7$</u>

<u>$\Delta\phi/\Delta L = 0.45°/\text{nm}$</u>

Potential Advantages of HCRF (cont.)

- Agility
  - Easier turn-on/turn-off
  - Variable inter-macropulse spacing
- Reduced development costs
  - Pulsed format allows inexpensive concept demonstrations and iteration
  - Synergy with other programs maximizes leverage of government funds

Olin

System Analysis for HCRF Space-Based FEL

Reasons for simple system analysis early in the technology program

- **To set technology goals (related to eventual utility in a mission)**
- **To establish motivation for funding (based on comparative value to applications)**

Caveat:

- **Of course, the degree of definition of goals and strength of motivation should be limited in early, inexpensive stages of development**
- **Even so, PI has completed very little systems analysis work to date**

Therefore we can answer questions like this –

- **What are rough beam power and accelerator efficiency goals for HCRF (based on approximate entry-level SDI mission requirements)**

But not questions such as –

- **How would a deployed HCRF-FEL system compare with CW SCRF FEL in terms of numbers of satellites, mass, size, cost, and effectiveness?**
- **How would HCRF compare with SB HF? With a GBL?**
- **What are balanced HCRF technology goals commensurate with an optimized system?**
- **What are realistic system performance growth limits for the HCRF technology?**

Olin

Comparative Analysis—HCRF FEL as a Space Laser

Anticipated strengths of HCRF in space-based laser applications

- vs. RF FEL – size, mass on orbit, efficiency, atmospheric penetration
- vs. HF – size, mass on orbit, particularly in growth scenario against responsive threat

Deployment regimes where PI hopes to support SDI-sponsored comparison with other concepts:

- Compact, low-mass, early application
  - Cost-effective initial SDI mission demonstrations, other applications (e.g. radar)
  - Growth scenario taking in-orbit systems toward full mission potential
- Standard mission set and launch limit
  - For ease of comparison with major space-based laser studies
  - Standard target sets and HLLV launch mass limits
- High-performance end of spectrum
  - Long range, higher altitude, high kill-rates against responsive threat – few satellites, highly robust and survivable
  - Scenario: First launch defends system, then assemble on orbit for full capability

PI has accomplished only the following systems analysis work:

- Established simple strawman accelerator technology performance requirements based on existing SDI-sponsored space-based laser systems studies using standard mission sets
- Defined very simple entry-level space-based HCRF FEL system design concepts

Olin

SDI Mission Requirements for SBL Systems

SPECIFIED REQUIREMENTS	NEARER-TERM SYSTEM ("down-excursion" scenario)	FAR-TERM SYSTEM ("up-excursion" scenario)
LIQUID BOOSTER		
Spot diameter (cm)		
Minimum edge intensity (kW/cm2)		
Fluence (kJ/cm2)		
SOLID BOOSTER		
Spot diameter (cm)		
Minimum edge intensity (kW/cm2)		
Fluence (kJ/cm2)		
POST-BOOST VEHICLE		
Spot diameter (cm)		
Minimum edge intensity (kW/cm2)		
Fluence (kJ/cm2)		
TOTAL Number of Targets (Boosters)		
FIRST SHOT (seconds after launch)		
WAR ENDS (seconds)		
TOTAL ENGAGEMENT TIME		

Lethality requirements and engagement scenarios based on SDIO Technical Guidelines Document for Phase II SBL systems studies.

Olin

HCRF Concept Based on Typical SB FEL Requirements

Derived Requirements	Nearer-Term System ("down-excursion")	Far-Term System ("up-excursion")	HCRF point design (to set technology goals)
Wavelength (microns)			0.4-[1.0]*
Altitude (km)			
Effective ranges (km)			
Number in constellation			
On-target-time per kill (s)			
Brightness (watts/ster)			[1]* - 4 x 10^{20}
Beam Diameter (m)			[5]* - 10
Laser power (MW)			[20]*
Run time (s)			
			*Entry level

NOTE: Space-based FEL system design requirements based on Lockheed Missiles and Space Company's SBL System Study Phase III. These top-level system designs are not optimized for the HCRF concept and are used to provide system and technology goals for HCRF at a scoping level only. The resulting HCRF point design is not suitable for size, weight, cost, and performance comparisons with other SBL's.

Olin
89-01-074

Immediate System Analysis Observations

Shorter wavelengths have obvious performance, cost, size, and weight advantages

- **Once initial proof-of-principle is complete, R&D should stress higher energies, lower emittance, and short-period wigglers**

Thermal control and run time dominate mass budget – therefore, efficiency is critical

- **Again, R&D should stress improving accelerator beam quality**

Optimization for HCRF probably lies both in nearer term, low cost development and demonstrations and in growth to high performance, long-range, robust systems in the far term

- **Simplicity of technology allows for quick, efficient development, demonstration, and iteration**
- **A relatively simple entry-level system could be launched in one shuttle flight for SDI weapon and other application demonstrations**
- **The ruggedness and simplicity of the technology allows for straightforward, cost-effective scaling to large, highly capable future systems**

Olin
88-101-001
89-01-082

Candidate Single - Shuttle HCRF SBFEL Launch Configuration

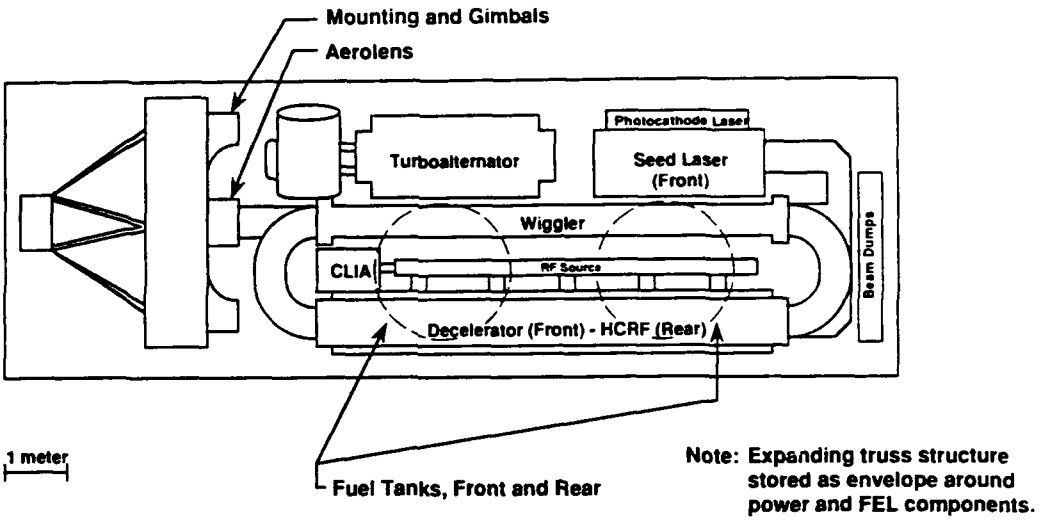

Note: Expanding truss structure stored as envelope around power and FEL components.

- 8 m Wiggler
- 4 m Beam Director
- 150 MeV, 75 MW Electron Beam
- 2 - 5 MW Optical Power at 1 μm

Olin
MF02.1

Deployed Configuration for Single - Shuttle - HCRF SBFEL Experiment

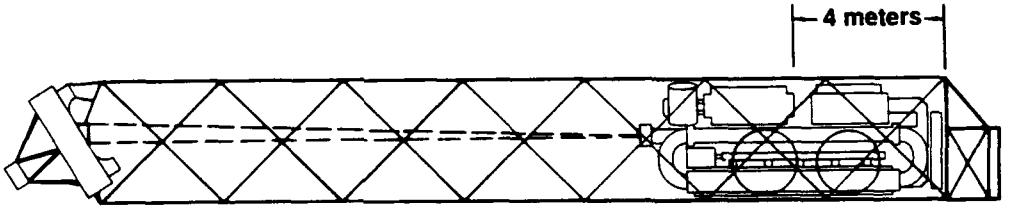

Expanding Truss With Aerolens Option

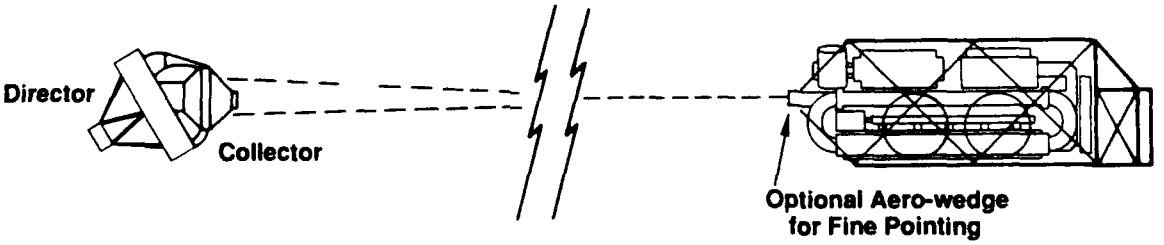

Detached Beam Director Option

Olin

HCRF Subsystem Block Diagram

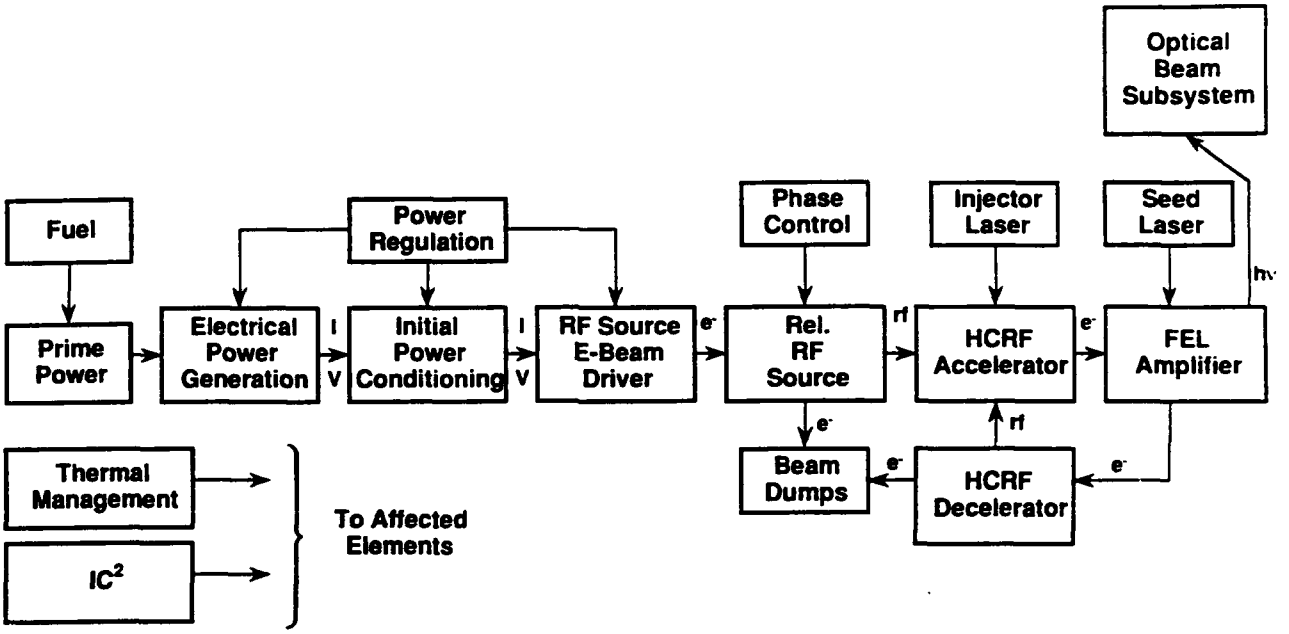

Shaded boxes show principal focus of present HCRF program

Olin

89-01-121

Accelerator-FEL System Efficiency Goals

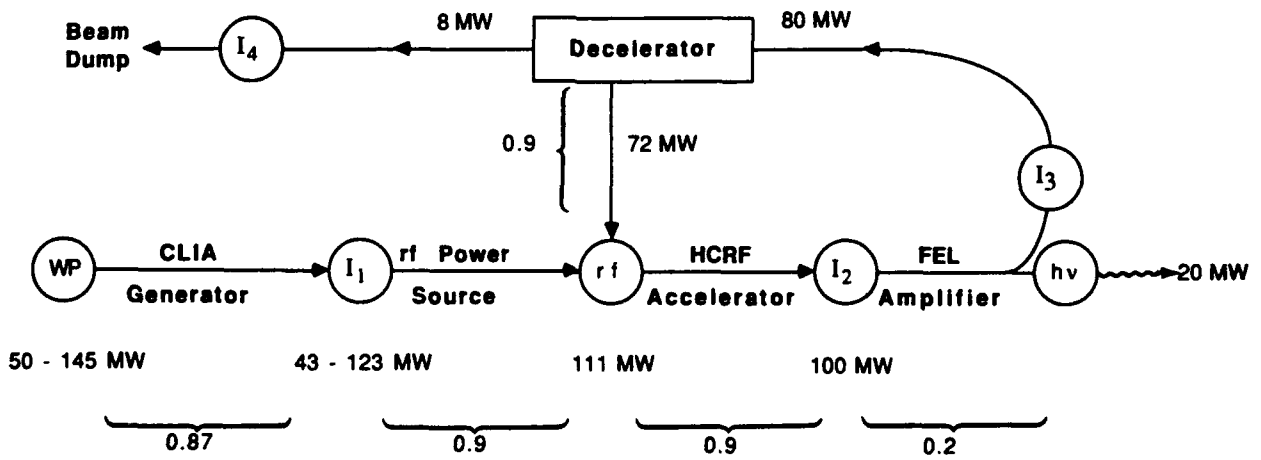

Wall-Plug-to-Light Efficiency Goal = 40 percent

Olin

89-01-095

HCRF Accelerator Parameters for Rough Conceptual Point Design

	During Micropulse	During Macropulse	Overall Average
Peak Electron Energy	200 MeV	200 MeV	200 MeV
Real Estate Gradient	20 MeV/m	20 MeV/m	20 MeV/m
Current	2 kA	50 A	0.5 A
Beam Power	400 GW	10 GW	100 MW
Beam Energy	20 J	30 kJ	$\int$ Pdt
Pulse Duration	50 ps	3 μs	NA
Pulse Repetition Rate	500 MHz	3.3 kHz	NA
Input rf Frequency	500 MHz	500 MHz	500 MHz
Duty Factor	NA	2.5×10^{-2}	2.5×10^{-4}

Olin

88-01-084

Key Accelerator Technology Issues Tree

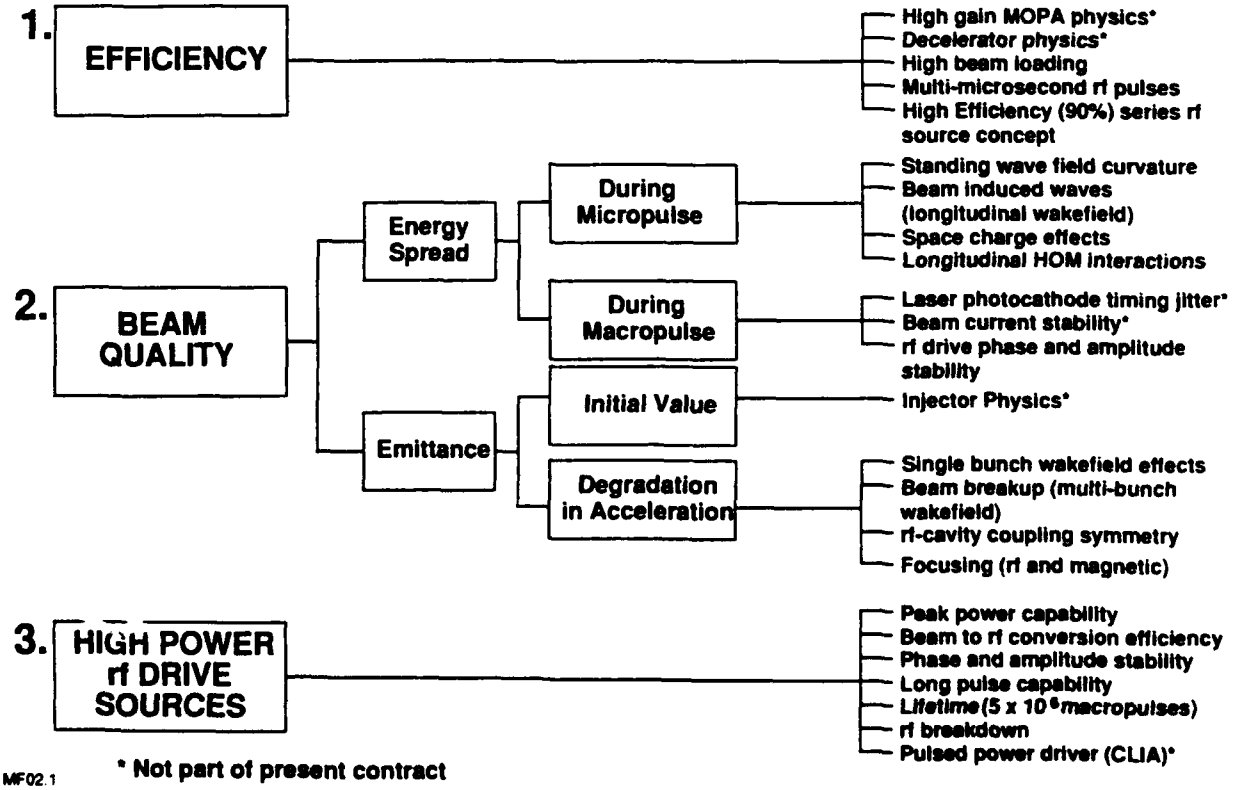

MF02.1

* Not part of present contract

HCRF Program Background

- Initial program proposed November 1987
- Study task initiated September 1988
- Study 50% complete

Olin

Top-Level HCRF Technology Roadmap as Originally Proposed

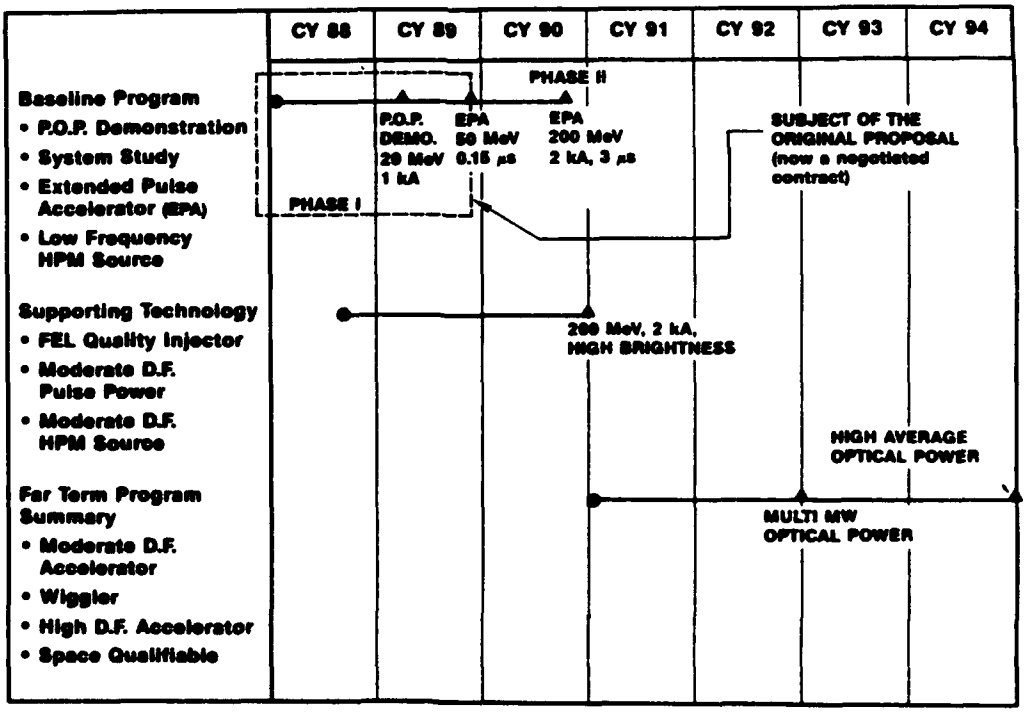

Olin

Original Baseline Technology Program (Phase I and Phase II)—Single Shot HCRF Demonstration

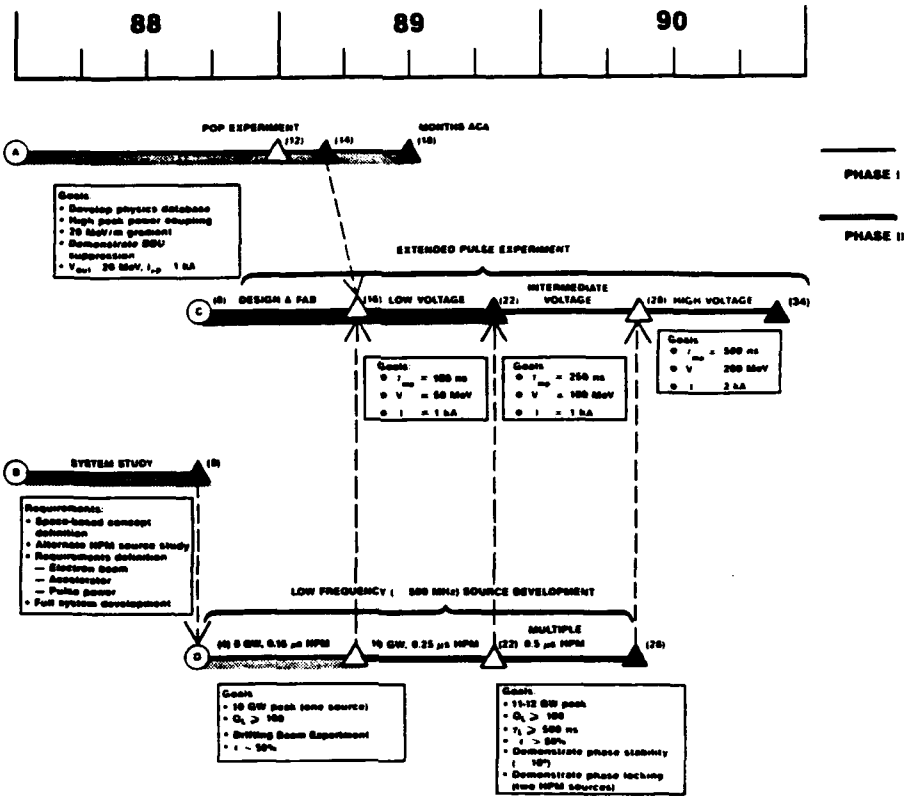

Olin
87 07 116

Original Supporting Technology Program

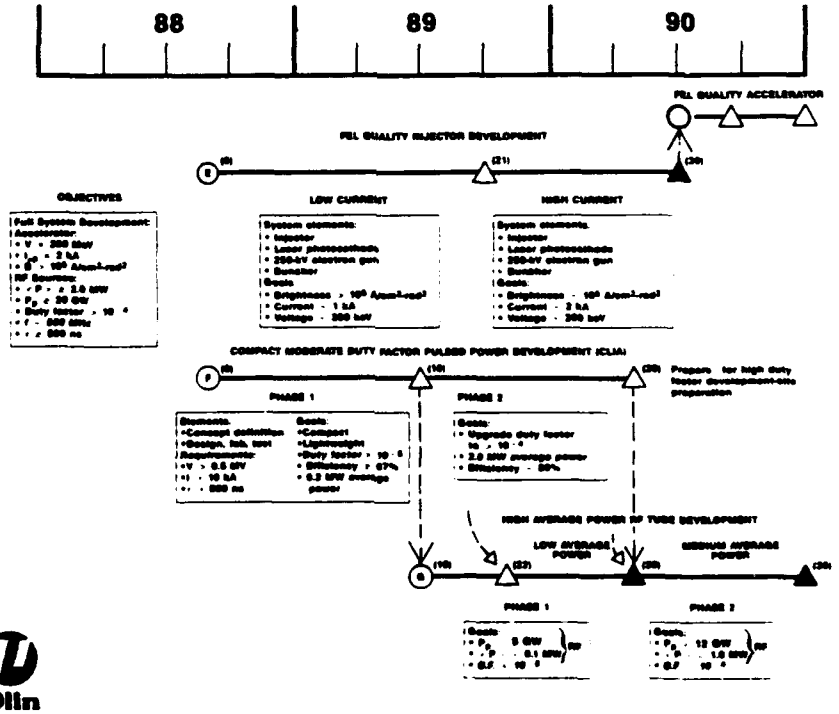

Olin
87 07 118

Original Far Term Program

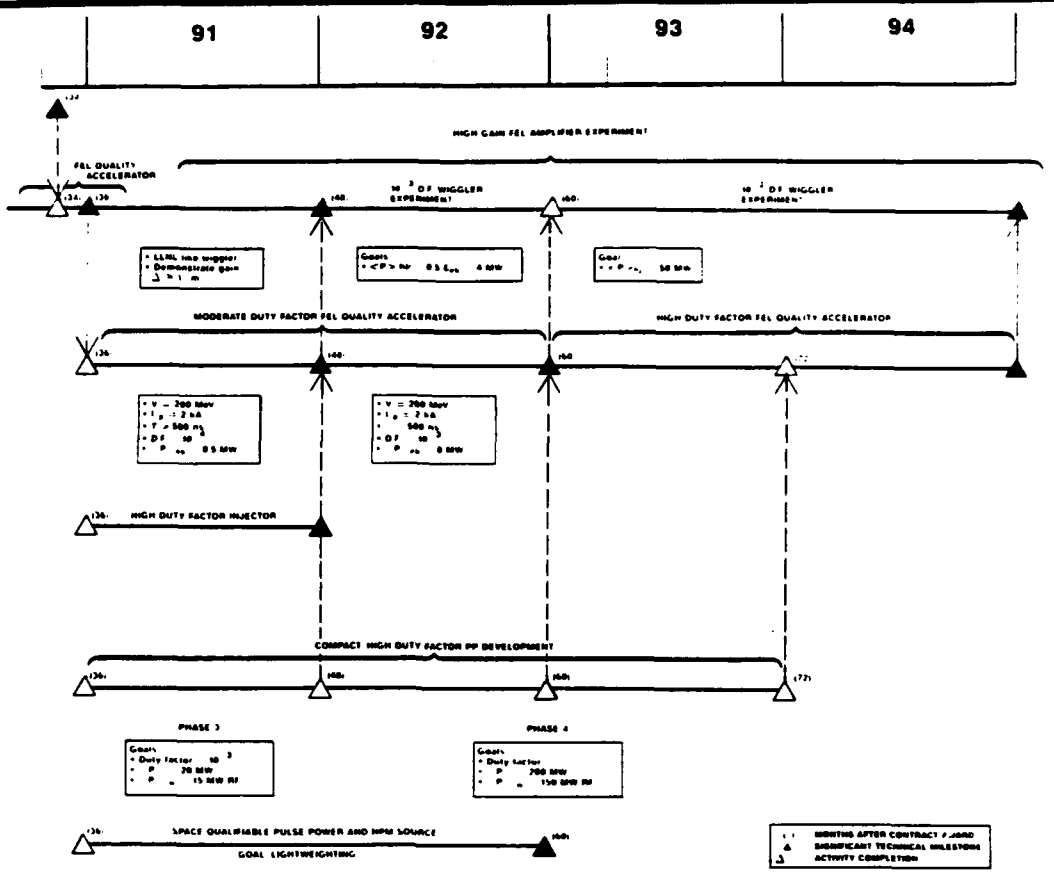

Olin

Top-Level Program Funding Summary ($M)

		Funded	Committed	Negotiated	To be Proposed (ROM)
Baseline Program	Phase I	0.2	0.4	3.9	0
	Phase II	0	0	0	2.2
Supporting Technology Program		0	0	0	5.0
Far-Term Program		0	0	0	TBD

Olin

Original Statement of Work for Initial Study ($200 k)

Descoped	1. Survey technical requirements for SBFEL
Bulk of Effort to Date	2. Establish performance requirements for HCRF
	3. Establish HCRF subsystem and component performance requirements
	4. Update technology goals for other three subprojects
Minimal Effort So Far	5. Compare HCRF to CW SCRF concept

Olin

HCRF Study Task Budget, and Costs to Date (Through 1-6-89)

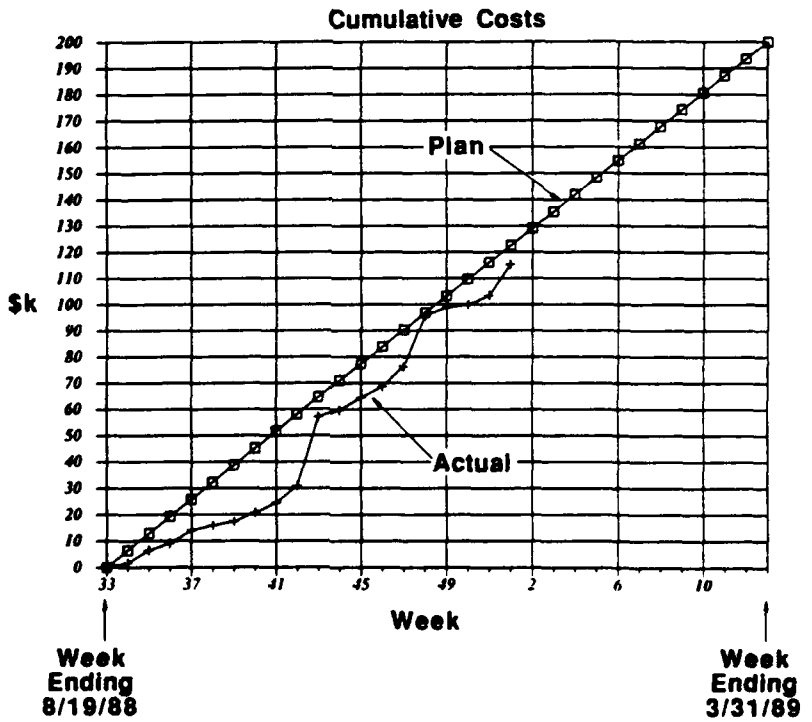

Olin

Impact of Study Results and Related Events Since Original Program Plan was Formulated

One year funding delay combined with synergistic technology developments in other programs has actually lowered risk of developing the HCRF concept:

- LANL photocathode results
- NRL L-band relativistic klystron development
- Availability of PI microsecond pulse generator (CAMEL X)
- CLIA development by BTI/DNA
- Advent of series rf source concept

Therefore, proposed program plan has been revised

Revised Baseline Technology Program (Phases I and II)

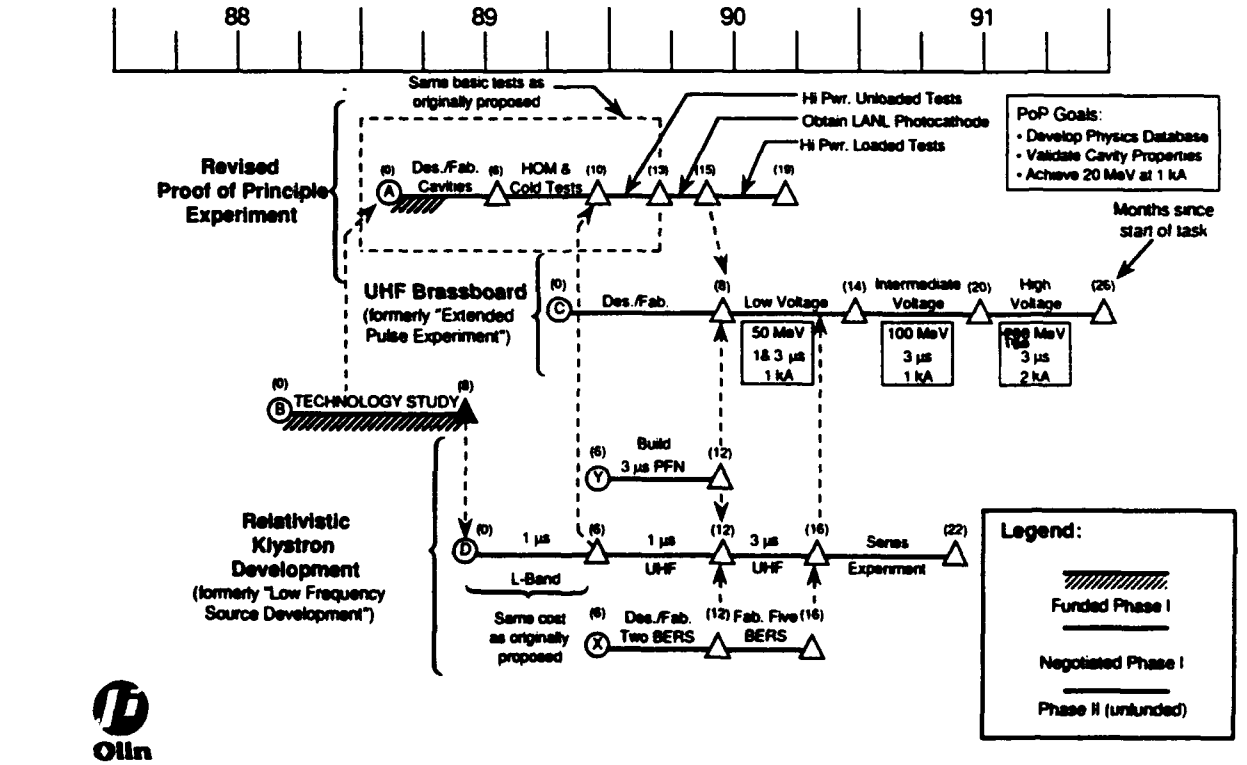

Selected Technology Extrapolations for Three HCRF Subsystems

Subsystem	Parameter	Brassboard Demonstrator Requirement	Far-Term SBFEL Requirement	Present State-of-the-Art*
Main Electron Accelerator	Gradient	20 MV/m	20 MV/m	5 MV/m
	Micropulse current	2 kA	2 kA	0.6-1.6 kA
	Micropulse charge	10^{-7} C	10^{-7} C	10^{-8} C
	Macropulse current	50 A	50 A	0.1 A
	Beam loading fraction	0.95	0.95	0.90
	Transverse Q	< 100	< 100	100-1000
	Wall loading	NA	350 kW/m	200-400 kW/m
	rf cycles per micropulse	1	1	
Relativistic rf Source	Frequency	500 MHz	500 MHz	1328 MHz
	Number of klystrons	10	10	1
	Peak rf power (per klystron)	1 GW	2 GW	0.5 GW
	Overall average rf power	10 GW	10 GW	0.5 GW
	Micropulses per macropulse	--	58	--
	Micropulse duration	--	30 ns	140 ns
	Macropulse duration	3.5 μs	3.5 μs	140 ns
	Electronic efficiency (per klystron)	0.5	0.5	0.4
	Overall electronic efficiency	0.9	0.9	--
	Amplitude stability	1%	1%	2%
	Phase stability	1%	1%	2%
	Macropulse repetition rate	--	3.3 kHz	--
	Lifetime	10^2	5 (10^6) shots	10^2-10^3
Relativistic Electron Beam Generator for rf Source	Electron energy	500 keV	500 keV	> 1 MeV
	Beam power per micropulse	2 GW	4 GW	> 10 GW
	Short pulse repetition rate	NA	20-30 MHz	10 MHz
	Short pulse duration	NA	30-50 ns	50 ns
	Long pulse repetition rate	3.3 kHz	3.3 kHz	5 kHz
	Long pulse duration	3.5 μs	3.5 μs	3 μs

*Not all state-of-the-art parameters achieved simultaneously

Olin

Conclusions

- The HCRF concept offers significant advantages to the SBL program
- Our analyses indicate that the basic concept is sound
- Further analysis and experiments are needed to validate the concept fully and to provide design data
- A program plan exists that maximizes the use of recent technology and leverages government funding considerably
- Program is only partially funded now. Proof-of-principle experiment needs to be started to preserve momentum.

Olin

HCRF Accelerator Efficiency and Beam Quality Issues

DAVID PRICE

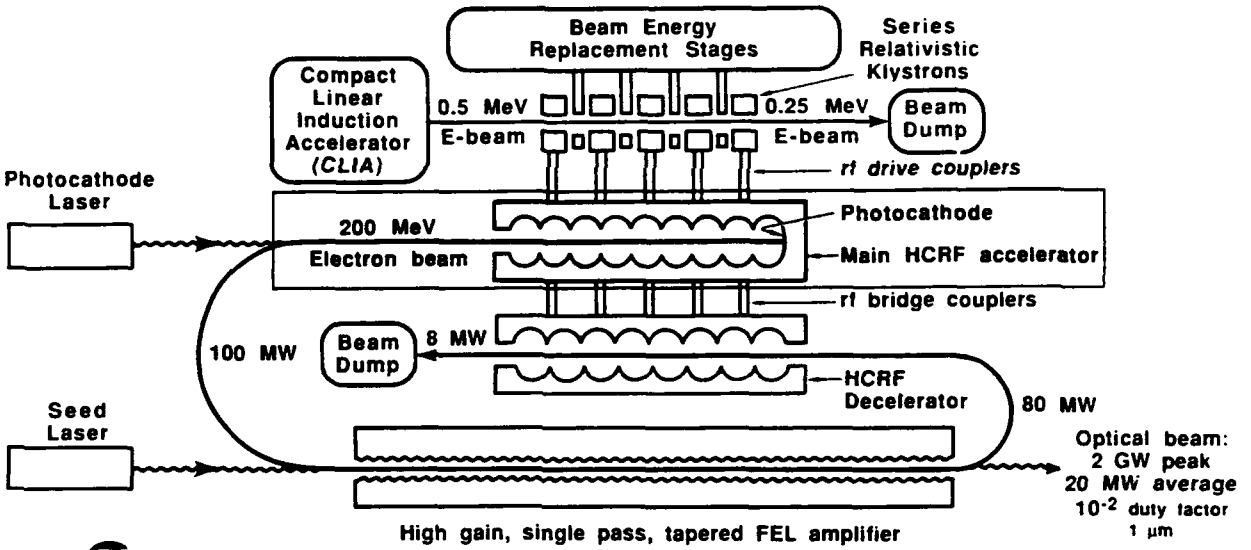

Olin

Key Accelerator Technology Issues Tree

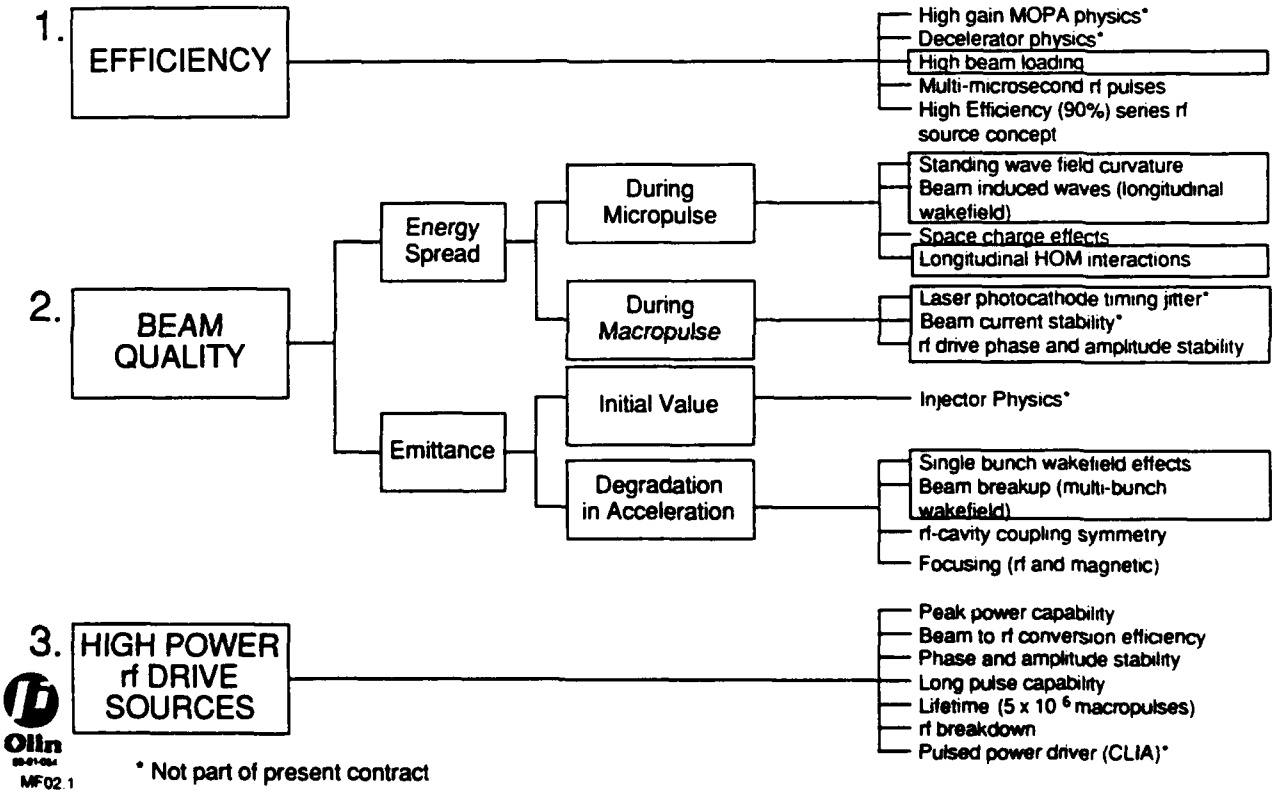

Olin

MF02.1

* Not part of present contract

1. Efficiency Issues

SUBSECTION OUTLINE

1.1 POINT DESIGN

1.2 PARAMETRIC DEPENDENCE OF RF → E-BEAM EFFICIENCY

1.3 PARAMETER OPTIMIZATION AND TRADEOFFS

Parameter	Conclusion
(1) Eg, gradient	• Peak rf electric field can be sustained • Transient thermal loading is not significant
(2) α, beam loading fraction	• Required implicit Q_0 values achievable • Single bunch loading should be estimated
(3) τ_0, rf pulse duration	• μs duration, HPM source development required

Olin

1.1 Point Design

ACCELERATOR PARAMETERS

Beam power during macropulse = 10^{10}W
(Avg. beam power 100 MW for 100 seconds)

Input Parameters:

Gradient	Eg = 20 MV/m
Frequency	f = 500 MHz
Pulse length	τ_0 = 3.0 μs
Accel. length	L = 10 m

Output Parameters:		SUPERFISH Output:
VSWR (beam on)	VSWR = 1.2	
Beam loading fraction	α = 0.95	
Shunt impedance	R/Q = 320 Ω/m*	R/Q = 296 Ω/m
Stored RF energy	U = 3.98 kJ	3.87 kJ
Minimum intrinsic Q	$Q_0 = 2.375\ (10^4)$	$3.8\ (10^4)$ (Al)
Beam Q	$Q_b = 1.25\ (10^3)$	
CW wall losses	$\langle P \rangle_{wall}$ = 526 kW/m	

*Longitudinal shunt impedance scaled from CEBAF design [H. A. Grunder, et al., "The Continuous Electron Beam Accelerator Facility," IEEE Particle Accelerator Conference, Washington, DC, p. 13 (1987)] $(R/Q)_{CEBAF}$ = 960, 1497 MHz.

Olin

1.1 Point Design (cont.)

BASELINE CELL DESIGN FOR 500 MHZ ACCELERATOR

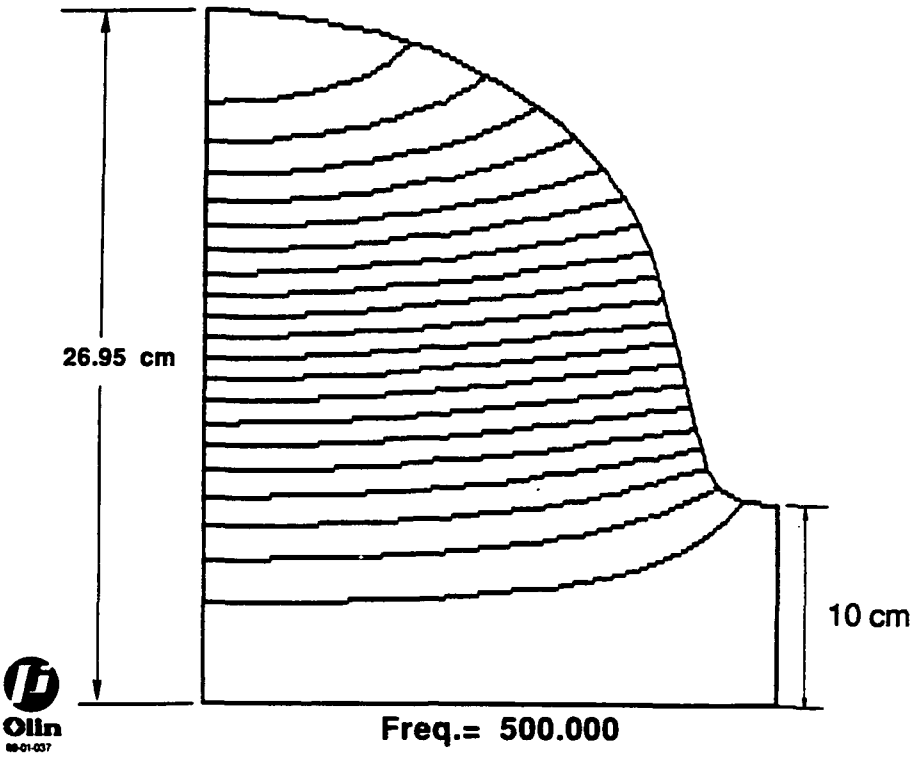

1.1 Point Design (cont.)

FIVE CELL CAVITY CONCEPT

- **Follows CERN SC design** (P. Bernard, et.al IEEE Trans. Nucl. Sci. Vol. NS-30, No. 4, August 1983) **but, with center cell input coupling.**

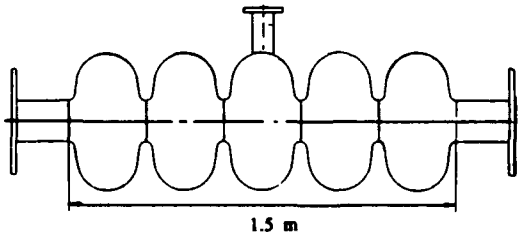

- **Initial SUPERFISH analysis shows suitable separation of normal modes**

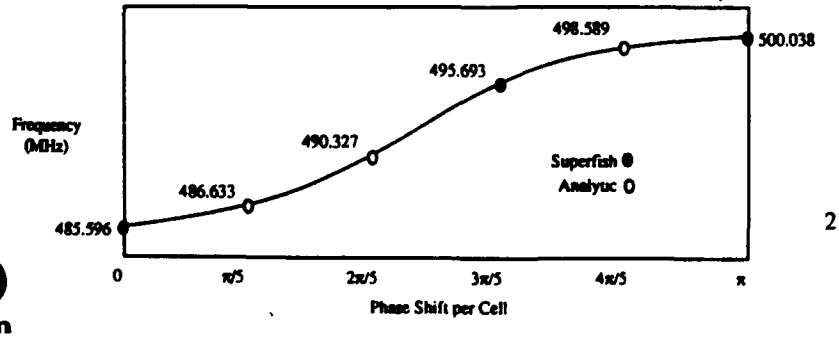

Bandwidth:

$$2\frac{(f_\pi - f_0)}{f_\pi + f_0} = 2.93\ \%$$

Olin
88-11-103

1.2 Parametric Dependence of RF → E-beam Efficiency

- The conversion efficiency from RF to e-beam power is the product of three factors

$$\eta = \left[\frac{4V}{(1+V)^2}\right] x [\alpha] x \left[1 - \frac{\tau_{fill}}{\tau_o}\right]^*$$

$$\left(\frac{\text{Coupled Power}}{\text{Source Power}}\right) x \left(\frac{\text{Beam Power}}{\text{Coupled Power}}\right) x \left(\frac{\text{Macropulse Duration}}{\text{rf Pulse Duration}}\right)$$

*(R. H. Miller, "Comparison of Standing-Wave and Traveling-Wave Structures," 1986 Linear Accelerator Conference Proceedings, SLAC-Report-303, p. 200).

$$\tau_{fill} = \tau \, Ln \left\{\frac{2\beta^{1/2} (RLP_{in})^{1/2}}{IRL}\right\}$$

$\tau = Q_o/\pi f (1 + \beta)$
f = frequency
Q_o = implicit Q
V = VSWR with e-beam on
β = VSWR with e-beam off
R = shunt impedance
L = accelerator length
I = macropulse current
P_{in} = coupled power

Olin

Macropulse Energy Account (No Recirculation)

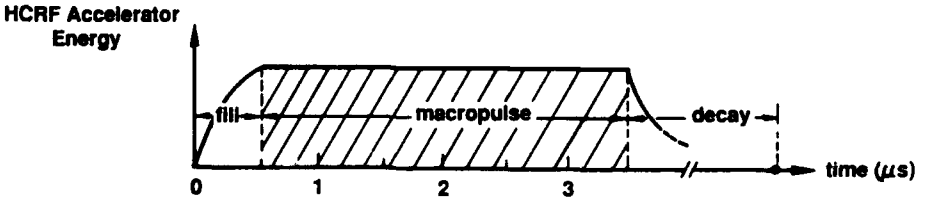

Channels	RF Energy (kJ)
Output e-beam	30
Stored	4
Wall Load	1.5
Fill time mismatch	1.0

$$\text{eff} = \frac{30}{30 + 4 + 1.5 + 1.0} = 82\%$$

Olin

1.3 Parameter Optimization and Tradeoffs

1.3.1 Variation of (RF → e-beam) efficiency, η, with VSWR (beam on), V, and beam loading fraction, α

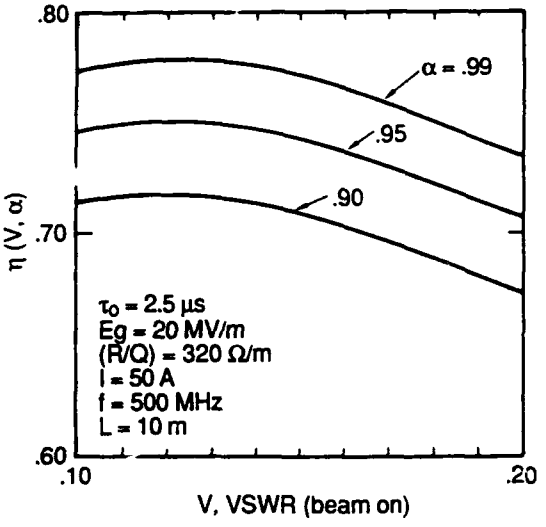

- Broad maximum near V = 1.2
- Two issues:
  - (i) High reflected power during filling time requires:
    - (a) high power isolator, with a
    - (b) high power load
  - (ii) Maximum achievable beam loading fraction limited by cavity material

Olin

Beam Loading Fraction = 95% with (Real Estate) Gradient = 20 MV/m in Aluminum Cavities is Achievable

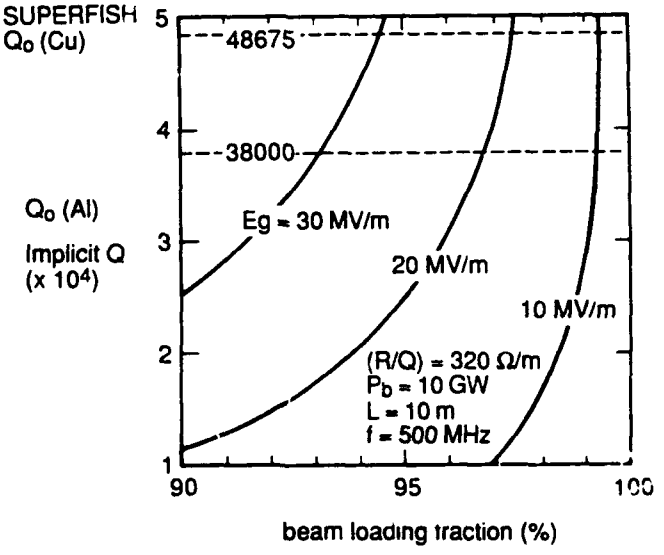

- Must evaluate longitudinal energy spread due to single bunch loading to further assess feasibility of very high beam loading fraction.

Olin

1.3 Parameter Optimization and Tradeoffs (cont.)

1.3.2 Variation of efficiency with (real estate) gradient, Eg, and rf pulse duration, τ_o

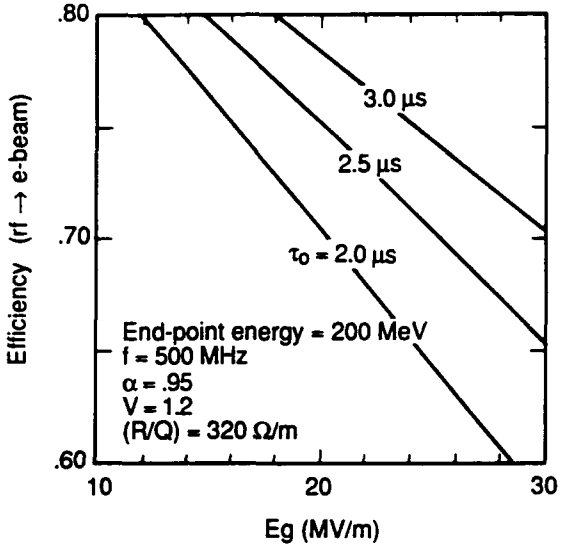

- Higher gradients require longer accelerator fill times
- Must extend rf pulse duration to preserve efficiency
- Two issues:
  - (i) Feasibility of 20 MV/m gradient
  - (ii) Development of μs HPM source

Olin

89-01-035

The Peak Electric Field in HCRF Can Be Sustained in rf Structures Without Breakdown

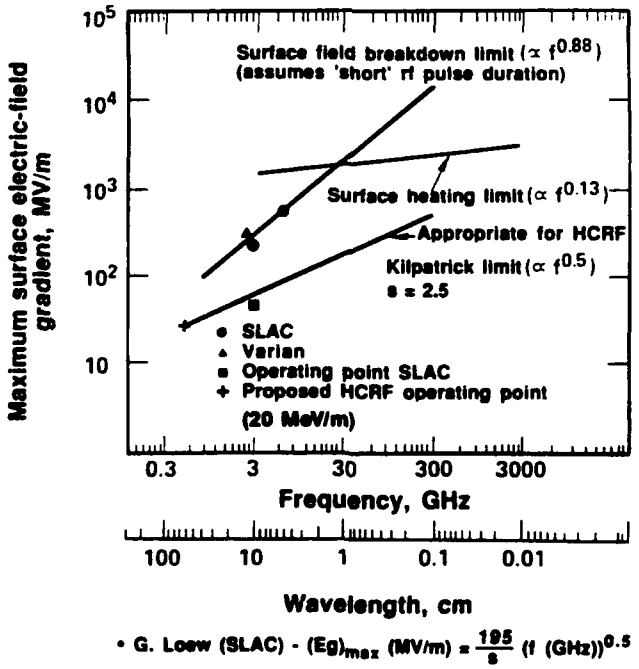

• G. Loew (SLAC) - $(Eg)_{max}$ (MV/m) = $\frac{195}{s}$ (f (GHz))$^{0.5}$

Olin

Peak Wall Loading (Per RF Pulse) Does Not Lead to Local Thermal Problems

- Analysis follows that from I. Wilson, W. Schnell, and H. Henke, "Design and Fabrication Studies of High Gradient Accelerating Structures for the CERN Linear Collider (CLIC)," 1988 Linear Accelerator Conference, Williamsburg, VA, Oct. 3-7, 1988.
- Maximum local heat flux (at position of maximum wall surface H_θ component) ~ 2 kW/cm^2
- Maximum surface temperature rise (per rf pulse) ~ 1.8°C

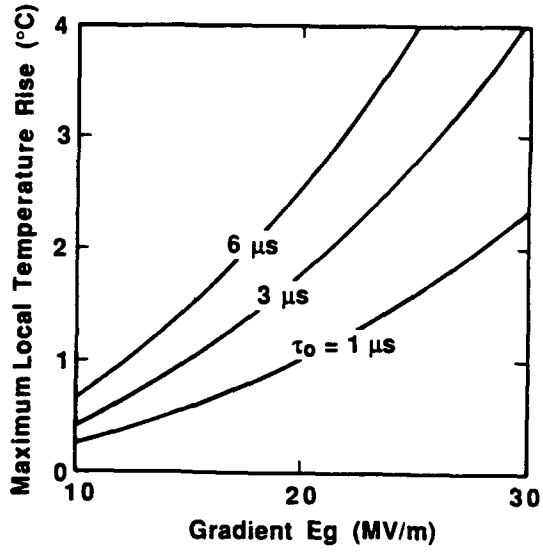

Olin
89-01-042

2. Beam Quality Issues

SUBSECTION OUTLINE

2.1 Energy Spread

2.1.1 During the Micropulse (FEL Limitation = 0.5%)
- Standing wave field curvature
- Beam induced waves (longitudinal wakefield)
- (Longitudinal HOM interactions)

2.1.2 During the Macropulse (FEL Limitation = 2.0%)
- Laser photocathode timing jitter
- Beam current stability
- rf drive phase and amplitude stability

Parameter	Conclusion
$\left(\frac{\nabla\gamma}{\gamma}\right)$, spread within micropulse micro	• .5% (FEL constraint can be achieved by injecting ahead of RF crest. Existing technology sufficient
$\left(\frac{\nabla E}{E}\right)$, spread within macropulse	• Need moderate laser technology extrapolation to achieve 2 % (FEL constraint)

Olin
89-01-051

2.1.1 (Energy Spread) During the Micropulse

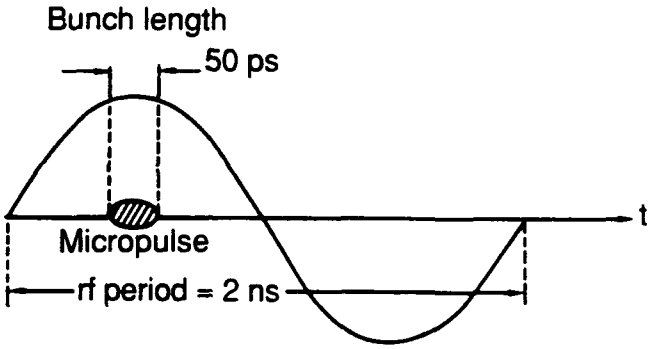

- $\frac{\Delta\gamma}{\gamma} \approx 0.31\%$
- This value consistent with more precise calculation which employs SUPERFISH calculated field structure
- This value also obtained with PARMELA

Olin

2.1.1 (Energy Spread) During the Micropulse

BEAM INDUCED WAVES (LONGITUDINAL WAKEFIELDS)

- Energy variation over a single (zero length) bunch due to TM_{010} fundamental mode

$$\frac{\Delta\gamma}{\gamma} = \frac{1}{2}\omega\left(\frac{R}{Q}\right)\frac{q}{Eg} \qquad \begin{cases} \omega = 2\pi\ (500\ \text{MHz}) \\ \left(\frac{R}{Q}\right) = 300\ \frac{\Omega}{m} \\ q = 10^{-7}\ \text{coul} \\ Eg = 20\ \text{MV/m} \end{cases} \qquad \rightarrow \left(\frac{\Delta\gamma}{\gamma}\right)^{\text{fund}}_{\text{micro}} = 0.24\%$$

- The fundamental theorem of beam loading: (P. B. Wilson, "High-Energy Electron Linacs: Applications to Storage Ring RF Systems and Linear Colliders," SLAC-PUB-2884, 1982) gives estimate lower by 1/2
- The total energy variation (over a micropulse) due to the fundamental and all HOM:

$$\left(\frac{\Delta\gamma}{\gamma}\right)_{\text{micro}} < 2\%$$

Olin

2.1.1 (Energy Spread) During the Micropulse

METHODS TO SUPPRESS BEAM INDUCED SPREADING

- **Balance the variation by moving the bunch ahead of the rf by θ degrees where:**

$$\left(\frac{\Delta\gamma}{\gamma}\right)_{micro} \approx \Delta\theta\tan\theta$$

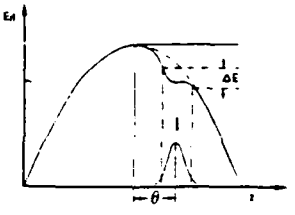

For the point design, $\theta \lesssim 6°$

- **Investigate: "Minimizing the Energy Spread Within a Single Bunch by Shaping its Charge Distribution," (G. Loew and J. Wang, SLAC/AP-25 1984).**

Olin

2.1.2 (Energy Spread) During the Macropulse

LASER PHOTOCATHODE TIMING JITTER

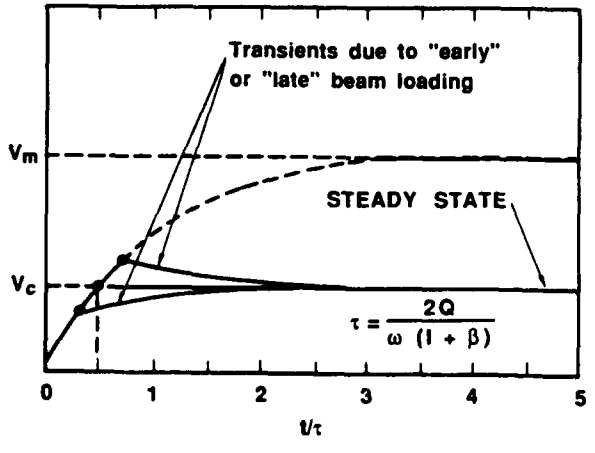

- Energy spread, $\frac{\Delta E}{E}$ due to timing jitter, Δt: $\frac{\Delta E}{E} \approx \frac{\Delta t}{2\tau_{fill}}$
- For the point design parameters: 0.1%/1 ns
- Nd YAG drive laser for LANL photocathode: temporal jitter = 4 ps

Olin

Therefore, demonstrated · laser technology easily fulfills HCRF timing jitter requirements.

2.1.2 (Energy Spread) During the Macropulse

BEAM CURRENT STABILITY

- Beam loading fraction scales proportionally with micropulse current, i:

$$\frac{\Delta E}{E} = \frac{\Delta i}{i} \approx 0.1\%$$

- Energy spectrum for 10 μs train of 28 ps micropulses through LANL two-cavity (photocathode) linac*

  1300 MHz
  10-40 π mm • mrad
  $> 600 \frac{A}{cm^2}$
  13.2 nC (from 1 cm^2)

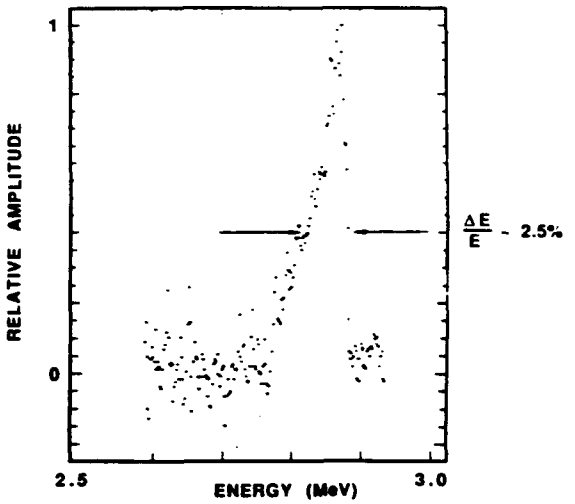

Therefore, demonstrated injector technology within an order of magnitude of HCRF requirements

Olin

* R. L. Sheffield, et al., "rf Photoelectron Gun Experimental Performance," 1988 Linear Accelerator Conference, Williamsburg, VA, Oct. 3-7, 1988.

2.1.3 (Energy Spread) During the Macropulse

rf Drive Phase and Amplitude Stability

- Phase jitter destroys micropulse - RF sync.

$$\frac{\Delta E}{E} \approx \phi\Delta\phi \approx 1\%$$

Therefore, for the point design: $\Delta\phi \sim \frac{1}{10}$ radian

- Beam loading fraction scales proportionally with RF drive amplitude, P:

Therefore: $\frac{\Delta E}{E} \approx \frac{\Delta P}{P} \approx 1\%$

Relativistic Klystrons· have demonstrated this stability at 0.5 GW.

Olin

·M. Friedman, J. Krall, Y. Y. Lau, and V. Serlin, "Externally Modulated Intense Relativistic Electron Beams," J. Appl. Phys. 64, 3353, 1988

2. Beam Quality Issues

SUBSECTION OUTLINE

2.2 Emittance

2.2.1 Degradation in Acceleration

- Single bunch wakefield effects
- Beam breakup (multi-bunch wakefield)

Parameter	Conclusion
$Q_\perp$, transverse mode Q	$Q_\perp \lesssim 100$ required to transport 50 A macropulse current
I, macropulse current	With sufficient damping design macropulse current is less than BBU thresholds. May require strong focusing in initial sections to control emittance growth

Olin
89-01-058

2.2 (Emittance) Degradation in Acceleration

SINGLE BUNCH WAKEFIELD EFFECTS (NO TRANSVERSE FOCUSING)

- Analysis follows: F. S. Felber, D. Mitrovich, R. K. Cooper, and P. B. Wilson, "Beam Breakup Instability in rf Linacs," IEEE Trans. Nucl. Sci. Vol. NS-30, Aug. (1983).
- Model neglects all but lowest frequency (dipole) mode of magnetic field generated by charge q, traveling a distance χ_o off-axis. The deflection a distance z down the accelerator:

$$\left(\frac{\chi}{\chi_o}\right) = 1 + \alpha z \,, \quad \alpha = \frac{q}{\varepsilon_o E g \, (0.4\,\lambda)^3}$$

- For the point design:

$$\left(\frac{\chi}{\chi_o}\right)_{z=L} = 1.4$$

- **Beam transmission is not threatened and emittance is not significantly degraded**

Olin
89-01-071

Required Brightness Not Threatened by Single Bunch Wakefields

- In the limit of no focusing*, the maximum emittance:

$$\varepsilon_{max} = \pi\alpha\,\chi_o^2\,(1 + \alpha L) = (0.18)\,\chi_o^2\ \text{m} \bullet \text{rad}$$

- To achieve the FEL brightness: $B = 2(10^{10})\ \text{A/m}^2 \bullet \text{rad}^2$ with a micropulse current, i = 2 kA, the required alignment:

$$B \le \frac{i}{(\varepsilon_{max}^2)(\gamma^2 - 1)}\,B \Rightarrow \boxed{\chi_o \le 2\ \text{mm}}$$

* With transverse focusing consistent with that observed in PARMELA:

$$\varepsilon_{max} = \frac{2}{L}\chi_o^2 = (0.2)\,\chi_o^2\ \text{m} \bullet \text{rad}$$

Olin

2.2 (Emittance) Degradation in Acceleration

BEAM BREAKUP (MULTI-BUNCH WAKEFIELD)

- Regenerative beam breakup (P. B. Wilson, "High-Energy Electron Linacs: Applications to Storage Ring rf Systems and Linear Colliders, "SLAC-PUB-2884, 1982)

  For a CW* standing wave accelerator, the starting current threshold (above which the backward wave-deflecting mode grows):

$$I_{Reg} = \frac{0.025\,\lambda^2 E_a}{Q_\perp\,L}.$$

Olin

2.2 (Emittance) Degradation in Acceleration (cont.)

BEAM BREAKUP (MULTI-BUNCH WAKEFIELD) (cont.)

For the point design parameters, the 50 A macropulse current is below this threshold if:

$$Q_{\perp} \leq 360 .$$

(Alternately, for $Q_{\perp} = 100$, $I_{Reg} = 180$ A)

---

* The starting current for a finite length beam, $I(\tau_p)$ is increased by the ratio:

$$\frac{I(\tau_p)}{I_{Reg}} = 1 + F_e \left(\frac{\tau}{\tau_p}\right),$$

where τ is the characteristic time of the structure and F_e is the amplification factor required to produce breakup from noise (typically $F_e \sim 10$ to 20). (For $Q_{\perp} = 100$, $F_e = 10$, $I(\tau_p) = 500$ A)

Olin

2.2 (Emittance) Degradation in Acceleration

BEAM BREAKUP (MULTI-BUNCH WAKEFIELD)

- Cumulative Beam Breakup

  For a constant gradient, pulsed accelerator without focusing the macropulse current which generates 20 e-fold growths over the accelerator length

$$I_{cum} \approx \frac{30\ Eg\ \lambda^2}{Lc\tau_p\ (R/Q)_{\perp}}$$

The point design parameters and $\left(\frac{R}{Q}\right)_{\perp} \sim 200\ \frac{\Omega}{m}$

$$I_{cum} \approx 120\ kA$$

Should investigate the effect of strong focusing

Olin

Stabilize Beam Breakup with Quadrupole Focusing

- (Saturated) cumulative beam breakup for an rf linac with side coupled cavities, utilizing quadrupole focusing* *

$$\left(\frac{x}{x_o}\right) \alpha \exp(\Gamma^{sat}),\ \Gamma^{sat} = \frac{n}{200} kQ_{\perp} \left[\frac{I}{17(10^3)}\right]$$

where n is the number of accelerating cells and k the coupling factor $\left(k = 10^{-10}\ \omega L\left(\frac{R}{Q}\right)_{\perp}\right)$.

- For the point design with $\left(\frac{R}{Q}\right)_{\perp} = 100\ \frac{\Omega}{m}$, $\Gamma^{sat} \approx 3$

Only three e-folds over the accelerator length

Olin 89-01-142

* V. K. Neil, L. S. Hall, and R. K. Cooper, "Further Theoretical Studies of the Beam Backup Instability," Particle Accelerators 9, 213 (1979)

HCRF Accelerator Efficiency and Beam Quality Issues

PRINCIPAL CONCLUSIONS

Issue	Principal Concern	Conclusion
Efficiency	High Beam Loading	• Assumed 20 MV/m gradient does not generate unreasonable localized thermal loads or electric stresses
Beam Quality	Longitudinal HOM Interactions	• Desire for high efficiency and small energy spread accents the importance of HPM source development. Injector requires only moderate extrapolation.
	BBU (Multi-bunch Wakefield)	• Beam will propagate through accelerator. Strong focusing required to limit emittance degradation

Olin 89-01-046

Accelerator Extrapolations

	Parameter	Brassboard Demonstrator Requirement	Far-Term SBFEL Requirement	Present State-of-the-Art
Injector	Micropulse charge	10^{-7} coul	10^{-7} coul	10^{-8} coul
	Micropulse current	2 kA	2 kA	600 A
	Repetition rate	500 MHz	500 MHz	108 MHz
	Lifetime	months	years	months
(Room-Temperature) Accelerating Structure	Accelerating gradient	20 MV/m	20 MV/m	5 MV/m
	Micropulse current	2 kA	2 kA	1.6 kA[1]
	Macropulse current	50 A	50 A	100 mA[2]
	Beam loading fraction	0.95	0.95	0.90[3]
	Transverse Q	< 100	< 100	100-1000
	Wall loading	--	550 kW/m	200-400 kW/m

[1] S. Takeda, et al., "High-Current Single Bunch Electron Linear Accelerator," IEEE Trans. Nucl. Sci., Vol. NS-32, No. 5, Oct., 1985.

[2] A. H. Lumpkin, et al., "On-Line Electron Beam Measurements for the Los Alamos Free-Electron Laser," IEEE Particle Accelerator Conference, Washington, DC, March 16-19, 1987.

[3] J. McKeown, et al., "High Power, On-Axis Coupled Linac Structure," Proceedings of the 1981 Linear Accelerator Conference, Santa Fe, New Mexico, Oct. 19-23, 1981.

Olin

Beam Transport in the HCRF

Robert J. Kares

Berkeley Research Associates
P O Box 241
Berkeley, CA 94701

Topics to be discussed:

- SUPERFISH results for RF fields of a single cell operated in π mode
- Layout of the prototype accelerator
- Structure of the beam pulse from the injector
- Focussing effect of the RF fields
- Case without external focussing
  - Emittance growth and longitudinal energy spread
  - Effect of varying initial beam radius
- Case of external focussing with quad doublets
- Summary and directions for future work

SUPERFISH Results for RF Fields of a Single Cell in π Mode

π Mode Field Lines in right half cell:

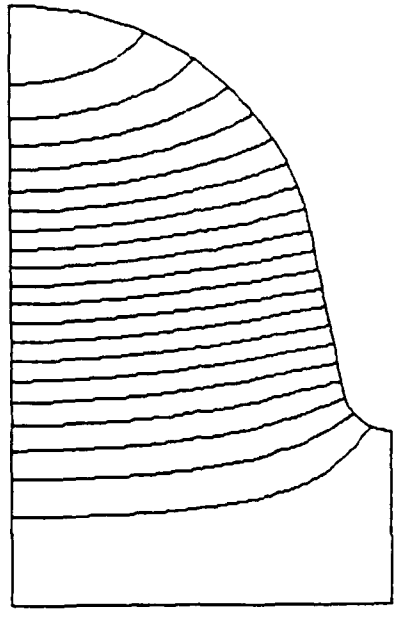

Full cell length L = 30 cm

π mode f = 500.038 MHz

Q = 48,675

Fourier Representation of Fields in π Mode

$$E_z(r,z,t) = E_0 \sum_{n=1}^{N} a_n I_0(k_n r)\cos\left[(2n-1)\frac{\pi z}{L}\right]\sin(\omega t + \phi_0)$$

with

$$k_n^2 = \left[(2n-1)\frac{\pi}{L}\right]^2 - \left[\frac{\omega}{c}\right]^2$$

Similarly for $E_r(r,z,t)$ and $B_\theta(r,z,t)$

- PARMELA uses first 14 terms in expansion to represent fields
  $a_1 = 1.55187 \quad a_2 = -0.10271 \quad a_3 = 0.01753$ ...
- Dominant term is n = 1 with small admixture of higher harmonics

$$\left[\frac{a_2}{a_1} = 6.6\,\%\right]$$

Maximum E_z Field Profile on Axis in Half Cell

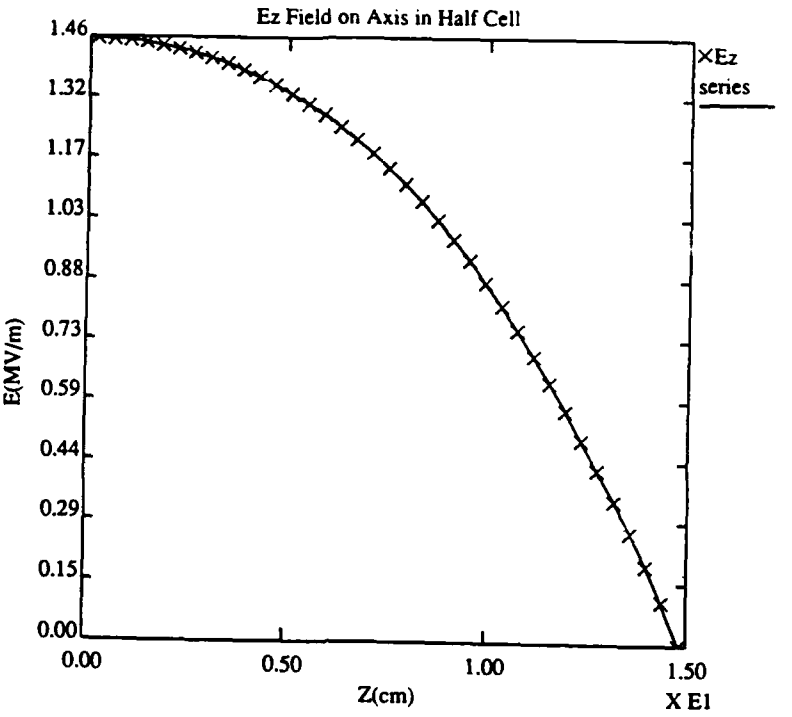

Geometrical Layout of Prototype Accelerator

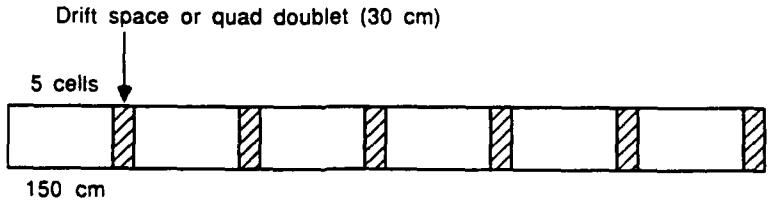

- Consists of 6 stages with 5 accelerating cells/stage
- Successive stages are separated by 30 cm gap containing either a drift space or quad doublet
- Effective accelerating gradient = 20 Mev/m
- Will separately consider two cases
  - No external focussing
  - External focussing with quad doublets

Structure of the Beam Pulse from the Injector

We assume:

- $B_N = 2\times10^{10}$ Amp/m^{2}rad^2 = $\left(\frac{2I}{\pi^2 \varepsilon_N^2}\right)$
- Flat current profile with I = 2 kA
- Hence initial normalized edge emittance = 142 mm-millirad
- 56 ps cylindrical pulse (10 deg in RF phase) with Q = 111 nC
- Pulse is monoenergetic with initial KE = 20 Mev
- Will examine 2 cases for the initial radius of the pulse, r_0 = 2 mm and r_0 = 1 cm

Focussing Effect of RF Fields

Initial beam X'-X and X-Y cross-sections for a case with r_0 = 1 cm and no external focussing:

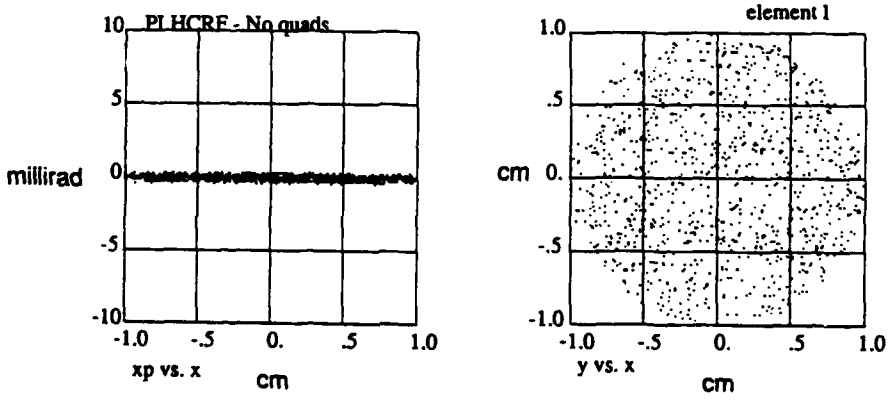

- RF E_r,B_θ fields exert a strong transverse focussing effect on the pulse

Beam X-Y Cross-section After Each Accelerator Stage for the Case

r_0 = 1 cm with No External Focussing

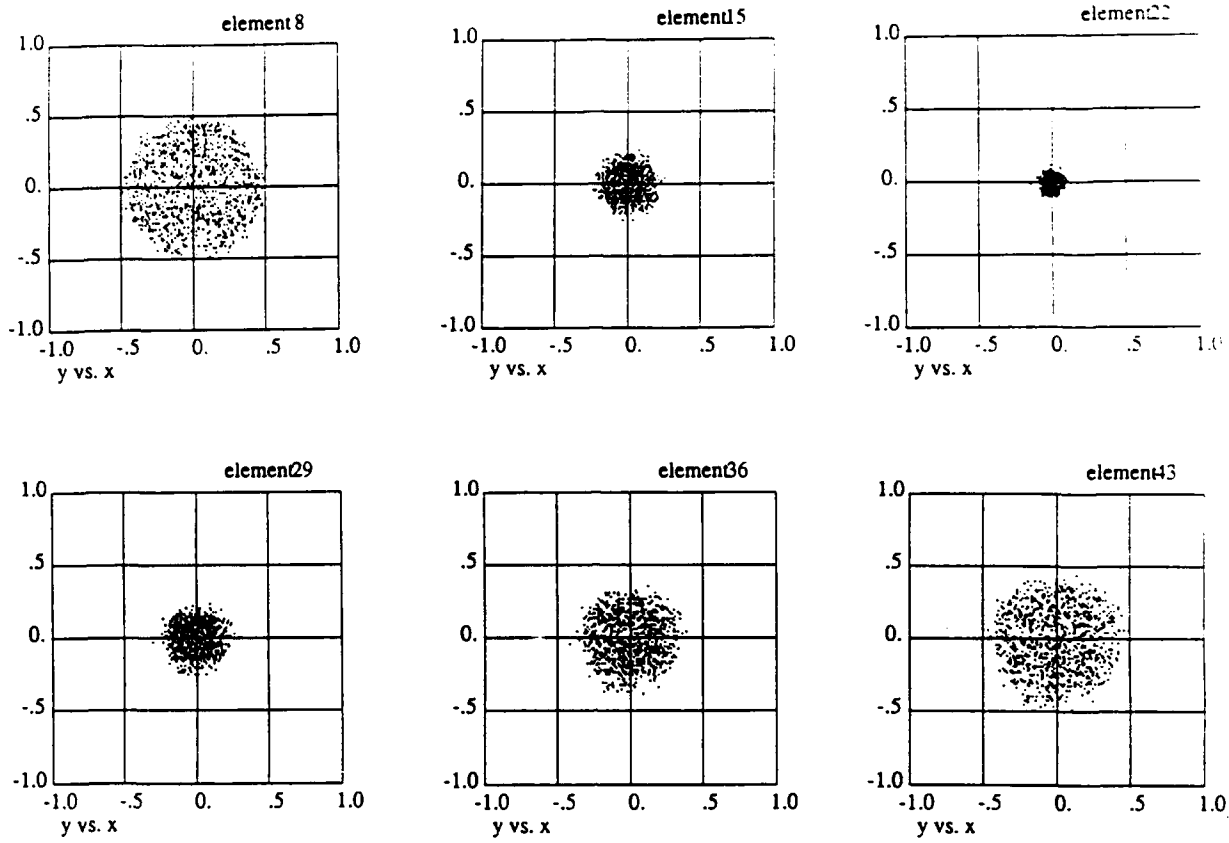

A Simple Theory of RF Focussing in π Mode

- Take $\beta_z = 1$
- Retain only the n = 1 term in the Fourier expansion of the fields so that:

  E_z is independent of r

  E_r and B_θ are linear in r

- For a particle in phase with the RF field find $\gamma(\phi)$ in closed form,

$$\gamma(\phi) = \gamma_0 + \alpha\left[\phi - \tfrac{1}{2}\sin(\phi)\right] \quad \phi = \omega t$$

where $\alpha = \dfrac{eE_0}{2mc\,\omega}$ = 3.742, the dimensionless RF strength parmeter

- Equation for transverse motion of particle becomes,

$$\frac{d}{d\phi}\left[\gamma(\phi)\frac{d\xi}{d\phi}\right] = -\alpha\sin(2\phi)\,\xi$$

where $\xi = \dfrac{r}{L}$, the normalized radial coordinate

Particle orbits starting from r = 1 cm (ξ = 1/30) with

r′ = -0.5, 0 or +0.5 millirad

(momentum spread consistent with the r_0 = 1cm case):

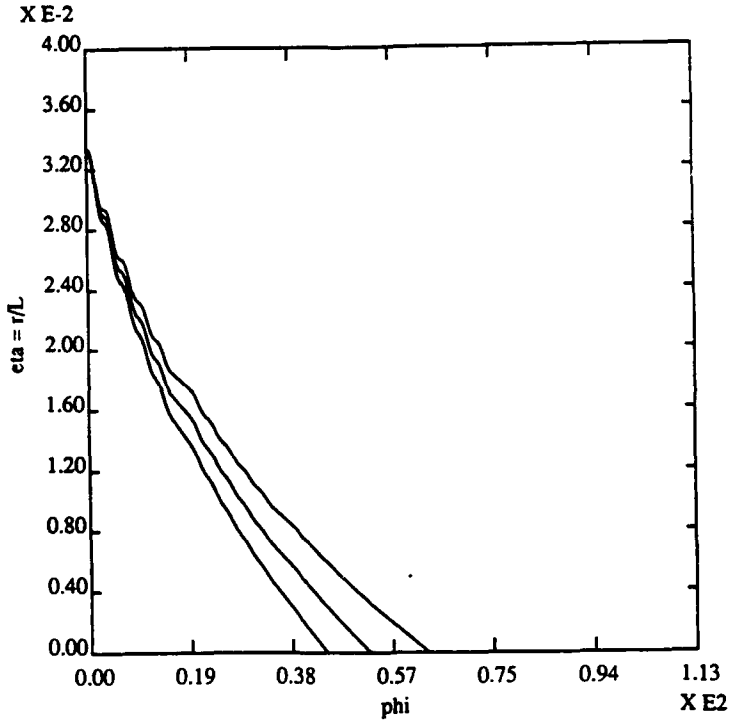

Particle orbits starting from r = 1 cm (ξ = 1/30) with

r′ = 0, 2, 4 or 6 millirad

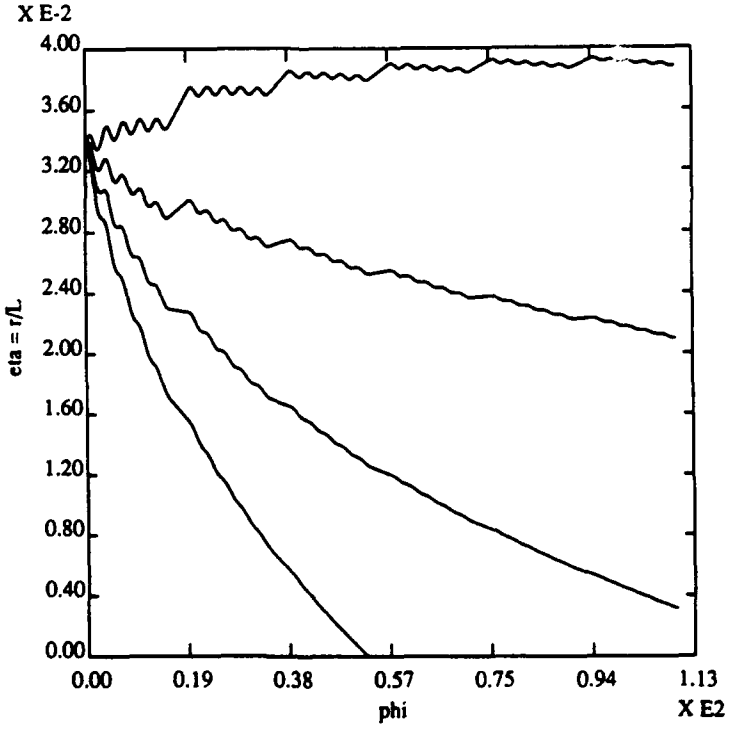

Initial Beam X'-X and X-Y Profile and X-Y Profiles After Accelerator Stages 3 and 6 for the Case r_0 = 2 mm with No External Focussing

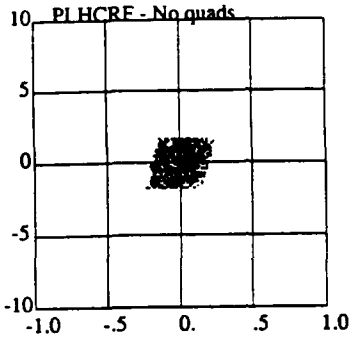

- Increased transverse momentum spread inhibits RF focussing

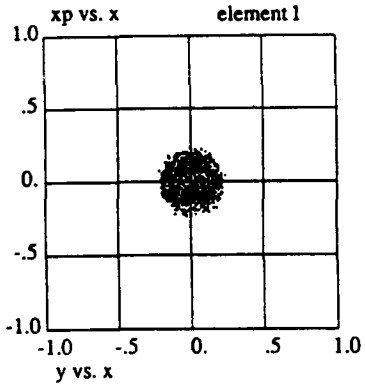

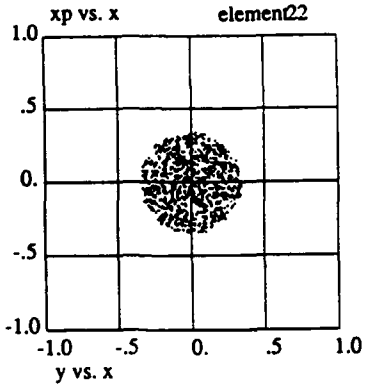

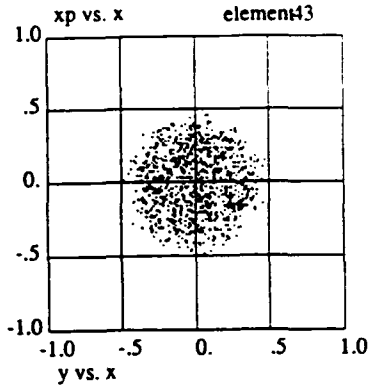

Particle orbits starting from r = 2 mm (ξ = .2/30) with

r' = 0 or 2 millirad

(momentum spread consistent with the r_0 = 2 mm case)

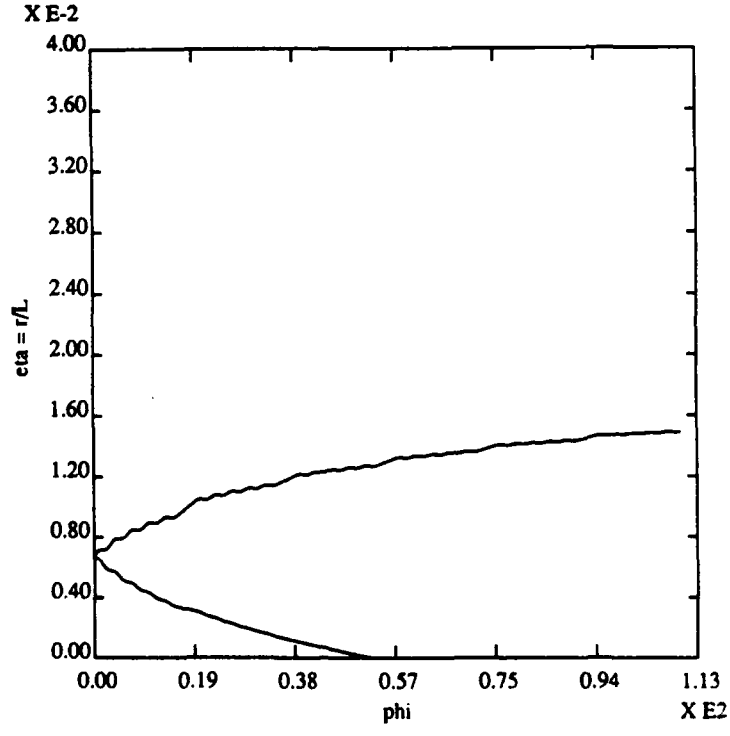

Transverse Emittance Growth with No External Focussing

- For r_0 = 1 cm an 11% growth in ε_N^{rms} is observed down the full length of the accelerator.
- This corresponds to a 19% reduction in B_N
- For r_0 = 2 mm the observed ε_N^{rms} growth is slightly higher, about 13%
- The space charge contribution to the transverse emittance growth is very small. The dominant contribution is from the RF fields.

Longitudinal Energy Spread

For a particle out of phase with the RF by $\Delta\phi$,

$$\gamma_f = \gamma_0 + \alpha\pi\cos(\Delta\phi)$$

After n cells,

$$\Delta\gamma = \gamma(\Delta\phi) - \gamma(0) = \alpha n\pi[\cos(\Delta\phi) - 1] \approx -\frac{n\pi\alpha}{2}\left(\Delta\phi\right)^2$$

- ΔE-$\Delta\phi$ distribution has a parabolic shape

Effect of Space Charge Forces on the ΔE -Δo Distribution

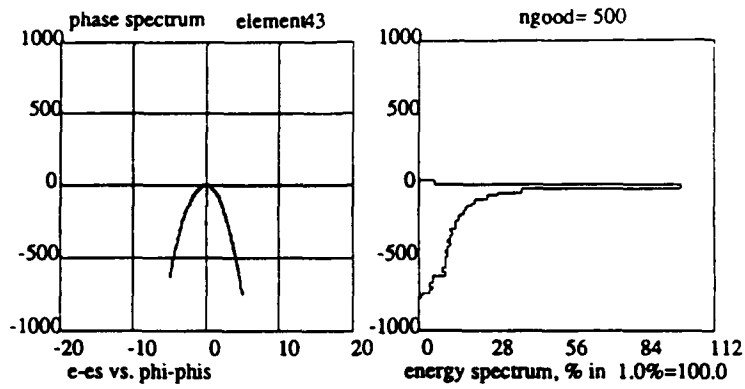

Without Space Charge

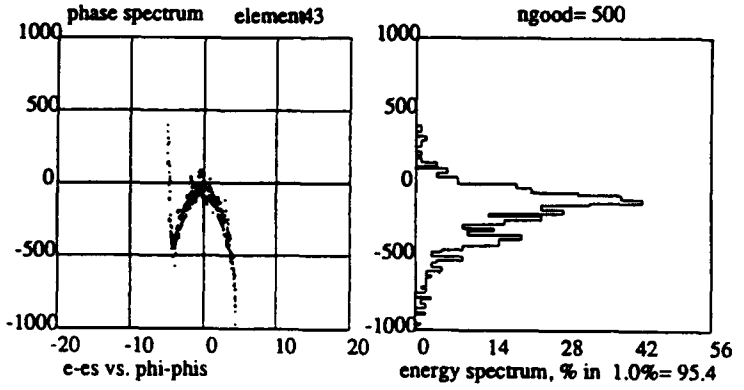

With Space Charge

Longitudinal Energy Spread (Continued)

- Space charge broadens body of distribution but has only a small effect on overall width

- With or without space charge effects,

  $\frac{\Delta E}{E}$ = 0.35 % at 10% of peak

Operation with Quad Doublet Focussing

- Choose $\frac{B_0}{\gamma a}$ = 4.062 G/cm for constant $\mu = 90^0$ down the length of the accelerator

Initial Beam X'-X and Y-X profiles for the r_0 = 2 mm case:

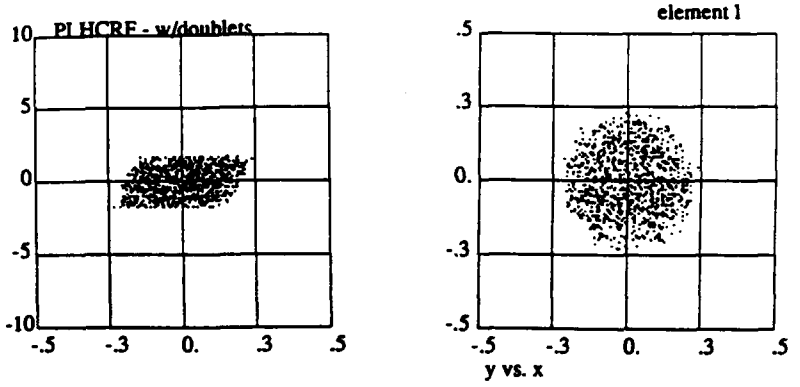

Beam X-Y Cross-section After Each Accelerator Stage for the Case r_0 = 2 mm with Quad Doublet Focussing

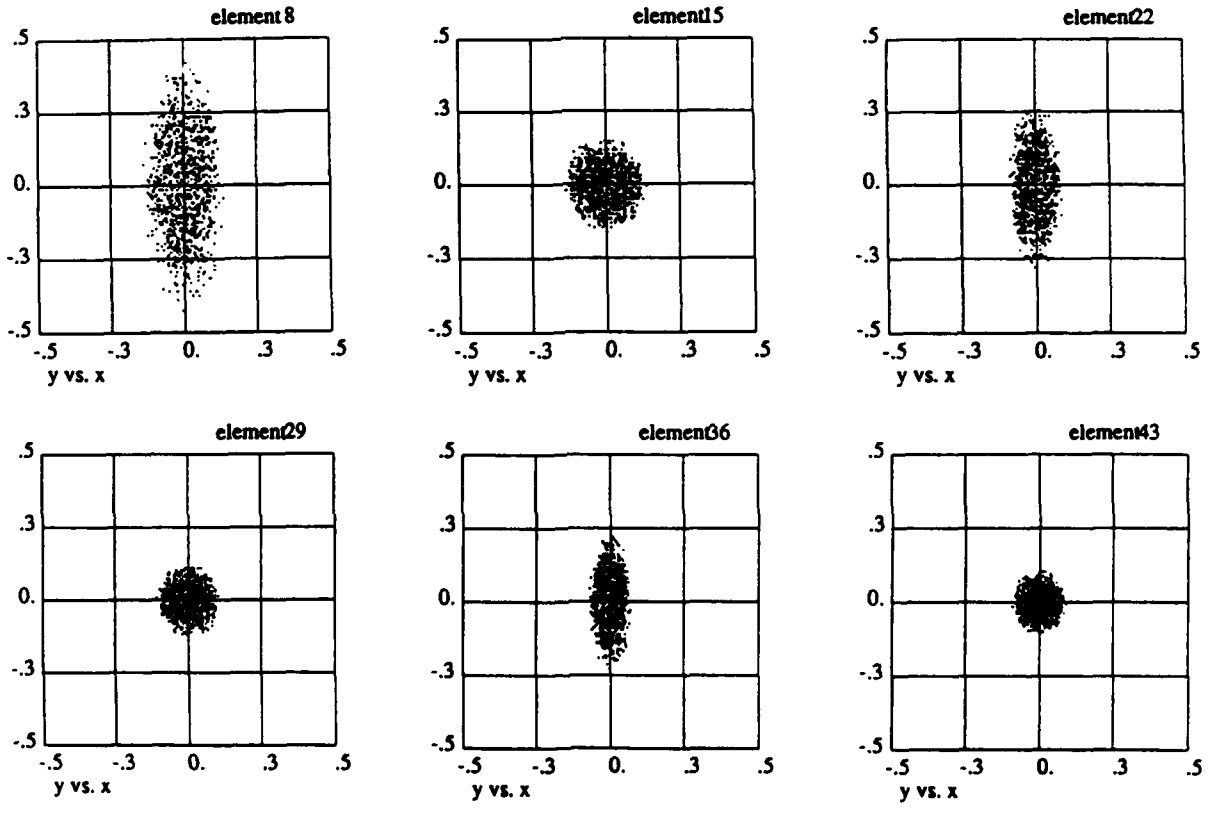

Emittance Growth and Energy Spread with Doublet Focussing

- For r_0 = 1 cm, ε_N^{rms} growth is about 26%
- However, for r_0 = 2 mm, growth is very small < 1%
- $\frac{\Delta E}{E}$ is about the same as for the case of no external focussing

Summary of Results to Date:

- Rf focussing is an important effect
- Simple theory of RF focussing is in good agreement with PARMELA results
- ε_N^{rms} growth ≈ 11% is observed in case of no external focussing. Inclusion of space charge forces has only a small effect on this result.
- $\frac{\Delta E}{E}$ ≈ 0.35% Space charge spreads out bulk of the $\Delta E - \Delta\phi$ distribution but has only a small effect on the width at 10% of peak.
- With quad doublet focussing and r_0 = 1 cm ε_N^{rms} growth ≈ 26% is observed.
  However, for r_0 = 2 mm the observed ε_N^{rms} growth is < 1%.

Directions for Future Work

- Study the BBU in greater detail.
- Study the laser-driven RF gun injector design.
- Continue to evaluate beam properties in the context of FEL performance.

A Program to Minimize BBU Effects

- Preliminary estimates of both cumulative and regenerative BBU growth have already been made. (They will be discussed elsewhere in this briefing.)
- To deal with cumulative BBU we will first study the relevant modes using URMEL.
- Then use Dick Cooper's BBU codes and theory to calculate growth along accelerator.
- Finally, reduce Q's of problem modes to suppress BBU growth to extent possible.
- For regenerative BBU we may be able to use MAFIA to study coupled-cavity problem.
- Once problem modes are identified, Cooper has theory and code to descibe BBU growth in coupled cavities.
- Fundamental constraint on BBU is set by FEL requirement that the beam not be displaced by more than about 10% of beam radius with r_b = 0.7 mm

A Program for Designing a Laser-Driven RF Gun Injector

- Apply recent analytic work of K. J. Kim at LBL to generate a rough design for a suitable laser-driven RF gun for the injector.
  - Estimate the exit rms ε, angular divergence and radius of pulse.
- Verify analytic estimates for gun with PARMELA calculations.
- Finally, use PARMELA to design a suitable transport system to bring the gun pulse up to 20 Mev.

PROTOTYPE FEL:

- Electron Beam:
  $\gamma mc^2 = 200$ MeV - electron beam energy
  $\Delta\gamma/\gamma = 0.005$ - energy spread
  $I = 2000$A - beam current
  $l_e = 100$ps - micropulse length
  $J_B = 2I/\pi^2\varepsilon_n^2 = 2\times10^6 \mathrm{A/cm^2 rad^2}$ - brightness
- Undulator:
  $\lambda_u \approx 5$cm - undulator period
  $K = e\bar{B}\lambda_u/2\pi mc^2 = 2.5$ - undulator parameter
  $L = 50$m - undulator length
  $N = 1000$ - # of undulator periods
  $\Delta\gamma/\gamma = 40\%$ - resonant energy taper
  $r_b \approx (\gamma\varepsilon\lambda_u/2\pi K)^{1/2} \approx 0.07$cm - beam radius
  $N_\beta = 6.4$ - number of betatron oscillations
- Radiation:
  $\lambda = 1\mu$m - radiation wavelength
  $w_0 \geq r_b$ - mode waist at beginning of undulator
- FEL:
  G(dB) ≈ 10.6dB/m - weak-field gain
  $\Delta\gamma/\gamma \approx \approx 0.02$ - gain bandwidth
  $N_{plasma} = 1$ - number of plasma oscillations
  $\eta = 20\%$ - FEL extraction efficiency
  $\varepsilon^* = 10^{-5}$cm-rad - critical emittance
  $\Delta\gamma^*/\gamma = 10^{-2}$ - critical energy spread
  $\sigma_z = 2\times10^4$ - slippage

RF Source Considerations

DAVID PRICE

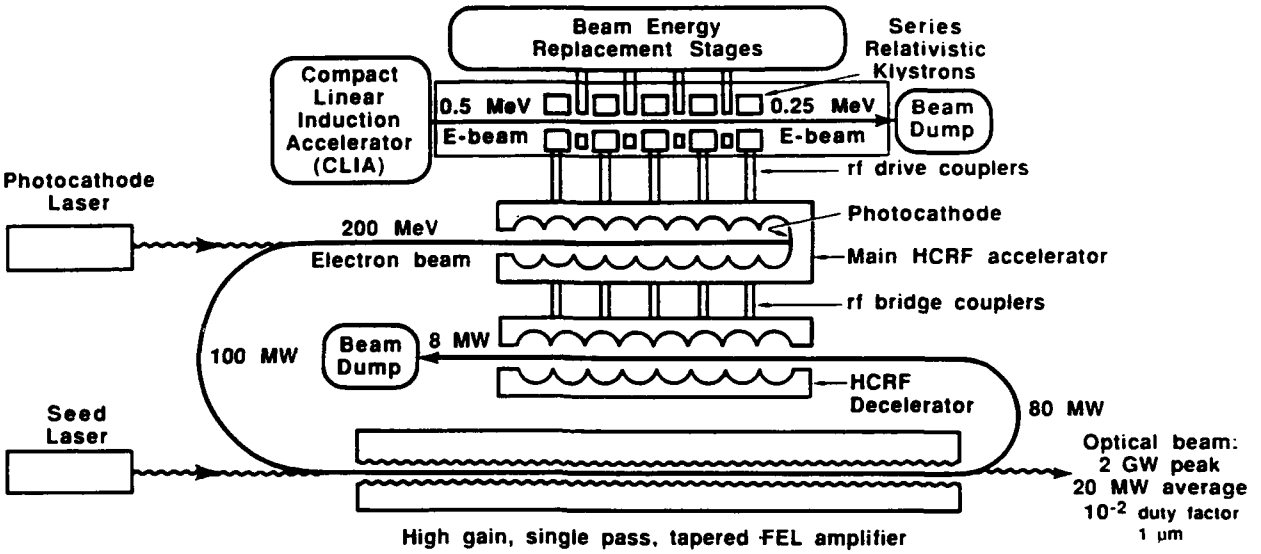

Olin

89-01-086

Key Accelerator Technology Issues Tree

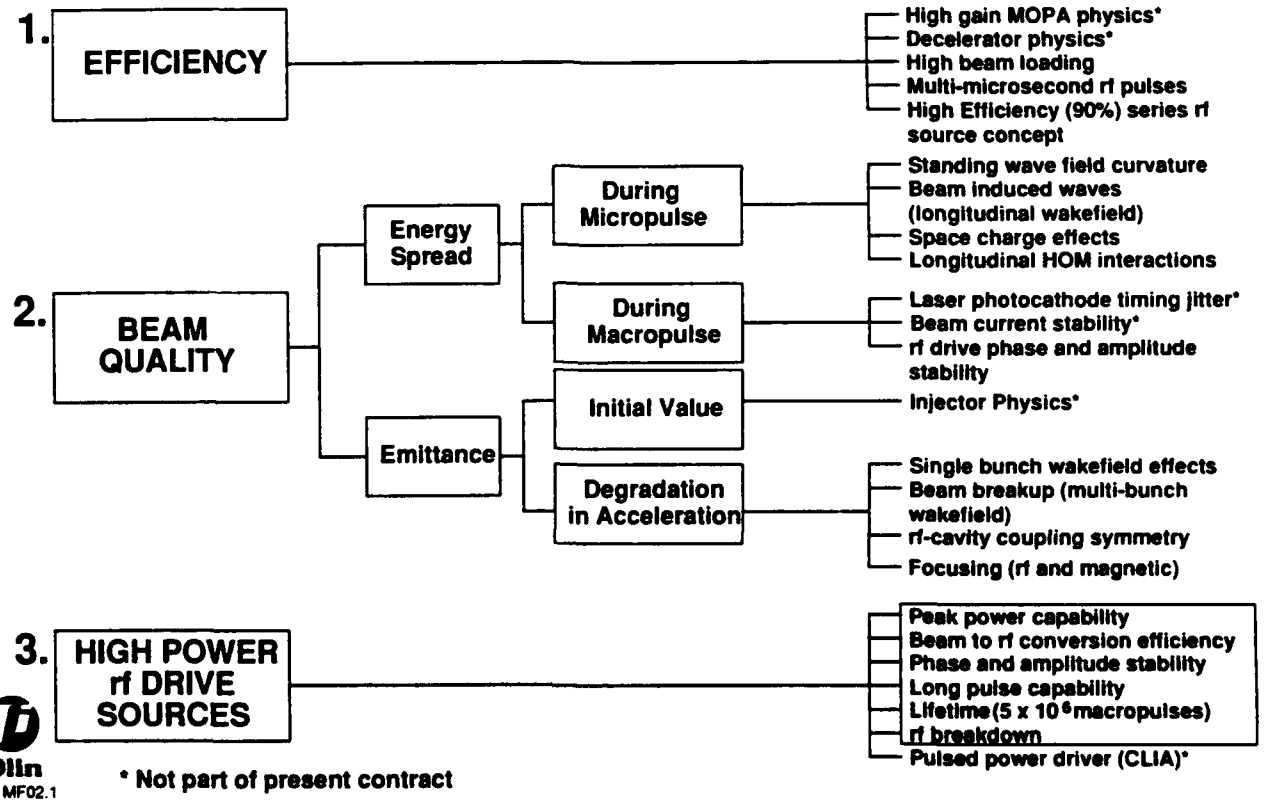

Olin

MF02.1

89-01-086

* Not part of present contract

RF Source Considerations

Section Outline

- Performance Requirements
- Demonstrated HPM Source Operation
- Electronic Efficiency Issues
- High Efficiency Series Relativistic Klystron Concept

Performance Requirements

• Peak Power Capability	10 GW
• Electronic Efficiency	90 %
• Phase Stability	2 %
• Amplitude Stability	1 %
• Pulse Duration	3.5 μs
• Repetition Rate	3.3 kHz
• Lifetime	5 (10^6) Shots

Demonstrated HPM Source Operation

		Brassboard Demonstrator Requirement	Relativistic Klystron[1]	Relativistic Magnetron[2]
Frequency	(MHz)	500	1328	2830
Peak Power Capacity	(GW)	10	0.5	3.6
Electronic Efficiency	(%)	90	40	30
Phase Stability	(%)	2	2	2
Amplitude Stability	(%)	1	2	(triangular pulse)
Pulse Duration	(ns)	3500	140	30
Repetition Rate	(kHz)	3.3	--	--
Lifetime	(no. shots)	5 (10^6)	--	--

1. M. Friedman, J. Krall, Y. Y. Lau, and V. Serlin, "Externally Modulated Intense Relativistic Electron Beams," J. Appl. Phys. 64, 3353 (1988).
2. H. Sze, B. Harteneck, J. Benford, T. S. T. Young, "Operating Characteristics of a Relativistic Magnetron with a Washer Cathode," IEEE Trans. Plasma Sci. Vol. PS-15, 327 (1987).

Olin
89-01-123

Demostrated HPM Source Operation

Further comparison of the NRL relativistic klystron and the PI relativistic magnetron.

	Klystron	Magnetron
Voltage	0.6 MeV	0.5 - 1 MV
Current	5 kA	3 - 10 kA
Magnetic Field	1 T	1 T
Extraction	Rectangular waveguide	Multiple rectangular waveguides
Pulse Duration Limitation	Drive pulse/ rf breakdown	Unknown
Electron Motion	Along field	Across field

The amplitude stability and the likelihood of extending the pulse duration of the relativistic klystron make it the less risky candidate for scaling

Olin
89-01139
MF02.1

Electronic Efficiency Issues

Relativistic Magnetron Efficiency Rule of Thumb:

(Experimental Efficiency) = 1/2 x (Theoretical Efficiency)

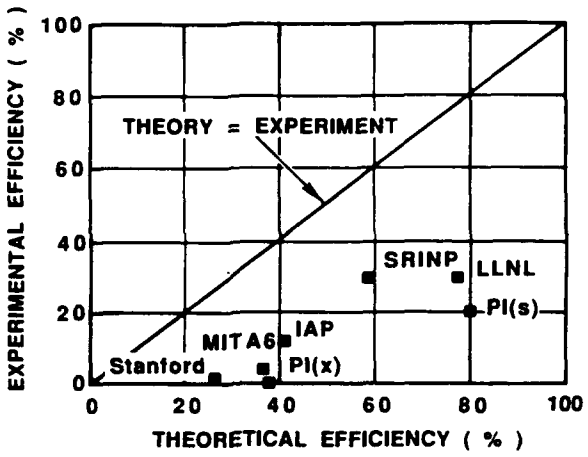

Olin
89-01-072

Series rf Source Concept

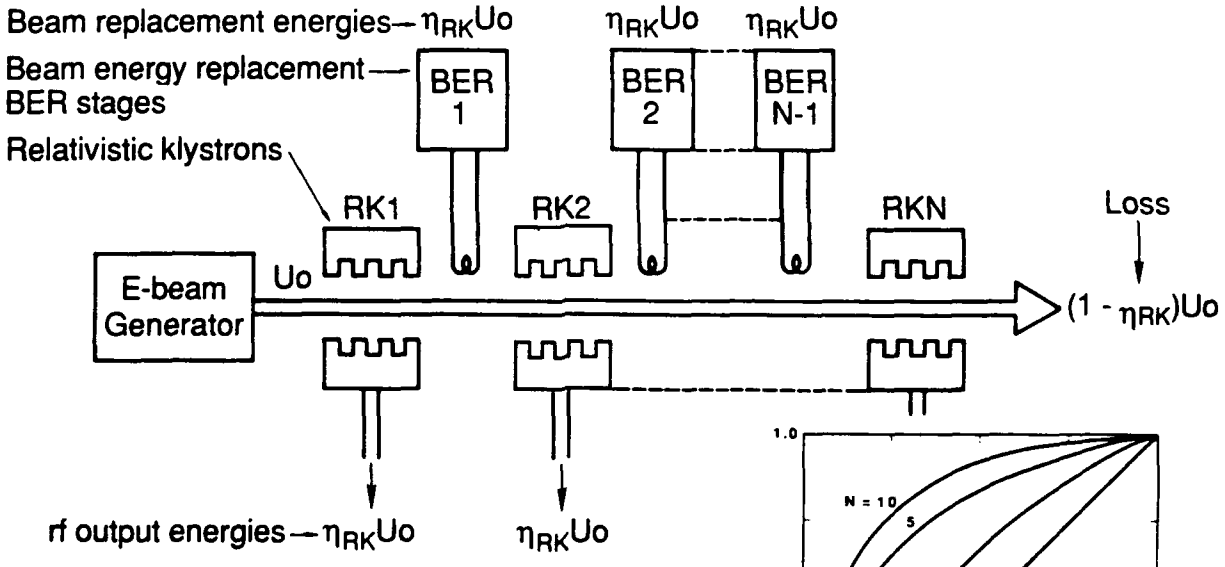

Total input energy = $(N-1)\,\eta_{RK}U_o + U_o$

Total rf output energy = $N\eta_{RK}U_o$

$$\therefore \text{Beam-to-rf efficiency} \equiv \eta_{TOT} = \frac{N}{N + \frac{1}{\eta_{RK}} - 1}$$

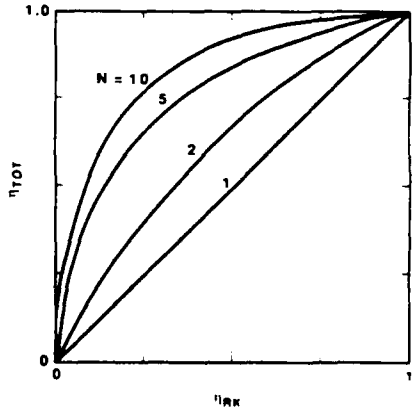

Olin
89-01-083

Details Peculiar to the Series HPM Source Concept

- Requirement of high current propagation over long distance makes transverse instability an issue
  (Resistive Wall Instability)
- Transverse emittance growth may affect microwave generation
- Must guarantee source-to-source phase coherency

Olin
89-01-137

Resistive Wall Instability Does Not Threaten Beam Propagation Through The Source

- **Exponential growth length for resistive wall instability (worst case)***

$$L = \frac{\pi}{2}\left(\frac{2}{3}\right)^{3/2}\left(\frac{\sigma\mu_0}{\tau_p}\right)^{1/2}\left(\frac{I_A}{I_b}\right)\gamma_0\, r_w^3$$

beam current, I_b	5 kA
beam pulse length, τ_p	500 ns
relativistic factor, γ_0	2 (600 kV)
Alfven current, I_A	37 kA

Only two e-fold lengths through the length of the source if r_w = 5 cm.

* Ken Takayama, "Beam Break-up and Relativistic Wall Instability in a Steady - State Free Electron Laser in the Microwave Regime," KEK Preprint 88-11 (1988)

Olin
89-01-089

rf Source Extrapolations

(BASELINE CONCEPT: SERIES RELATIVISTIC KLYSTRONS)

Parameter	Brassboard Demonstrator Requirement	Far-Term SBFEL Requirement	Present State-of-the-Art
Frequency	500 MHz	1328 MHz	
Number of klystrons	10	10	1
Peak rf power (per klystron)	1 GW	2 GW	0.5 GW
Overall average rf power	10 GW	10 GW	0.5 GW
Micropulses per macropulse	--	58	--
Micropulse duration	--	30 ns	140 ns
Macropulse duration	3.5 μs	3.5 μs	140 ns
Electronic efficiency (per klystron)	0.5	0.5	0.4
Overall electronic efficiency	0.9	0.9	--
Amplitude stability	1%	1%	2%
Phase stability	1%	1%	2%
Macropulse repetition rate	--	3.3 kHz	--
Lifetime	10^2	5 (10^6) shots	10^2-10^{-3}

Olin
89-01-116

CLIA Considerations for the High Current RF Linac Basic Concept

PETER SINCERNY

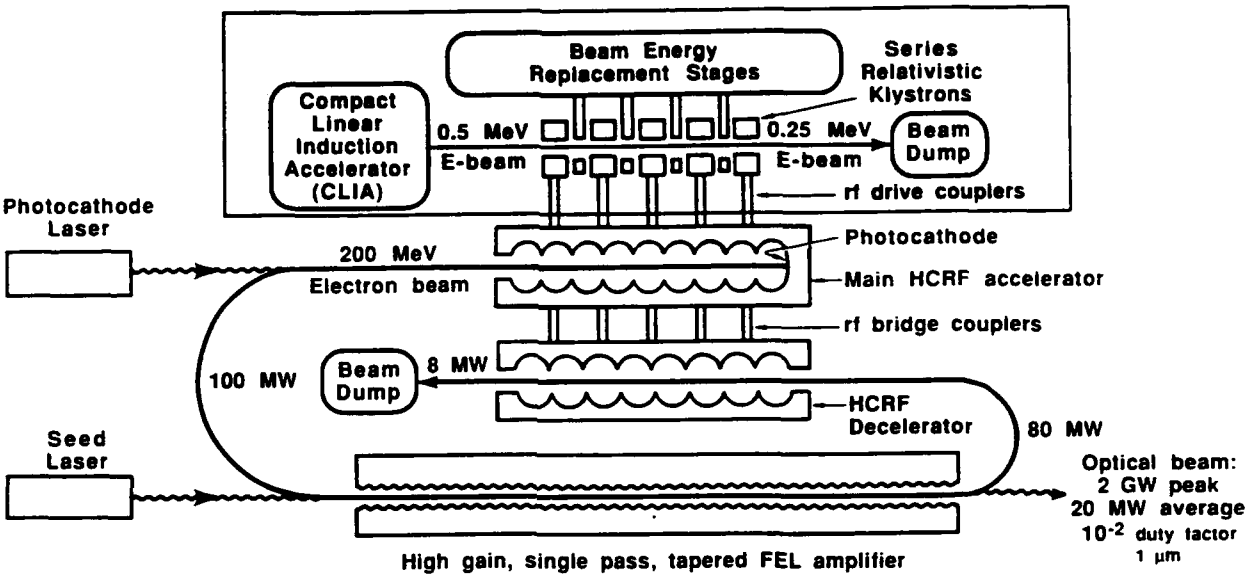

Olin

Consider Two Ways to Produce the Required 3.5 μs Electron Beam

1. Conventional high voltage PFN
   - Fairly simple to build today but not scalable to:
     - Either high repetition rate or
     - Compact, lightweight configurations
2. Compact Linear Induction Accelerator (CLIA)
   - All magnetic, inherently repetitive switching
   - Scalable to compact space-qualifiable hardware requirements

Series rf Source Concept

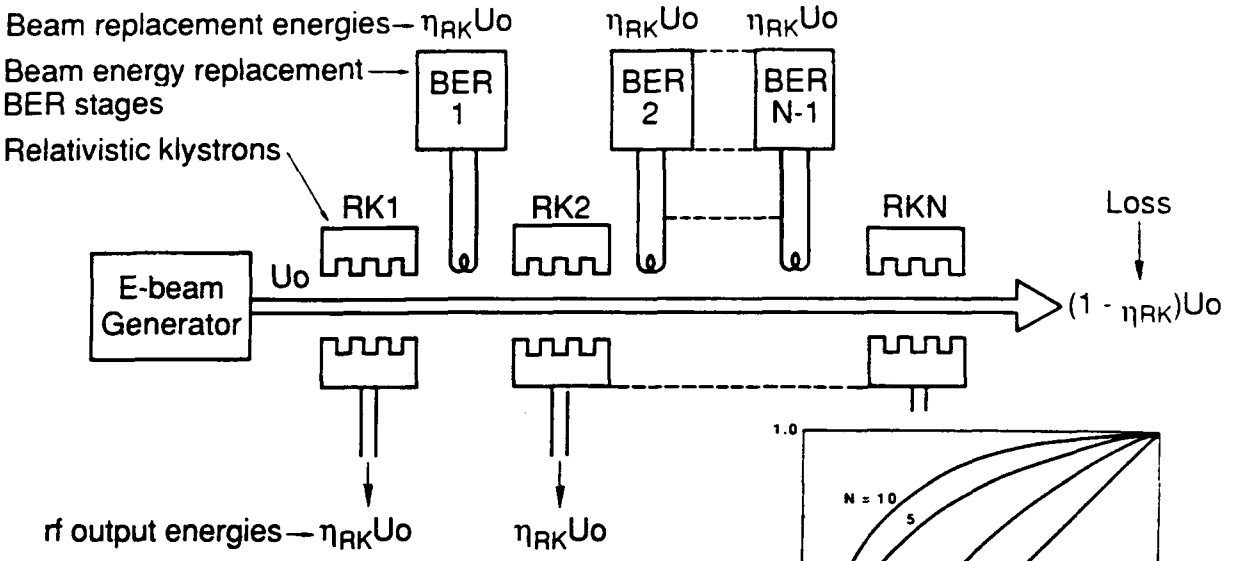

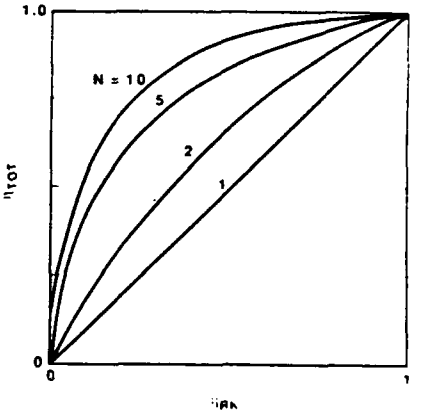

Total input energy = $(N-1)\,\eta_{RK}U_o + U_o$

Total rf output energy = $N\eta_{RK}U_o$

$$\therefore \text{Beam-to-rf efficiency} \equiv \eta_{TOT} = \frac{N}{N + \frac{1}{\eta_{RK}} - 1}$$

Olin

The CLIA Concept for HCRF SBFEL

Replace the conventional e-beam generator with a linear induction accelerator

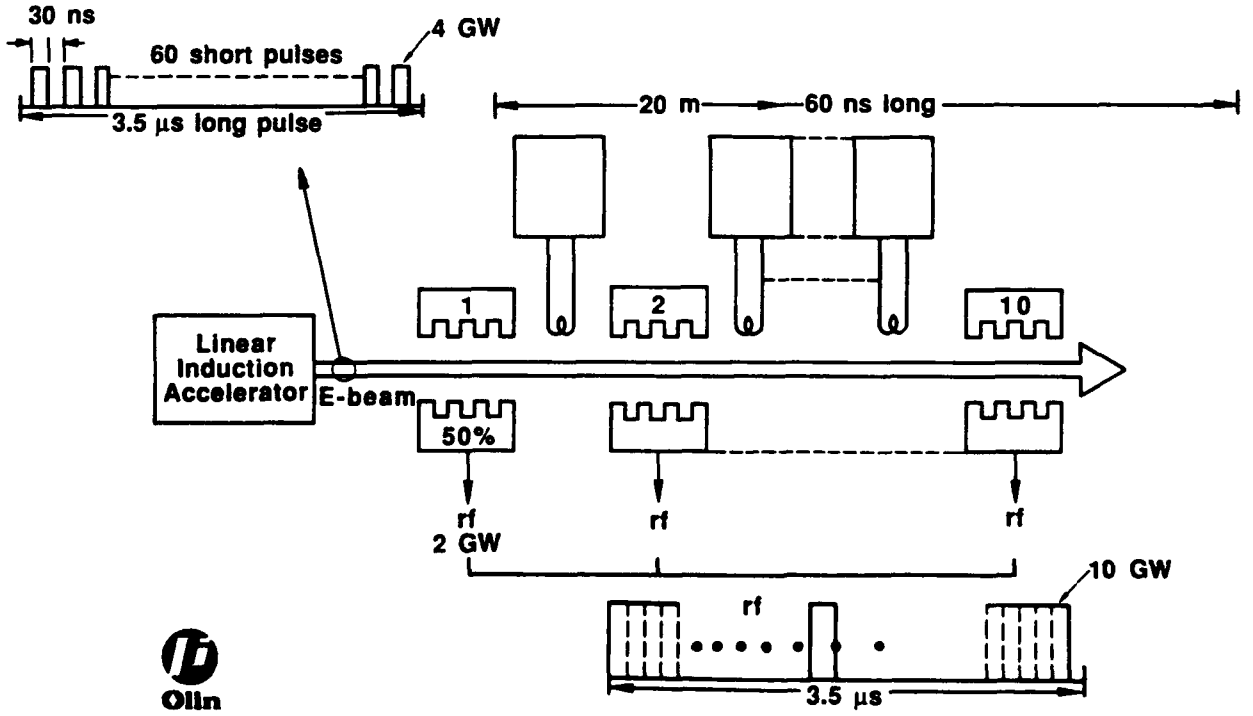

Olin

• **Note: Long pulse is repeated at 3.3 kHz**

The PI/CLIA Program

Purpose: Produce rep-rated (100 to 200 Hz) high power microwaves (300 MW, S-band) for lethality testing

Status:

- System design is completed (BTI funds)
- Accelerator fabrication completed (Olin Research Council funds)
- Full system fabrication and assembly funded (BTI) and will be completed by October 1989

Olin

The PI/CLIA Program (cont.)

Relevance to HCRF-SBFEL:

- Demonstrate full power single short pulse e-beam capability at 200 Hz
- Demonstrate first rf stage peak short pulse power
- Can serve as a 2 pulse series klystron test bed
- Phase 3 will demonstrate 10-short-pulse format

Olin

CLIA with HPM Load

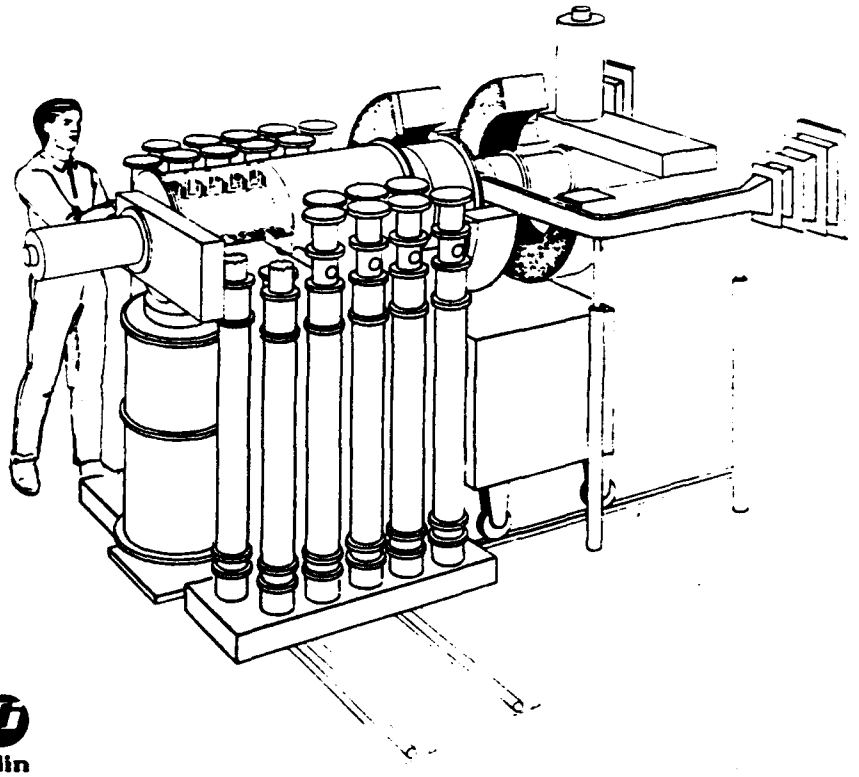

Olin

What Is CLIA?
Compact Linear Induction Accelerator

- CLIA is a pulsed-power conditioning system able to drive a wide variety of HPM sources
    - L-, S-, X-band magnetrons (1 to 20 GHz)
    - Vircators (0.4 to 10 GHz)
    - Free electron masers (2 to 10 GHz)
    - BWO
    - Relativistic klystron
- It can produce total outputs of 12 kJ during a 200 Hz, 5-second burst
- It is compact (2.0 M x 2.0 M x 4.0 M), lightweight, and can readily be made transportable

Olin

Definition of CLIA Pulse Formats

- 200 Hz Pulse Format:
  (Phase I and 2)

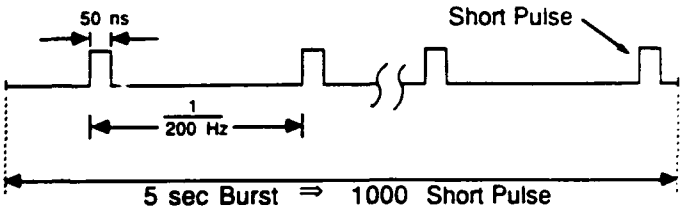

- 10 MHz Smart Long Pulse Format:
  (Phase 3)

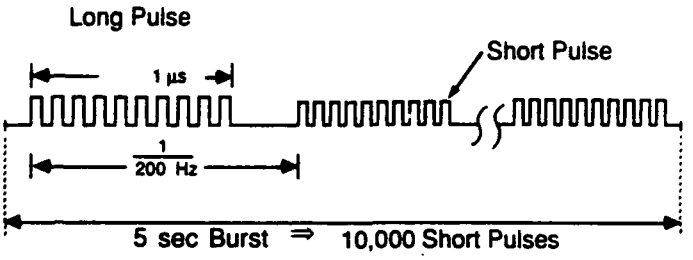

Radiation in the S Band ⇒ 3.0 GW, 100 J / short pulse
E-Beam parameters ⇒ 15 GW, 750 J/ short pulse (Flat Top)

Olin
88-01-133

CLIA Program

FY-88/89
- Develop/Facilitize CLIA for Indoor Testing at PI

FY-90
- Modify CLIA for Transportability
- Facilitize for Outdoor Testing
- Investigate "Smart" HPM Applications

FY-91
- Finish "Smart" HPM Investigation
- Investigate Advanced Microwave Concepts
  - Frequency Tunable, Beat Wave, FEM

Olin
88-12-047

Motivation for Building CLIA

- CLIA will verify specific threats of interest to BTI
- CLIA will explore electronic vulnerability as a function of repetition rate
- CLIA will provide testing capability for ongoing DARPA medium power microwave (MPM) program
- CLIA will exceed published Soviet microwave capability (peak power at 200 Hz) by an order of magnitude

Olin

HPM Systems Comparison: Soviet LIA and CLIA

	Soviet LIA	CLIA
V (kV)	300 to 500	750
1 (kA)	≤ 5 to 6	10 (Phase I) 20 (Phase II)
τ (1) (ns) (Electrical FWHM)	60	60
Repetition Frequency (Hz)	160 burst 50 CW	200 CW
Burst Duration	3 pulses*	5 s
RF-Like Pulse Format (10 MHz, burst)	?	Yes (second & third year)
Magnetron Peak Power	380 MW	3.0 GW

*Limited by duration of Bz magnetic field before magnetron goes out of resonance.

(1) Saturation requirements for induction cells are consistent with 0.25 μs pulse at 500 keV electron energy.

Olin

CLIA PHASE I Network

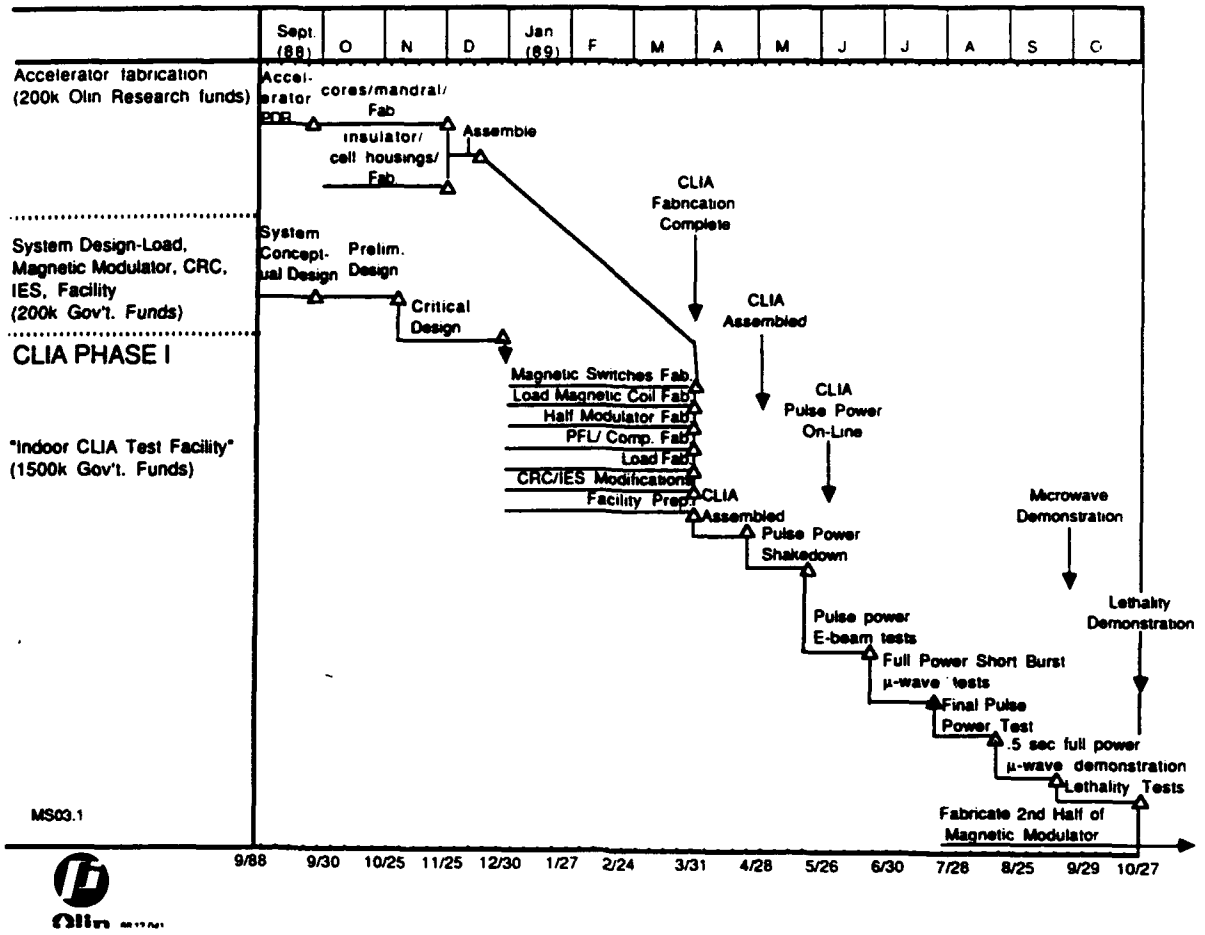

BLOCK DIAGRAM OF CLIA DEVICE

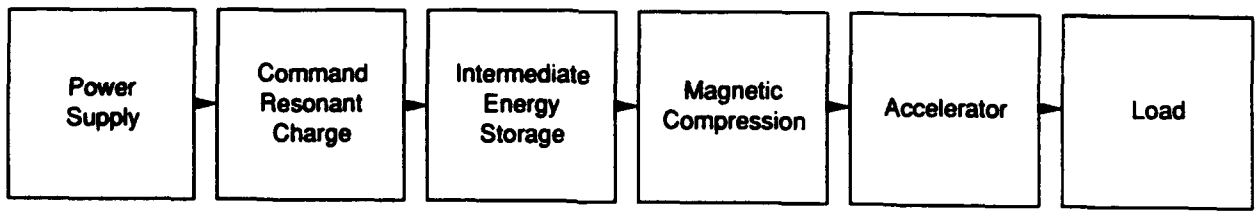

- V_{DC} = +45 kV
- I_{avg} = 6.1 A
- P_{avg} = 275 kW

- I_{pk} = 507 A
- I_{rms} = 49 A
- dI/dT = 15.9 A/μs
- f = 200 Hz

- V_{pk} = 78 kV
- I_{pk} = 20 kA
- I_{rms} = 280 A
- dI/dT = 26 kA/μs
- f = 200 Hz

- Three stages of compression
- τ_{charge} = 2.9 μs
- τ_{pulse} = 60 ns
- V_{out} = 75 kV
- E_{in} = 1100 J
- f = 200 Hz

- Ten cells
- V_{cell} = 75 kV
- $I_{cell} \leq$ 22 kA
- Z_{cell} = 3.41Ω
- E_{load} = 1000 J
- f = 200 Hz

- V_{load} = 750 kV
- $I_{pulse} \leq$ 22 kA
- Z_{load} = 34Ω
- $\tau_{rise} \leq$ 9 ns
- τ_{pulse} = 60 ns (FWHM)
- E_{load} = 1000 J
- f = 200 Hz

CRC AND IES MODULATOR SCHEMATIC AND PULSE CHARACTERISTICS

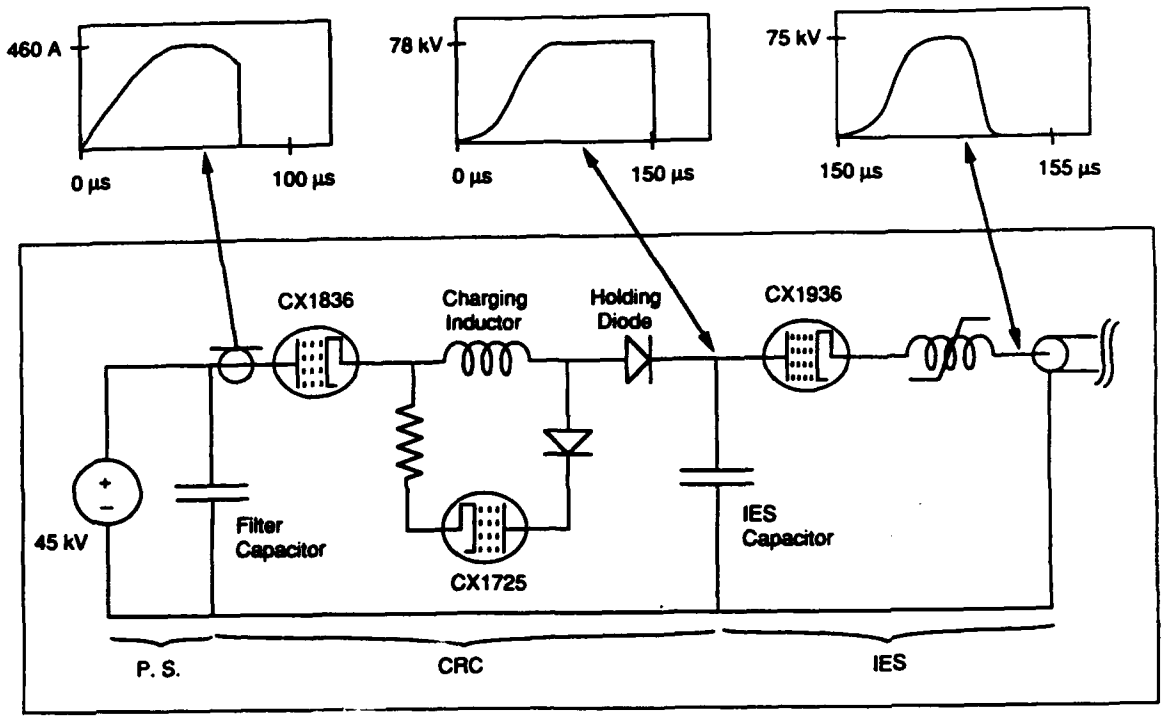

MAGNETIC COMPRESSION UNIT - SIMPLIFIED SCHEMATIC

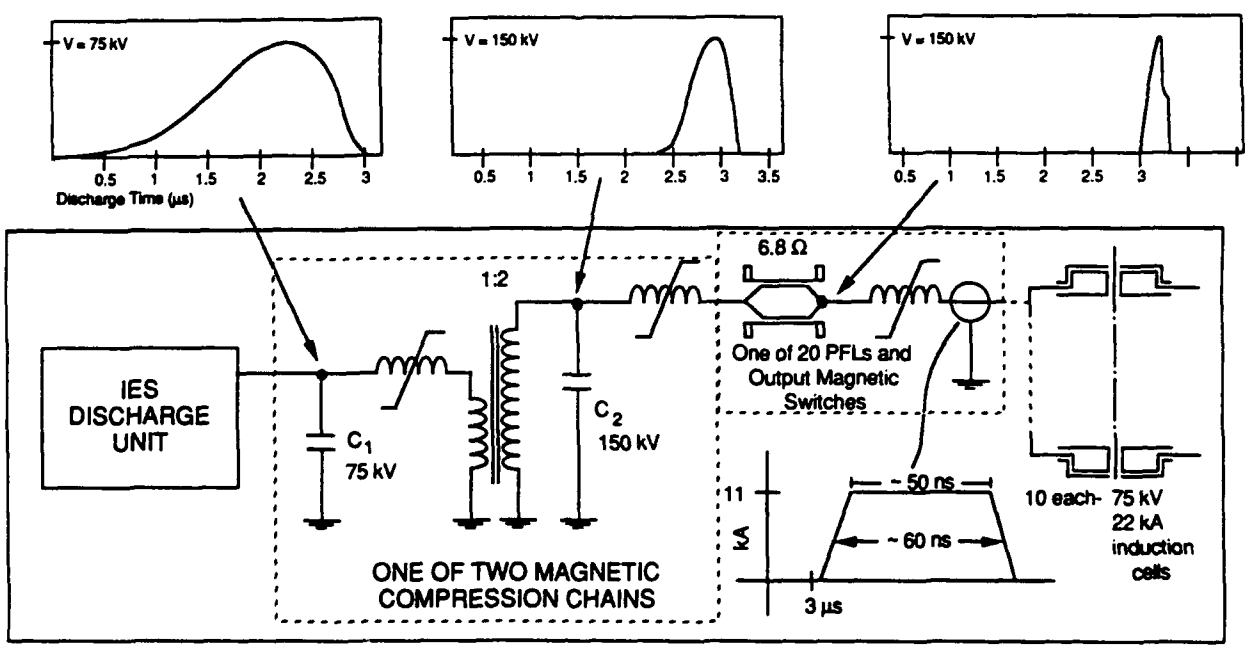

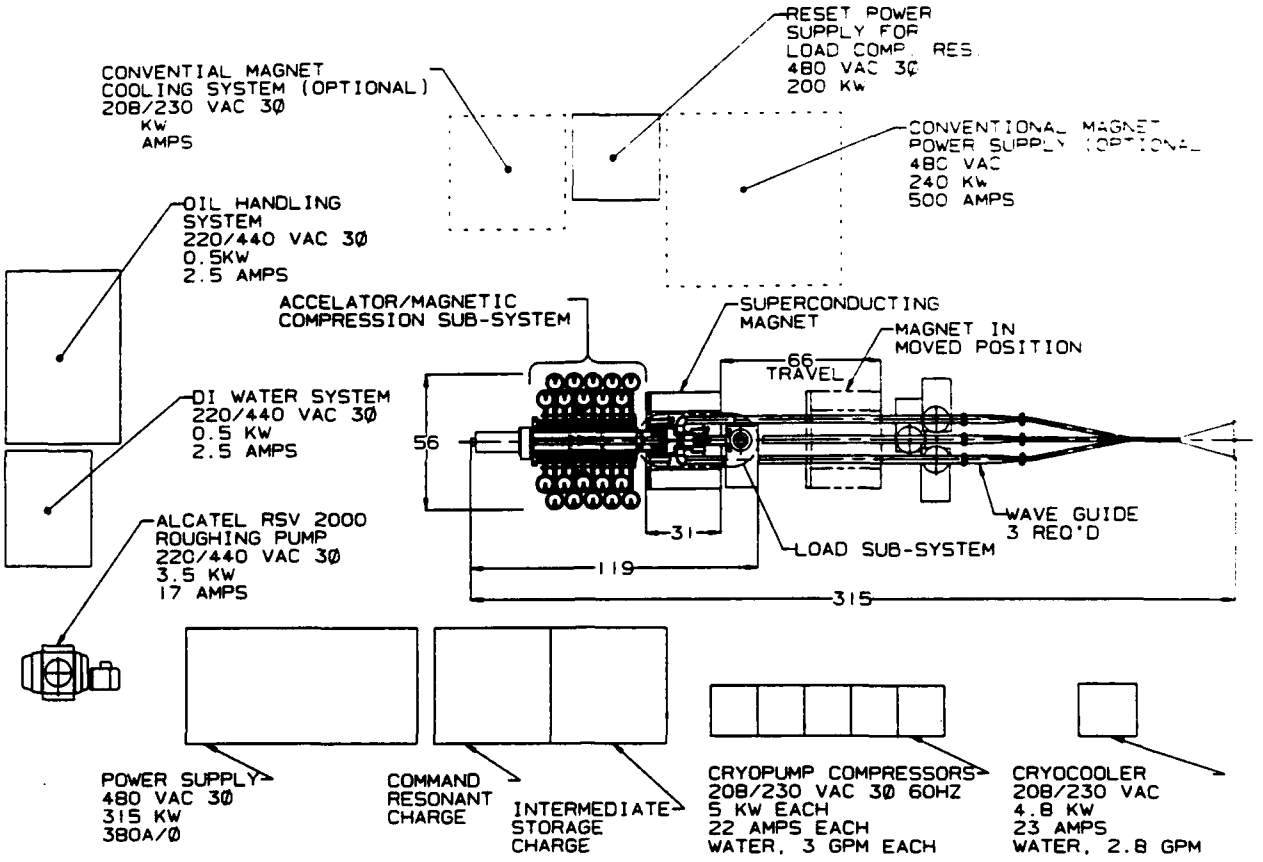

CLIA SYSTEM: PLAN VIEW

CLIA with S-Band Magnetron and Extraction Waveguides, Side Elevation

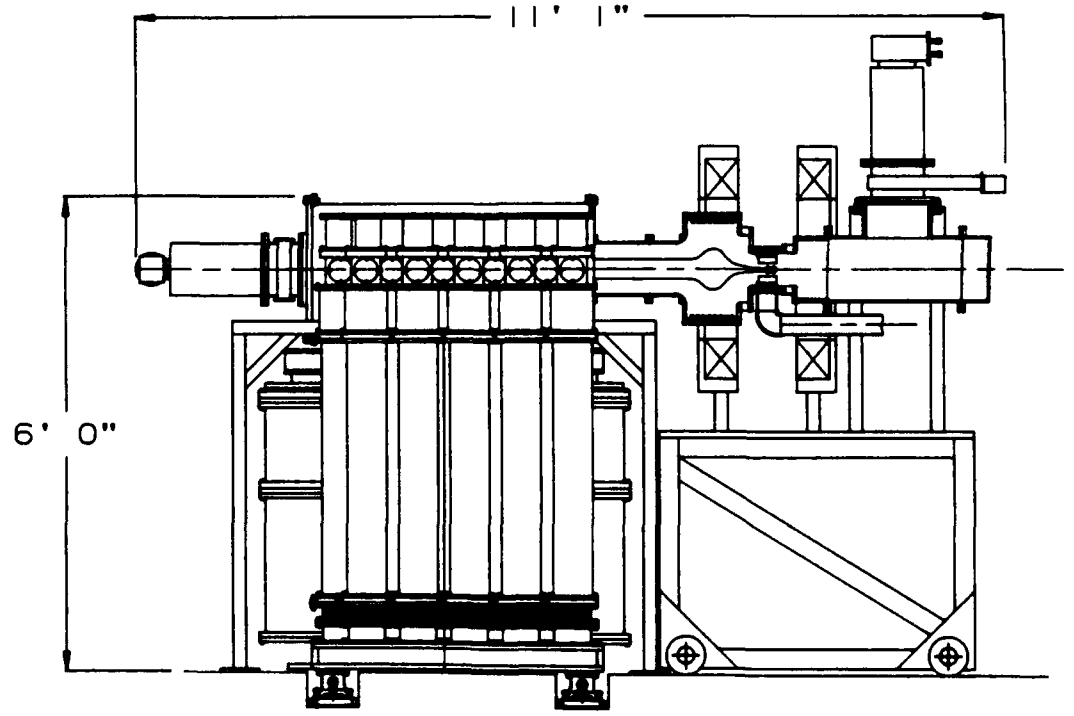

Olin

CLIA with S-Band Magnetron and Extraction Waveguides, Plan View

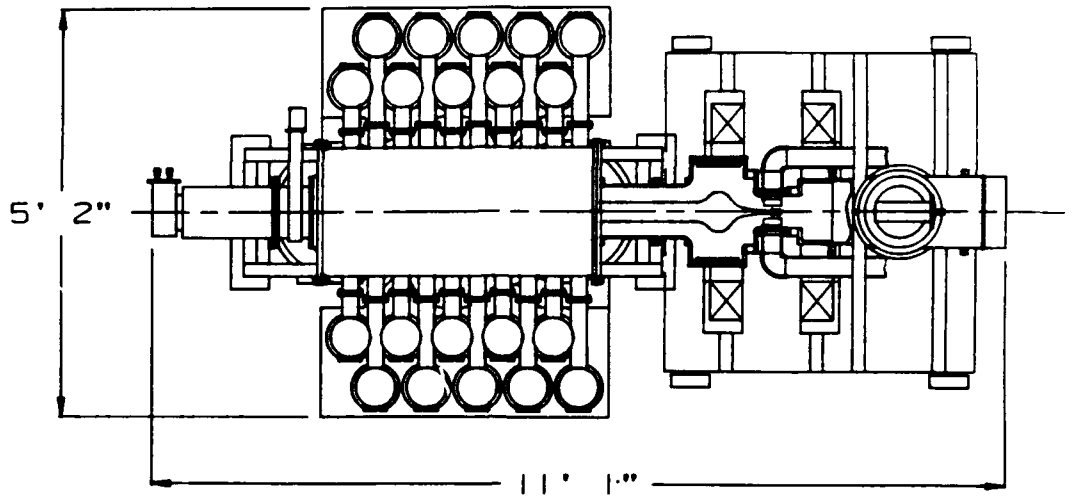

Olin

CLIA Accelerator Plan View Cross Section

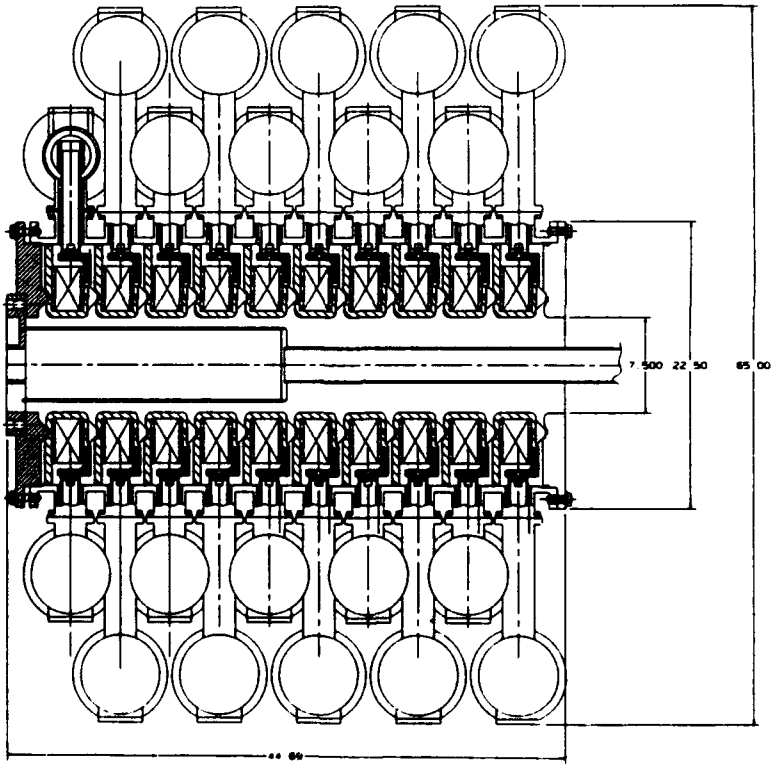

CLIA Accelerator End View

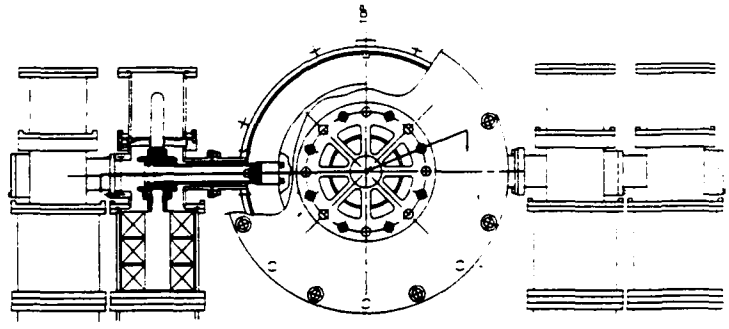

88-11-086

Comparison PI/CLIA Program with HCRF Requirements

PI/CLIA PROGRAM

	Phase I Funded 1989	Through Phase III By 1991	HCRF-SBFEL Requirements
E-beam power/ short pulse	7.5 GW	15 GW	4 GW
E-beam energy/ short pulse	375 J	750 J	120 J
rf power radiated per source	300 MW	6 GW	2 GW
Number of short pulses per long pulse	1	10	60
Repetition frequency of the long pulse	200 Hz	1.0 kHz	3.0 kHz

Olin

PoP Experiment Plan

DAVID PRICE

SECTION OUTLINE

- What is necessary to prove the basic HCRF accelerator concept?
- Recent technology breakthroughs motivating revised baseline program plan
- Revised Baseline Technology Program (Phases I and II)
- PoP scaled parameters
- Four sets of tests will demonstrate the HCRF concept

Olin

89-01-132

What is Necessary to Prove the Basic HCRF Accelerator Concept?

Demonstrate the following:

- High peak current micropulse
- High macropulse current
- High real estate gradient
- High beam quality

Olin

89-01-100

Recent Technology Breakthroughs Motivating Revised Baseline Program

- NRL relativistic klystron
- LANL photocathode
- PI PFN pulse duration extension
- PI Compact Linear Induction Accelerator

Olin
88-01-115

Revised Baseline Technology Program (Phases I and II)

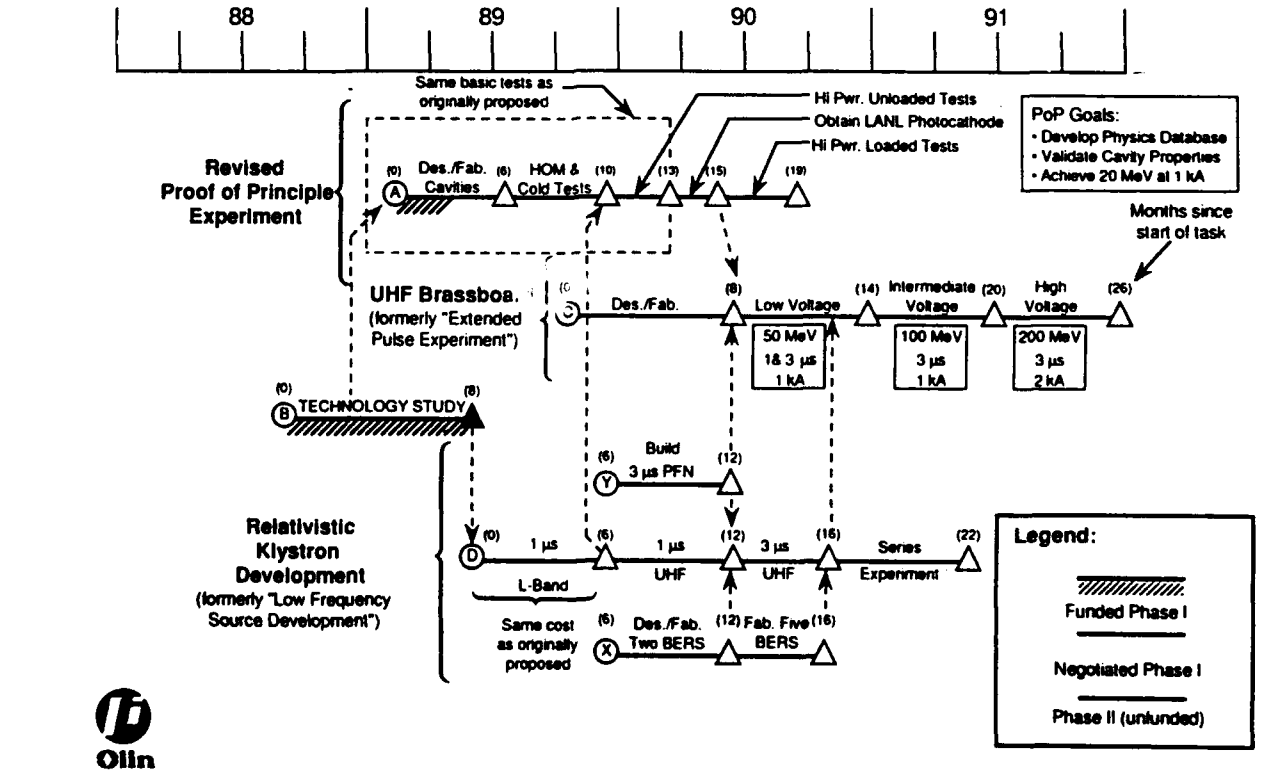

Olin
MF02.1
89-01-134

PoP Scaled Parameters

	Parameters	HCRF	PoP	Comments
rf	Frequency	500 MHz	1328 MHz	
	Pulse Duration	3.5 μs	1 μs	
	Power	10 GW	0.5 GW	
Cavity	Gradient	20 MV/m	20 MV/m	
	Characteristic Time	1 μs	250 ns	
	Shunt Impedance (R/Q)	300 Ω/m	800 Ω/m	$(R/Q) \propto \lambda^{-1}$
Beam	Micropulse Charge	10^{-7} Coul	10^{-8} Coul	
	Micropulse Current	2 kA	1 kA	
	Macropulse Current	50 A	5 A	$I_{threshold} \propto \lambda^2$
	Power	10 GW	0.1 GW	
	Energy	200 MeV	20 MeV	Two cavities
	Rep. Rate	3.3 kHz		
	$Q_\perp$	<100	<100	

Olin
89-01-052

Four Sets of Tests Will Demonstrate the HCRF Concept

Low Power rf
1. Single cell
2. Five cell cavity

High Power rf
3. Unloaded cavity
4. Loaded cavity

A single macropulse is sufficient for No. 4

Olin
89-01-054

Objectives of the PoP Experiment

1. (LOW POWER rf) SINGLE CELL TESTS

- Evaluate HOM damping effectiveness of advanced cavity design

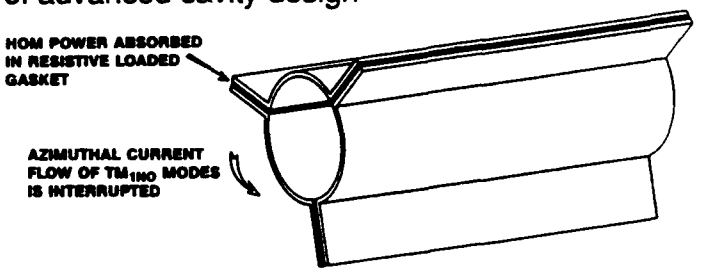

Demonstrate $Q_\perp < 100$

Olin
89-01-126

Objectives of the PoP Experiment

2. (LOW POWER rf) FIVE CELL CAVITY

- Measure π-mode frequency
- Measure $\frac{R}{Q}$, Q and f for spatial harmonics of lowest order longitudinal modes
- Measure $\left(\frac{R}{Q_\perp}\right)$, $Q_\perp$ and f for lowest order dipole modes

Determine RF properties and demonstrate HOM damping—$Q_\perp$ variability

Olin
89-01-127

Objectives of the PoP Experiment

3. (HIGH POWER RF) UNLOADED CAVITY

- Match source and cavity (determine iris size empirically, measure coupled and reflected beam)
- Measure gradient employing low intensity beam
- Explore surface conditioning

Demonstrate 20 $\frac{MV}{m}$ Gradient

Olin
89-01-129

Objectives of the PoP Experiment

4. (HIGH POWER RF) LOADED CAVITY

- Investigate energy transients versus beam injection timing
- Measure micropulse and macropulse current
- Measure beam energy
- Measure longitudinal energy spread
- Measure transverse emittance
- Parametrically study BBU

Demonstrate (single macropulse) design parameters

Olin
89-01-130

Summary and Conclusions (1)

We have reviewed the HCRF Accelerator concept for driving spaced-based free electron lasers. If developed fully, the concept offers many advantages.

- Reduced accelerator weight and volume
- Simpler, smaller wiggler
- Smaller, more robust space platform
- Pulse agility
- Reduced development costs

Olin

Summary and Conclusions (2)

These technical advantages promise to offer significant SBL mission advantages:

- Low size and mass on orbit
- Midcourse interactive discrimination (MID)
- Atmospheric penetration
- Compact, low mass early application capability

Further analysis is needed to validate and quantify such advantages.

Olin

Summary and Conclusions (3)

We have established preliminary design and performance goals for three levels of HCRF accelerators

	Proof of Principle Experiment	Brassboard Demonstrator	Far Term SBFEL Driver
Electron Energy	20 MeV	150 MeV	200 MeV
Gradient	20 MV/m	20 MV/m	20 MV/m
Micropulse Current	1 kA	2 kA	2 kA
Macropulse Current	5 A	50 A	50 A
rf Frequency	1328 MHz	500 MHz	500 MHz
Average Beam Power	NA	75 MW	100 MW

Olin

Summary and Conclusions (4)

We have identified the key accelerator technology issues

- Efficiency
- Beam quality
- rf drive sources

and have mapped out a two-phase baseline program plan to address them.

Olin

Summary and Conclusions (5)

Our baseline program has four elements

1. A technology study (50 percent complete)
2. Proof-of-principle experiments (15 percent funded)
3. A Brassboard demonstrator
4. Series Relativistic Klystron development

We have maximized the use of available technology to lower risk, leverage government funding and reduce long-term costs.

Olin

Summary and Conclusions (6)

We have reached several important accelerator technology conclusions so far:

- High beam loading (95%) looks feasible for high efficiency (> 80%)
- Series relativistic klystron can provide required power, pulse duration, amplitude stability, and efficiency. Two-beam accelerator experiments lend high confidence to concept
- Segmented cavity HOM damping promises $Q_{\perp} < 100$
- $(Z/Q)_{\perp} < 100\ \Omega$ is required to damp BBU and minimize emittance
- Strong focussing is required to suppress BBU-induced emittance growth. PARMELA indicates that quadrapole doublets cause < 1% additional normalized emittance growth for r_o = 2 mm and minimal additional energy spread
- An aperture size consistent with a 500 MHz fundamental frequency
- rf focussing is an important effect

Olin

Summary and Conclusions (last chart)

In conclusion:

- HCRF offers advantages
- The concept appears sound
- Reasonable technology goals are set
- Reasonable extrapolations from current state-of-the-art can meet the goals
- The benefit-to-cost ratio appears high

Olin

APPENDIX B

LISTING OF THE SYSTEM DESIGN CODE SOURCE PROGRAM

```
DECLARE SUB FixInp (Var!, Fld!, f$, sc!)
DECLARE SUB GetConfig ()
DECLARE SUB IncDec (D!(), inc!)
DECLARE SUB Message (text$)
DECLARE SUB MessageWait (text$)
DECLARE SUB OutSc (D!(), scan!())
DECLARE SUB PrLin (D!(), Fld!, f$)
DECLARE SUB ScanSub (D!(), s%, Fld!, f$, InScan())
DECLARE SUB SetConfig (BestMode%)
DECLARE SUB SetupArray (D!())
DECLARE SUB Units (a!, b!, unit$)
DECLARE SUB UpDown (D!(), f$, inc!, Fld)


' ================================================================================
'                                    HCRF
' ================================================================================


' Parameter definitions
' element (0,0)    1=input,2=output
' element (0,1)    minimum value for input
' element (0,2)    maximum value for input
' element (0,3)    step size for input
' element (0,4)    0 = not input being scanned, 1 = input being scanned
' element (0,5)    present value
' element (0,6)    Scale Factor for printing
' element (0,7)    Units Code 0=none, 1=Watts, 2=kg, 3=meter, 4=sec, 5=eV,
'                  6=mm-mrad, 7=Amps, 8=Coulombs, 9=Ohms, 10=Joules,
'                  11=v/meter, 12=Hz, 13=W/meter, 14=ohm-meter, 15=kg/cu meter
'                  16=kg/meter, 17=Volts, 18=%
' element (0,8)    Default Value
' elements (1,0) through (1,10)      values for the scan


'    FEL Parameters          meaning                    Units
DIM EtaFel(1, 10)         'FEL Efficiency             none
DIM PoFEL(1, 10)          'FEL Optical Output Power   Watts
DIM lenfel(1, 10)         'FEL Physical Length        Meters
DIM KgFEL(1, 10)          'FEL Weight                 Kilograms
DIM PiFel(1, 10)          'FEL Input Power            Watts
DIM TBurFel(1, 10)        'FEL Burst Duration         seconds
DIM KKFEL AS SINGLE       'FEL Weight Scaling         kg/kW


'Accelerator Parameters     meaning                    Units

DIM EAcc(1, 10)           'Beam Kinetic Energy        eV
DIM epsacc(1, 10)         'Beam Emittance             mm-mrad
DIM delacc(1, 10)         'Micropulse energy spread   none
DIM IuPAcc(1, 10)         'Micropulse peak current    Amperes
DIM QuPAcc(1, 10)         'Micropulse charge          Coulombs
DIM TuPAcc(1, 10)         'MicroPulse Duration        sec
DIM VSWRAcc(1, 10)        'Accelerator VSWR           none
DIM AlphaAcc(1, 10)       'Beam Loading               none
DIM RovQAcc AS SINGLE     'Shunt impedance            Ohms
DIM URFAcc(1, 10)         'Accelerator stored energy  Joules
DIM Q0Acc(1, 10)          'Intrinsic Q                none
```

```
DIM qBAcc(1, 10)          'Beam Q Value                        none
DIM EgAcc(1, 10)          'Real estate gradient                v/meter
DIM LenAcc(1, 10)         'Accelerator Length                  meters
DIM EtaAcc(1, 10)         'Accelerator Efficiency              none
DIM PRFAcc(1, 10)         'Macropulse rep-rate                 Hz
DIM PWllAcc(1, 10)        'Wall losses                         W
DIM PwlMAcc(1, 10)        'Wall Losses per meter               W/meter
DIM RhoAcc(1, 10)         'Accelerator Mat'l rho               Ohm-meter
DIM raptacc(1, 10)        'Aperture radius                     meter
DIM FAcc(1, 10)           'Frequency                           Hz
DIM IMPacc(1, 10)         'Macropulse Current                  Amps
DIM TMPAcc(1, 10)         'Macropulse duration                 sec
DIM PBmAvgAcc(1, 10)      'Avg E-Beam Power                    Watts
DIM PBmPkAcc(1, 10)       'Peak Beam Power                     Watts
DIM TFllAcc(1, 10)        'Fill time                           sec
DIM TRFAcc(1, 10)         'RF Pulse Duration                   sec
DIM KgAcc(1, 10)          'Accelerator Weight                  kg
DIM ccavacc(1, 10)        'Cells per Cavity                    none
DIM ncavacc(1, 10)        'Number of cavities                  none
DIM scavacc AS INTEGER    'Segments per cavity                 none
DIM fcavacc(1, 10)        'Feeds per cavity                    none
DIM rffdacc(1, 10)        'Sources per feed                    none
DIM rfsacc(1, 10)         'Total sources needed                none
DIM diaacc(1, 10)         'Diameter of Accelerator             meters
DIM DenAcc AS SINGLE      'density of accelerator mat'l        kg/m3
DIM kgmacc(1, 10)         'weight per length                   kg/m
DIM DutAcc(1, 10)         'Accelerator Duty Factor             none

'RF source set               meaning                           Units

DIM PPkRF(1, 10)          'RF peak power                       Watts
DIM PAvgRF(1, 10)         'RF Avg Power                        Watts
DIM EtaRF(1, 10)          'RF Sources Efficiency               none
DIM VRF AS SINGLE         'RF Drive beam energy                eV
DIM IRF(1, 10)            'RF drive beam current               Amps
DIM KKRF AS SINGLE        'RF Source weight scaling            kg/kW
DIM KgRF(1, 10)           'RF weight                           kg
DIM PiRF(1, 10)           'Power Input to RF Sources(Avg)      Watts

'Pulsed Power                meaning                           Units

DIM PiPFNtoXFMR(1, 10)    'Avg Power into the Transformer      Watts
DIM PiPFN(1, 10)          'Avg Power into the PFN(s)           Watts
DIM EsPFN(1, 10)          'Energy per pulse stored in PFN      Joules
DIM PiCRC(1, 10)          'Avg CRC Power                       watts
DIM EsFB(1, 10)           'Filter Bank Storage                 Joules
DIM npfn(1, 10)           'Number of pfn's                     none
DIM wpfn(1, 10)           'Energy stored in pfn's              Joules
DIM ippfn(1, 10)          'Peak discharge current              Amps
DIM KCPFN AS SINGLE       'capacitor weight scaling            kg/kJ
DIM KLPFN AS SINGLE       'inductor weight scaling             kg/kJ
DIM KTPFN AS SINGLE       'thyratron weight scaling            compound
DIM KXFMR AS SINGLE       'Transformer weight scaling          kg/kj
DIM KCRC AS SINGLE        'CRC weight scaling                  kg/kW
DIM KFil AS SINGLE        'Filter bank weight scaling          kg/kJ
DIM vpfn(1, 10)           'PFN Voltage                         Volts
```

```
DIM KgPFN(1, 10)          'PFN Weight                        kg
DIM nxfmr(1, 10)          'Transformer turns ratio           none
DIM KgXFMR(1, 10)         'Transformer weight                kg
DIM KgCRC(1, 10)          'CRC weight                        kg
DIM KgFil(1, 10)          'Filter bank Weight                kg


'Burst Power                meaning                          Units

DIM PBptoFB(1, 10)        'Burst Power                       Watts
DIM KBur AS SINGLE        'Burst power weight scaling        kg/kw
DIM KCom AS SINGLE        'Combustor weight scaling          kg/kw
DIM KTur AS SINGLE        'Turbine weight scaling            kg/kw
DIM KBurM AS SINGLE       'Burst Misc weight scaling         kg/kw
DIM KgBur(1, 10)          'Burst Power weight                kg


'Fuel & Baseload            meaning                          Units

DIM kglox(1, 10)          'LOX weight                        kg
DIM kglh2(1, 10)          'LH2 weight                        kg
DIM kgtank(1, 10)         'Tankage weight                    kg
DIM kgplat(1, 10)         'Platform weight                   kg
DIM WBase AS SINGLE       'Baseload Power                    Watts
DIM KgBase AS SINGLE      'Baseload Power weight             kg
DIM KgPoint AS SINGLE     'Pointing/tracking weight          kg


'Recirculation              meaning                          Units

DIM EtaRec(1, 10)         'Recirculation Efficiency          none


DIM InScan(15)            'input scan parameters (0:10) data, (11:12) scaling
DIM OutScan(15)           'output scan parameters (0:10) data, (11:12) scaling

DIM Limits(11) AS INTEGER
'limits contains mask for limits that have been exceeded,
' i.e. if on scan step four limits 3 and 5 were exceeded,
' then limits(4)=20 (10100 binary)


'=================================================================


' Constants for key codes and column positions
CONST ENTER = 13, ESCAPE = 27, PgDn = 81
CONST DOWNARROW = 80, UPARROW = 72, LEFTARROW = 75, RIGHTARROW = 77
CONST TABKEY = 9, INSKEY = 82, HOME = 71

CONST COL0 = 5, COL1 = 20, COL2 = 50

CONST NInp = 11, ROW = 9

'Initialize Values
GOSUB init

'Do graphics screen determination
```

```
' Constants for best available screen mode
CONST EGA = 9, CGA = 2
CONST RCTA = 1, DECL = 0
ScreenType% = CGA
RecType% = DECL

ScnFlg% = 0
DO    'Main do loop for entire program

  DO  ' Do loop for input section

    ' Display key instructions
    CLS
    LOCATE 1, COL1
    PRINT "DOWN / UP ................. Move to next field"
    LOCATE 2, COL1
    PRINT "LEFT / RIGHT ............. Decrease field value"
    LOCATE 3, COL1
    PRINT "INS ..................... Enter Value directly"
    LOCATE 4, COL1
    PRINT "TAB .... Activate/Deactivate scan of this value"
    LOCATE 5, COL1
    PRINT "ENTER .... Perform Analysis with current values"
    LOCATE 6, COL1
    PRINT "PgDn ...................Alternate Input Screen"
    LOCATE 7, COL1
    PRINT "ESCAPE ......................... Quit Program"

    ' Redefine Cursor to Filled Block
    LOCATE ROW, COL1, 1, 1, 12

    ' Display Input Parameters
    LOCATE ROW, COL0: PRINT "FEL Ouput Power (MW)";
    CALL PrLin(PoFEL(), 0, "##.#")

    LOCATE ROW + 1, COL0: PRINT "FEL Efficiency ";
    CALL PrLin(EtaFel(), 1, "#.##")

    LOCATE ROW + 2, COL0: PRINT "Burst Duration (Seconds)";
    CALL PrLin(TBurFel(), 2, "####")

    LOCATE ROW + 3, COL0: PRINT "Accelerator Kinetic Energy (MeV)";
    CALL PrLin(EAcc(), 3, "###")

    LOCATE ROW + 4, COL0: PRINT "Cavity Resistivity (microOhm-cm)";
    CALL PrLin(RhoAcc(), 4, "####")

    LOCATE ROW + 5, COL0: PRINT "Accelerator Frequency (GHz)";
    CALL PrLin(FAcc(), 5, "##.##")

    LOCATE ROW + 6, COL0: PRINT "RF Source Set Efficiency ";
    CALL PrLin(EtaRF(), 6, "#.##")

    LOCATE ROW + 7, COL0: PRINT "Accelerator Length (Meters)";
    CALL PrLin(LenAcc(), 7, "###.#")

    LOCATE ROW + 8, COL0: PRINT "FEL Beam Recirculaion Efficiency";
    CALL PrLin(EtaRec(), 8, "#.##")
```

```
LOCATE ROW + 9, COL0: PRINT "Macropulse Duration (microseconds)";
CALL PrLin(TMPAcc(), 9, "##.##")

LOCATE ROW + 10, COL0: PRINT "Macropulse Rep-rate (kHz)";
CALL PrLin(PRFAcc(), 10, "##.##")

LOCATE ROW + 11, COL0: PRINT "Micropulse Peak Current (kA)";
CALL PrLin(IuPAcc(), 11, "##.##")

'make sure fld is not left too high from output section of code
' reset it to first parameter
Fld = 0
Calc = 0

' Update parameter values based on keystrokes
DO
  ' Put cursor on field
  LOCATE ROW + Fld, COL2 + 2
  ' Get a key and strip null off if it's an extended code
  DO
    K$ = INKEY$
  LOOP WHILE K$ = ""
  ky = ASC(RIGHT$(K$, 1))

  SELECT CASE ky

    CASE ESCAPE                    ' End program
      CLS : END

    CASE UPARROW, DOWNARROW        ' Change Parameter at which we Point
      IF ky = DOWNARROW THEN inc = 1 ELSE inc = -1
      Fld = Fld + inc
      IF Fld = -1 THEN Fld = NInp
      IF Fld = NInp + 1 THEN Fld = 0

    CASE RIGHTARROW, LEFTARROW, INSKEY  'Change Value of Parameter
      inc = 0   'Assume INS Key at first
      IF ky = RIGHTARROW THEN inc = 1
      IF ky = LEFTARROW THEN inc = -1
      SELECT CASE Fld
        CASE 0                              ' FEL Power
          CALL UpDown(PoFEL(), "##.#", inc, Fld)
        CASE 1                              ' FEL Efficiency
          CALL UpDown(EtaFel(), "#.##", inc, Fld)
        CASE 2                              ' Burst Length
          CALL UpDown(TBurFel(), "####", inc, Fld)
        CASE 3                              ' Accelerator Beam Energy
          CALL UpDown(EAcc(), "###", inc, Fld)
        CASE 4                              ' Rho of Accelerator Matl
          CALL UpDown(RhoAcc(), "###.#", inc, Fld)
        CASE 5                              ' Accelerator Frequency
          CALL UpDown(FAcc(), "##.##", inc, Fld)
        CASE 6                              ' RF Efficiency
          CALL UpDown(EtaRF(), "#.##", inc, Fld)
        CASE 7                              ' Length of Acc
          CALL UpDown(LenAcc(), "###.#", inc, Fld)
        CASE 8                              ' Recirc Efficiency
```

```
      CALL UpDown(EtaRec(), "#.##", inc, Fld)
    CASE 9                              ' Macropulse Duration
      CALL UpDown(TMPAcc(), "##.##", inc, Fld)
    CASE 10                             ' Macropulse RepRate
      CALL UpDown(PRFAcc(), "##.##", inc, Fld)
    CASE 11                             ' Micropulse Current
      CALL UpDown(IuPAcc(), "##.##", inc, Fld)
    CASE ELSE
  END SELECT

CASE TABKEY         'Change from single value to scan or vice versa
  SELECT CASE Fld
    CASE 0                              ' FEL Power
      CALL ScanSub(PoFEL(), ScanFlg%, Fld, "##.#", InScan())
      InStr$ = "FEL Output Power"
    CASE 1                              ' FEL Efficiency
      CALL ScanSub(EtaFel(), ScanFlg%, Fld, "#.##", InScan())
      InStr$ = "FEL Efficiency"
    CASE 2                              ' Burst Length
      CALL ScanSub(TBurFel(), ScanFlg%, Fld, "####", InScan())
      InStr$ = "Burst Length"
    CASE 3                              ' Accelerator Beam Energy
      CALL ScanSub(EAcc(), ScanFlg%, Fld, "###", InScan())
      InStr$ = "Accelerator Beam Energy"
    CASE 4                              ' Rho of Accelerator Matl
      CALL ScanSub(RhoAcc(), ScanFlg%, Fld, "###.#", InScan())
      InStr$ = "Accelerator Resistivity"
    CASE 5                              ' Accelerator Frequency
      CALL ScanSub(FAcc(), ScanFlg%, Fld, "##.##", InScan())
      InStr$ = "Accelerator Frequency"
    CASE 6                              ' RF Efficiency
      CALL ScanSub(EtaRF(), ScanFlg%, Fld, "#.##", InScan())
      InStr$ = "RF Source Efficiency"
    CASE 7                              ' Length of Acc
      CALL ScanSub(LenAcc(), ScanFlg%, Fld, "###.#", InScan())
      InStr$ = "Accelerator Length"
    CASE 8                              ' ReCirc Efficiency
      CALL ScanSub(EtaRec(), ScanFlg%, Fld, "#.##", InScan())
      InStr$ = "Recirculation Efficiency"
    CASE 9                              ' Macropulse Duration
      CALL ScanSub(TMPAcc(), ScanFlg%, Fld, "##.##", InScan())
      InStr$ = "Macropulse Duration"
    CASE 10                             ' Macropulse PRF
      CALL ScanSub(PRFAcc(), ScanFlg%, Fld, "##.##", InScan())
      InStr$ = "Macropulse PRF"
    CASE 11                             ' Micropulse Current
      CALL ScanSub(IuPAcc(), ScanFlg%, Fld, "##.##", InScan())
      InStr$ = "Micropulse Current"
    CASE ELSE
  END SELECT

CASE ENTER          'Exit input section and start calculation
  Calc = 1
  EXIT DO

CASE PgDn
  GOSUB OthInp
  EXIT DO
```

```
      CASE ELSE

    END SELECT
  LOOP
LOOP WHILE Calc = 0

'Now do set up for calc's
 CALL SetupArray(PoFEL())
 CALL SetupArray(EtaFel())
 CALL SetupArray(TBurFel())
 CALL SetupArray(EAcc())
 CALL SetupArray(RhoAcc())
 CALL SetupArray(FAcc())
 CALL SetupArray(EtaRF())
 CALL SetupArray(LenAcc())
 CALL SetupArray(EtaRec())
 CALL SetupArray(TMPAcc())
 CALL SetupArray(PRFAcc())
 CALL SetupArray(IuPAcc())

 '  Now were ready to do the real calculations

IF ScanFlg% = 1 THEN lim% = 10 ELSE lim% = 0     'is this a scan?

FOR i = 0 TO lim%  'Main loop to do 1 or 11 Calculations

  'First, the FEL

  PiFel(1, i) = PoFEL(1, i) / EtaFel(1, i)

  'That was simple, now the accelerator

  'Gradient is Energy over Length
  EgAcc(1, i) = EAcc(1, i) / LenAcc(1, i)

  'Average Beam Power is Power in to FEL
  PBmAvgAcc(1, i) = PiFel(1, i)

  'Duty Factor is pulse length times PRF
  DutAcc(1, i) = TMPAcc(1, i) * PRFAcc(1, i)

  'Peak Power out is Average power divded by duty Factor
  PBmPkAcc(1, i) = PBmAvgAcc(1, i) / DutAcc(1, i)

  'Macropulse Current is Power over Voltage
  IMPacc(1, i) = PBmPkAcc(1, i) / EAcc(1, i)

  'MicroPulse Charge is MP I over Freq
  QuPAcc(1, i) = IMPacc(1, i) / FAcc(1, i)

  'Micropulse length is charge over current
   TuPAcc(1, i) = QuPAcc(1, i) / IuPAcc(1, i)

  'Q0 is reduced from standard value by the sqrt of the ratio of rho
  Q0Acc(1, i) = 48675 / (SQR(RhoAcc(1, i) / 1.72))

  'Stored Energy is Eg^2 L / wF(R/Q)
  URFAcc(1, i) = EgAcc(1, i) ^ 2 * LenAcc(1, i) / (6.28 * FAcc(1, i) * RovQAcc)
```

```
'Beam Q is 2PI F U / (EI)
qBAcc(1, i) = 6.28 * FAcc(1, i) * URFAcc(1, i) / (EAcc(1, i) * IMPacc(1, i))

'Alpha is related to q0, qB
AlphaAcc(1, i) = 1 / (1 + qBAcc(1, i) / Q0Acc(1, i))

'VSWR is related to Alpha
VSWRAcc(1, i) = 1 / (1 / AlphaAcc(1, i) - 1)

'Fill Time Is a function of lots of things
VSWR = VSWRAcc(1, i)
LogTerm = LOG(2 * VSWR / (VSWR - 1))
TF11Acc(1, i) = Q0Acc(1, i) / (3.14 * FAcc(1, i) * (1 + VSWR)) * LogTerm

TRFAcc(1, i) = TMPAcc(1, i) + TF11Acc(1, i)

'Accelerator Efficiency is related to Alpha and fill time ratio
EtaAcc(1, i) = AlphaAcc(1, i) * (1 - TF11Acc(1, i) / TRFAcc(1, i))

'Average wall losses
Temp = 6.28 * FAcc(1, i) * URFAcc(1, i) / Q0Acc(1, i)
PW11Acc(1, i) = Temp * TRFAcc(1, i) * PRFAcc(1, i)

'Average wall losses/meter
Pw1MAcc(1, i) = PW11Acc(1, i) / LenAcc(1, i)

'No go on to the RF source set
PPkRF(1, i) = PBmPkAcc(1, i) / EtaAcc(1, i)
PAvgRF(1, i) = PPkRF(1, i) / (TRFAcc(1, i) * PRFAcc(1, i))
IRF(1, i) = (PPkRF(1, i) / EtaRF(1, i)) / VRF

IF RecType% = RCTA THEN   'do calcs for rectenna type recirculation
  PiRF(1, i) = PAvgRF(1, i) / (.6 * EtaRF(1, i))
  Temp = PiFel(1, i) * (1 - EtaFel(1, i)) * EtaRec(1, i)
  PiPFNtoXFMR(1, i) = PiRF(1, i) / EtaXFMR - Temp
  PiPFN(1, i) = PiPFNtoXFMR(1, i) / EtaPFN
  EsPFN(1, i) = PiPFN(1, i) / PRFAcc(1, i)
  PiCRC(1, i) = PiPFN(1, i) / EtaCRC
  EsCRC(1, i) = EsPFN(1, i) / EtaCRC
  EsFB(1, i) = 10 * EsCRC(1, i)
  Temp = .9 * (PiRF(1, i) - PAvgRF(1, i))
  PBptoFB(1, i) = PiCRC(1, i) - Temp
ELSE
END IF
'do weight scalings
KgFEL(1, i) = PoFEL(1, i) * KKFEL / 1000
KgAcc(1, i) = DenAcc * VolAcc(1, i) / 1000
KgRF(1, i) = KKRF * PAvgRF(1, i) / 1000
KgXFMR(1, i) = KKXFMR * EsPFN(1, i) / 1000
KgPFN(1, i) = (KKCPFN + KKLPFN) * EsPFN(1, i)
KgPFN(1, i) = (KgPFN(1, i) + KKTPFN * PiPFNtoXFMR(1, i)) / 1000
KgCRC(1, i) = KKCRC * PiPFN(1, i) / 1000
KgFil(1, i) = KKFIL * EsFB(1, i) / 1000
KgBur(1, i) = (KKBur + KCom + KTur) * PBptoFB(1, i) / 1000
KgFuel(1, i) = TBurFel(1, i) * PBptoFB(1, i) * ScalingFactor / 1000
KgTot(1, i) = KgFEL + KgAcc(1, i) + KgRF(1, i) + KgXFMR(1, i)
KgTot(1, i) = KgTot(1, i) + KgPFN(1, i) + KgCRC(1, i) + KgFil(1, i)
```

```
    KgTot(1, i) = KgTot(1, i) + KgBur(1, i) + KgFuel(1, i) + KgBase + KgPoint

    IF ScanFlg% = 0 THEN GOSUB printrout    ' if it wasn't a scan, just print

  NEXT i

  'do output scan stuff now

  IF ScanFlg% = 1 THEN      '  If it was a scan, do plot stuff
    RTI = 0
    CONST Nout = 15, ROWO = 6
    Fld = 0
    scr% = 1
    DO

      ' Display key instructions
      CLS
      LOCATE 1, COL1
      PRINT "DOWN / UP ..................... Move to next field"
      LOCATE 2, COL1
      PRINT "ENTER ..... Graph this Parameter vs Input Parameter"
      LOCATE 3, COL1
      PRINT "PgDn ..................... Alternate Output Screen"
      LOCATE 4, COL1
      PRINT "ESCAPE ..................... Return to Input Screen"

      ' change to Block cursor
      LOCATE ROWO, COL1, 1, 1, 12

      ' Display possible Parameters to plot
      IF scr% = 1 THEN
        LOCATE ROWO, COL0: PRINT "FEL Average Input Power";
        LOCATE ROWO + 1, COL0: PRINT "Accelerator Gradient";
        LOCATE ROWO + 2, COL0: PRINT "Average Accelerator Beam Power";
        LOCATE ROWO + 3, COL0: PRINT "Accelerator Duty Factor";
        LOCATE ROWO + 4, COL0: PRINT "Peak Accelerator Beam Power";
        LOCATE ROWO + 5, COL0: PRINT "Peak MacroPulse Current";
        LOCATE ROWO + 6, COL0: PRINT "Micropulse Charge";
        LOCATE ROWO + 7, COL0: PRINT "Micropulse duration";
        LOCATE ROWO + 8, COL0: PRINT "Accelerator Q";
        LOCATE ROWO + 9, COL0: PRINT "Accelerator Stored Energy";
        LOCATE ROWO + 10, COL0: PRINT "Accelerator Beam Loading";
        LOCATE ROWO + 11, COL0: PRINT "Accelerator VSWR";
        LOCATE ROWO + 12, COL0: PRINT "Accelerator Fill Time";
        LOCATE ROWO + 13, COL0: PRINT "Accelerator Efficiency";
        LOCATE ROWO + 14, COL0: PRINT "Average Wall Losses per Meter";
        LOCATE ROWO + 15, COL0: PRINT "Acc";
      ELSE
        LOCATE ROWO, COL0: PRINT "FEL Weight";
        LOCATE ROWO + 1, COL0: PRINT "Accelerator Weight";
        LOCATE ROWO + 2, COL0: PRINT "RF Sources Weight";
        LOCATE ROWO + 3, COL0: PRINT "Transformer Weight";
        LOCATE ROWO + 4, COL0: PRINT "PFN Weight";
        LOCATE ROWO + 5, COL0: PRINT "CRC Weight";
        LOCATE ROWO + 6, COL0: PRINT "Filter Bank Weight";
        LOCATE ROWO + 7, COL0: PRINT "Burst Power Weight";
        LOCATE ROWO + 8, COL0: PRINT "Fuel Weight";
        LOCATE ROWO + 9, COL0: PRINT "Total Platform Weight";
```

```
END IF

RTO = 0   'flag to control screen

' Update outscan values
DO
  ' Put cursor on field
  LOCATE ROWO + Fld, COL0
  ' Get a key and strip null off if it's an extended code
  DO
    K$ = INKEY$
  LOOP WHILE K$ = ""
  ky = ASC(RIGHT$(K$, 1))

  SELECT CASE ky
    CASE ESCAPE       'Return to Input Screen
      RTI = 1

    CASE UPARROW, DOWNARROW  ' Select different parameter
      IF ky = DOWNARROW THEN inc = 1 ELSE inc = -1
      Fld = Fld + inc
      IF Fld = -1 THEN Fld = Nout
      IF Fld = Nout + 1 THEN Fld = 0

    CASE ENTER
      IF scr% = 1 THEN
        SELECT CASE Fld
          CASE 0
            OutStr$ = "FEL Average Input Power"
            CALL OutSc(PiFel(), OutScan())
          CASE 1
            OutStr$ = "Accelerator Gradient"
            CALL OutSc(EgAcc(), OutScan())
          CASE 2
            OutStr$ = "Average Accelerator Beam Power"
            CALL OutSc(PBmAvgAcc(), OutScan())
          CASE 3
            OutStr$ = "Accelerator Duty Factor"
            CALL OutSc(DutAcc(), OutScan())
          CASE 4
            OutStr$ = "Peak Accelerator Beam Power"
            CALL OutSc(PBmPkAcc(), OutScan())
          CASE 5
            OutStr$ = "Macropulse Peak Current"
            CALL OutSc(IMPacc(), OutScan())
          CASE 6
            OutStr$ = "MicroPulse Charge"
            CALL OutSc(QuPAcc(), OutScan())
          CASE 7
            OutStr$ = "MicroPulse Duration"
            CALL OutSc(TuPAcc(), OutScan())
          CASE 8
            OutStr$ = "Accelerator Q"
            CALL OutSc(Q0Acc(), OutScan())
          CASE 9
            OutStr$ = "Accelerator Stored Energy"
            CALL OutSc(URFAcc(), OutScan())
```

```
        CASE 10
          OutStr$ = "Accelerator Beam Loading"
          CALL OutSc(AlphaAcc(), OutScan())
        CASE 11
          OutStr$ = "Accelerator VSWR"
          CALL OutSc(VSWRAcc(), OutScan())
        CASE 12
          OutStr$ = "Accelerator Fill Time"
          CALL OutSc(TFllAcc(), OutScan())
        CASE 13
          OutStr$ = "Accelerator Efficiency"
          CALL OutSc(EtaAcc(), OutScan())
        CASE 14
          OutStr$ = "Accelerator Average Wall Losses per Meter"
          CALL OutSc(PwlMAcc(), OutScan())
        CASE 15
        CASE ELSE
      END SELECT
    ELSE
      SELECT CASE Fld
        CASE 0
          OutStr$ = "FEL Weight"
          CALL OutSc(KgFEL(), OutScan())
        CASE 1
          OutStr$ = "Accelerator Weight"
          CALL OutSc(KgAcc(), OutScan())
        CASE 2
          OutStr$ = "RF Sources Weight"
          CALL OutSc(KgRF(), OutScan())
        CASE 3
          OutStr$ = "Transformer Weight"
          CALL OutSc(KgXFMR(), OutScan())
        CASE 4
          OutStr$ = "PFN Weight"
          CALL OutSc(KgPFN(), OutScan())
        CASE 5
          OutStr$ = "CRC Weight"
          CALL OutSc(KgCRC(), OutScan())
        CASE 6
          OutStr$ = "Filter Bank Weight"
          CALL OutSc(KgFil(), OutScan())
        CASE 7
          OutStr$ = "Burst Power Weight"
          CALL OutSc(KgBur(), OutScan())
        CASE 8
          OutStr$ = "Fuel Weight"
          CALL OutSc(KgFuel(), OutScan())
        CASE 9
          OutStr$ = "Total Platform Weight"
          CALL OutSc(KgTot(), OutScan())
        CASE ELSE
      END SELECT
      END IF
    GOSUB Graphics
    RTO = 1  'fall through first loop put up output screen again

  CASE PgDn  'put up other screen
    IF scr% = 1 THEN scr% = 2 ELSE scr% = 1
```

```
            RTO = 1
          CASE ELSE

        END SELECT

      LOOP WHILE (RTI = 0) AND (RTO = 0)

    LOOP WHILE (RTI = 0) AND (RTO = 1)

  END IF

LOOP

END  'Physical end of program - logically never reached


 '+++++++++++++++++++++++++++++++++++++++++++++++++++++++++=++++++++++++++++++++
init:

'initialize arrays for input parameters

  PoFEL(0, 0) = 1: PoFEL(0, 1) = 2000000!: PoFEL(0, 2) = 4E+07
  PoFEL(0, 3) = 2000000!: PoFEL(0, 4) = 0: PoFEL(0, 5) = 1E+07
  PoFEL(0, 6) = 1000000!: PoFEL(0, 7) = 1: PoFEL(0, 8) = 1E+07

  EtaFel(0, 0) = 1: EtaFel(0, 1) = .05: EtaFel(0, 2) = .5
  EtaFel(0, 3) = .05: EtaFel(0, 4) = 0: EtaFel(0, 5) = .3
  EtaFel(0, 6) = 1: EtaFel(0, 7) = 0: EtaFel(0, 8) = .3

  TBurFel(0, 0) = 1: TBurFel(0, 1) = 50: TBurFel(0, 2) = 1000
  TBurFel(0, 3) = 50: TBurFel(0, 4) = 0: TBurFel(0, 5) = 500
  TBurFel(0, 6) = 1: TBurFel(0, 7) = 4: TBurFel(0, 8) = 500

  EAcc(0, 0) = 1: EAcc(0, 1) = 5E+07: EAcc(0, 2) = 2.5E+08
  EAcc(0, 3) = 1E+07: EAcc(0, 4) = 0: EAcc(0, 5) = 1.2E+08
  EAcc(0, 6) = 1000000!: EAcc(0, 7) = 5: EAcc(0, 8) = 1.2E+08

  RhoAcc(0, 0) = 1: RhoAcc(0, 1) = .5: RhoAcc(0, 2) = 75
  RhoAcc(0, 3) = .5: RhoAcc(0, 4) = 0: RhoAcc(0, 5) = 55
  RhoAcc(0, 6) = 1: RhoAcc(0, 7) = 14: RhoAcc(0, 8) = 55

  FAcc(0, 0) = 1: FAcc(0, 1) = 1E+08: FAcc(0, 2) = 1E+10
  FAcc(0, 3) = 1E+08: FAcc(0, 4) = 0: FAcc(0, 5) = 5E+08
  FAcc(0, 6) = 1E+09: FAcc(0, 7) = 12: FAcc(0, 8) = 5E+08

  EtaRF(0, 0) = 1: EtaRF(0, 1) = .05: EtaRF(0, 2) = 1
  EtaRF(0, 3) = .01: EtaRF(0, 4) = 0: EtaRF(0, 5) = .85
  EtaRF(0, 6) = 1: EtaRF(0, 7) = 0: EtaRF(0, 8) = .85

  LenAcc(0, 0) = 1: LenAcc(0, 1) = 5: LenAcc(0, 2) = 50
  LenAcc(0, 3) = .5: LenAcc(0, 4) = 0: LenAcc(0, 5) = 13.5
  LenAcc(0, 6) = 1: LenAcc(0, 7) = 3: LenAcc(0, 8) = 13.5

  EtaRec(0, 0) = 1: EtaRec(0, 1) = 0: EtaRec(0, 2) = 1
  EtaRec(0, 3) = .02: EtaRec(0, 4) = 0: EtaRec(0, 5) = .8
  EtaRec(0, 6) = 1: EtaRec(0, 7) = 0: EtaRec(0, 8) = .8

  TMPAcc(0, 0) = 1: TMPAcc(0, 1) = .000001: TMPAcc(0, 2) = .00001
```

```
TMPAcc(0, 3) = .0000002: TMPAcc(0, 4) = 0: TMPAcc(0, 5) = .0000032
TMPAcc(0, 6) = .000001: TMPAcc(0, 7) = 4: TMPAcc(0, 8) = .0000032

PRFAcc(0, 0) = 1: PRFAcc(0, 1) = 1000: PRFAcc(0, 2) = 10000
PRFAcc(0, 3) = 100: PRFAcc(0, 4) = 0: PRFAcc(0, 5) = 3100
PRFAcc(0, 6) = 1000: PRFAcc(0, 7) = 12: PRFAcc(0, 8) = 3100

IuPAcc(0, 0) = 1: IuPAcc(0, 1) = 500: IuPAcc(0, 2) = 5000
IuPAcc(0, 3) = 100: IuPAcc(0, 4) = 0: IuPAcc(0, 5) = 1000
IuPAcc(0, 6) = 1000: IuPAcc(0, 7) = 7: IuPAcc(0, 8) = 1000

'Scaling and Unit values for calculated parameters

AlphaAcc(0, 6) = 1: AlphaAcc(0, 7) = 0
PiFel(0, 6) = 1000000!: PiFel(0, 7) = 1
EgAcc(0, 6) = 1000000!: EgAcc(0, 7) = 11
PBmAvgAcc(0, 6) = 1000000: PBmAvgAcc(0, 7) = 1
TuPAcc(0, 6) = 1E-12: TuPAcc(0, 7) = 4
DutAcc(0, 6) = 1: DutAcc(0, 7) = 0
PBmPkAcc(0, 6) = 1E+09: PBmPkAcc(0, 7) = 1
IMPacc(0, 6) = 1: IMPacc(0, 7) = 7
IuPAcc(0, 6) = 1000: IuPAcc(0, 7) = 7
QuPAcc(0, 6) = 1E-09: QuPAcc(0, 7) = 8
Q0Acc(0, 6) = 1: Q0Acc(0, 7) = 0
qBAcc(0, 6) = 1: qBAcc(0, 7) = 0
URFAcc(0, 6) = 1: URFAcc(0, 7) = 10
PwlMAcc(0, 6) = 1000: PwlMAcc(0, 7) = 13
PWllAcc(0, 6) = 1000000: PWllAcc(0, 7) = 1
VSWRAcc(0, 6) = 1: VSWRAcc(0, 7) = 0
TFllAcc(0, 6) = .000001: TFllAcc(0, 7) = 4
EtaAcc(0, 6) = 1: EtaAcc(0, 7) = 0
KgFEL(0, 6) = 1: KgFEL(0, 7) = 2
KgAcc(0, 6) = 1: KgAcc(0, 7) = 2
KgRF(0, 6) = 1: KgRF(0, 7) = 2
KgXFMR(0, 6) = 1: KgXFMR(0, 7) = 2
KgPFN(0, 6) = 1: KgPFN(0, 7) = 2
KgPFN(0, 6) = 1: KgPFN(0, 7) = 2
KgCRC(0, 6) = 1: KgCRC(0, 7) = 2
KgFil(0, 6) = 1: KgFil(0, 7) = 2
KgBur(0, 6) = 1: KgBur(0, 7) = 2
KgFuel(0, 6) = 1: KgFuel(0, 7) = 2
KgTot(0, 6) = 1: KgTot(0, 7) = 2

' values for constants

KKFEL = .001      'FEL Weight Scaling              kg/kW
scavacc = 3       'Segments per cavity             none
VRF = 250         'RF Drive beam energy            eV
RovQAcc = 320     'Accelerator R/Q                 none
KKRF = .03        'RF Source weight scaling        kg/kW
DenAcc = 9000     'density of accelerator mat'l    kg/m3
KCPFN = .06       'capacitor weight scaling        kg/kJ
KLPFN = .001      'inductor weight scaling         kg/kJ
KTPFN = 1         'thyratron weight scaling        compound
KXFMR = 40        'Transformer weight scaling      kg/kj
KCRC = .02        'CRC weight scaling              kg/kW
KFil = .06        'Filter bank weight scaling      kg/kJ
KBur = .02        'Burst power weight scaling      kg/kw
```

```
  KCom = .02          'Combustor weight scaling          kg/kw
  KTur = .02          'Turbine weight scaling            kg/kw
  KBurM = .02         'Burst Misc weight scaling         kg/kw
  WBase = 40000000    'Baseload Power                    Watts
  KgBase = 4000       'Baseload Power weight             kg
  KgPoint = 1000      'Pointing/tracking weight          kg
  EtaXFMR = .99       'Transformer Efficiency
  EtaPFN = .95        'PFN Efficiency
  EtaCRC = .95        'CRC Efficiency

RETURN


printrout:
  CLS
  PRINT
  CALL Units(PiFel(0, 6), PiFel(0, 7), u$)
  PRINT USING "FEL Avg Input Power =  ####.## & "; PiFel(1, i) / PiFel(0, 6); u$
  CALL Units(EgAcc(0, 6), EgAcc(0, 7), u$)
  PRINT USING "Accelerator Gradient =  ####.## & "; EgAcc(1, i) / EgAcc(0, 6); u$
  CALL Units(PBmAvgAcc(0, 6), PBmAvgAcc(0, 7), u$)
  PRINT USING "Accelerator Avg Beam Power =  ####.## & "; PBmAvgAcc(1, i) /
PBmAvgAcc(0, 6); u$
  CALL Units(DutAcc(0, 6), DutAcc(0, 7), u$)
  PRINT USING "Accelerator Duty Factor =  ####.## & "; DutAcc(1, i) / DutAcc(0, 6);
u$
  CALL Units(PBmPkAcc(0, 6), PBmPkAcc(0, 7), u$)
  PRINT USING "Accelerator Peak Beam Power =  ####.## & "; PBmPkAcc(1, i) /
PBmPkAcc(0, 6); u$
  CALL Units(IMPacc(0, 6), IMPacc(0, 7), u$)
  PRINT USING "Macropulse Peak Current =  ####.## & "; IMPacc(1, i) / IMPacc(0, 6);
u$
  CALL Units(QuPAcc(0, 6), QuPAcc(0, 7), u$)
  PRINT USING "Micropulse Charge =  ####.## & "; QuPAcc(1, i) / QuPAcc(0, 6); u$
  CALL Units(TuPAcc(0, 6), TuPAcc(0, 7), u$)
  PRINT USING "Micropulse Duration =  ####.## & "; TuPAcc(1, i) / TuPAcc(0, 6); u$
  CALL Units(Q0Acc(0, 6), Q0Acc(0, 7), u$)
  PRINT USING "Accelerator Qo = #####.# & "; Q0Acc(1, i) / Q0Acc(0, 6); u$
  CALL Units(URFAcc(0, 6), URFAcc(0, 7), u$)
  PRINT USING "Accelerator Stored Energy =  ####.## & "; URFAcc(1, i) / URFAcc(0,
6); u$
  CALL Units(qBAcc(0, 6), qBAcc(0, 7), u$)
  PRINT USING "Accelerator Beam Q =  ####.## & "; qBAcc(1, i) / qBAcc(0, 6); u$
  CALL Units(AlphaAcc(0, 6), AlphaAcc(0, 7), u$)
  PRINT USING "Accelerator Beam Loading =  #.### & "; AlphaAcc(1, i) / AlphaAcc(0,
6); u$
  CALL Units(VSWRAcc(0, 6), VSWRAcc(0, 7), u$)
  PRINT USING "Accelerator VSWR = ###.# & "; VSWRAcc(1, i) / VSWRAcc(0, 6); u$
  CALL Units(TF11Acc(0, 6), TF11Acc(0, 7), u$)
  PRINT USING "Accelerator Fill Time = ##.## & "; TF11Acc(1, i) / TF11Acc(0, 6); u$
  CALL Units(EtaAcc(0, 6), EtaAcc(0, 7), u$)
  PRINT USING "Accelerator Efficiency = #.### & "; EtaAcc(1, i) / EtaAcc(0, 6); u$
  CALL Units(PW11Acc(0, 6), PW11Acc(0, 7), u$)
  PRINT USING "Avg Wall Losses =  ####.## & "; PW11Acc(1, i) / PW11Acc(0, 6); u$
  CALL Units(Pw1MAcc(0, 6), Pw1MAcc(0, 7), u$)
  PRINT USING "Avg Wall losses per Meter =  ####.## & "; Pw1MAcc(1, i) / Pw1MAcc(0,
6); u$
  CALL MessageWait("")
```

```
  'printer output
    LPRINT USING "FEL Ouput Power ##.# MW"; PoFEL(1, 0) / PoFEL(0, 6)
    LPRINT USING "FEL Efficiency #.##"; EtaFel(1, 0) / EtaFel(0, 6)
    LPRINT USING "Burst Duration #### Sec"; TBurFel(1, 0) / TBurFel(0, 6)
    LPRINT USING "Accelerator Kinetic Energy ### MeV"; EAcc(1, 0) / EAcc(0, 6)
    LPRINT USING "Cavity Resistivity #### microOhm-Meters"; RhoAcc(1, 0) / RhoAcc(0,
6)
    LPRINT USING "Accelerator Frequency ##.## GHz"; FAcc(1, 0) / FAcc(0, 6)
    LPRINT USING "RF Source Set Efficiency #.##"; EtaRF(1, 0) / EtaRF(0, 6)
    LPRINT USING "Accelerator Length ###.# Meters"; LenAcc(1, 0) / LenAcc(0, 6)
    LPRINT USING "FEL Beam Recirculaion Efficiency #.##"; EtaRec(1, 0) / EtaRec(0,
6)
    LPRINT USING "Macropulse Duration ##.## microseconds"; TMPAcc(1, 0) / TMPAcc(0,
6)
    LPRINT USING "Macropulse Rep-rate ##.## kHz"; PRFAcc(1, 0) / PRFAcc(0, 6)
    LPRINT USING "Micropulse Peak Current ##.## kA"; IuPAcc(1, 0) / IuPAcc(0, 6)


RETURN


Graphics:
  '       We enter this subroutine with the following Knowledge
  '
  '               InScan(0:10) - the eleven values of the input parameter
  '               OutScan(0:10) - the eleven values of the output parameter
  '               InScan(11) - the scale factor for the input
  '               OutScan(11) - the scale factor for the output
  '               InScan(12) - the units for the input
  '               OutScan(12) - the units for the output
  '               InStr$ - The name of the input parameter
  '               OutStr$ - The name of the output parameter
  '
  '  First, convert to units and get the maxes and mins
  mindx = 1E+20: maxdx = -1E+20: mindy = 1E+20: maxdy = -1E+20
  FOR i = 0 TO 10
    OutScan(i) = OutScan(i) / OutScan(11)
    IF OutScan(i) > maxdy THEN maxdy = OutScan(i)
    IF OutScan(i) < mindy THEN mindy = OutScan(i)
    IF InScan(i) > maxdx THEN maxdx = InScan(i)
    IF InScan(i) < mindx THEN mindx = InScan(i)
  NEXT i

  '  The x limits are the data limits, but we need better scaling for y
  ydspr = maxdy - mindy

  IF ydspr = 0 THEN  'Output parameter is constant - no graph
    CALL MessageWait(OutStr$ + " is constant =" + STR$(maxdy))
    RETURN
  END IF

  test = 0      'find the lowest  per div value that contains the data
  sc = .0001
NextOOM:
  fac = 1
  GOSUB testsc
  IF test = 1 THEN GOTO done
  fac = 2
```

```
  GOSUB testsc
  IF test = 1 THEN GOTO done
  fac = 2.5
  GOSUB testsc
  IF test = 1 THEN GOTO done
  fac = 5
  GOSUB testsc
  IF test = 1 THEN GOTO done
  sc = sc * 10
  GOTO NextOOM
testsc:
  ydiv = sc * fac
  ygmin = INT(mindy / ydiv) * ydiv
  ygmax = ygmin + 6 * ydiv
  IF (ygmin < mindy) AND (ygmax > maxdy) THEN test = 1
RETURN

done:
  dropout = 0
  DO
    CLS
    SCREEN ScreenType%              'use screen to get screen dumps
    SHELL "graphics"      'allow screen dump

    'Draw graph and label axes
    WINDOW (-.2, -.245)-(1.1, 1.14)
    LINE (0, 0)-(0, 1): LINE (0, 1)-(1, 1): LINE (1, 1)-(1, 0): LINE (1, 0)-(0, 0)
    FOR i = 0 TO 10: LINE (i / 10, -.01)-STEP(0, .01): NEXT i
    FOR i = 2 TO 8 STEP 2
      LINE (i / 10, 0)-(i / 10, 1), , , &HF800
    NEXT i
    FOR i = 0 TO 6: LINE (-.01, i / 6)-STEP(.01, 0): NEXT i
    FOR i = 2 TO 4 STEP 2
      LINE (0, i / 6)-(1, i / 6), , , &HF800
    NEXT i
    FOR i = 3 TO 21 STEP 6
      LOCATE i, 1
      PRINT USING "####.###"; ygmin + (21 - i) / 3 * ydiv
    NEXT i
    LOCATE 22, 9
    PRINT USING "####.###"; InScan(0)
    LOCATE 22, 22
    PRINT USING "####.###"; InScan(2)
    LOCATE 22, 34
    PRINT USING "####.###"; InScan(4)
    LOCATE 22, 47
    PRINT USING "####.###"; InScan(6)
    LOCATE 22, 59
    PRINT USING "####.###"; InScan(8)
    LOCATE 22, 72
    PRINT USING "####.###"; InScan(10)

    'draw data
    xspr = InScan(10) - InScan(0)
    ygspr = 6 * ydiv
    xmin = InScan(0)
    ygmin = ygmin
    FOR i = 0 TO 9
```

```
  xc = (InScan(i) - xmin) / xspr
  xn = (InScan(i + 1) - xmin) / xspr
  yc = (OutScan(i) - ygmin) / ygspr
  yn = (OutScan(i + 1) - ygmin) / ygspr
  IF (xc >= 0) AND (xc <= 1) THEN            'don't draw outside graph
    IF (xn >= 0) AND (xn <= 1) THEN
      IF (yn >= 0) AND (yn <= 1) THEN
        IF (yc >= 0) AND (yc <= 1) THEN
          LINE (xc, yc)-(xn, yn)
        END IF
      END IF
    END IF
  END IF
NEXT i

' make up title for graph
CALL Units(InScan(11), InScan(12), Iu$)
IF Iu$ = "" THEN Iu$ = "" ELSE Iu$ = " (" + Iu$ + ")"
CALL Units(OutScan(11), OutScan(12), Ou$)
IF Ou$ = "" THEN Ou$ = "" ELSE Ou$ = " (" + Ou$ + ")"
Title$ = OutStr$ + Ou$ + " vs. " + InStr$ + Iu$
LOCATE 1, 40 - INT(LEN(Title$) / 2)
PRINT Title$

'instructions to continue
LOCATE 24, 16
PRINT "S to rescale, P for new Output Parameter, I for new Inputs";
LOCATE 1, 1

DO

  DO
    K$ = INKEY$
  LOOP WHILE K$ = ""
  ky = ASC(RIGHT$(K$, 1))

  SELECT CASE ky
    CASE 83, 115  'S - ReScale graph
      LOCATE 24, 16
      PRINT SPACE$(62);
      LOCATE 23, 16
      INPUT "New Minimum Vertical Value", newV
      ygmin = newV
      DO
        LOCATE 23, 16
        PRINT SPACE$(54);
        LOCATE 23, 16
        INPUT "New Maximum Vertical Value", newV
      LOOP UNTIL newV > ygmin
      ydiv = (newV - ygmin) / 6
      EXIT DO

    CASE 80, 112  'P - Leave and select output parameter
      dropout = 1
      EXIT DO

    CASE 73, 105  'I - Leave and redo input
      dropout = 1
```

```
          RTI = 1
          EXIT DO

        CASE ELSE
      END SELECT
    LOOP
  LOOP WHILE dropout = 0
  CLS
  SCREEN 0
 RETURN


OthInp:

' Constants for key codes and column positions

  CONST sRow = 6
  CONST SNInp = 18
  SR = 0: RTI = 0
  DO
    CLS
    LOCATE 1, COL1
    PRINT "DOWN/UP ................... Move to Next Field"
    LOCATE 2, COL1
    PRINT "INS ..................... Enter Value Directly"
    LOCATE 3, COL1
    PRINT "HOME ...... Save or Retrieve Input Parameters"
    LOCATE 4, COL1
    PRINT "PgDn ................. Alternate Input Screen"

    LOCATE sRow, COL1, 1, 1, 12

    LOCATE sRow, COL0: PRINT "FEL Weight Scaling Factor (kg/kW)";
    LOCATE sRow, COL2: PRINT USING "[ #.#### ]"; KKFEL;

    LOCATE sRow + 1, COL0: PRINT "RF Drive Beam Energy (keV)";
    LOCATE sRow + 1, COL2: PRINT USING "[ ####.# ]"; VRF / 1000;

    LOCATE sRow + 2, COL0: PRINT "Accelerator R/Q (Ohms)";
    LOCATE sRow + 2, COL2: PRINT USING "[ ####.# ]"; RovQAcc;

    LOCATE sRow + 3, COL0: PRINT "RF Source Weight Scaling (kg/kW)";
    LOCATE sRow + 3, COL2: PRINT USING "[ #.#### ]"; KKRF;

    LOCATE sRow + 4, COL0: PRINT "Accelerator Material Density (kg/m3)";
    LOCATE sRow + 4, COL2: PRINT USING "[ ####.# ]"; DenAcc / 1000;

    LOCATE sRow + 5, COL0: PRINT "Capacitor Weight Scaling (kg/kJ)";
    LOCATE sRow + 5, COL2: PRINT USING "[ #.#### ]"; KCPFN;

    LOCATE sRow + 6, COL0: PRINT "Inductor Weight Scaling (kg/kJ)";
    LOCATE sRow + 6, COL2: PRINT USING "[ #.#### ]"; KLPFN;

    LOCATE sRow + 7, COL0: PRINT "Thyratron Weight Scaling (kg/kW)";
    LOCATE sRow + 7, COL2: PRINT USING "[ #.#### ]"; KTPFN;

    LOCATE sRow + 8, COL0: PRINT "Transformer Weight Scaling";
```

```
      LOCATE sRow + 8, COL2: PRINT USING "[ #.#### ]"; KXFMR;

      LOCATE sRow + 9, COL0: PRINT "CRC Weight Scaling (kg/kW)";
      LOCATE sRow + 9, COL2: PRINT USING "[ #.#### ]"; KCRC;

      LOCATE sRow + 10, COL0: PRINT "Filter Bank Weight Scaling (kg/kJ)";
      LOCATE sRow + 10, COL2: PRINT USING "[ #.#### ]"; KFil;

      LOCATE sRow + 11, COL0: PRINT "Burst Power Weight Scaling (kg/kW)";
      LOCATE sRow + 11, COL2: PRINT USING "[ #.#### ]"; KBur;

      LOCATE sRow + 12, COL0: PRINT "Combustor Weight Scaling (kg/kW)";
      LOCATE sRow + 12, COL2: PRINT USING "[ #.#### ]"; KCom;

      LOCATE sRow + 13, COL0: PRINT "Turbine Weight Scaling (kg/kW)";
      LOCATE sRow + 13, COL2: PRINT USING "[ #.#### ]"; KTur;

      LOCATE sRow + 14, COL0: PRINT "Baseload Power Requirement (MW)";
      LOCATE sRow + 14, COL2: PRINT USING "[ #####. ]"; WBase / 1000000;

      LOCATE sRow + 15, COL0: PRINT "Baseload Power Weight (kg)";
      LOCATE sRow + 15, COL2: PRINT USING "[ #####. ]"; KgBase;

      LOCATE sRow + 16, COL0: PRINT "Pointing/Tracking Weight (kg)";
      LOCATE sRow + 16, COL2: PRINT USING "[ ##### ]"; KgPoint;

      LOCATE sRow + 17, COL0: PRINT "Recirculation Type";
      LOCATE sRow + 17, COL2:
      IF RecType% = RCTA THEN PRINT "[  RCTA ]";  ELSE PRINT "[  DECL ]";

      LOCATE sRow + 18, COL0: PRINT "Computer Screen Type";
      LOCATE sRow + 18, COL2:
      IF ScreenType% = EGA THEN PRINT "[  EGA  ]";  ELSE PRINT "[  CGA  ]";

      Fld = 0

      DO
        LOCATE sRow + Fld, COL2 + 2
        DO
          DO
            K$ = INKEY$
          LOOP WHILE K$ = ""
          ky = ASC(RIGHT$(K$, 1))
        LOOP WHILE NOT ((ky = UPARROW) OR (ky = DOWNARROW) OR (ky = HOME) OR (ky =
PgDn) OR (ky = INSKEY))

        SELECT CASE ky

          CASE UPARROW, DOWNARROW
            IF ky = DOWNARROW THEN inc = 1 ELSE inc = -1
            Fld = Fld + inc
            IF Fld = -1 THEN Fld = SNInp
            IF Fld = SNInp + 1 THEN Fld = 0

          CASE INSKEY
            SELECT CASE Fld
              CASE 0
                CALL FixInp(KKFEL, Fld, "#.####", 1)
```

```
      CASE 1
        CALL FixInp(VRF, Fld, "####.#", 1000)
      CASE 2
        CALL FixInp(RovQAcc, Fld, "####.#", 1)
      CASE 3
        CALL FixInp(KKRF, Fld, "#.####", 1)
      CASE 4
        CALL FixInp(DenAcc, Fld, "####.#", 1000)
      CASE 5
        CALL FixInp(KCPFN, Fld, "#.####", 1)
      CASE 6
        CALL FixInp(KLPFN, Fld, "#.####", 1)
      CASE 7
        CALL FixInp(KTPFN, Fld, "#.####", 1)
      CASE 8
        CALL FixInp(KXFMR, Fld, "#.####", 1)
      CASE 9
        CALL FixInp(KCRC, Fld, "#.####", 1)
      CASE 10
        CALL FixInp(KFil, Fld, "#.####", 1)
      CASE 11
        CALL FixInp(KBur, Fld, "#.####", 1)
      CASE 12
        CALL FixInp(KCom, Fld, "#.####", 1)
      CASE 13
        CALL FixInp(KTur, Fld, "#.####", 1)
      CASE 14
        CALL FixInp(WBase, Fld, "###.##", 1000000)
      CASE 15
        CALL FixInp(KgBase, Fld, "#####.", 1)
      CASE 16
        CALL FixInp(KgPoint, Fld, "#####.", 1)
      CASE 17
        LOCATE sRow + 17, COL2 + 3
        IF RecType% = RCTA THEN
          RecType% = DECL
          PRINT "DECL";
        ELSE
          RecType% = RCTA
          PRINT "RCTA";
        END IF

      CASE 18
        LOCATE sRow + 18, COL2 + 3
        IF ScreenType% = EGA THEN
          ScreenType% = CGA
          PRINT "CGA";
        ELSE
          ScreenType% = EGA
          PRINT "EGA";
        END IF
      CASE ELSE
    END SELECT
  CASE HOME
    GOSUB SaveRoutine
    RTI = 1
    EXIT DO
  CASE PgDn
```

```
          RTI = 1
          EXIT DO
        CASE ELSE
      END SELECT
    LOOP
  LOOP WHILE RTI = 0
RETURN


SaveRoutine:
  DO
    CLS
    LOCATE 1, COL1: PRINT "S ..... Save Current Input Parameters"
    LOCATE 2, COL1: PRINT "R ..... Retrieve A Saved Parameter Set"
    LOCATE 3, COL1: PRINT "ESC ..... Return to Input Screen"
    DO
      DO
        K$ = INKEY$
      LOOP WHILE K$ = ""
      ky = ASC(RIGHT$(K$, 1))
    LOOP WHILE NOT ((ky = ESCAPE) OR (ky = ASC("S")) OR (ky = ASC("s")) OR (ky =
ASC("R")) OR (ky = ASC("r")))

    SELECT CASE ky

      CASE ESCAPE
        RTI = 1
        EXIT DO

      CASE ASC("s"), ASC("S")
        LOCATE 6, 1
        PRINT "Enter File Name (Including Path if different from current Default)"
        LOCATE 7, 1
        INPUT "File Name... ", Fil$
        ON ERROR GOTO LocErr
        OPEN "O", 1, Fil$
        WRITE #1, ScanFlg%
        FOR i = 0 TO 1
          FOR j = 0 TO 10
            WRITE #1, PoFEL(i, j), EtaFel(i, j), TBurFel(i, j), EAcc(i, j)
            WRITE #1, RhoAcc(i, j), FAcc(i, j), EtaRF(i, j), LenAcc(i, j)
            WRITE #1, EtaRec(i, j), TMPAcc(i, j), PRFAcc(i, j), IuPAcc(i, j)
          NEXT j
        NEXT i
        WRITE #1, KKFEL, VRF, RovQAcc, KKRF
        WRITE #1, DenAcc, KCPFN, KLPFN, KTPFN, KXFMR, KCRC, KFil
        WRITE #1, KBur, KCom, KTur, KBurM, WBase, KgBase, KgPoint
        CLOSE #1
        ON ERROR GOTO 0

      CASE ASC("R"), ASC("r")
        LOCATE 6, 1
        PRINT "Enter File Name (Including Path if different from current Default)"
        LOCATE 7, 1
        INPUT "File Name... ", Fil$
        ON ERROR GOTO LocErr
        OPEN "I", 1, Fil$
        INPUT #1, ScanFlg%
```

```
        FOR i = 0 TO 1
          FOR j = 0 TO 10
            INPUT #1, PoFEL(i, j), EtaFel(i, j), TBurFel(i, j), EAcc(i, j)
            INPUT #1, RhoAcc(i, j), FAcc(i, j), EtaRF(i, j), LenAcc(i, j)
            INPUT #1, EtaRec(i, j), TMPAcc(i, j), PRFAcc(i, j), IuPAcc(i, j)
          NEXT j
        NEXT i
        INPUT #1, KKFEL, VRF, RovQAcc, KKRF
        INPUT #1, DenAcc, KCPFN, KLPFN, KTPFN, KXFMR, KCRC, KFil
        INPUT #1, KBur, KCom, KTur, KBurM, WBase, KgBase, KgPoint
        CLOSE #1
        ON ERROR GOTO 0

      CASE ELSE

    END SELECT
  LOOP

RETURN

LocErr:

  LOCATE 10, 1
  PRINT "File Operation not Sucessful"
  CALL MessageWait("")
  GOTO SaveRoutine

END

DEFINT A-Z
' ================================ Delay ============================
'   Delay based on time so that wait will be the same on any processor.
'   Notice the check for negative numbers so that the delay won't
'   freeze at midnight when the delay could become negative.
' ===================================================================
'
SUB Delay (Seconds!) STATIC

   Begin! = TIMER
   DO UNTIL (TIMER - Begin! > Seconds!) OR (TIMER - Begin! < 0)
   LOOP

END SUB

DEFSNG A-Z
SUB FixInp (Var, Fld, f$, sc)
   DO
     BEEP
     LOCATE sRow + Fld, COL2: PRINT "[" + SPACE$(LEN(f$) + 2) + "]";
     LOCATE sRow + Fld, COL2 + 2: INPUT NewVal
   LOOP WHILE NewVal < 0
   Var = NewVal * sc
   LOCATE sRow + Fld, COL2: PRINT SPACE$(79 - COL2 - 2);
   LOCATE sRow + Fld, COL2: PRINT USING "[ " + f$ + " ]"; Var / sc;
END SUB

' ============================ IncDec ================================
'   Returns the Current value adjusted by Inc and rotated if necessary
```

```
'   so that it falls within the range of Lower and Upper.
' ====================================================================
'
SUB IncDec (D(), inc)

   ' Calculate the next value
   OldValue = D(0, 5)
   D(0, 5) = D(0, 5) + inc * D(0, 3)
   ' Handle special cases of rotating off top or bottom
   IF D(0, 5) >= D(0, 2) THEN D(0, 5) = D(0, 2)
   IF D(0, 5) <= D(0, 1) THEN D(0, 5) = D(0, 1)

END SUB

DEFINT A-Z
' ============================== Message ==============================
'   Displays a status message followed by blinking dots.
' ====================================================================
'
SUB Message (text$) STATIC
   LOCATE 24, 1: PRINT SPACE$(60);
   LOCATE 24, 1
   COLOR 7        ' White
   PRINT text$;
'   COLOR 23       ' Blink
   IF text$ <> "" THEN
     PRINT " . . .";
   END IF
   COLOR 7        ' White
END SUB

DEFSNG A-Z
'============================== MessageWait ==============================
'        This routine displays a message on the last line and then waits
'   for the user to strike a key before continuing.  It then blanks the
'   message and returns.
'=========================================================================
SUB MessageWait (text$) STATIC
   LOCATE 24, 1: PRINT SPACE$(60);
   LOCATE 24, 1
   COLOR 7        ' White
   PRINT text$ + "  (Any Key to Continue)";

   PRINT " . . .";
   COLOR 7        ' White

   DO
   K$ = INKEY$
   LOOP WHILE K$ = ""
   CALL Message("")
END SUB

SUB OutSc (D(), scan())
  FOR i = 0 TO 10
    scan(i) = D(1, i)
  NEXT i
  scan(11) = D(0, 6)
  scan(12) = D(0, 7)
```

```
END SUB

SUB PrLin (D(), Fld, f$)
   IF D(0, 4) = 0 THEN
     LOCATE ROW + Fld, COL2
     PRINT USING "[ " + f$ + " ]"; D(0, 5) / D(0, 6);
   ELSE
     LOCATE ROW + Fld, COL2
     PRINT USING "[ " + f$ + " - " + f$ + " ]"; D(1, 0) / D(0, 6); D(1, 10) / D(0,
6)
   END IF
END SUB

SUB ScanSub (D(), s%, Fld, f$, InScan())
'================================ ScanSub ================================
'       This routine handles changing input from a ten value scan
'   to a single value and vice versa.  S% is 1 when any scan is active
'   for any parameter, d(0,4) is 1 when this particular parameter is
'   being scanned.  If a scan of this parameter is activated, this
'   routine fills (1,0) through (1,10) with equally spaced values before
'   returning.
'=========================================================================
   IF (s% = 1) AND (D(0, 4) = 0) THEN
      MessageWait ("Deactivate Other Scan First")
   ELSEIF D(0, 4) = 1 THEN
      D(0, 4) = 0
      D(0, 5) = D(1, 0)
      s% = 0
   ELSEIF (s% = 0) AND (D(0, 4) = 0) THEN
      DO
         LOCATE ROW + NInp + 2, COL0
         INPUT "Enter Minimum Value for Scan...  ", min
         LOCATE ROW + NInp + 3, COL0
         INPUT "Enter Maximum Value for Scan...  ", max
         LOCATE ROW + NInp + 2, COL0
         PRINT SPACE$(50)
         LOCATE ROW + NInp + 3, COL0
         PRINT SPACE$(50)
      LOOP UNTIL min <> max
      D(0, 4) = 1
      s% = 1
      D(1, 0) = min * D(0, 6)
      InScan(0) = D(1, 0) / D(0, 6)
      D(1, 10) = max * D(0, 6)
      InScan(10) = D(1, 10) / D(0, 6)
      FOR i = 1 TO 9
         D(1, i) = D(1, 0) + i * (D(1, 10) - D(1, 0)) / 10
         InScan(i) = D(1, i) / D(0, 6)
      NEXT i
      InScan(11) = D(0, 6)
      InScan(12) = D(0, 7)
   END IF
   LOCATE ROW + Fld, COL2 + 2
   IF D(0, 4) = 0 THEN
      PRINT USING f$ + " ]           "; D(0, 5) / D(0, 6)
   ELSE
      PRINT USING f$ + " - " + f$ + " ]"; D(1, 0) / D(0, 6); D(1, 10) / D(0, 6)
```

```
   END IF
END SUB

'============================ SetupArray ==================================
'       This simple routine fills the (1,1) through (1,10) positions
'   of the array with the value in the (0,5) position unless (0,4)=1
'   which indicates this is a scanned parameter.
'==========================================================================
SUB SetupArray (D())
IF D(0, 4) = 0 THEN
  FOR i = 0 TO 10
    D(1, i) = D(0, 5)
  NEXT i
END IF
END SUB

SUB Units (a, b, unit$)
   SELECT CASE a
      CASE 1E-12
         sc$ = "p"
      CASE 1E-09
         sc$ = "n"
      CASE .000001
         sc$ = "u"
      CASE .001
         sc$ = "m"
      CASE .01
         sc$ = "c"
      CASE 1
         sc$ = ""
      CASE 1000
         sc$ = "k"
      CASE 1000000
         sc$ = "M"
      CASE 1E+09
         sc$ = "G"
      CASE 1E+12
         sc$ = "T"
      CASE ELSE
   END SELECT
   SELECT CASE b
      CASE 0
         un$ = ""
      CASE 1
         un$ = "W"
      CASE 2
         un$ = "kg"
      CASE 3
         un$ = "m"
      CASE 4
         un$ = "s"
      CASE 5
         un$ = "eV"
      CASE 6
         un$ = "mm-mrad"
      CASE 7
         un$ = "A"
      CASE 8
```

```
            un$ = "C"
         CASE 9
            un$ = "Ohms"
         CASE 10
            un$ = "J"
         CASE 11
            un$ = "V/m"
         CASE 12
            un$ = "Hz"
         CASE 13
            un$ = "W/m"
         CASE 14
            un$ = "uOhm-cm"
         CASE 15
            un$ = "kg/m^3"
         CASE 16
            un$ = "kg/m"
         CASE 17
            un$ = "V"
         CASE ELSE
      END SELECT
      unit$ = sc$ + un$
END SUB

'============================== UpDown ==================================
'           Used to increment, decrement, or input a new value directly.
'      First requires that an active scan of this parameter be disabled.
'      Calls IncDec to do the inc/dec function but handles the direct
'      entry right here.
'========================================================================
'
SUB UpDown (D(), f$, inc, Fld)
  IF D(0, 4) = 1 THEN
    MessageWait ("Deactivate Scan First")
  ELSEIF inc <> 0 THEN
    CALL IncDec(D(), inc)
    PRINT USING f$; D(0, 5) / D(0, 6)
  ELSE
    LOCATE ROW + NInp + 2, COL0
    INPUT "Enter New Value...  ", NewVal
    LOCATE ROW + NInp + 2, COL0
    PRINT SPACE$(50)
    D(0, 5) = NewVal * D(0, 6)
    LOCATE ROW + Fld, COL2 + 2
    IF D(0, 4) = 0 THEN PRINT USING f$ + " ]          "; D(0, 5) / D(0, 6)
  END IF
END SUB
```

APPENDIX C

SRI REPORT ON ULTRA-WIDEBAND SEA CLUTTER MEASUREMENTS

SRI International

Final Report • December 1990

ULTRA-WIDEBAND SEA CLUTTER MEASUREMENTS

Michael D. Cousins, Senior Research Engineer
Roger S. Vickers, Senior Research Physicist
Geoscience and Engineering Center

SRI Project 1309

Prepared for:

Physics International Company
2700 Merced Street
San Leandro, California 94577

Attn: George Frazier

Subcontract B84038MC

333 Ravenswood Avenue • Menlo Park, CA 94025-3493 • (415) 326-6200 • FAX: (415) 326-5512 • Telex: 334486

Final Report • December 1990

ULTRA-WIDEBAND SEA CLUTTER MEASUREMENTS

Michael D. Cousins, Senior Research Engineer
Roger S. Vickers, Senior Research Physicist
Geoscience and Engineering Center

SRI Project 1309

Prepared for:

Physics International Company
2700 Merced Street
San Leandro, California 94577

Attn: George Frazier

Subcontract B84038MC

Approved:

Murray J. Baron, Director
Geoscience and Engineering Center

John P. McHenry, Vice President
Advanced Development Division

SRI International 333 Ravenswood Avenue • Menlo Park, CA 94025-3493 • (415) 326-6200 • FAX: (415) 326-5512 • Telex: 334486

CONTENTS

ILLUSTRATIONS

TABLES

I INTRODUCTION

Recent interest in ultra-wideband (UWB) radar systems and their possible application to ship defense against low-altitude missiles (sea skimmers) has led to the realization that very little data is available in the literature on ocean backscatter from UWB systems. Of particular interest is the region from 400 MHz down to the resonant frequencies of possible sea-skimming targets (around 60 MHz). The effort described in this report supports a NOSC program to provide measurements from 200 to 1000 MHz on ocean backscatter and on the visibility of certain specific targets in the presence of the radar clutter from the ocean.

The study reported here is Phase I of a two-phase effort in which a high-power UWB radar system will be operated at the NOSC facility at Point Loma (San Diego), California, to collect a sample suite of UWB data. In this first phase, the wideband feeds for both the receiver and transmitting antennas were designed and tested and the receiver design was completed.

II ANTENNA FEED DESIGN CONSIDERATIONS

The objective of this work has been to devise an antenna having a small beamwidth (and consequently high gain) that will transmit and/or receive ultra-wideband (UWB) radar signals with little overall distortion. Because the purpose of the antenna is to serve as the transmission and receiving element in a radar system directed at the study of sea clutter, a beamwidth having the smallest practical value is desired. The signals of interest cover the spectrum from 200 MHz to 1000 MHz. Because a 30-ft parabolic reflector is the largest reasonably transportable antenna element available to us, it has been chosen as the principal antenna aperture to be illuminated. We recognized, as others have (Walton and Sundberg, 1964), that an appropriately designed horn illuminating the reflector aperture can result in an antenna system with approximately constant gain and beamwidth over the frequency range covered. The desired feed horn would provide full illumination of the parabolic reflector at the lowest frequency to be used and increasingly narrower beams of illumination at higher frequencies. The available 30-ft reflector has a focus-to-diameter ratio of 0.35, which results in an angle subtended at the prime focus of approximately 110°. Thus, this establishes the desired horn beamwidth at the lowest operating frequency.

A broadband double-ridge waveguide derived horn has been selected for the feed horn to provide the widest possible bandwidth and small size (to limit feed blockage). Devices of the general design required have been described in the literature (Walton and Sundberg, 1964; Kerr, 1973) and are commercially available covering the 200 MHz to 2000 MHz frequency range. SRI has used such broadband horns extensively in previous UWB radar work and thus we have developed a degree of confidence in utilizing them for the present application. Figure 1 shows the E- and H- field patterns for the available broadband horn at 200 MHz and 1000 MHz. At the low-frequency end, the horn pattern is quite suitable for use in illuminating the 30-ft parabolic dish, owing to the well-balanced E- and H- patterns. The situation is not as favorable at higher frequencies (1 GHz, for example). The E- and H- patterns are not as well balanced or as narrow as desired. The horn provides a reasonable and useful 6-dB edge taper at 200 MHz that will help minimize unwanted sidelobes. The double-ridged broadband horn available for experimental application at SRI displays moderate dispersion. In the past, this effect has been ameliorated by resistive loading at the aperture and in the waveguide section. Overall efficiency of the broadband horns has been observed to be low. Furthermore, these inefficiencies are almost certainly a result of the E-plane phase errors across the horn aperture, as reported in Walton and Sundberg (1964). These problems have led others to apply dielectric correcting lenses to the antenna to compensate for the nonideal nature of the otherwise desirable antenna. Left uncompensated, the aperture phase errors are manifested by reduced efficiency and increased beamwidth owing to an effective aperture that is substantially smaller than the physical horn dimensions.

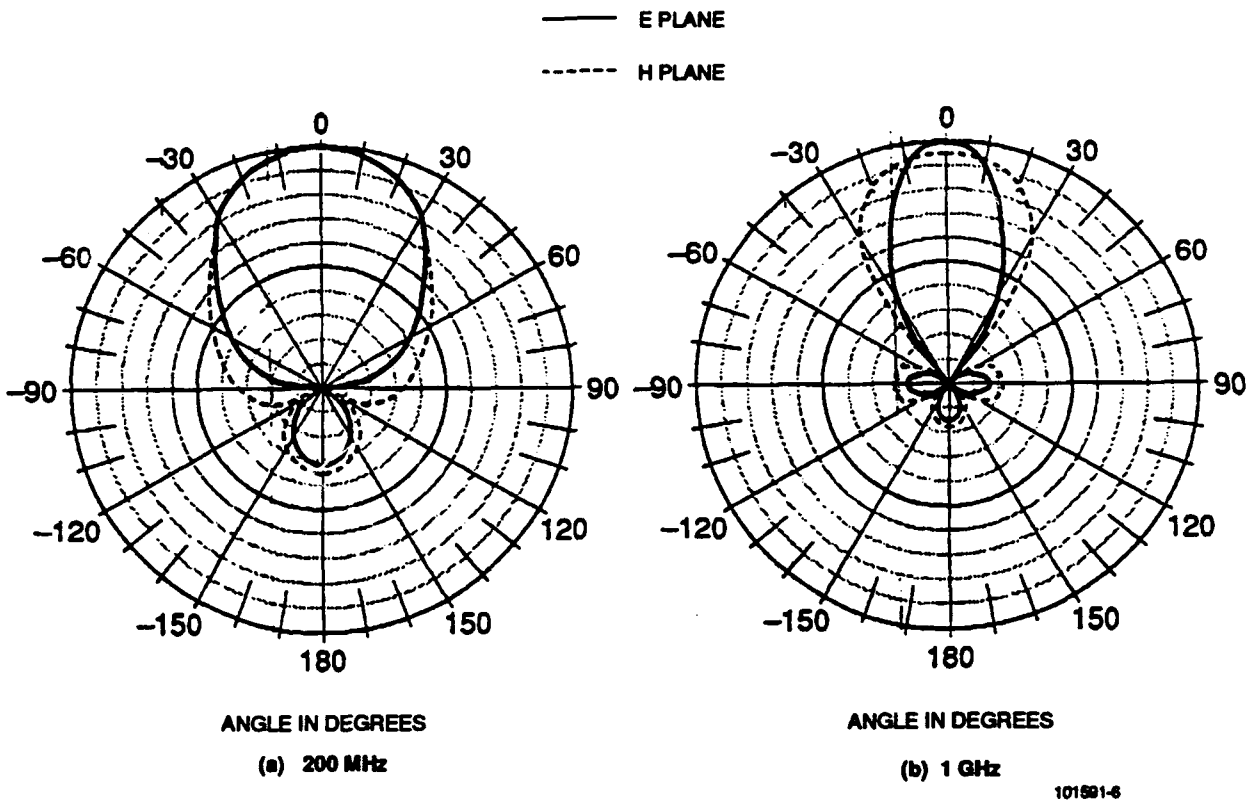

FIGURE 1 E- AND H- PATTERNS OF BROADBAND HORN AT 200 MHz AND 1 GHz

Each ring = 0.10 (relative voltage)

Our approach has been to:

- Apply the known broadband horn as an unmodified feed
- Measure the overall results obtained when radiating signals of the expected kind
- Determine the resultant suitability of the antenna for the job or any requirement for and efficacy of further modification.

At the outset, it was understood that any feed to be used at the high peak-power levels desired for the work would require special high-voltage design treatment (to be applied by Physics International). The broadband horn is mechanically and electrically well-suited to those treatments and no unusual difficulties are expected in implementing the design in a high-power version. Specifically, it will be necessary to pressurize the high-power horn with sulfur hexafluoride to mitigate the effects of air breakdown.

The polarization of the feed and resulting antenna system is linear. Either horizontal or vertical polarization may be chosen by physically rotating the feed horn. Quadraridge waveguide horn designs are available (from Watkins-Johnson, for example) that would make possible the nearly simultaneous (on alternate pulses, perhaps) excitation and reception of both polarizations. Because no simple means were readily available to direct the high-power pulse source to the two input ports of such an antenna, the use of a quadraridge waveguide horn option was not pursued.

III FIELD TESTS OF THE ANTENNA FEED

A. TEST GEOMETRY

Field tests of the broadband ridged horn feed antenna with the 30-ft dish (proposed for use in this program) were conducted at SRI's Stanford field site. A transmission path of approximately 200 m was established between the transmitting antenna and a receiving broadband horn located across a deep gully from the transmitter.

B. SWEPT FREQUENCY MEASUREMENTS

Simple swept-frequency measurements were made of the connecting cables to be used, of the two horn antennas together with the cables to establish the horn gain, and finally of the full horn-fed-dish transmitter and horn receiver setup. The boresight direction was established by noting the peak of the received signal as the dish azimuth and elevation were varied. Measurements of swept spectra were then made at 1° increments in azimuth and elevation through the main lobe of the beam. The results of these measurements, summarized in Tables 1 and 2 and in Figures 2 and 3, show that the beamwidth of the 30-ft dish fed with the available broadband horn is close to the expected 10° range at the low end of the spectrum of usage but that the beamwidth narrows considerably as frequency increases. This indicates that the horn beamwidth is not diminishing with the increase in frequency as rapidly as required (because of the horn aperture phase errors and subsequent reduced effective aperture). The gain of the dish-horn combination also varies with frequency, as one would expect. The measured gain, averaged over the band, is indicative of an effective aperture efficiency of about 20%. The resulting antenna combination, while not perfect, has a broad frequency range of usefulness in the most desired band of 200 to 500 MHz where the high-power source energy is concentrated. The excess gain (and consequent narrower beamwidth) frequencies above 500 MHz will tend to compensate for the fall-off in energy from the source at high frequencies, thus increasing the effective system bandwidth. Further improvement will be effected in Phase II of this program, if necessary, by the addition of a phase correcting plate to both antenna feed horns.

Subsequent tests explored sidelobe and backlobe power to estimate the amount of unwanted electromagnetic energy that might be present at and near the transmitter installation. Our findings of observed power level relative to the main beam power are in Table 3.

Table 1

GAIN AS A FUNCTION OF FREQUENCY AND AZIMUTH OFFSET
FOR BROADBAND HORN FEEDING 30-FT DISH

Frequency	Gain (dB) for Indicated Azimuth Offset						
(MHz)	0	+1°	+2°	+3°	+4°	+5°	−2°
200	19.9	20.1	19.3	18.5	17.4	17.1	18.8
280	24.8	23.9	20.9	22.6	20.1	19.3	23.4
360	25.2	24.9	23.8	22.7	21.3	17.0	23.5
440	25.5	25.2	24.1	21.4	17.8	12.4	22.2
520	26.5	27.0	25.2	21.2	15.2	9.8	23.3
600	27.4	27.6	27.9	21.1	17.8	10.1	23.3
680	29.8	27.9	26.5	21.0	17.8	13.4	25.1
760	30.6	29.9	26.4	21.0	15.5	12.8	25.1
840	30.9	28.7	26.6	21.1	15.9	14.8	25.5
920	32.7	32.7	28.6	21.2	18.5	17.1	27.2
1000	31.1	29.5	26.7	19.1	17.1	15.8	22.6

Table 2

GAIN AS A FUNCTION OF FREQUENCY AND ELEVATION OFFSET
FOR BROADBAND HORN FEEDING 30-FT DISH

Frequency	Gain (dB) for Indicated Elevation Offset			
(MHz)	+1°	+2°	+4°	+6°
200	19.6	19.3	18.5	16.0
280	23.9	23.9	21.2	16.3
360	25.1	23.8	20.8	14.2
440	26.0	24.7	20.6	12.4
520	26.1	24.5	19.2	12.5
600	25.7	23.8	18.3	17.0
680	29.5	26.0	19.7	13.9
760	28.9	24.5	21.0	14.1
840	29.3	24.6	22.2	11.0
920	30.8	27.2	25.3	13.0
1000	28.6	25.1	22.9	17.1

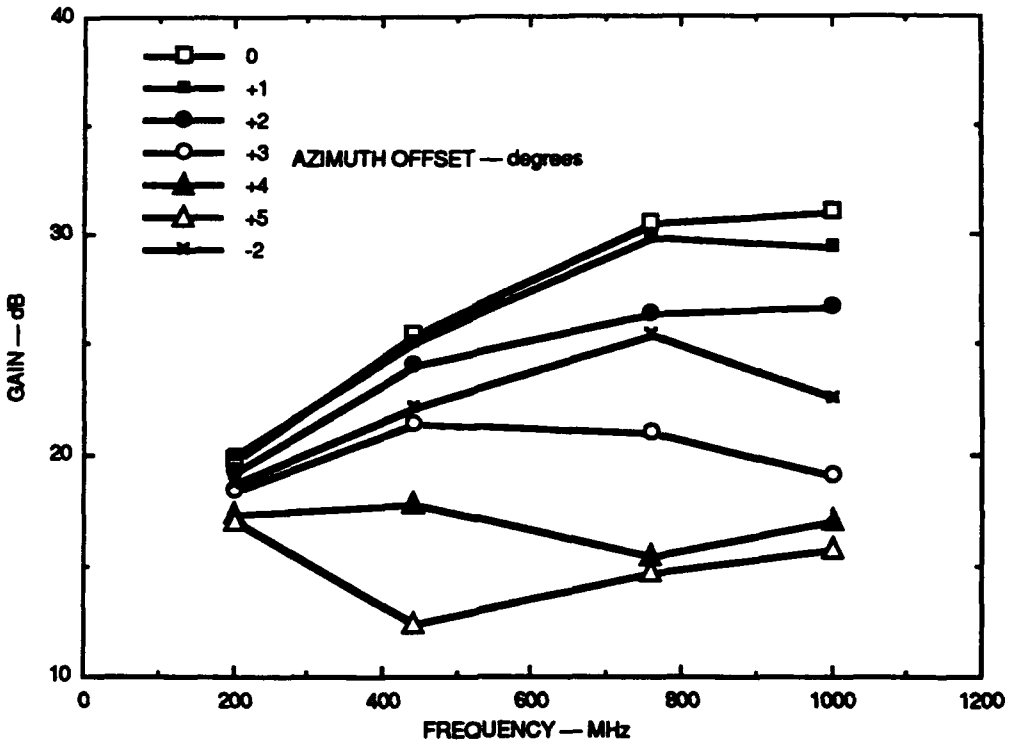

FIGURE 2 GAIN AS A FUNCTION OF ANGLE PARAMETRIC IN FREQUENCY FOR BROADBAND HORN FEEDING 30-FT DISH

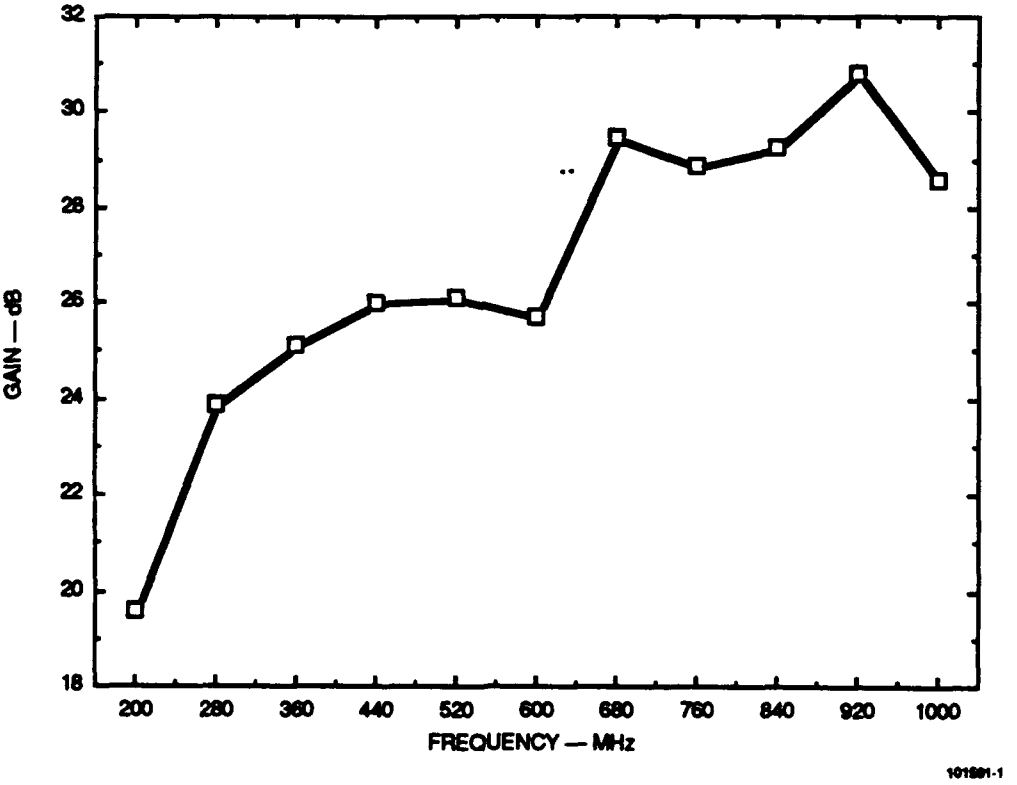

FIGURE 3 GAIN AS A FUNCTION OF FREQUENCY WITH ANGLE OFFSET = +1 FOR BROADBAND HORN FEEDING 30-FT DISH

Table 3

SIDELOBE AND BACKLOBE MEASUREMENTS
FOR BROADBAND HORN FEEDING 30-FT DISH

Angle (deg)	Level (dBm) at Frequency 200 MHz	300 MHz	400 MHz
0	–31	–34	–31
30	–56	–58	
60	–65	–58	
90	–65	–67	–58
120	–76	–70	
150	–70		
180	–61	–67	–75

C. PULSED MEASUREMENTS

The principal field measurements conducted were the determination of electric fields transmitted by the horn and dish combination using a low power pulse source (approximately 3-kV pulses). The high-power source to be used for later ocean clutter characterization has an output waveform that is understood to be very similar to the waveform from the lower power source used in these tests. The electromagnetic signals transmitted were sensed at the 200-m distant receiving site by an E-field probe and by a broadband horn antenna. Measurements of the transmitted waveform (by both sensors) were recorded as a function of angle off boresight in azimuth and elevation. Some examples of these data are presented in Figure 4. The raw data obtained were made available to Physics International for their analysis, which resulted in the curves of peak-to-peak power for the n^{th} cycle of the received signal as a function of azimuth and elevation, as shown in Figure 5. Our concern was with the preservation of the characteristic shape of the transmitted signal as a function of angles. With the expected constant gain and beamwidth as a function of frequency, the received signal should vary in amplitude only as a function of the angles. We observed that this is generally the case within the main beam, but that there are perturbations and distortions visible both within the main beam (where they are overridden by the average waveform) and at the beam edges (where they are unimportant because of the overall low power). These variations may result from the presence of unaccounted reflections in the test setup at the field site (since the receive antenna had very wide beamwidth) as well as nonideal behavior of the transmit antenna assembly. Figure 6 shows waveform peak amplitude as functions of azimuth and elevation.

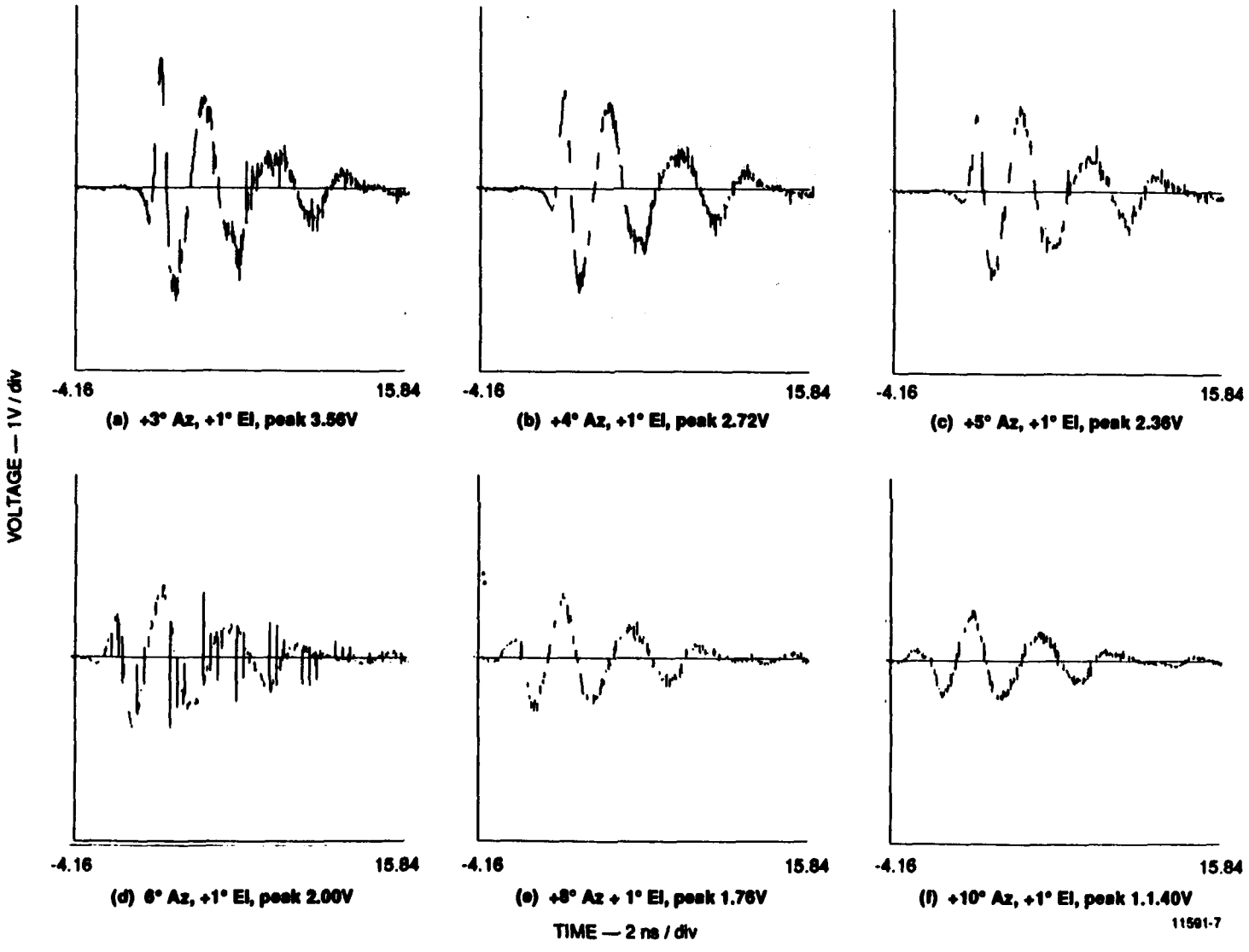

FIGURE 4 TYPICAL RECEIVED WAVEFORMS AS A FUNCTION OF AZIMUTH OFFSET FROM PEAK READING POSITION

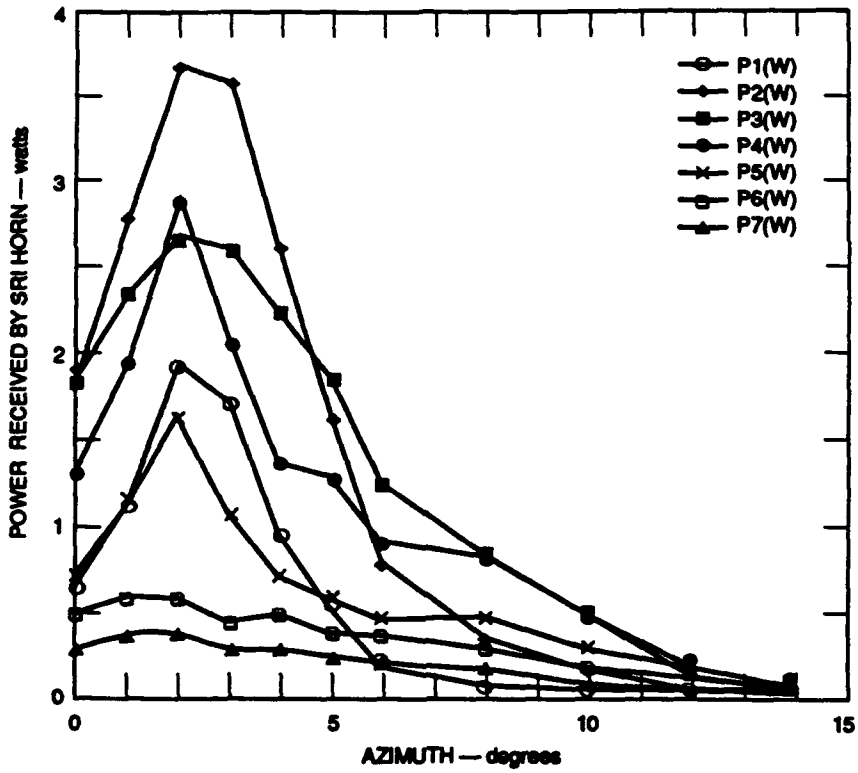

(a) AS A FUNCTION OF AZIMUTH OFFSET (RELATIVE)

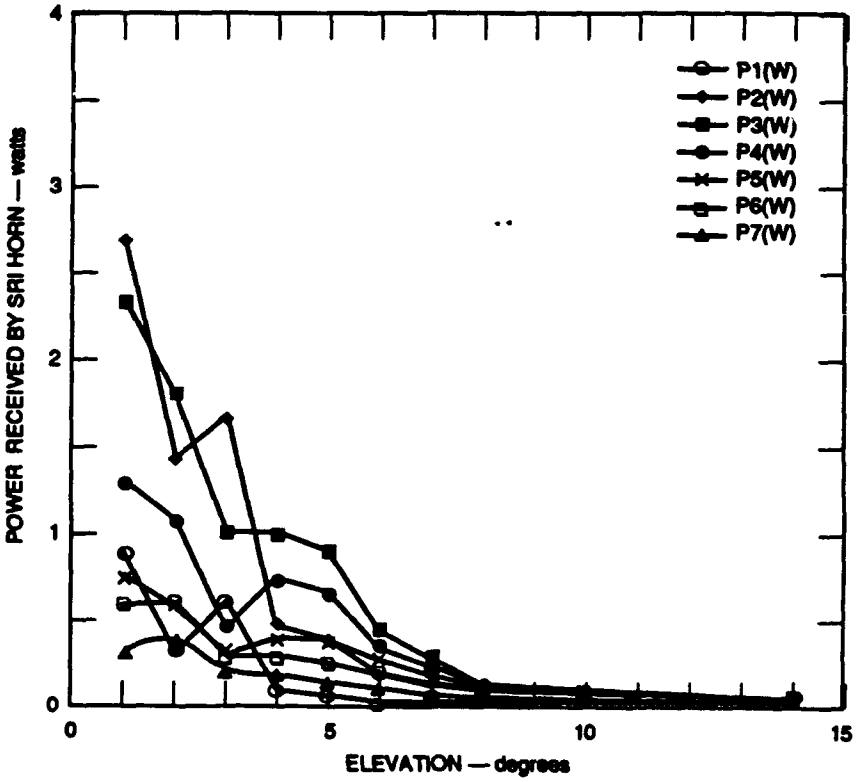

(b) AS A FUNCTION OF ELEVATION OFFSET (RELATIVE)

FIGURE 5 PEAK POWER IN n^{th} CYCLE OF WAVEFORM

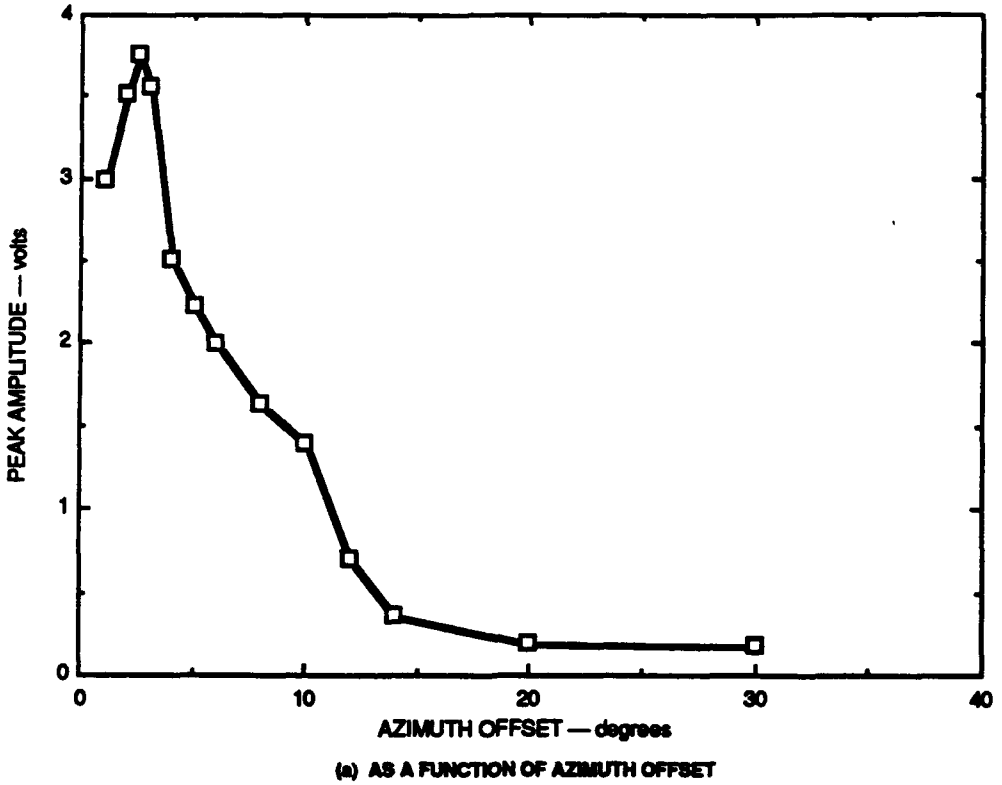

(a) AS A FUNCTION OF AZIMUTH OFFSET

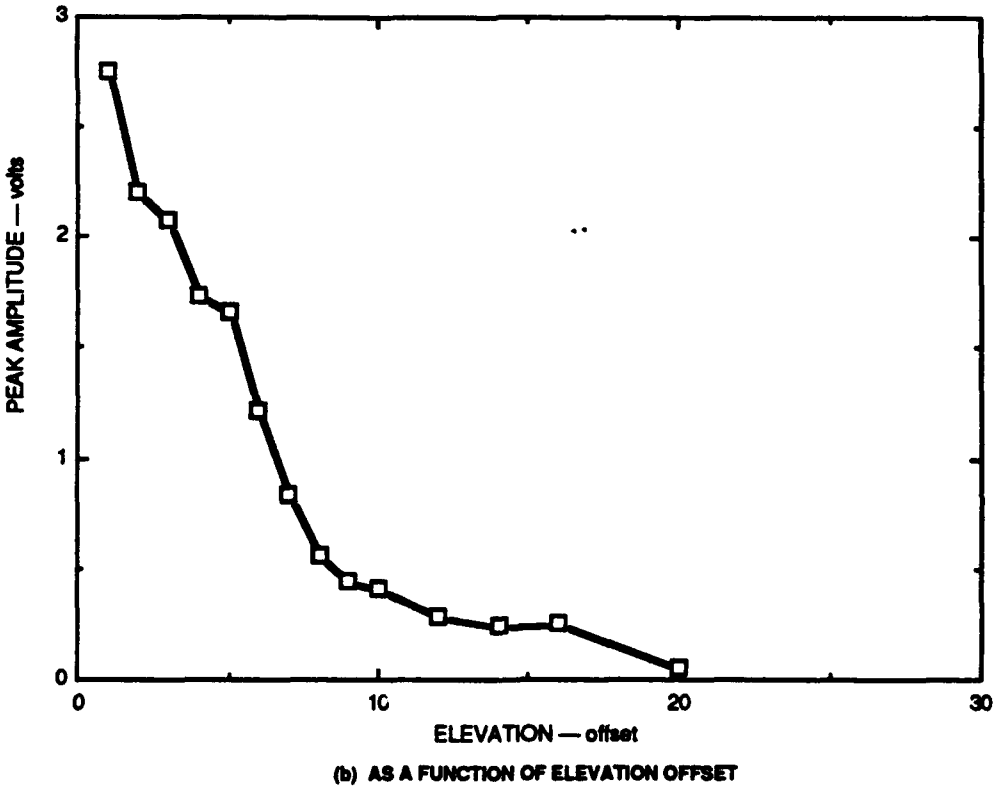

(b) AS A FUNCTION OF ELEVATION OFFSET

101581-4

FIGURE 6 PEAK AMPLITUDE OF SIGNAL

For the waveform measurements reported here no filtering or amplifier was applied at the receiver site. A 12-dB attenuator was placed between the receive horn and the digitizing signal analyzer (Tektronix DSA-602). For the low-power pulse source provided by Physics International, peak signals viewed by the receiver horn at boresite reached a maximum of 15 V at the antenna terminals.

IV DESIGN OF THE RECEIVER AND DATA SYSTEM

The principal challenge in the design of the receiver and data system is a consequence of the large signal bandwidth. In many situations, sampling techniques can be used to transpose these frequencies to a lower and therefore less-demanding spectral region. However, this requires a stationary target field over the sampling reconstruction period. In our case, the repetition rate of the source will not permit such an approach and we are left with the necessity of digitizing each radar pulse repetition interval (PRI) at the full bandwidth. The transient digitizer planned for this project is the Tektronix DSA-602, which has a maximum digitizing rate of 2000 MHz, giving us a maximum usable analog bandwidth of 1000 MHz. The instrument has been tested with a sample receiver and impulse signal, and software has been completed to record and display a sequence of transient records using this digitizer. Like all high-speed digitizers, the DSA-602 is limited in its dynamic range, which is eight bits (48 dB). We can extend this a little by applying time-varying gain to the received signal (commonly called *sensitivity time control*, or STC), so that the distant signals are amplified more than those close-in. Provided that the noise—either man-made or natural—does not start to fill the dynamic range of the receiver, this approach can gain us another 40 dB. Data from the digitizer are stored as ASCII files on IBM-PC-compatible disks for archiving and later analysis. The system is capable of recording data at 160 transients per second, which is substantially higher than the proposed transmitter can operate, and will not be the limiting factor in the final radar system.

The receiver is a relatively simple design, using no local oscillators and a single preselecting filter stage. We anticipate some problems with the high amplitude of the direct pulse from the transmitting antenna (the "main bang") and plan to handle that with some robust limiting stages as shown in Figure 7. Within the amplifier chain are three cascaded STC stages, each supplying a maximum of 15 dB of range-dependent voltage gain. Thus, it should be possible to compensate for the $1/R^4$ losses before the digitizing stage. The gain and noise levels through the amplifier are shown in Figure 8. We estimate that the noise level looking out to sea will be approximately 5 dB over thermal (kTB) in the 200 to 1000 MHz spectral range.

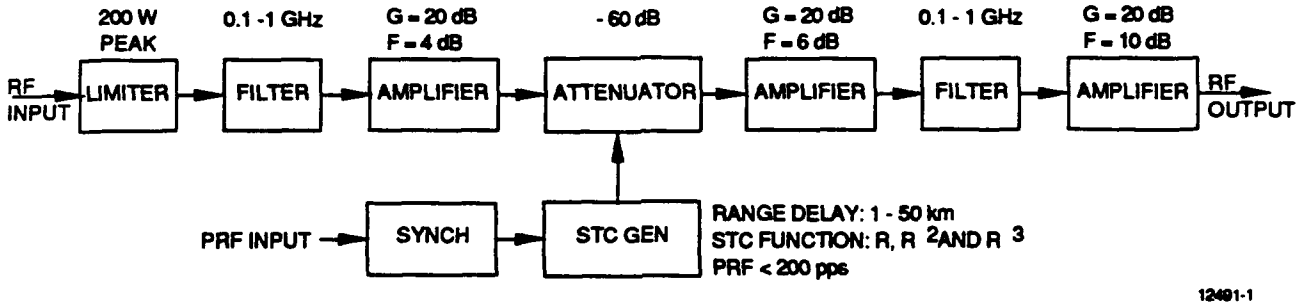

FIGURE 7 BLOCK DIAGRAM OF SEA-CLUTTER RADAR RECEIVER

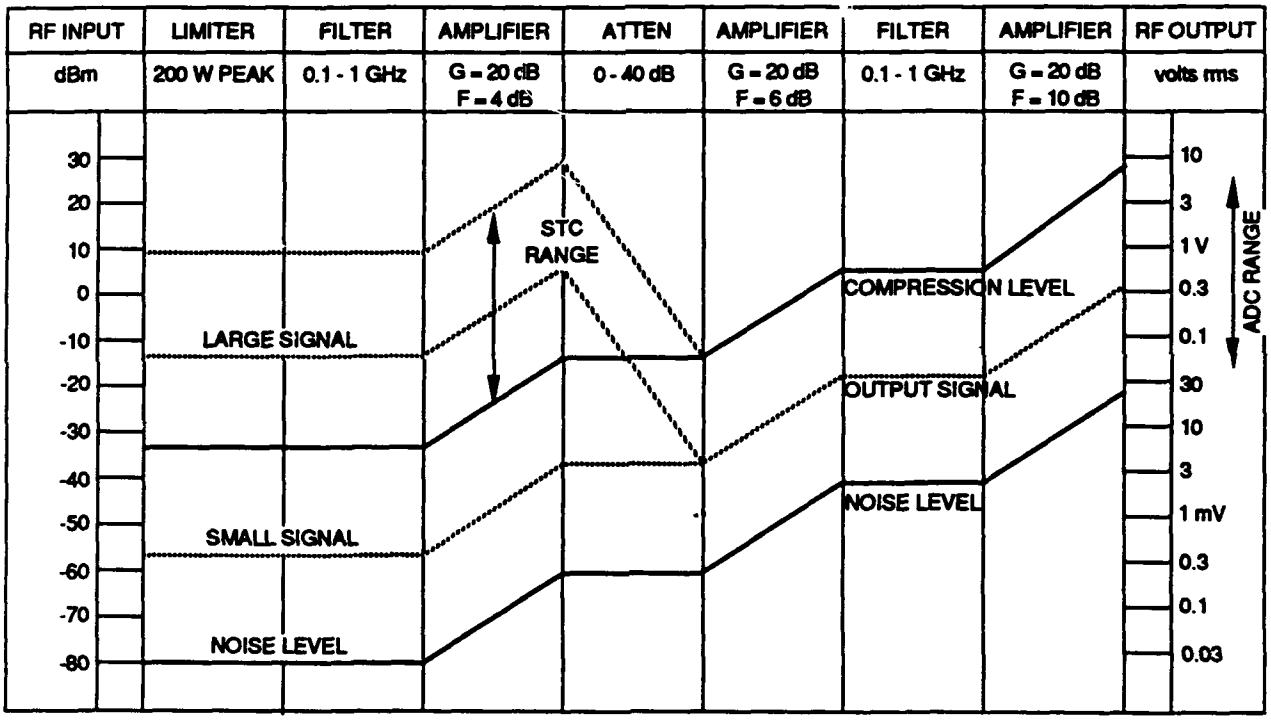

FIGURE 8 DYNAMIC RANGE OF SEA-CLUTTER RADAR

V NOSC SUPPORT

During the Phase I project, we have supported a number of project meetings at the NOSC and PI facilities. In addition, we have assisted NOSC in their search for a 30-ft transmitter dish, both by locating a number of government dishes that were available and by inspecting and reporting on a particular dish operated by Lockheed Missiles and Space Division at the request of NOSC personnel.

VI PROJECTED SCHEDULE FOR PHASE II

The elapsed time from the start of the Phase II contract until we will be ready to put the receiving system in the field will be eight weeks minimum. This is primarily controlled by the time necessary to mobilize the 30-ft dish now at SRI's field site and by delivery times of critical components. Wherever possible, we will use and replace components in stock that are not urgently needed by other projects. However, in the case of mechanical components for the 30-ft dish, this will not be possible and components must be ordered from vendors. Thus, if we are to take measurements in March, we must have contractual authorization to start work by the end of January. A detailed schedule is shown in Figure 9.

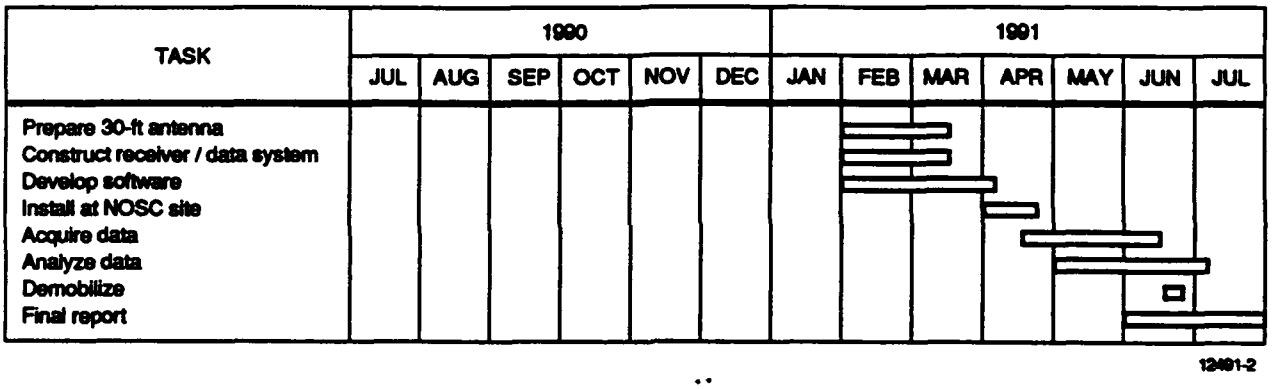

FIGURE 9 EXPERIMENT SCHEDULE, PRESUMING FEBRUARY 1 START DATE

VII CONCLUSIONS

We have designed and tested an antenna system that will broadcast 200- to 1000-MHz energy in a beam approximately ±5° from the boresight at the 3-dB points. The actual receive dish to be used on the program has been calibrated in this mode. The receiver design has been completed, allowing for rejection of the large direct feed-through pulse from the transmitter, and the necessity for increasing the dynamic range of the system through the use of STC. We anticipate that the system will be able to detect low RCS targets out to approximately 20 km and to make measurements of sea clutter sufficient to fill in the voids present in the published literature on the subject. We anticipate some difficulty in measuring sea clutter in low sea state conditions, based on the productions of the NOSC team that the backscatter could be as low as –90 dB at grazing angles. While this is good for detection of targets (because it implies a high signal-to-clutter ratio), it complicates the job of characterizing the sea clutter.

REFERENCES

Kerr, J.L., 1973: "Short Axial Length Broadband Horns," *IEEE Trans Ant. & Prop.*, pp 711-714 (September).

Walton, K.L., and V.C. Sundberg, 1964: "Broadband Ridged Horn Design," *Microwave J.*, Vol. 7, pp 96-101 (March 1964).

APPENDIX D

CONCEPTUAL DESIGN OF A HIGH POWER ELECTRON BEAM POST-ACCELERATION EXPERIMENT

The final technical task of the HCRF program was the conceptual design of an experiment to investigate producing RF energy by using a linear series of relativistic klystrons powered by a single electron beam that is re-accelerated after passing through each klystron. The re-acceleration (post-acceleration) replaces energy extracted as RF from the klystrons. The efficiency of converting electron beam energy to RF energy increases as the number of klystrons increases. The motivation for designing the experiment and its relevance to the HCRF program was explained in Section 2.4 of this report. The primary motivation was to provide a reasonable point of departure for meaningful future work on the HCRF concept should SDIO choose to restart the effort later. For economy, the design effort was constrained to use existing hardware wherever possible. The final conclusion of the effort was that some new accelerator hardware would be required to make the experiment viable. The details that led to this conclusion follow.

D.1 DESIGN OVERVIEW.

The post-acceleration experiment was designed around using PI's CLIA (see Section 2.4) and a set of existing L-band relativistic klystron amplifier (RKA) hardware owned by SDIO. Use of these existing parts was the main design constraint. To provide separated regions for primary and post-acceleration, the ten induction cells in CLIA are split into two portions, one with seven acceleration cells, and the other with three cells. The seven-cell portion is used to drive the RKA. The bunched beam produced by the RKA is then post-accelerated by the three-cell section of CLIA before arriving at the RF extraction cavity. Ideally, the accelerating gap would be placed at the location where the beam from the RKA is optimally bunched. A truly relativistic post-acceleration substantially increases the kinetic energy of the beam without disturbing the beam bunching. Therefore, more kinetic energy of the beam is available for conversion to RF energy in the extraction cavity downstream of the post-acceleration gap. The source emsemble efficiency increases with multiple extraction of the microwave energy from the post-accelerated bunched beam because the relativistic beam does not debunch until most of its kinetic energy is converted into RF energy. Furthermore, the post-acceleration/multiple extraction cycle can be repeated to achieve high system efficiency. The post-acceleration needs only to refurbish the energy extracted in the previous cycle.

Figure D.1 illustrates a concept geometry for the post-acceleration experiments in the single-shot regime. The seven-cell accelerator delivers a 500-kV, 5-kA annular electron beam, at the cathode-anode gap, to the modulating cavity where the beam is initially velocity modulated. The RKA magnet provides the guide field for transporting the e-beam down the drift tube. When

In

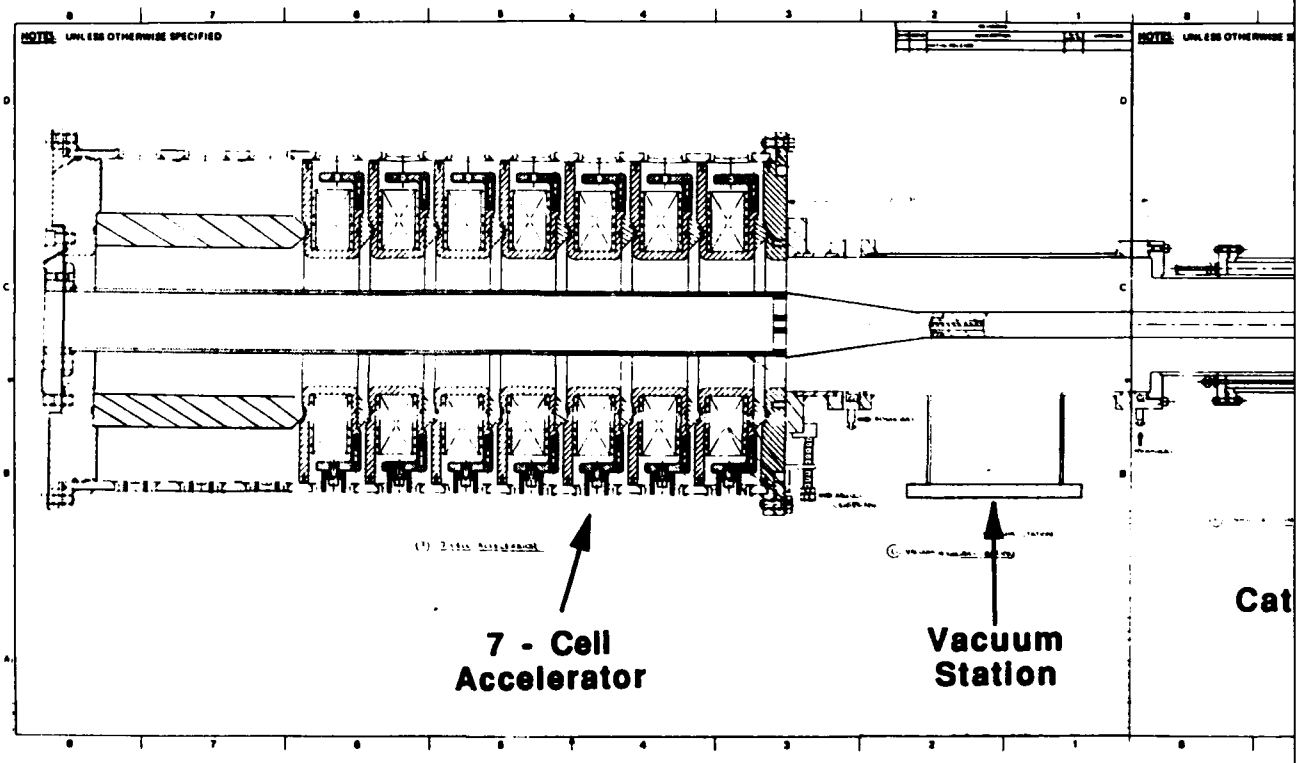

Cat

1

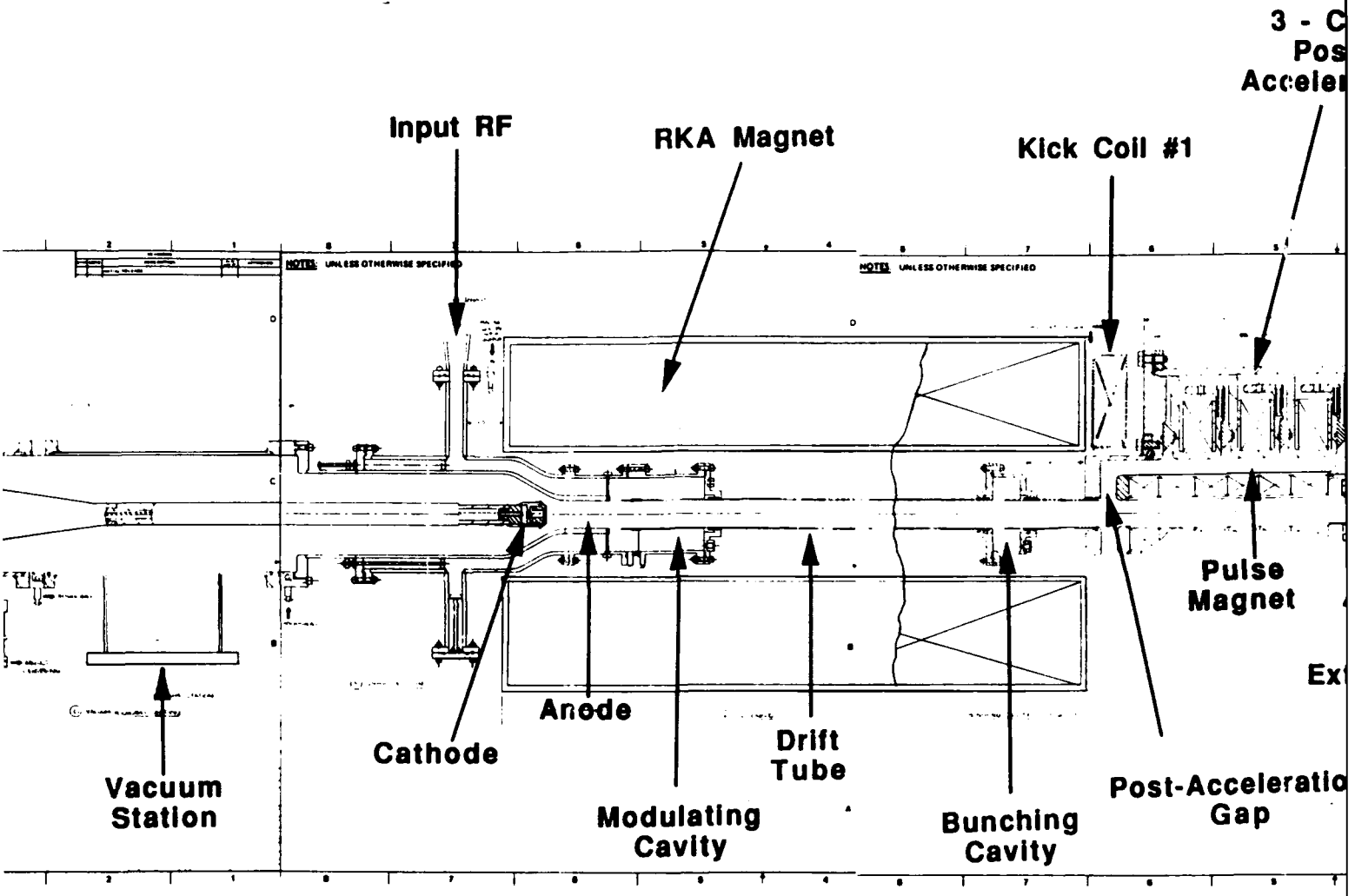

Figure D-1. A concept geometry for the po CLIA.

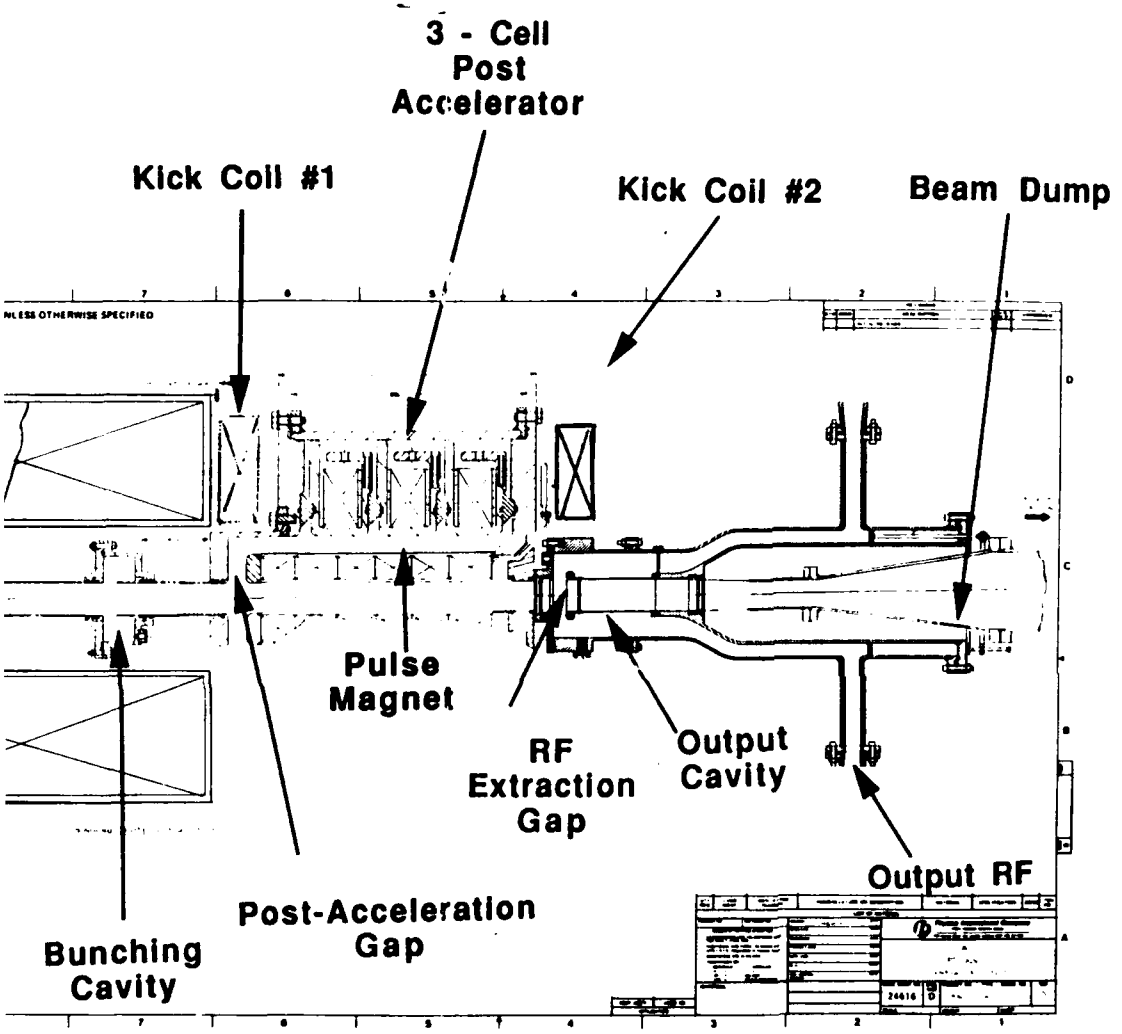

D-1. A concept geometry for the post-acceleration experiment on CLIA.

the beam passes the bunching cavity, it gets excited to a high RF electric field. This excitation causes more bunching in the beam as it propagates farther downstream. Previous L-band RKA experiments on CLIA have demonstrated that the bunched beam can contain an RF current as high as 3 kA. The 210-kV post-acceleration gap, powered by the three-cell accelerator, substantially increases the beam energy. The two kick coils and the pulse magnet in the three-cell accelerator structure supply the guiding magnetic field for the electron beam to propagate through the accelerator to the RF extraction/output cavity, whose design is identical to the RKA version. This cavity couples out the RF power in the beam modulation to the rectangular waveguides. The electron beam is eventually collected by the beam dump.

D.2 DESIGN ISSUES.

Various design issues had to be addressed. They include impedance matching for the pulsed power system, electric field in the post-acceleration cell, magnetic field effects on the Metglas accelerator cores of CLIA, the design of the magnetic guide field and the bunched beam transport from the post-accelerator gap to the extraction cavity. Those issues are discussed below, starting with the beam transport and working backward towards the matching of the pulsed power system.

D.2.1 Bunched Beam Transport.

Rob Ryne at Los Alamos provided the computer code RKIS that was used to study transport of the modulated electron beam from the post-accelerating gap to the output cavity. The parameters of the calculation are given in Table D.1.

Table D.1. Parameters used in the beam transport calculation.

DC Beam Current	5 kA
Beam Energy	750 kV
Beam Modulation	Square Wave, or $1+e\cos(\omega t)$; e = 90%, 60% or 30%
Modulation Frequency	1.32 GHz
Beam Radius	1.9 cm
Drift Tube Radius	2.32 cm
Drift Tube Length	1 m

The beam model in the calculation is a solid beam of 1.9 cm radius in a drift tube of 2.32 cm radius. This beam is different from the thin (3 mm width) annular RKA beam of the same outer radius and drift tube radius. The charge density in the annular beam is about 3 times larger than that in the solid beam used in the code calculation. The high charge density is likely to enhance the beam debunching.

Figure D.2 shows the calculated amplitude of the first harmonic in the transported beam as a function of distance downstream of the post-acceleration gap for a square wave and three different modulations. Previous RKA experiments indicate that a 60% modulated, 750-kV, 5-kA (d.c. current) beam should exit the post-accelerating gap. After propagating a 50-cm distance from the post-acceleration gap to extraction gap spacing in the present design, the initial 3 kA of modulation at the first harmonic would be reduced to 1.8 kA. The power content available for RF extraction is reduced from 1.5 GW to 1.35 GW (from 500 kV x 3 kA to 750 kV x 1.8 kA). In this case, post-acceleration will not increase the microwave output. Using existing hardware restricts the design geometry, and limits options for optimizing RF extraction. For this reason, other issues associated with the intense beam transport, such as beam phase stability versus voltage and current, bunch integrity, and energy spread versus drift length were not studied at this time.

D.2.2 Beam Guiding Magnetic Field.

D.2.2.1 Static Analysis of the Guide Field. The on-axis beam guiding magnetic field was treated as a static (dc) field. The guide field is generated by four magnets, a large solenoid for the bunching section, kick-coil No. 1 located immediately downstream of the main solenoid, a pulsed magnet inside the accelerator section, and kick-coil No. 2 for the klystron extraction section. The magnetic fields (Figure D.3) were calculated using a standard solenoid formula with end corrections, under the assumption that no magnetic material is present in the vicinity. The beam radius under the influence of the static guide field was also calculated. The result from this simplified analysis indicates that the beam may be contained within the drift tube throughout the post-accelerator.

The effects of transients and the presence of high-μ material have been ignored in the above analysis, but their impact must be considered in the design of the guide field. Figure D.4 shows the post-acceleration region in the concept geometry (in the following discussion, please refer to this figure unless stated otherwise). The large RKA solenoid is dc-excited so transient effects can be ignored. However, the presence of high permeability material must be included. Design of the

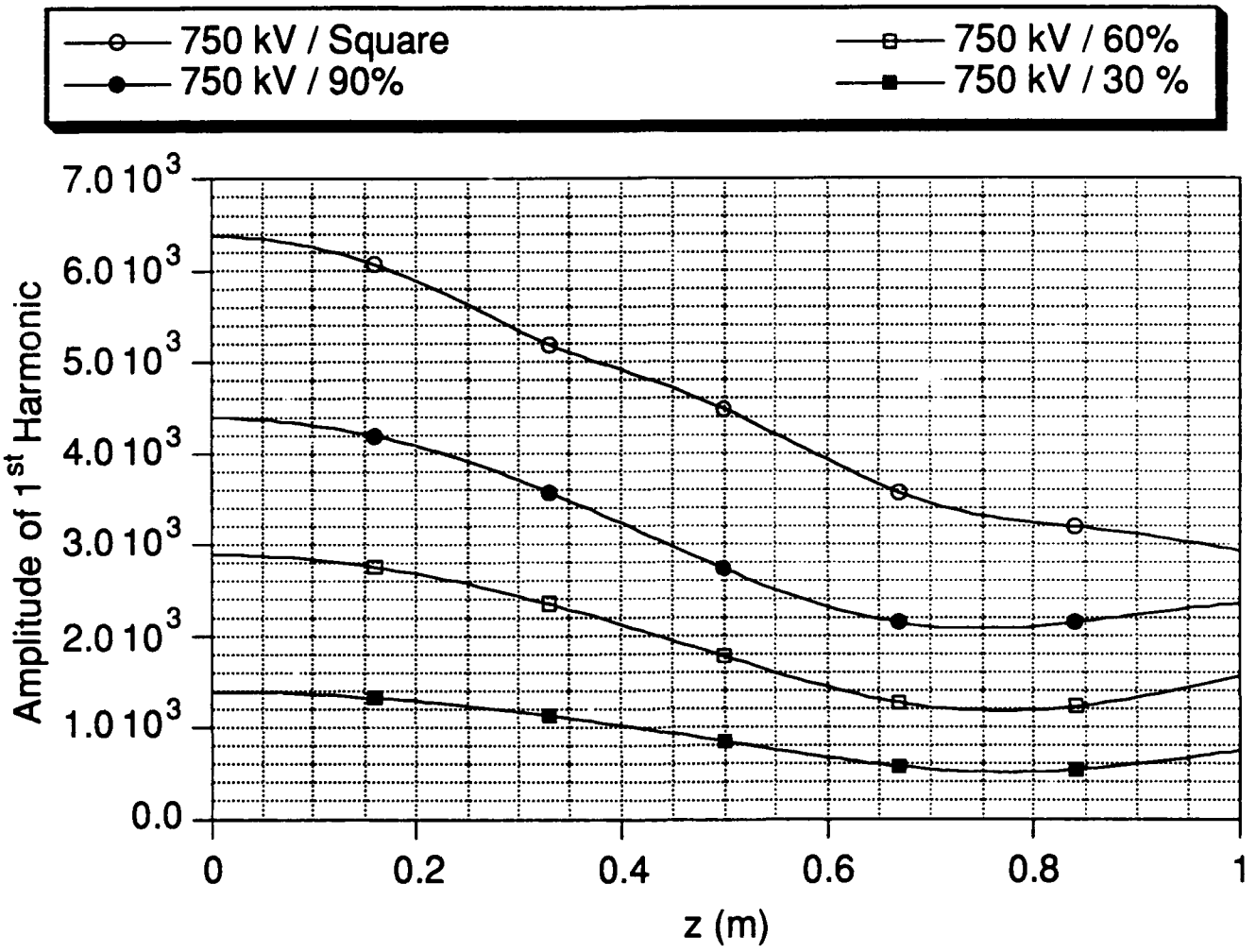

Figure D-2. Dependence of the first harmonic amplitude on the beam transport distance.

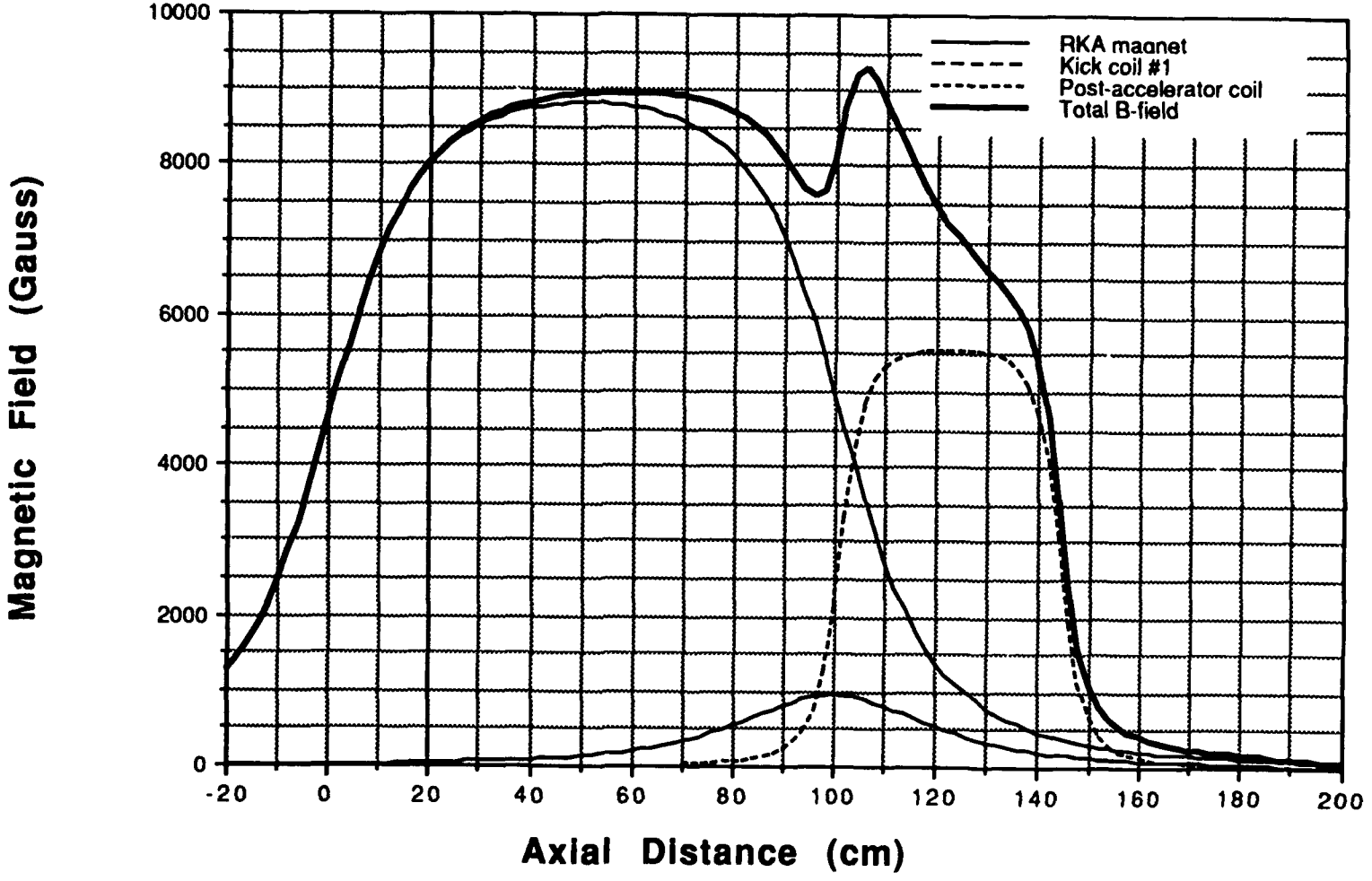

Figure D-3. **Axial magnetic field distribution in the post-acceleration region from a DC calculation of fields. Note that Kick coil #2 was not included in this static calculation.**

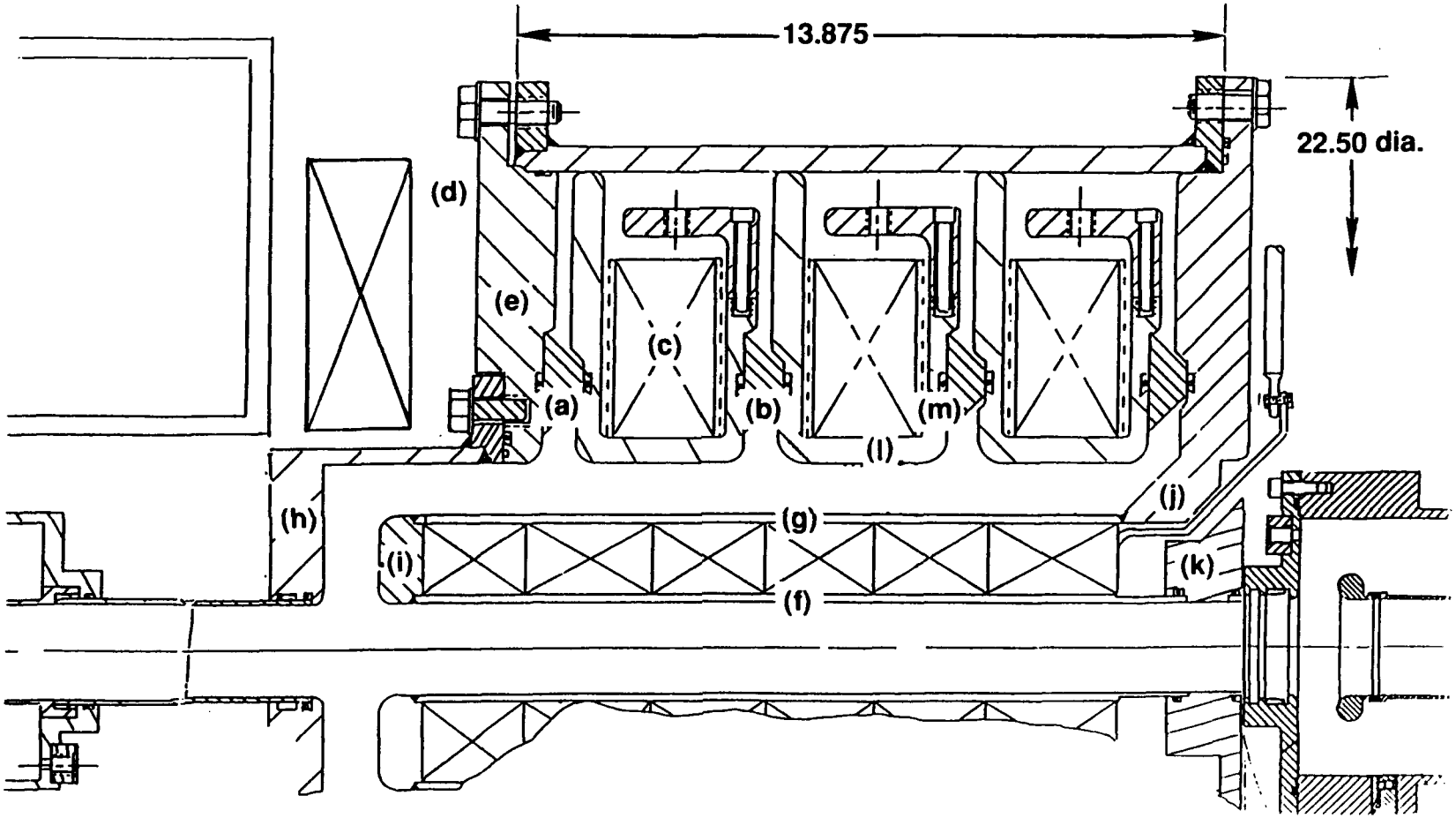

Figure D-4. Post-acceleration region in the concept geometry.

kick-coils and post-accelerator pulsed magnet will require inclusion of high permeability materials, transient effects, or both depending on temporal pulse length.

D.2.2.2 High Permeability Materials. Unshielded high permeability materials such as the Metglas cores in CLIA "pull" flux from the surrounding regions and alter the magnetic field. The leftmost Metglas core (area c), if unshielded, could alter the field produced by the dc excited coil by a few hundred Gauss at the beam location. A similar effect could be produced for the pulsed coil if the pulse length is sufficiently long.

If a shield is imposed to protect the Metglas core from the dc field, it will also affect the magnetic field at the beam location. However, it is not clear whether the effect will be larger or smaller than that for the unshielded core. The effect depends on the location of the shield and where the comparison is made.

D.2.2.3 Transient Effects. Current is induced in any continuous, electrically conducting ring when the pulsed magnet is fired. This current will alter the magnetic field and will decay in time. Thus the statistically calculated field distribution will be obtained only if the temporal pulse length is sufficient to permit the current to decay to negligible levels. The decay times associated with several rings in the proposed concept were estimated.

Note that the current decay times can be significantly longer than the "skin times" frequently associated with the diffusion of magnetic fields in conducting media. The skin time is the time for flux to diffuse into the material. In the case of the conceptual geometry, sufficient flux must diffuse through the material to fill in space inside the ring. The appropriate decay time is the L/R time of the ring.

If the innermost wall (area f) of the post-acceleration cavity is 3/16-inch stainless steel; the L/R time is about 0.1 ms. Thus the static field would be approached in perhaps 0.5 ms. The coil's external wall (area g) has a decay time of about 0.25 ms if it has the same wall thickness. If the wall thickness is increased to enhance the mechanical strength of the assembly, the decay time will increase proportionately.

The 1-inch-thick ring (area h) to the left of the pulsed coil has an L/R time of about 0.5 ms. However, such an estimate assumes that the field is diffusing from both sides of the ring. Since the conceptual geometry involves imposing the field from only one side, a time of 2 ms is probably more reasonable. However, this ring is relatively far from the pulsed coil, and its effect on the

field is relatively small. Thus the static distribution will be approached in a smaller number of decay times. It would be desirable to reduce the thickness both of this ring and the one at the end of the coil (area i) if possible.

The plate (area j) and ring (area k) at the right end of the coil are even thicker. The difference in cross hatching and seals makes it appear that these are distinct parts. These parts will inhibit the diffusion of the magnetic field into the extraction cavity that is presumably required. In addition, the structure of the left end of the extraction cavity poses a similar problem. The ring (k) has an L/R time of about 4 ms. The current decay time for the plate (j) is somewhat longer. Adding the extraction cavity parts would increase the decay time to 10-20 ms. This would require a pulse length of perhaps 100 ms to achieve the static field distribution. Redesign of this region should be considered to reduce the thickness of the parts unless a 100-ms pulse length is reasonable.

If the rings discussed so far were the only ones in the system and if the parts near the extraction cavity were made thinner, a pulse length of 5 ms would probably be sufficient to use static analysis of the field distribution. However, the Metglas cores are wound on aluminum mandrels. The L/R time associated with the inner wall of these mandrels (area l) is about 20 ms, and the time associated with the radial walls (area m) is even longer. If the pulse length is very long, say 1 second, then the Metglas cores must be included in the analysis. If the pulse length is only 5 ms, then these surfaces should be assumed to constrain the return flux for the pulsed coil. This could lower the field inside of the coil by as much as 15%.

If the magnetic field must be held constant within the post-acceleration cell to better than about 25%, the effects discussed in this section will be important and should be included in the design, or an experimental effort should be anticipated to obtain a satisfactory guide field. There are a number of computer codes available commercially that could be used to address these issues.

The best approach is probably to thin the parts near the extraction cavity and use a few-millisecond excitation pulse for the magnet. This would avoid involving the Metglas cores in the pulsed magnetic field, although it would require including the core mandrels in the analysis.

D.2.2.4 <u>Interaction between Magnetic Fields and Metglas Cores</u>. A very crude estimate yields a 1-kG field at the intended location of the leftmost Metglas core (area c). If the core were not to perturb the magnetic field, this would essentially be the magnetic induction in the

material and is small compared with the 30-kG flux swing available. However, the core material has a very high DC permeability (which is anisotropic due to the construction of the core). Thus the core will "pull" flux from the surrounding region and increase the internal B-field. If the resulting field is enhanced by more than a factor of three, the performance of the system might be adversely affected.

It would be desirable to shield the Metglas core from the imposed magnetic fields by inserting an annular mild steel ring between the core and the DC magnet coil. This annulus could be placed in the gap presently occupied by the unneeded insulator (area a), external to the post-acceleration cell (area d), or the nominal 1-inch-thick endplate (area e) could be made from mild steel.

While the inclusion of a high permeability shield will affect the magnetic field distribution, it is not clear that the effect will be substantially worse than that of an unshielded Metglas core. This subject is discussed in more detail in the following section.

The shield should extend radially from near the inner radius of the Metglas core to at least the outer radius of the core. The shield must be sufficiently thick to conduct the required flux without saturating the shield material. A thickness of 1/2 inch should be more than sufficient, and 1/4 inch might work.

D.2.3 Electric Fields in the Post-accelerator Cell.

The re-entrant anode configuration of the post-accelerator cell is less favorable than a re-entrant cathode with respect to the peak electric fields generated on cathode surfaces which are potential electron emitters. The geometry of the concept is shown in Figure D.5. The leftmost insulator (area a) is not needed, and is replaced by a metal ring of the same shape in this concept geometry. The next insulator (area b) is located in the accelerating gap which produces the highest electric fields on the cathode surfaces. This region has been analyzed with JASON (a Poisson solver) as shown in Figure D.6. Analysis of expanded views of the two cathode corners yields a peak surface field of 95 kV/cm on the left corner and 65 kV/cm on the right corner. These fields are acceptable provided that the left corner is free of scratches and pits that produce additional enhancements.

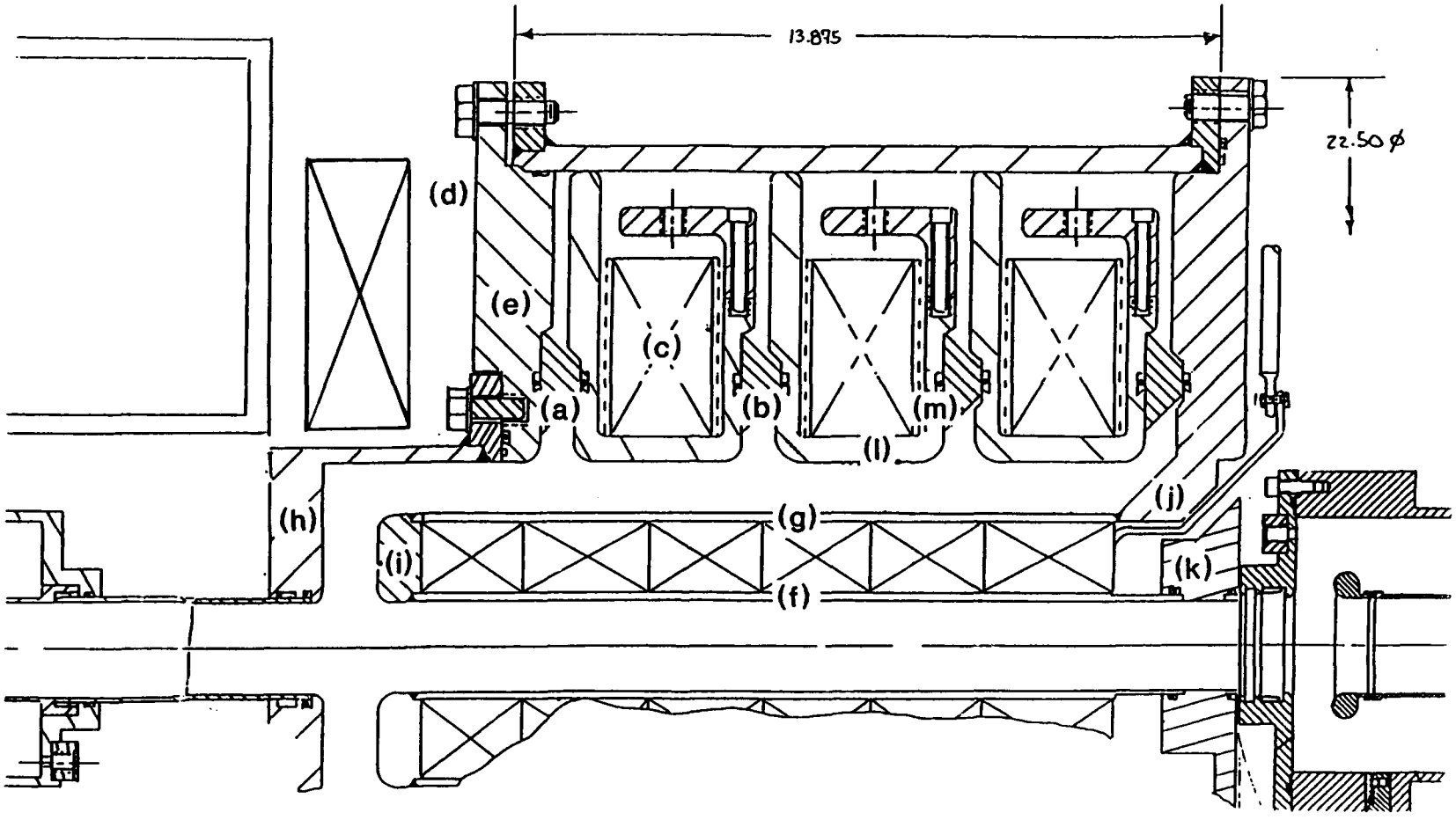

Figure D-5. Concept of the concept using electric fields in the post accelerator cell.

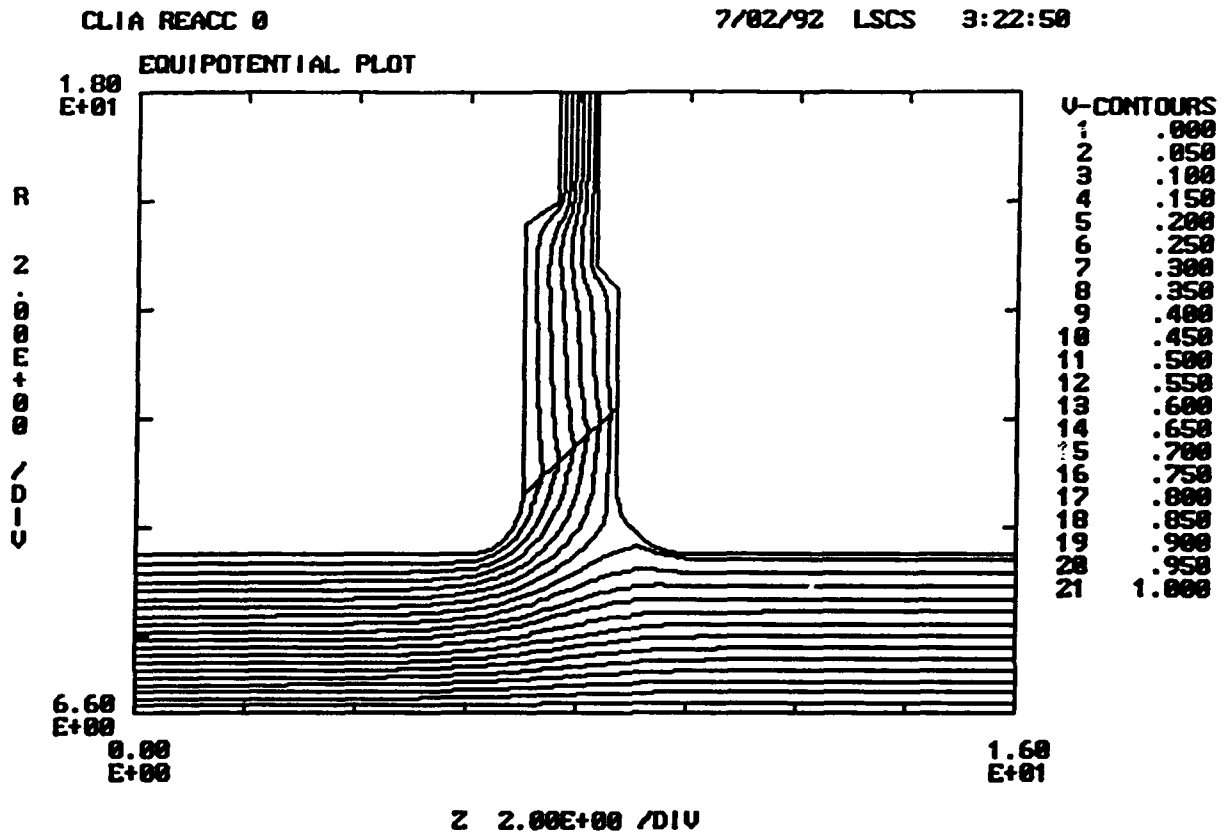

Figure D-6. Equipotential distribution in the high stress area of the post-accelerator.

D.2.4 Impedance Matching.

The impedance match between the RKA load and the seven-cell CLIA proposed in this design is different from that in the present RKA experiments which operate CLIA with the full ten-cell accelerator. When the operating voltage is increased to obtain 500 kV with only seven accelerator cells, the transients due to mismatch may pose electrical stress problems in the accelerator. It would be prudent to fill the CLIA "compensation" resistors with a resistive solution that would limit the mismatch to at most a factor of 1.5. For the purposes of estimating the required resistance, the accelerator cores can be considered to draw 1 kA of magnetization current, and the beam should be considered to be a constant current load to the reacceleration cell.

In conclusion, some resistive matching should be incorporated into the experiments, electric fields are acceptable, shielding of the Metglas cores is desirable, and the design of the guide field is a complex issue which will require either empirical or sophisticated design techniques. Beam transport from post-acceleration to extraction cavity will decrease the RF energy content of the beam for the design geometry due to the hardware restrictions.

D.3 SUMMARY.

A preliminary conceptual design was executed for a post-acceleration experiment on CLIA to study the high current RF source for the high gradient standing wave accelerator. The details of various design issues and methods to deal with them were studied. The conceptual post-acceleration experiment may not increase the RKA output if only the existing CLIA and RKA hardware is used. Voltage from the split CLIA is insufficient to properly post-accelerate the bunched electron beam out of the RKA. Additional CLIA hardware is needed to increase the voltage enough to make the post-acceleration experiment viable as a proof-of-principle experiment in using post-acceleration as the energy replacement stage in the high current source.